Ph.D Thesis
2009

SYNTHESIS AND CHARACTERISATION OF NEW TRANSITION METAL COMPLEXES OF SCHIFF BASES DERIVED FROM 3-HYDROXYQUINOXALINE-2-CARBOXALDEHYDE AND APPLICATION OF SOME OF THESE COMPLEXES AS HYDROGENATION AND OXIDATION CATALYSTS

V. Arun

DEPARTMENT OF APPLIED CHEMISTRY
COCHIN UNIVERSITY OF SCIENCE AND TECHNOLOGY
KOCHI-682 022, KERALA, INDIA

SYNTHESIS AND CHARACTERISATION OF NEW TRANSITION METAL COMPLEXES OF SCHIFF BASES DERIVED FROM 3-HYDROXYQUINOXALINE-2-CARBOXALDEHYDE AND APPLICATION OF SOME OF THESE COMPLEXES AS HYDROGENATION AND OXIDATION CATALYSTS

Thesis submitted to the
Cochin University of Science and Technology
In partial fulfilment of the requirements
for the degree of

DOCTOR OF PHILOSOPHY
IN
CHEMISTRY
Under the Faculty of Science

By

V. ARUN

DEPARTMENT OF APPLIED CHEMISTRY
COCHIN UNIVERSITY OF SCIENCE AND TECHNOLOGY
KOCHI-682 022, KERALA, INDIA

JUNE 2009

SYNTHESIS AND CHARACTERISATION OF NEW TRANSITION METAL COMPLEXES OF SCHIFF BASES DERIVED FROM 3-HYDROXYQUINOXALINE-2-CARBOXALDEHYDE AND APPLICATION OF SOME OF THESE COMPLEXES AS HYDROGENATION AND OXIDATION CATALYSTS

Thesis submitted to the

Cochin University of Science and Technology

In partial fulfilment of the requirements

For the degree of

Doctor of philosophy

In

Chemistry

Under the faculty of Science

By

V. ARUN

DEPARTMENT OF APPLIED CHEMISTRY

COCHIN UNIVERSITY OF SCIENCE AND TECHNOLOGY

KOCHI-682 022, KERALA, INDIA

JUNE 2009

I dedicate this thesis to my

Parents and brothers

Certificate

Certified that the thesis entitled "**Synthesis and characterisation of new transition metal complexes of Schiff bases derived from 3-hydroxyquinoxaline-2-carboxaldehyde and application of some of these complexes as hydrogenation and oxidation catalysts**", *submitted by Mr. V. Arun is an authentic record of research work carried out by him under my supervision at the Department of Applied Chemistry in partial fulfillment of the requirements for the degree of Doctor of Philosophy in Chemistry of the Cochin University of Science and Technology and the work embodied in this thesis has not been included in any other thesis submitted previously for the award of any other degree.*

Kochi-682 022

17-06-2009

Dr. K.K.Mohammed Yusuff
Professor
Department of Applied Chemistry
Cochin University of Science and Technology
Kochi-682 022
Kerala, India

Declaration

I hereby declare that the thesis entitled "**Synthesis and characterisation of new transition metal complexes of Schiff bases derived from 3-hydroxyquinoxaline-2-carboxaldehyde and application of some of these complexes as hydrogenation and oxidation catalysts**" submitted for the award of Ph.D. the degree of Doctor of Philosophy in Chemistry of the Cochin University of Science and Technology is based on the original work done by me under the guidance of Prof. Dr. K. K. Mohammed Yusuff, Professor, Department of Applied Chemistry, Cochin University of Science and Technology, Kochi-682 022 and this work has not been included in any other thesis submitted previously for the award of any other degree.

Kochi-682 022 **V. Arun**

17-06-2009

Acknowledgment

I gratefully acknowledge my deep sense of gratitude to all who provided help and support to me during the course of my research work. I invariably feel short of words to express my heartfelt gratitude and deep indebtedness to Prof. Dr. K. K. Mohammed Yusuff, my supervising guide for his efficient guidance through the awesome path of research with great patience. His constant encouragement, fruitful discussions and valuable suggestions at different stages were really a great inspiration. He is truly a "Guru" for me in the calmness of mind, hard work and patience towards others.

I would like to express my deep gratitude and heartfelt thanks to Prof. Dr. K. Girish Kumar, Head, Department of Applied Chemistry for providing the necessary advice and facilities for carrying out my research. Former heads of the Department Prof. Dr. S. Sugunan and Prof. Dr. M. R. Prathapachandra Kurup were of immense help to me during the initial stages of my research. I express my gratitude to them.

The support and encouragement of Dr. N. Sridevi in the whole stages of research, was of immense help and I am extremely thankful to her for the same. I sincerely appreciate the help rendered by Dr. Rani Abraham during the preparation of my thesis.

The help and useful advice offered by the faculty members, Prof. Dr. K. Sreekumar, Dr. S. Prathapan, Dr. N. Manoj, Dr. P. V.Mohanan, Dr. P. A. Unnikrishnan, Ms. P. M. Sabura Begum and Dr. M. Ravindranathan of this department during the crucial stages of my work and at times when I was confronted with chaos and confusion had been of much value and I am grateful to all of them for their kind heartedness.

I recall with gratitude the selfless help and involvement of my lab mates P. P Robinson, Ms. Annu Anna Varghese, Manju Sebastian, Ms. P. Leeju, Ms. G. Varsha and Digna Varghese at different stages of my work. I am also thankful to all of my seniors who gave me support and reassurance in different ways.

My friends were the chief contributors to what all I had been able do as part of research and I am heavily indebted to all of my friends in the Department of Applied Chemistry, various other departments of CUSAT and other research institutions.

I am immensely grateful to Dr. A. Ajayaghosh, NIIST, Trivandrum; Prof. Dr. K. Krishankutty, University of Calicut; Prof. Dr. K. K. Aravindhakshan, University of Calicut; Prof. Dr. K. Natarajan, Bharathiar University, Coimbatore and Prof. Dr. P. R. Athappan, Madurai Kamaraj University, for the help offered by them for various analyses.

I am happy to acknowledge the services of SAIF at STIC, CUSAT; CDRI, Lucknow; IIT, Mumbai and SAIF, IISc, Bangalore for the help in sample analyses.

I express my heartfelt gratitude to my parents and brothers for their love, affection and encouragement.

Above all my praises are due to God, without the grace of whom the whole episode would have had reduced to nothing.

Arun

Preface

The thesis deals with studies on the synthesis, characterisation and catalytic applications of some new transition metal complexes of the Schiff bases derived from 3-hydroxyquinoxaline-2-carboxaldehyde. Schiff bases which are considered as 'privileged ligands' have the ability to stabilize different metals in different oxidation states and thus regulate the performance of metals in a large variety of catalytic transformations. The catalytic activity of the Schiff base complexes is highly dependant on the environment about the metal center and their conformational flexibility. Therefore it is to be expected that the introduction of bulky substituents near the coordination sites might lead to low symmetry complexes with enhanced catalytic properties. With this view new transition metal complexes of Schiff bases derived from 3-hydroxyquinoxaline-2-carboxaldehyde have been synthesised. These Schiff bases have more basic donor nitrogen atoms and the presence of the quinoxaline ring may be presumed to build a favourable topography and electronic environment in the immediate coordination sphere of the metal.

The aldehyde was condensed with amines 1,8-diaminonaphthalene, 2,3-diaminomaleonitrile, 1,2-diaminocyclohexane, 2-aminophenol and 4-aminoantipyrine to give the respective Schiff bases. The oxovanadium(IV), copper(II) and ruthenium(II) complexes of these Schiff bases were synthesised and characterised. All the oxovanadium(IV) complexes have binuclear structure with a square pyramidal geometry. Ruthenium and copper form mononuclear complexes with the Schiff base derived from 4-aminoantipyrine while binuclear square planar complexes are formed with the other Schiff bases.

The catalytic activity of the copper complexes was evaluated in the hydroxylation of phenol with hydrogen peroxide as oxidant. Catechol and hydroquinone are the major products. Catalytic properties of the oxovanadium(IV) complexes were evaluated in the oxidation of cyclohexene with hydrogen peroxide as the oxidant. Here allylic oxidation products rather than epoxides are formed as the major products. The ruthenium(II) complexes are found to be effective catalysts for the hydrogenation of benzene and toluene. The kinetics of hydrogenation was studied and a suitable mechanism has been proposed.

Contents

Page No

Chapter 7

Chapter 8

Chapter 1

Introduction

Contents

Schiff bases have been playing an important part in the development of coordination chemistry. Schiff base metal complexes have been studied extensively because of their attractive chemical and physical properties and their wide range of applications in numerous scientific areas. These types of complexes have been vigorously explored in recent years and such studies have been the subject of many papers and reviews. Many of them are centered on the catalytic activity of Schiff base complexes in a large number of homogeneous and heterogeneous reactions. It is difficult to cover in this chapter the literature on Schiff base metal complexes, which embraces very wide and diversified subjects comprising vast areas of organometallic compounds and various aspects of bioinorganic chemistry. Therefore, the introduction part is limited to a brief discussion on the Schiff bases, their metal complexes and general applications of Schiff base complexes with an emphasis on catalytic applications.

1. Schiff base ligands

Schiff base was first reported by Hugo Schiff in 1864 [1]. Schiff bases can be prepared by condensing carbonyl compounds and amines in different conditions and in different solvents with the elimination of water molecules. The presence of a dehydrating agent normally favours the formation of Schiff bases. Though the

Schiff bases are stable solids, care should be taken in the purification steps as it undergoes degradation. Chromatographic purification of Schiff bases on silica gel is not recommended as they undergo hydrolysis. The common structural feature of these compounds is the azomethine group with a general formula RHC=N-R', where R and R' are alkyl, aryl, cyclo alkyl or heterocyclic groups which may be variously substituted. Presence of a lone pair of electrons in an sp^2 hybridised orbital of nitrogen atom of the azomethine group is of considerable chemical importance and impart excellent chelating ability especially when used in combination with one or more donor atoms close to the azomethine group. Examples of a few compounds are given in Figure 1. This chelating ability of the Schiff bases combined with the ease of preparation and flexibility in varying the chemical environment about the C=N group makes it an interesting ligand in coordination chemistry.

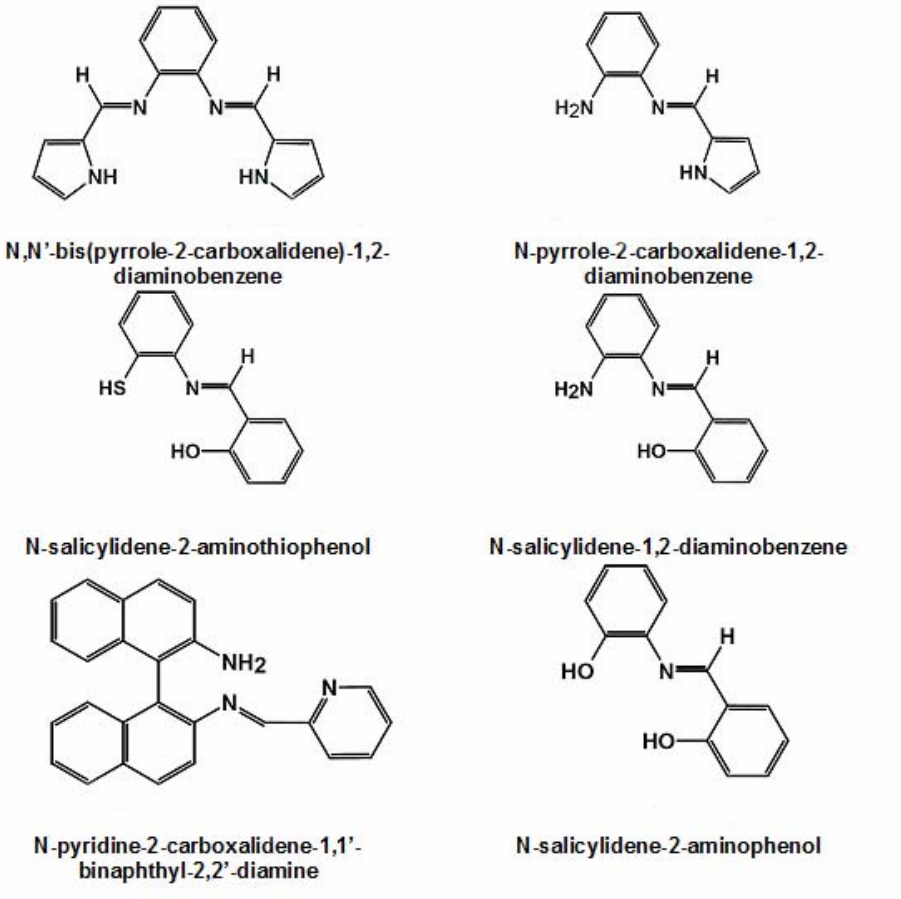

Figure 1: Some examples of Schiff bases

When aldehyde is a salicylaldehyde derivative and amine is a diamine derivative, the condensation produces interesting N_2O_2 Schiff base compounds (Figure 2). The so called salen ligands are very much like porphyrins and, unlike the latter, can be easily prepared. Although the term salen was originally used only to describe the tetradentate Schiff bases derived from salicylaldehyde and ethylenediamine, the term salen-type is now used in the literature to describe the class of (O, N, N, O) tetradentate bis-Schiff ligands. Stereogenic centers or other elements of chirality (planes, axes) can be introduced in the synthetic design of Schiff bases (Figure 2).

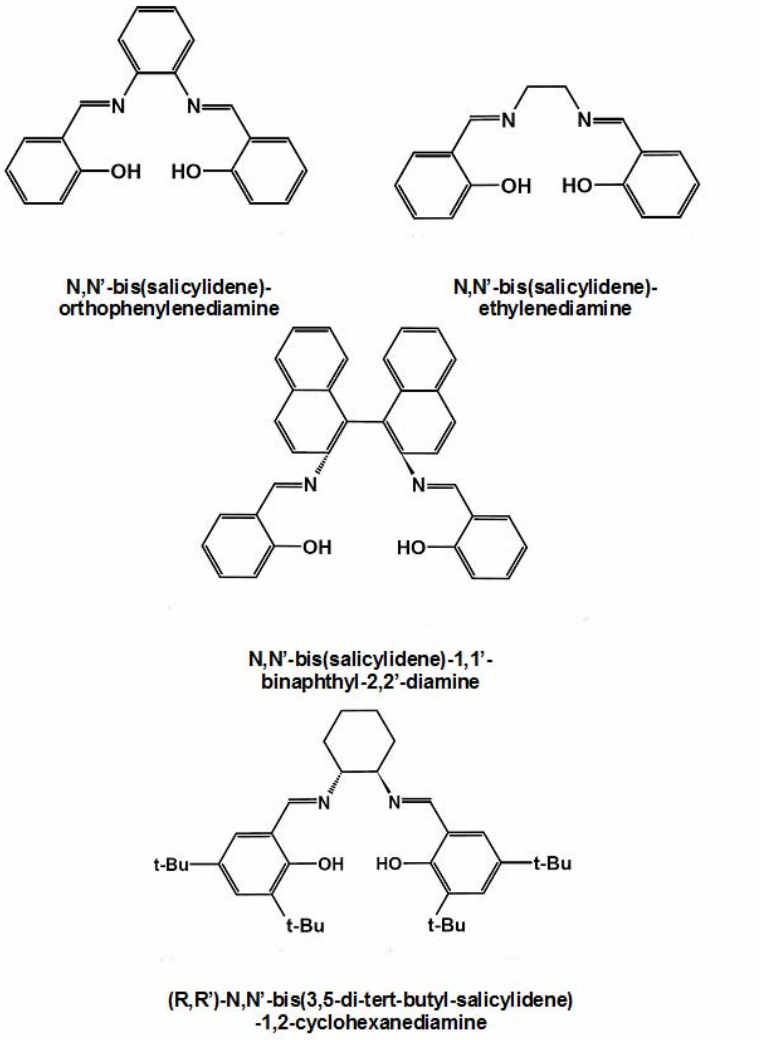

Figure 2: N_2O_2 Schiff base compounds

In addition to these, Schiff base macrocycles (Figure 3) have been prepared by well known self condensation reaction of appropriate formyl- or keto- and primary amine precursors and find wide applications in macrocyclic and supramolecular chemistry [2,3]. Schiff bases easily form stable complexes with most transition metal ions and stabilize them in various oxidation states.

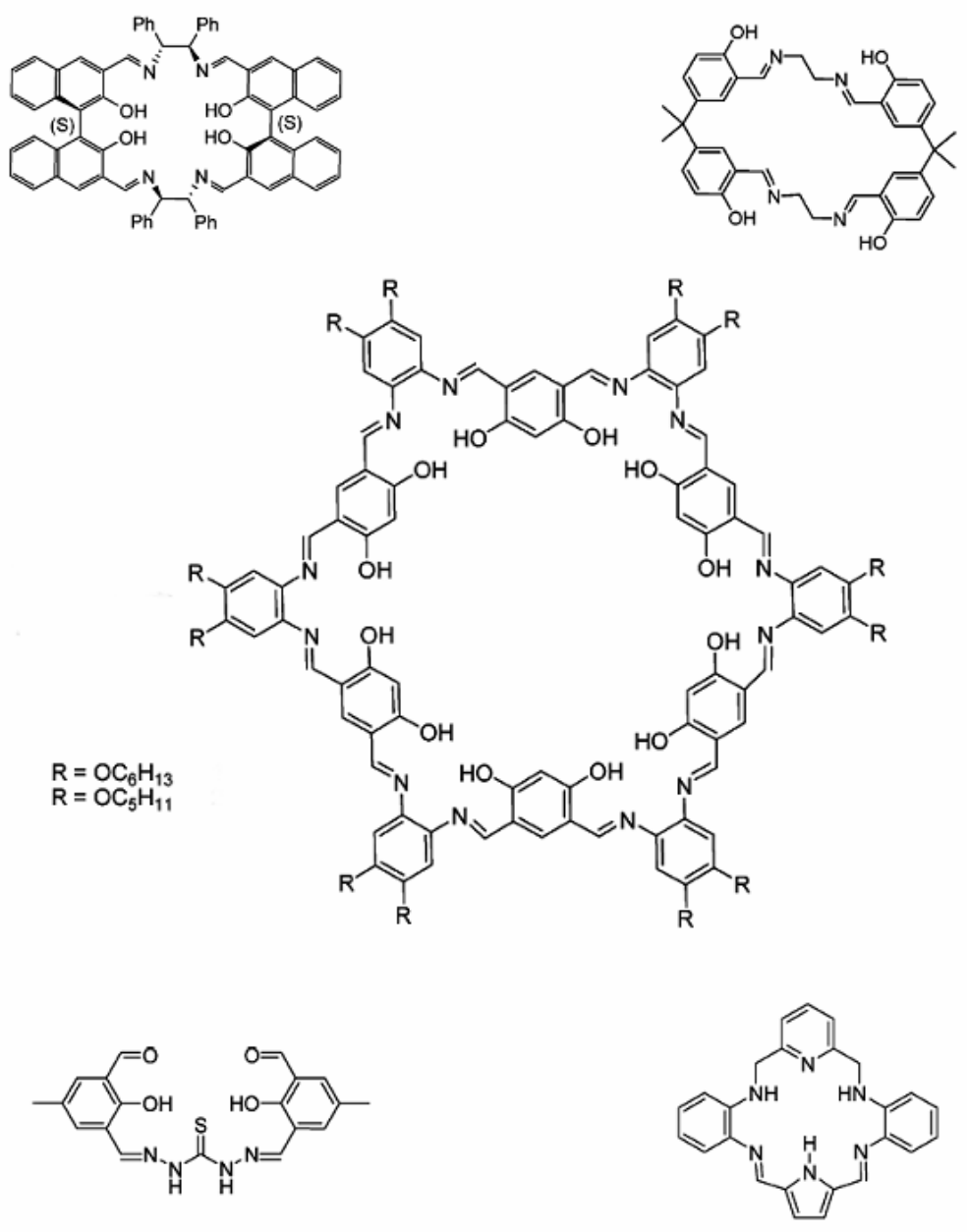

Figure 3: Macrocyclic Schiff base compounds

2. Schiff base transition metal complexes

Metal complexes of the Schiff bases are generally prepared by treating metal salts with Schiff base ligands under suitable experimental conditions. However, for some catalytic application the Schiff base metal complexes are prepared in situ in the reaction system. Cozzi in his review has outlined five synthetic routes that are commonly employed for the preparation of Schiff base metal complexes and these are depicted in Scheme 1 [4].

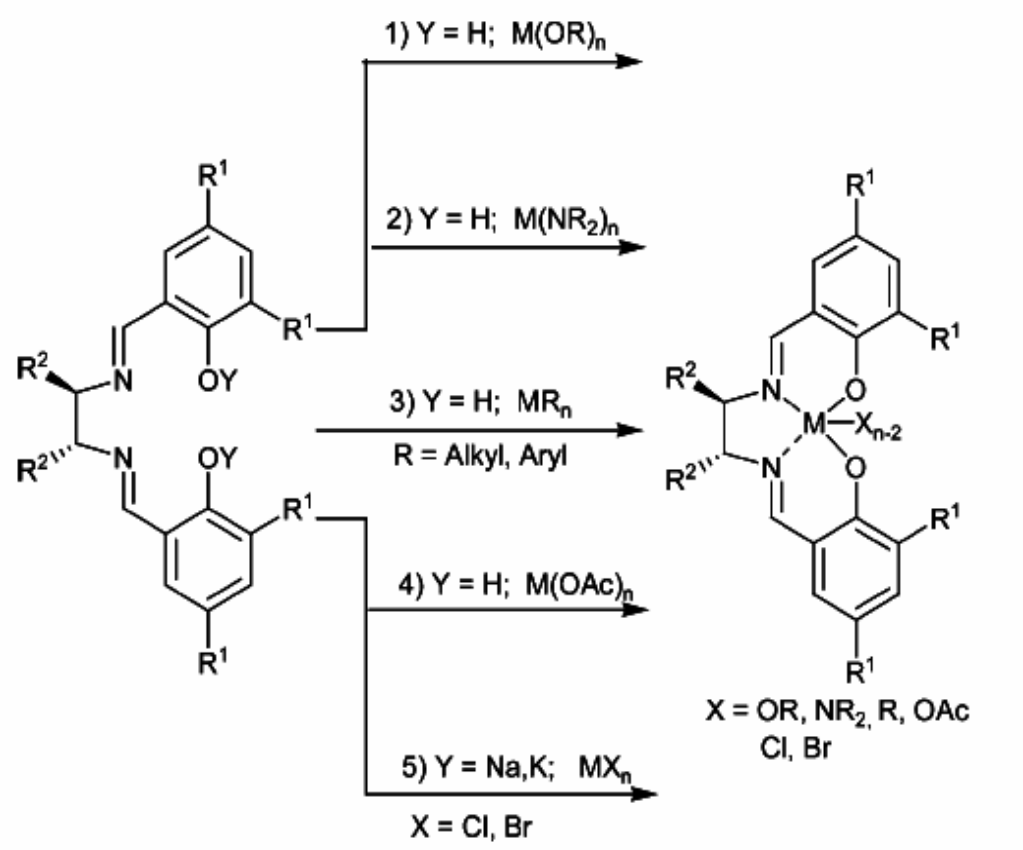

Scheme 1: Preparation of Schiff base complexes

Route 1 involves the use of metal alkoxides ($M(OR)_n$). Alkoxides of early transition metals (M = Ti, Zr), are commercially available and easy to handle. The use of other alkoxide derivatives is not easy, particularly in the case of highly moisture-sensitive derivatives of lanthanides. Metal amides $M(NMe_2)_4$ (M = Ti, Zr)

are also employed as the precursors in the preparation of Schiff base metal complexes (Route 2). The reaction occurs via the elimination of the acidic phenolic proton of the Schiff bases through the formation of volatile $NHMe_2$. Other synthetic routes include treatment of metal alkyl complexes with Schiff bases (Route 3) or treatment of the Schiff base with the corresponding metal acetate under reflux conditions (Route 4). The synthetic scheme presented in route 5 which is quite effective in obtaining salen-type metal complexes consists of a two-step reaction involving the deprotonation of the Schiff bases followed by reaction with metal halides. Deprotonation of the acidic phenolic hydrogen can be effectively done by using NaH or KH in coordinating solvents and the excess sodium or potassium hydride can be eliminated by filtration. The deprotonation step is normally rapid at room temperature, but heating the reaction mixture to reflux does not cause decomposition.

An elaborate discussion on synthesis and characterisation of Schiff base metal complexes is not attempted here, as there are numerous literature reviews on these aspects [2,5-7]. The synthesis of the well known Schiff base complex, N,N'-bis(3,5-di-tert-butylsalicylidene)-1,2-cyclohexanediaminomanganese (III)chloride, is presented in Scheme 2. This manganese complex is known as Jacobsen's catalyst. The Schiff base can be successfully prepared by the condensation between *trans*-1,2-diaminocyclohexane and 3,5-di-*tert*-butyl-2-hydroxybenzaldehyde and finally Jacobsen's catalyst can be prepared from the ligand by treatment with manganese(II) acetate followed by oxidation with air.

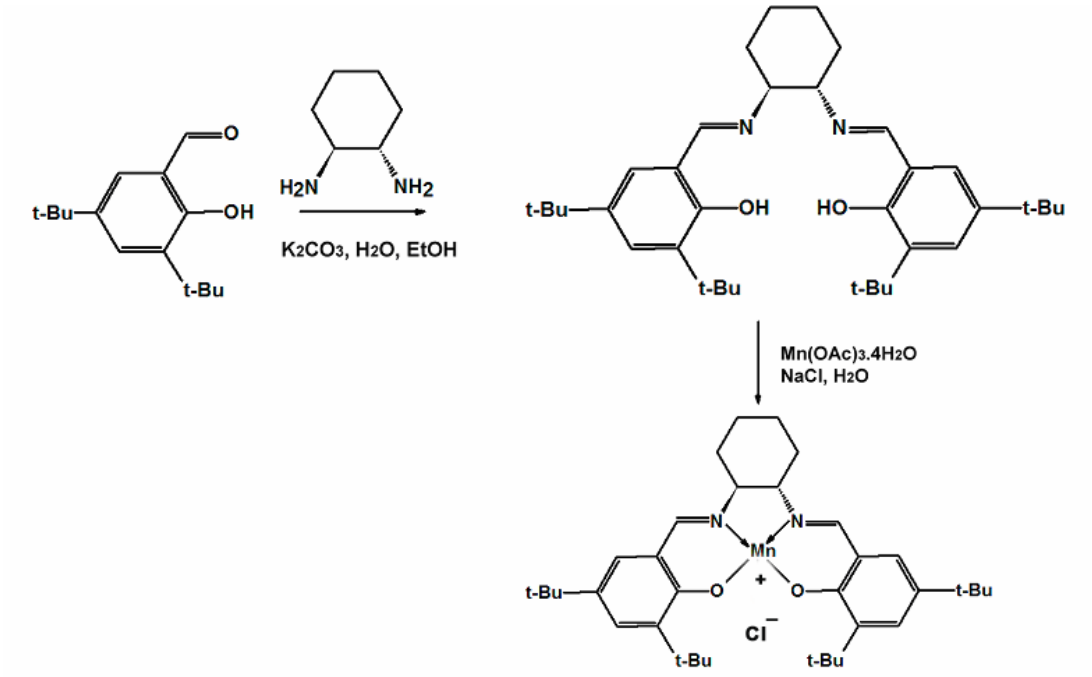

Scheme 2: Synthesis of Jacobsen's catalyst

3. Applications of Schiff base transition metal complexes

The major applications of the Schiff base complexes are in catalysis and will be discussed in detail in Section 4. The Schiff base complexes do have a number of other applications which are discussed briefly in this section.

3.1 As electroluminescent materials

Organic electroluminescent (EL) devices are useful in novel-type flat-panel displays since Tang and Van Styke first reported on high-performance organic EL devices [8]. Their discovery was based on employing a multilayer device structure containing an emitting layer and a carrier transport layer of suitable organic materials. Organic dyes, chelate metal complexes and polymers are three major categories of materials used in the fabrication of organic EL devices. Out of the three, chelate metal complexes having high-luminance blue emitting nature find use as materials for RGB (red, green, and blue) emission.

Schiff base complexes, especially those of Zn(II), are now a days used as electroluminescent materials [9,10]. Zinc complex of the Schiff base, N,N'-bis(2-hydroxy-1-naphthylidene)-3,6-dioxa-1,8-diaminooctane, emits blue light with an emission peak at 455 nm having maximum brightness of 650 cd m^{-2}, when it is used as the emitting layer in an electroluminescence device. Fabrication of EL devices employing this kind of zinc complexes as blue electroluminescent material was carried out by thermal vacuum-deposition. Wei et al. prepared blue luminescent zinc and beryllium complexes of the Schiff bases derived from calixarene [11]. These Schiff bases complexes have good solubility in normal solvents and can easily form thin films. Xie et al. reported the crystal structure, thermal stability and optoelectronical properties of bis[salicylidene(4-dimethylamino)aniline]zinc(II) [12]. This complex exhibits very good light emission and charge transporting performance in organic light emitting diodes (OLEDs). These experimental reports point to the possible application of Schiff base complexes as emitting materials in full colour flat-panel displays.

3.2 In non-linear optical devices

Nonlinear optics (NLO) deals with the interactions of applied electromagnetic fields with various materials to generate new electromagnetic fields, altered in frequency, phase, or other physical properties. Such materials that are able to manipulate photonic signals efficiently are of importance in optical communication, optical computing, and dynamic image processing [13-17]. In this connection transition metal complexes have emerged as potential building blocks for nonlinear optical materials due to the various excited states present in these systems as well as due to their ability to tailor metal-organic-ligand interactions [18-23]. Compared to the more common organic molecules, the metal complexes offer a large variety of novel structures, the possibility of enhanced thermal stability, and a diversity of tunable electronic behaviours by virtue of the coordinated metal center and hence they may find use as NLO materials with unique magnetic and electrochemical properties [24-26]. The investigations on NLO properties of metal

complexes are being pursued by several research groups [19,20,27-33]. It has been reported by Di Bella and co-workers that bis(salicylaldiminato) metal Schiff base complexes exhibit good second order NLO properties [34-40].

3.3 In electrochemical sensors

Schiff bases have been used as carriers in the preparation of potentiometric sensors for determining cations and anions [41-50]. A ruthenium(III) Schiff base complex was used in the fabrication of chloride PVC-based membrane sensor [51]. The sensor with a composition of 30% PVC, 62% benzyl acetate, 5% ruthenium(III) Schiff base complex and 3% hexadecyltrimethyl ammonium bromide displays near-Nernstian behavior over a wide concentration range. It shows high selectivity toward chloride ions over several organic and inorganic anions and was successfully applied for the determination of chloride in serum samples. It could also be used as an indicator electrode in the potentiometric titration of chloride ions with silver nitrate solution. Gupta et al. recently reported a potentiometric aluminium sensor based on the use N,N'-bis(salicylidene)-1,2-cyclohexanediamine as a neutral carrier in poly(vinyl chloride) matrix [52]. It was successfully applied for direct determination of aluminium(III) in biological, industrial and environmental samples. The electrode could be used in the pH range of 2.0–9.0 and mixtures containing up to 20% (v/v) non-aqueous content. It has been used as an indicator electrode in potentiometric titration of aluminium ion with EDTA. The Schiff base, N,N′,N″,N‴-1,5,8,12-tetraazadodecane-bis(salicylaldiminato), has been used as ionophore for preparing Mn^{2+} selective sensor [53]. The sensor was found to be sufficiently selective for Mn^{2+} over a number of alkali, alkaline and heavy metal ions and could therefore be used for the determination of manganese in various samples by direct potentiometry.

3.4 In medicinal chemistry

Many Schiff bases are known to be medicinally important and used to design medicinal compounds [54-57]. It was seen that the biological activity of Schiff bases either increase or decrease upon chelation with metal ions [58-60].

Cobalt(II), nickel(II) and copper(II) complexes of Schiff bases derived from 3-substituted-4-amino-5-mercapto-1,2,4-triazole and 8-formyl-7-hydroxy-4-methylcoumarin show potent antibacterial activity against *Escherichia coli*, *Staphylococcus aureus*, *Streptococcus pyogenes*, *Pseudomonas aeruginosa* and *Salmonella typhi* and antifungal activities against *Aspergillus niger*, *Aspergillus flavus* and *Cladosporium* [61].

Ru(II)–PPh_3/$AsPh_3$ complexes, containing hydrazone oxime ligands, show considerable activity against selected bacterial species and are capable of binding to Herring sperm DNA in mixed modes [62]. The Cr(III), Fe(III) and Co(III) complexes formed form tetradentate (ONNO) Schiff base ligands, 1,4-bis[3-(2-hydroxy-1-naphthaldimine)propyl]piperazine and 1,8-bis[3-(2-hydroxy-1-naphthaldimine)-*p*-menthane, show moderate antimicrobial activity [63] compared to standard antibiotics [64]. The antibacterial activity of the tridentate Schiff base, formed by condensation of 2-amino-3-carboxyethyl-4,5-dimethylthiophene with salicylaldehyde, was found to increase on chelation with transition metal ions [65]. Co(II), Ni(II), Cu(II) and Zn(II) complexes of the Schiff base derived from vanillin and DL-α-aminobutyric acid were also found to exhibit higher antibacterial activity compared to the free Schiff bases [66]. Several mono and binuclear transition metal complexes of the Schiff base derived from phenylaminoacetohydrazide and dibenzoylmethane, are more potent bactericides and fungicides than the ligand [67]. Sharma and Piwnica-Worms reported Schiff base complexes that target hemozoin aggregation like the antimalarial drug, chloroquine [68-70].

Investigations on the interactions of DNA with transition metal complexes provide leads for rational drug design, as well as means for the development of

sensitive chemical probes for DNA [71-83]. These interactions would be either covalent or non-covalent. In covalent binding the labile part of the complexes is replaced by a nitrogen base of DNA. On the other hand, the non-covalent DNA interactions include intercalative, electrostatic and groove binding of cationic metal complexes along periphery of the DNA helix, the major or minor groove. Intercalation involves the partial insertion of aromatic heterocyclic rings between the DNA base pairs.

Gupta and co-workers reported DNA binding properties of a series of transition metal complexes having potential NNO-tridentate donor Schiff bases derived from the condensation of 2,6-dibenzoyl 4-methylphenol with diamines [84-90]. DNA binding studies of the cationic Ni^{II} complex of the 5-triethyl ammonium methyl salicylideneortho-phenylendiimine ligand, shows that the metal complex strongly interacts with DNA [91]. Zn(II) and Cu(II) complexes of this Schiff base interact with native calf thymus DNA by groove or intercalating binding mode [92]. The cobalt(II) and nickel(II) complexes of salicylaldehyde-2-phenylquinoline-4-carboylhydrazone interact with calf-thymus DNA via a groove binding mode [93]

The interaction of chromium(III) Schiff base complexes, $[Cr(salen)(H_2O)_2]^+$ where salen = N,N'-ethylenebis(salicylideneimine) and $[Cr(salprn)(H_2O)_2]^+$ where salprn = N,N'-propylenebis(salicylideneimine) with calf thymus DNA (CT-DNA), has been reported [94]. Chromium(III) complexes derived from chiral binaphthyl Schiff base ligands (R- and S-2,2'-bis(salicylideneamino)1,10-binaphthyl) are also found to interact with CT-DNA through groove binding [95]. Binuclear copper(II) complexes having the Schiff base ligand, N,N'-bis(3,5-tert-butylsalicylidene-2-hydroxy)-1,3-propanediamine, are found to be effective in the cleavage of plasmid DNA without the addition of any external agents and in the presence of hydrogen peroxide at pH = 7.2 and 37 °C. DNA cleavage mechanism studies show that complexes examined here may be capable of promoting DNA cleavage through an oxidative DNA damage pathway [96].

Silvestri et al. showed that the interaction between native calf thymus deoxyribonucleic acid (DNA) and Fe^{III}-N,N'-ethylene-bis (salicylideneiminato)-chloride, Fe(Salen)Cl, take place through an electrostatic binding between the $Fe(Salen)^{+}$ cation and the phosphate groups of DNA [97]. The Mn(II) complex, MnL (L = sodium (E)-3-(1-carboxyethylimino)methyl)-4-hydroxybenzenesulfonate), is capable of intercalating into the double-stranded salmon sperm DNA [98]. Chaviara et al. reported a series of Cu(II) complexes of the Schiff bases derived by the condensation of diethylenetriamine with 2-thiophene-carboxaldehyde/2-furaldehyde/2-pyrrole-2-carboxaldehyde [81]. The DNA electrophoretic mobility studies show that these compounds interact with DNA either by a simple mode of coordination, leading to the formation of a DNA complex cationic adduct or by acting as chemical nucleases able to promote its degradation.

4. Schiff base transition metal complexes in catalysis

Schiff base complexes play a central role in various homogeneous catalytic reactions and the activity of these complexes varies with the type of ligands, coordination sites and metal ions. Literature reports reveal that a large number of Schiff base metal complexes exhibit catalytic activities. Chiral Schiff base complexes are more selective in various reactions such as oxidation, hydroxylation, aldol condensation and epoxidation. A discussion on the catalytic activity of Schiff base metal complexes in various reactions are outlined in this section.

4.1 Oxidation reactions

Uchida and Katsuki reported the activity of cationic cobalt(III)salen complexes in Baeyer–Villiger oxidation of 3-phenyl cyclobutanone with H_2O_2 or urea hydrogen peroxide adduct [99]. The analoguos [Zr(salen)] catalysts are also active in Baeyer–Villiger oxidation of cyclobutanone derivatives to produce lactones in 75–99% yields and 69–78% ee in the presence of H_2O_2 as an oxidant [100]. Reddy and Thornon reported that complexes **1** and **2** catalyse the oxidation of a range of ketone silyl enol ethers to give α-hydroxyketones using iodosylbenzene as

oxidant in acetonitrile at room temperature [101]. Later, Waldemar et al. showed that **1** also catalyses the asymmetric oxidation of silyl ketene acetals in high enantioselectivity [102].

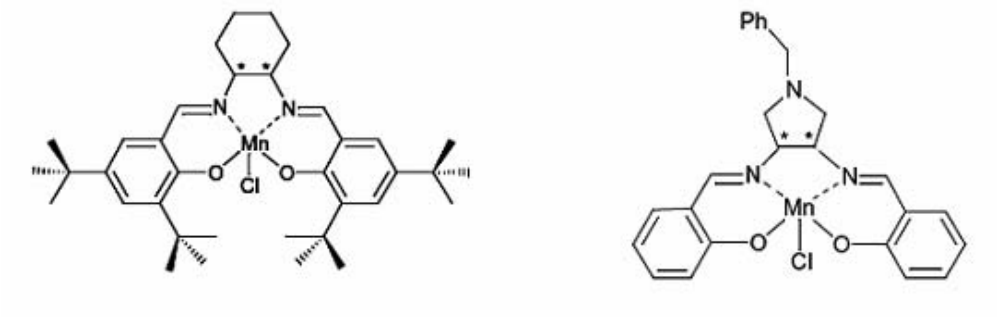

1 **2**

In 1986 Nakajima et al. studied the application of chiral Schiff base complexes in enantioselective sulfide oxidations [103]. Using tetradentate Schiff base-oxovanadium(IV) complex, **3**, as catalyst, they could achieve an enantioselectivity of 42% ee in the oxidation of methylphenyl sulfide to the corresponding sulfoxide. The oxovanadium(V) complex, **4**, having an amino acid-derived tridentate –O-N-O-type Schiff base as ligand was reported to catalyse the asymmetric oxidation of sulphoxide [104]. The catalytic behaviour of the complexes formed in-situ from Schiff base derivatives of salicylaldehyde and aminophenol, **5**, and vanadyl acetylacetonate is remarkable for the oxidation of sulphides [105]. Vetter and Berkessel reported the enantioselectivities associated with the sulfoxidations of vanadium catalysts derived from Schiff-base ligands **6-8** [106]. Katsuki and coworkers extended this study using **9** as ligand and vanadium as the metal [107].

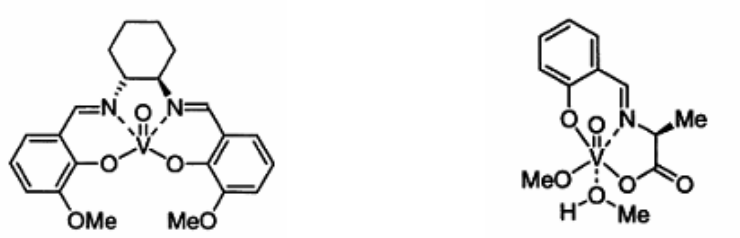

3 **4**

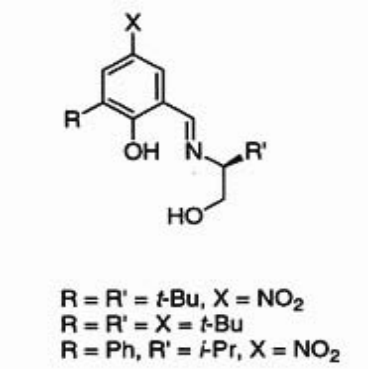

5

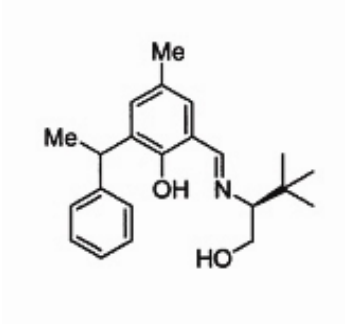

6

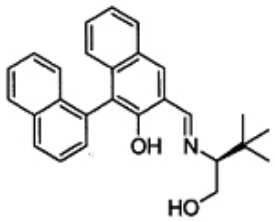

7

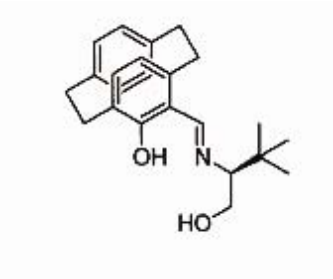

8

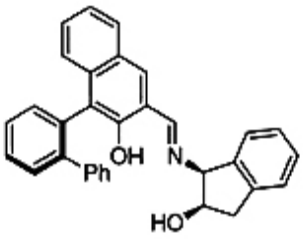

9

Titanium(IV), vanadium(IV), copper(II) or zinc(II) complexes of chiral Schiff base ligands of –O-N-O- type were used in various asymmetric chemical transformations. The addition of trimethylsilylcyanide (TMSCN) to benzaldehyde in the presence of titanium(IV) ions resulted in trimethylsilyl cyanohydrins **10** in 40–85% enantioselectivity (Scheme 3) [108,109].

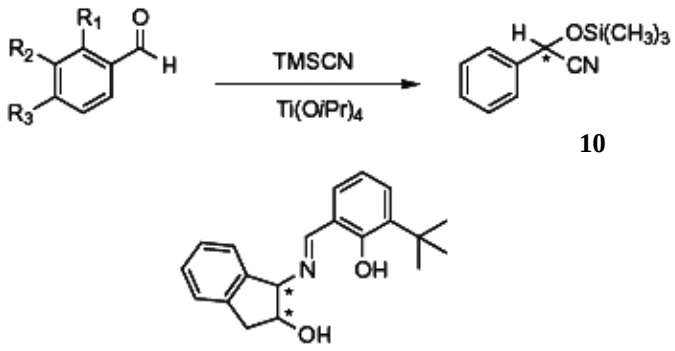

10

Scheme 3: Schiff base catalysed synthesis of trimethylsilyl cyanohydrins

The binuclear palladium Schiff base complex, **11**, was found to be effective catalysts in direct oxygenation of unfunctionalized hydrocarbons and phenols [110-114]. Dinuclear Schiff base complexes of copper(II) ions **12** were used successfully in hydroxylation of phenol [115].

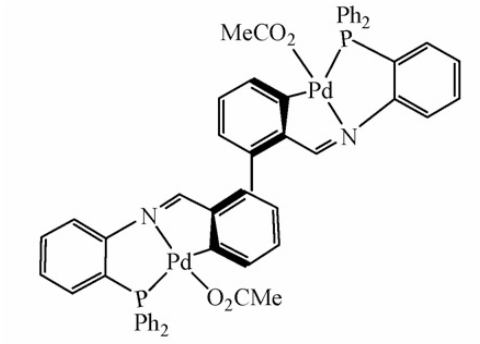

11

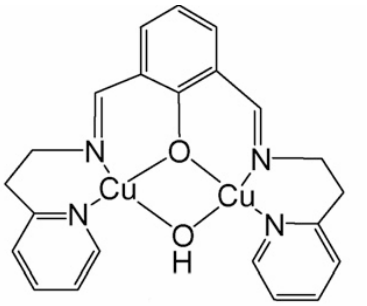

12

Co(salen) and its analogues, **13-17**, have been used for catalysing the oxidation of phenols and alcohols with dioxygen as oxidant [116]. Reports on oxidation of alkenes also exist [117,118]. In order to efficiently bind dioxygen and to be catalytically active, Co(salen) needs an axial ligand (Figure 4). The dioxygen is coordinated orthogonally to the square planar coordination sphere of Co(salen). The axial ligand is needed to fill the sixth coordination site, opposite to dioxygen. Pyridine is the most common axial ligand used in the Co(salen) catalysed oxidation reactions [116]. Other bases, for example, imidazole and pyrimidine have also been used [119]. An alternative way to provide an axial ligand is to use modified salen structure, which has extra nitrogen, for intramolecular axial coordination in the ligand frame (Figure 4).

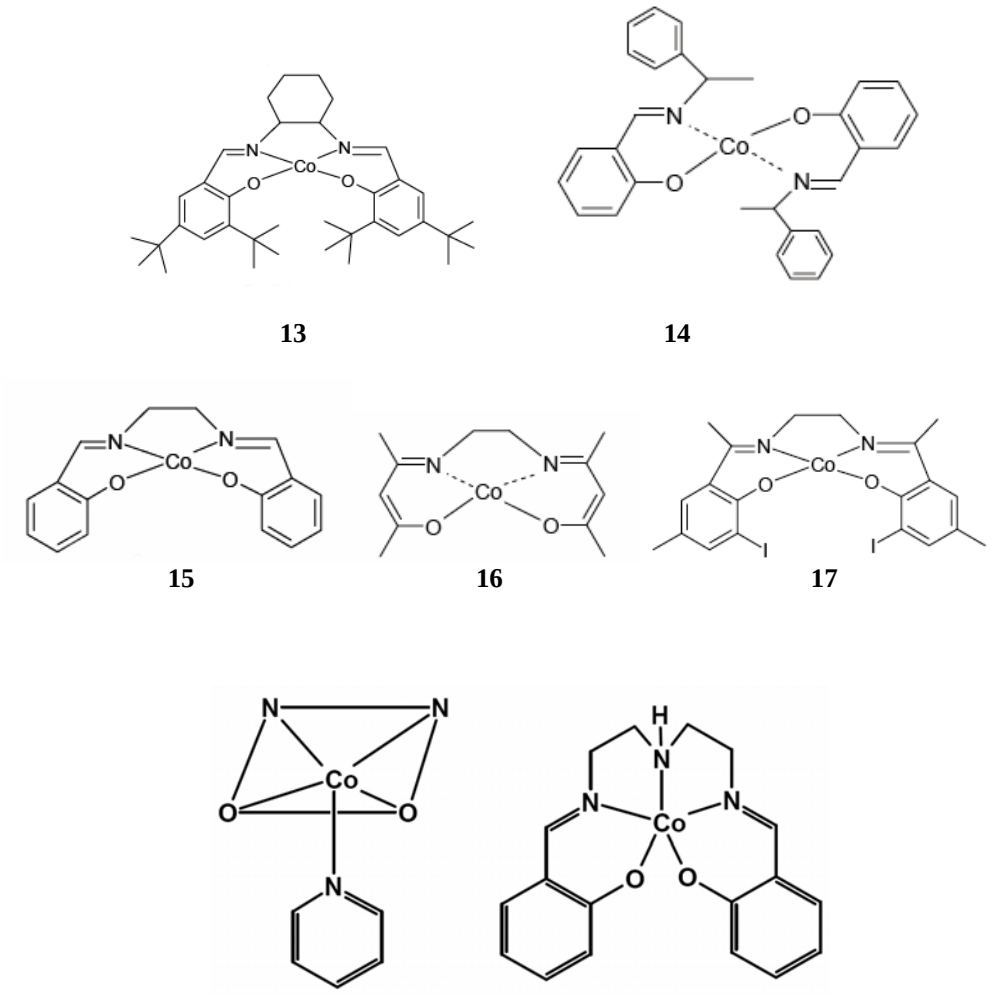

Figure 4: Axial ligand in cobalt Schiff base complexes

Reports on the studies with ruthenium complexes containing salen-type Schiff base ligands in the catalysis of hydrocarbon oxidation are noticeably few in literature [120].

4.2 Epoxidation reactions

McGarrigle and Gilheany have given a detailed discussion on the achiral and asymmetric epoxidations of alkenes catalysed by chromium and manganese-salen complexes [121]. They mainly focussed on the mechanism, catalytic cycle, intermediates, and mode of selectivity. Among these Mn-(salen)-type complexes,

Jacobsen's complex, **1**, has been demonstrated to be very effective for the enantioselective epoxidation of unfunctionalised olefins [122,123]. However, the second-generation Mn-(salen) catalysts introduced by Katsuki and co-workers, **18**, have surpassed Jacobsen's catalyst in terms of selectivity and activity, but they are not as synthetically accessible, and this has limited their application [124-126].

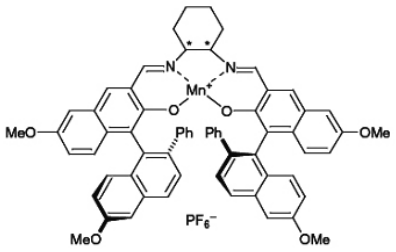

18

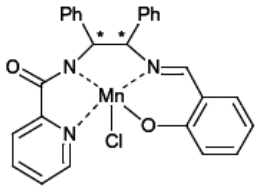

19

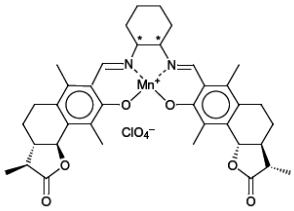

20

The manganese Schiff base chelate, **19**, synthesised by Zhao et al. exhibit moderate asymmetric induction (31–74% ee) in the epoxidation of dihydronaphthalene with higher turnover number [127]. Fernandez et al. epoxidised various unfunctionalised olefins with very high yield and poor asymmetric induction in presence of the manganese Schiff base complex, **20** [128].

Ruthenium complexes of trans-$[RuCl_2(bpydip)]$ and trans-$[Ru(OH)_2(bpydip)](PF_6)_2$ with tetradentate Schiff base ligand N,N'-bis(7-methyl-2-pyridylmethylene)-1,3-diiminopropane (bpydip) were used as remarkable catalysts in the epoxidation of cyclohexene in the presence of iodosobenzene [129]. Kureshy et al. have reported the catalytic activity of the nickel(II) Schiff base complexes of N,N'-bis(2-hydroxyphenyl)ethylenediimine, **21**, and N,N'-(2-hydroxyphenyl)acetylaldimine N-(2-hydroxyphenyl)acetamide, **22**, in the epoxidation of olefins such as cyclohexene, 1-hexene, *cis*- and *trans* stilbenes, indene with sodium hypochloride [130].

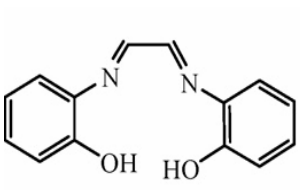

21

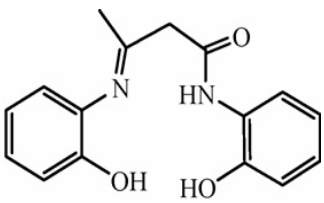

22

Potentially tetradentate binaphthyl N_2O_2 Schiff bases, **23**, were prepared by the condensations of aromatic aldehydes with amines like 2,2′-diamino-1,1′-binaphthyl or 2-amino-2′-hydroxy-1,1′-binaphthyl. Metal complexes of these Schiff bases have wide application in catalysis especially in asymmetric epoxidation of unfunctionalised olefins [131].

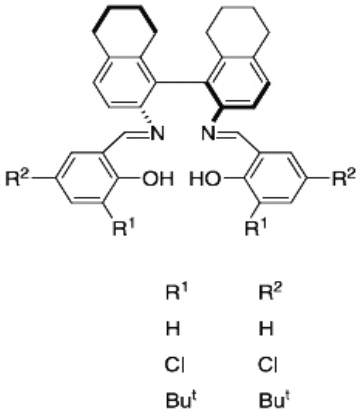

23

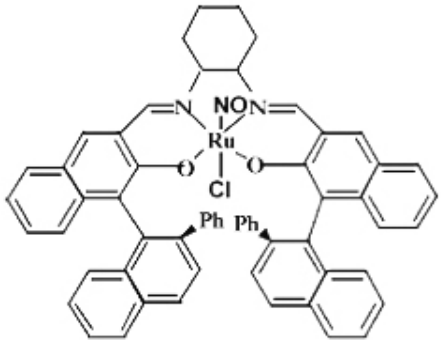

24

Katsuki and co-workers first reported the synthesis and catalytic application of ruthenium(II)-complex, **24**, containing chiral tetradentate (N_2O_2) Schiff base ligand in the asymmetric epoxidation of conjugated olefins in the presence of various terminal oxidants [132,133].

Mezzetti and co-workers have carried out the asymmetric epoxidation using ruthenium(II) complexes containing tetradentate chiral Schiff base ligands with N_2P_2 donors, **25–27**, with hydrogen peroxide as terminal oxidant [134,135].

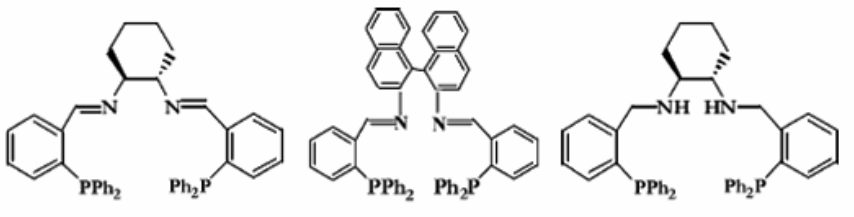

25 **26** **27**

Ruthenium(III) complexes, **28-30**, of the tetradentate Schiff base ligands obtained by the condensation of 3-acetyl-6-methylpyran-2,4-dione with various diamines, exhibit catalytic activity in the asymmetric epoxidation of styrene and substituted styrenes [136].

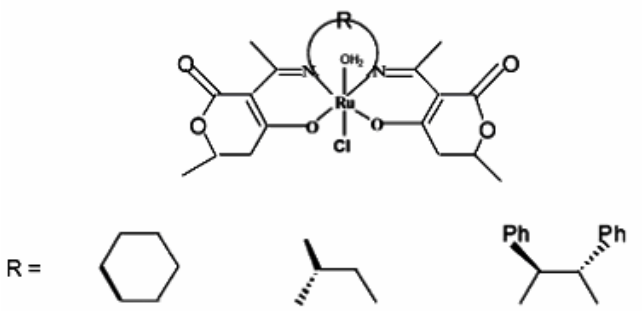

28 **29** **30**

4.3 Polymerization reactions

Reports on varios polymerisation reactions catalyzed by Schiff base metal complexes are found in the literature. Verpoort et al. reported a detailed discussion on catalytic activity in the atom transfer radical polymerization and ring opening metathesis polymerization of various substrates using Ru-catalysts having salicylaldiminato-type Schiff bases as one of the ligands, **31-36** [137].

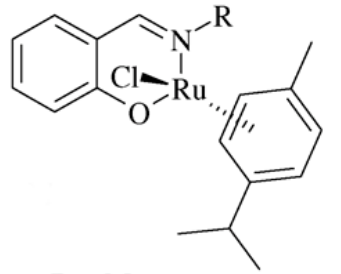

R = Me
R = *t*-Bu
R = 2,6-Me_2-4-BrC_6H_2

31

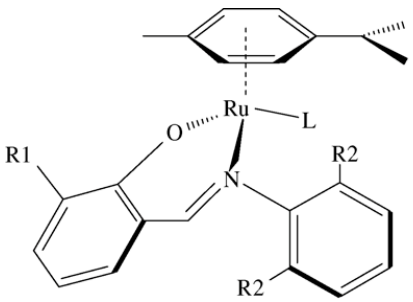

L = Cl, R_1 = *t*-Bu, R_2 = *i*-Pr.
L = C_6F_5, R_1 = *t*-Bu, R_2 = *i*-Pr.

32

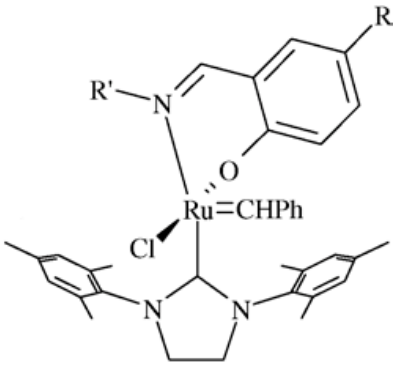

R = H, R' = Me
R = NO_2, R' = Me
R = H, R' = 2,6-Me_2-4-BrC_6H_2
R = NO_2, R' = 2,6-Me_2-4-BrC_6H_2
R = H, R' = 2,6-*i*-$Pr_2C_6H_3$
R = NO_2, R' = 2,6-*i*-$Pr_2C_6H_3$

33

R = H, R' = Me
R = NO_2, R' = Me
R = H, R' = 2,6-Me_2-4-BrC_6H_2
R = NO_2, R' = 2,6-Me_2-4-BrC_6H_2
R = H, R' = 2,6- *i*-$Pr_2C_6H_3$
R = NO_2, R' = 2,6- *i*-$Pr_2C_6H_3$

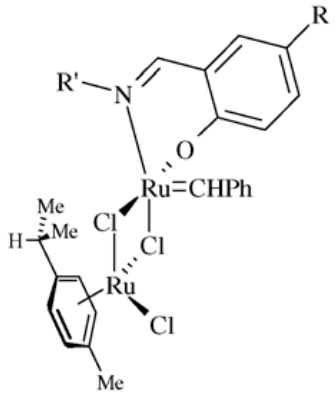

34

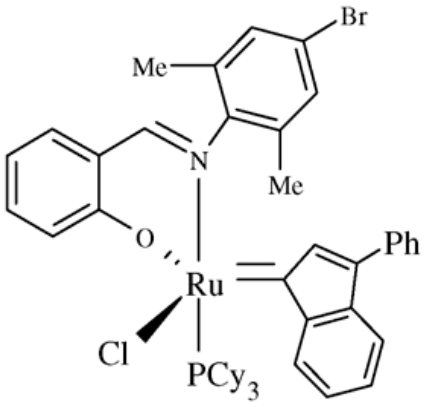

35

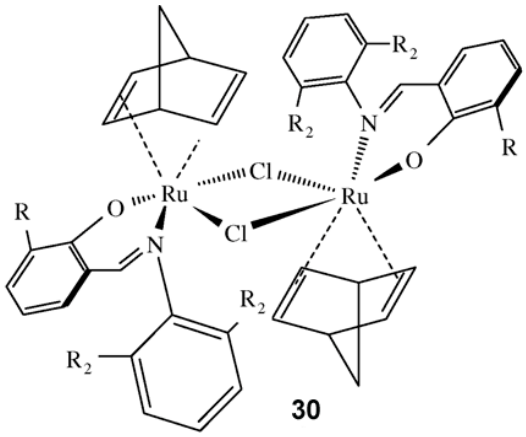

30

diolefine = norborane diene
R_1 = t-Bu, R_2 = i-Pr

36

Aluminum complexes of a series of tridentate Schiff base ligands, **37-40**, were found to catalyse the polymerization of ethylene [138].

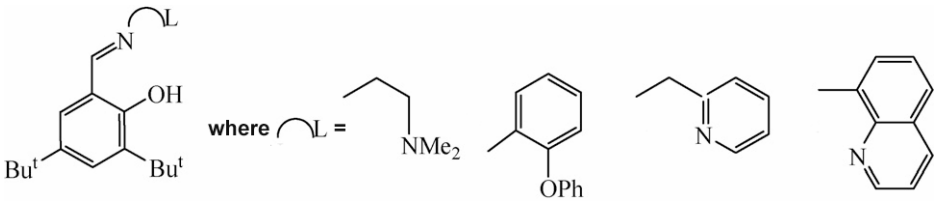

37 **38** **39** **40**

A number of pyridyl bis(imide) complexes and phenoxy imine complexes are used as catalysts in the polymerization of ethylene [139-142]. Pyridine bis(imine) complexes of iron(III) and cobalt(II) show significant activity in the polymerization of ethylene and copolymerization of ethylene with 1-hexene [143]. The salicylaldiminato complexes of zirconium were found to be effective catalysts in ethylene polymerization and promoted radical decomposition in certain cases [144]. Polymethylmethacrylate was prepared in presence of Cr(III) and Ni(II)salen complexes as catalysts for the controlled radical polymerization of the methylmethacrylate monomer [145].

4.4 Hydrogenation reactions

Schiff base complexes of transition metals are efficient catalysts in carrying out asymmetric reduction of dialkyl ketones [146-149]. The catalytic activity in the transfer hydrogenation of aliphatic and aromatic ketones in the presence of isopropanol and KOH has been investigated with ruthenium(III) Schiff base complexes of general formula [RuX(EPh_3)(LL')] where X = Cl or Br, E = P or As and LL' = [ONNO] donor of the heterocyclic Schiff base ligands, **41-43** [150]. Venkatachalam and Ramesh also reported the transfer hydrogenation of imines to amines mediated by ruthenium(III) bis-bidentate Schiff base complexes [151].

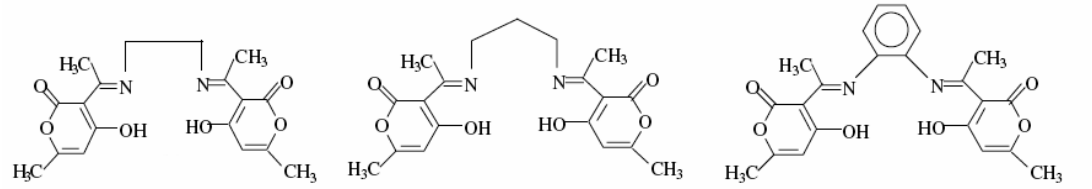

41 **42** **43**

A series of palladium(II) complexes of Schiff bases with the nitrogen ligands have been synthesised and their catalytic activity in the hydrogenation of alkenes and alkynes in mild conditions (with 1 atm dihydrogen pressure at 40 °C) has been studied by Costa et al. [152]. Two representative examples of these Schiff base complexes are given below (**44,45**).

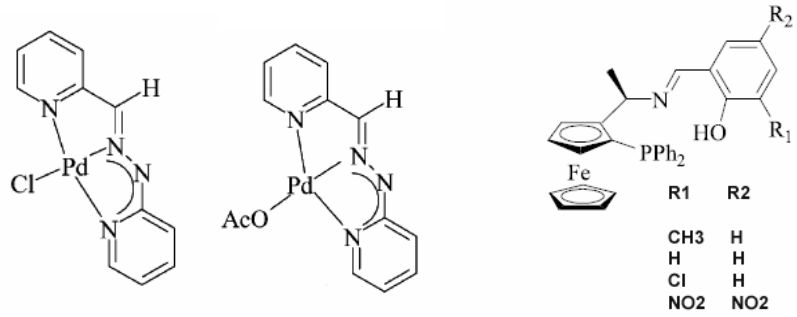

44 **45** **46**

Mono and dinuclear Pd(II) complexes of Schiff bases having sterically constrained tert butyl groups on the salicyl ring exhibit very good catalytic activity towards hydrogenation of nitrobenzene and cyclohexene [153,154].

In situ generated ruthenium complexes of the chiral P,N,O Schiff bases, **46**, derived from substituted salicylaldehyde and (R)-1-[(S)-2-(diphenylphosphino) ferrocenyl] ethylamine and $Ru(DMSO)_4Cl_2$ were found to be effective catalysts for the asymmetric transfer hydrogenation of methyl aryl ketones with 2-propanol as the hydrogen donor [155]. A series of chiral N_4-Schiff bases, containing amine or sulfonamide functionalities has been synthesized by Karame at al. [156]. Coupled with ruthenium catalysts, these Schiff bases induce interesting results in the hydrogenation of acetophenone. The asymmetric hydrogenation reaction was

carried out under hydrogen pressure (30 bar) at room temperature in the presence of the chiral catalyst prepared in situ.

4.5 Miscellaneous reactions

In addition to the above mentioned three major types of catalytic reactions, some other reactions are also catalysed by the Schiff base complexes. Chiral Schiff base lanthanum(III) complexes displayed catalytic activity in the asymmetric Diels–Alder reaction of 3-(2-propenoyl)-2-oxazolidinone with cyclopentadiene [157]. Schiff base complex catalyzed acylation of 4-furyl-4- *N*-benzylaminobut-1-enes with maleic anhydride produced 4-oxo-3 aza-10-oxatricyclo[5.2.1.0]dec-8-ene-6-carboxylic acid via amide formation through intramolecular Diels–Alder reaction of furan [158,159]. The new family of enantiomerically enriched Schiff base chromium(III) complexes, **47,** were also used as catalysts in Diels–Alder reactions [159].

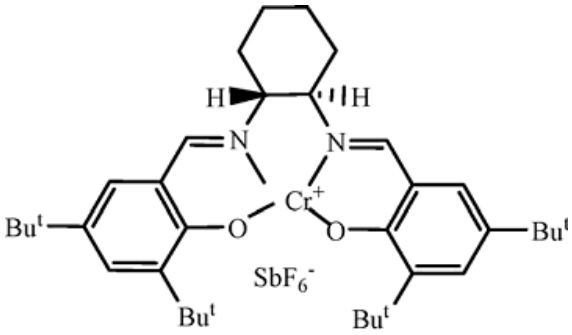

47

Jacobsen et al. have has also achieved the asymmetric hetero-Diels–Alder reaction between [(2-chlorobenzoyl)oxy]-acetaldehyde and 1-methoxy-3-[(trimethylsilyl)oxy]buta-1,3-diene in the presence of 2 mol% Cr(salen) using a noncoordinating ethereal solvent at 230 °C in the presence of dried 4 Å molecular sieve [160]. Aluminum(III) chiral complexes of binaphthal Schiff base ligand are used as catalysts in the aldol addition/acyl transfer reactions between 5-methoxyoxazoles and aldehydes [161], which afforded corresponding (4S, 5S)-

oxazoline products with 98% ee and 60% turnover number. Schiff base complexes of aluminum(III) were active in the reaction between 5-methoxyoxazoles and benzaldehydes to produce optically active *cis*-oxazoline adducts with >99% ee [161].

The ring-opening of cyclohexa-1,4-diene monoepoxide was carried out by Jacobsen's group [162] under solvent free conditions in presence of 7.5 mol% of **48** and azidotrimethylsilanolate to produce the azido silyl ether in 92% enantiomeric excess (Scheme 4).

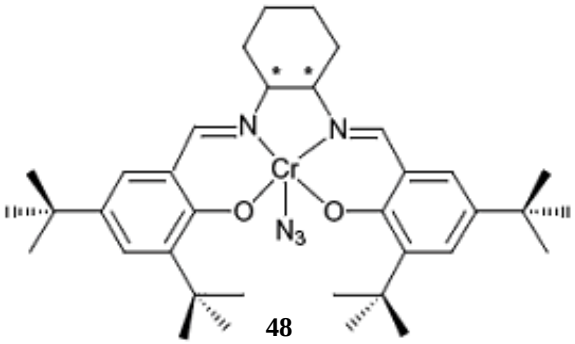

48

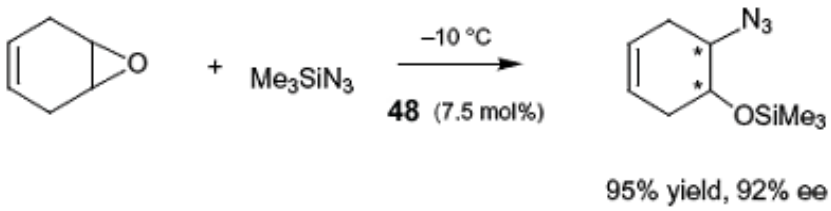

95% yield, 92% ee

Scheme 4

Jacobsen also discovered [163] that the Co(salen) complex **49** was active in the hydrolytic kinetic resolution of racemic epoxides which enables access to terminal epoxides and diols in high enantiomeric purity (Scheme 5).

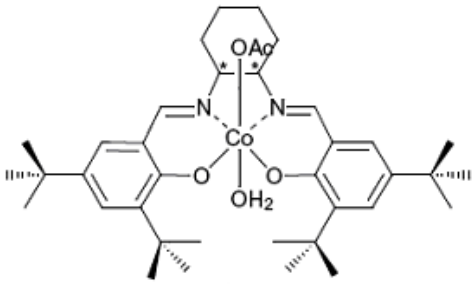

49

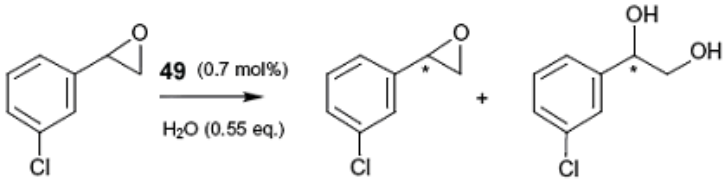

Scheme 5

The synthesis of Ru(salen) without the nitrosyl group was difficult to realize, until Nguyen et al. reported that ruthenium(II) salen complexes are very efficient catalysts for cyclopropanation of olefins [164]. The synthesis of Ru(salen) was realized using a nitrosyl as precursor [165]. N_2P_2–Ru(II) complexes **50** were activated by silver triflate to catalyze the asymmetric cyclopropanation of styrene with ethyl diazoacetate but observed enantioselectivity was low [166].

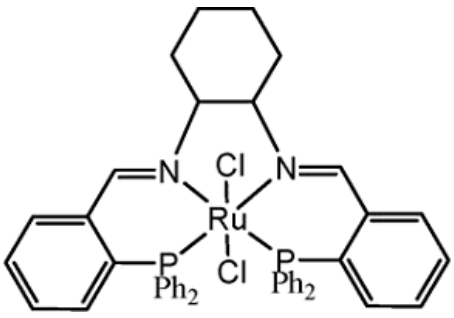

50

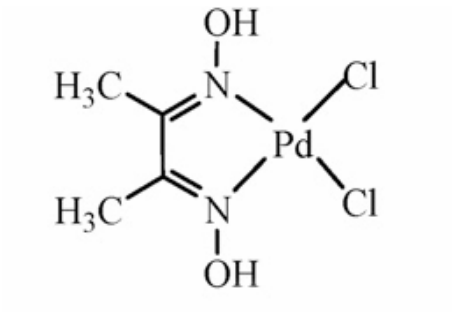

51

Palladium(II) complexes of nitrogen Schiff base ligands showed higher catalytic activity in Heck reaction than that of commercially used phosphene Schiff base complexes [167]. High yields of the E-cinnamates and E-stilbenes obtained by

the Mizoroki–Heck reaction with Pd(II) complexes of dimethyl glyoxime, **51**, 8-hydroxyquinoline, salen and picolinic acid ligands.

In addition to the homogeneous catalytic reaction, supported transition metal Schiff base complexes also find wide application in catalysis [168-176]. Among these polymer supported [177-189] and zeolite encapsulated Schiff base complexes are the most widely used in heterogeneous catalysis [190-195].

Most of the afore mentioned Schiff base complexes are derivatives of salicylaldehyde. It is clear from the above discussion that they have wide applications in various fields especially in that of catalysis. There are many reports to prove that the catalytic properties of the Schiff base complexes can be altered by changes in the Schiff base portion [196-198]. In the present investigation, we have employed an electron rich and bulky 3-hydroxyquinoxaline-2-carboxaldehyde for the preparation of Schiff bases to know whether their complexes have structures and catalytic activities different from that of the salen complexes. Metal complexes of the Schiff bases derived from quinoxaline-2-carboxaldehyde and 3-hydroxyquionxaline-2-carboxaldehyde are rare [199-203]. However there are many reports on the synthesis, biological and other applications of the compounds having quinoxaline rings. So a brief discussion on these types of compounds is included here.

5. Chemistry of quinoxaline compounds

The chemistry of quinoxaline (which are known as “benzopyrazine”) and its derivatives attracts continuous attention because of their wide applicability in various areas. A discussion on the synthesis of quinoxalines and their metal complexes and their optoelectronic and biological applications are included in this section.

5.1 Synthesis of quinoxalines

A number of synthetic strategies have been developed for the synthesis of substituted quinoxalines and the most common method relies on the condensation of an aryl 1,2-diamine with 1,2 dicarbonyl compound in refluxing ethanol or acetic acid [204-209]. Thirumurugan et al. reported a simple and convenient method for the synthesis of quinoxaline derivatives from cinnamils in water under reflux/microwave irradiation conditions (Scheme 6) and these quinoxaline derivatives show good photophysical properties and stable fluorescence [210].

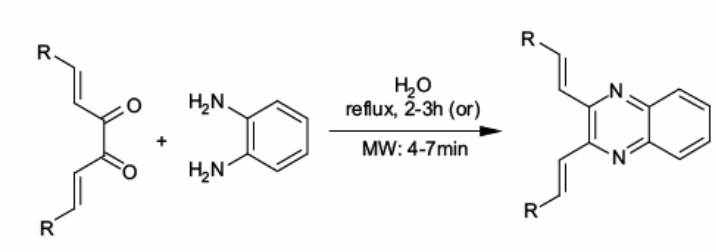

Scheme 6: Synthesis of quinoxalines

Binary metal oxides supported on Si-MCM- 41 mesoporous molecular sieves were employed as catalysts in the synthesis of quinoxaline derivatives (Scheme 7) by the condensation of 1,2-diamine with 1,2 dicarbonyl compounds [211].

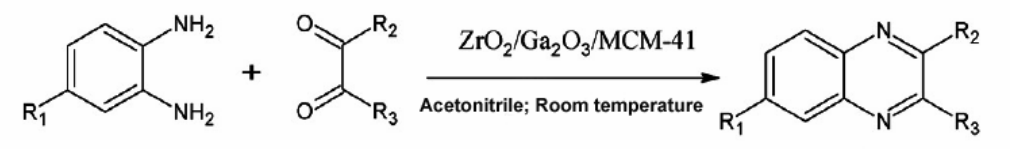

Scheme 7: Quinoxaline synthesis

Palladium-catalyzed Suzuki-Miyaura coupling of 2,3-dichloroquinoxaline with various boronic acids results in the formation of symmetrical and unsymmetrical 2,3-disubstituted quinoxalines [212]. Li et al. reported a novel approach for the synthesis of 6,7-disubstituted-1H-quinoxalin-2-ones starting from substituted phenylamines and chloroacetyl chloride through the efficient sequence of acylation, nitration, reduction, intramolecular alkylation, and oxidation [213]. Lewis acid-promoted addition of allyltri-n-butylstannane to o-quinonediimines afforded

tetrahydroquinoxaline derivatives or allylated amides depending on the nature of the substituent on imine nitrogen [214].

Mamedov et al. developed a new and effective procedure for the synthesis of 3-ethylquinoxalin-2(1H)-one from o-phenylenediamine and ethyl 2-oxobutanoate [215]. Gui et al. synthesized quinoxalines through the condensation reaction of o-phenylenediamine with aryl aldehydes or ketones [216]. Various biologically important quinoxaline derivatives were efficiently synthesized in excellent yields using molecular iodine as catalyst [217]. o-Phenylenediamines react with an array of vicinal-diols in diglyme in the presence of a catalytic amount of a ruthenium catalyst along with KOH to afford the corresponding quinoxalines in good yields [218,219]. A series of new quinoxalines has been obtained from a one pot, three-component reaction of (2-arylsulfanyl-3-aryl-2-oxiranyl)(aryl)methanones with o-phenylenediamine in the presence of a catalytic amount of acetic acid. This reaction presumably involves a tandem oxirane aminolysis-cyclisation-elimination-air oxidation-condensation sequence [220]. Hui et al. reported the synthesis of various pharmacologically active non-symmetrical 2,3-disubstituted quinoxalines [221]. Quinoxaline derivatives have been synthesized with excellent yields by the condensation of 1,2-diamines with aliphatic or aromatic 1,2-dicarbonyl compounds or benzilmonoxime with solid acid catalyst, silica sulphuric acid [222].

Wu and Gorden reported the synthesis of potentially bioactive 2-quinoxalinol salen ligands suitable for metal coordination [223]. Gris et al. employed biocatalysis or microwave irradiation for the synthesis of quinoxaline derivatives. Some of these quinoxalinone derivatives exhibited good inhibitor activity against some human tumoral cells and the lymphoma related to HIV-1 [224]. A cheap and efficient method for the synthesis of quinoxaline derivatives catalysed by N,N,N-trimethyl-N-propanesulfic acid ammonium hydrogen sulphate was reported by Dong et al. [225].

5.2 Metal complexes of quinoxalines

The quinoxaline class of ligands meet the expectations of modern metallo-organic chemistry with their low-lying LUMOs, two nitrogen atoms in para-position, suitable for bridging and easy functionalization [226]. Xie et al. reported the crystal structure of tetraaquabis[2,3-bis(5-methyl-1,3,4-thiadiazol-2-ylsulfanylmethyl) quinoxaline]nickel(II) bis(perchlorate) acetone disolvate in which the Ni^{II} center adopts a slightly distorted octahedral coordination geometry, with two N atoms from two distinct ligands and four O atoms from water molecules [227]. Rotondo et al. reported the synthesis and ^{1}H and ^{13}C NMR study of Pt^{II} complexes of [6,7-dimethyl-2,3-bis(2-pyridyl)quinoxaline] (DMeDPQ) and the crystal structure of $[Pt(DMeDPQ)(bipy)](PF_6)_2$ [228]. The rigid seven-membered chelate quinoxaline ligand holds the fused aromatic rings nearly perpendicular to the Pt^{II} coordination plane, generating the peculiar L-shaped structure.

The compound, $[Cu(C_9H_5N_2O_3)_2(C_2H_6O_S)_2]$, consists of octahedrally coordinated Cu^{II} ions, with the 3-oxo-3,4-dihydroquinoxaline-2-carboxylate ligands acting in a bidentate manner [229]. Lee et al. reported the crystal structure of paddle wheel-type centrosymmetric dinuclear complex, $[Cu_2(C_7H_5O_2)_4(C_8H_6N_2)_2]$, containing four bridging benzoate groups and two terminal quinoxaline ligands [230]. The reaction of 1,4-dihydro-2,3-quinoxalinedione (H_2L) with $CuCl_2$ in the presence of LiOH in DMF has led to a three dimensional coordination polymer $[Cu_3L_2Cl_2(DMF)_4]_n$ where L^{2-} is 2,3-dioxyquinoxalinate [231]. Variable-temperature (2−300 K) magnetic susceptibility and variable-field (0−5 T) magnetization studies of this complex reveal that L^{2-} propagates weak antiferromagnetic exchange interactions through its “quinoxaline” moiety.

In $[RuCl(C_{10}H_{14})(C_{20}H_{16}N_4)]PF_6{\cdot}CH_3CN$, the coordination of one pyridyl ring and of one N atom of the quinoxaline unit to ruthenium imposes considerable distortion on the 6,7-dimethyl-2,3-dipyridin-2-ylquinoxaline ligand. Here the pyridyl ring and the quinoxaline unit are in almost coplanar [232]. The electrochemical and

photophysical properties of a series of luminescent ruthenium(II) amidodipyridoquinoxaline biotin complexes have been investigated [233]. Luminescent tricarbonylrhenium(I) dipyridoquinoxaline indole complexes are sensitive for indole-binding proteins [234].

In the crystal structure of dibromidobis(quinoxaline)zinc(II), the quinoxaline ligands are monocoordinated to the Zn^{II} atom and, with the bromide ions, form a distorted tetrahedral geometry [235]. The combination of π-stacking interactions between inversion-related quinoxaline ligands and the bridging Zn creates layers parallel to the *bc* plane. Novel mercury(II) complexes of 2,3-bis(1H-pyrrol-2-yl)quinoxaline-functionalized Schiff bases were prepared and characterized [236]. They were found to be fluorescent and highly selective for mercury(II) ion in aqueous solution. In the crystal structure of dichlorodiquinoxaline zinc(II), the two quinoxaline ligands are mono-coordinated to a Zn^{II} atom. With the two chloride ions, they form distorted tetrahedral coordination geometry and a combination of π stacking interactions between inversion-related quinoxaline ligands and the coordination to zinc creates layers parallel to the *bc* plane [237].

The use of dipyrido[3,2-d:2′,3′-f]quinoxaline (Dpq) combined with three structurally related benzene dicarboxylic acid ligands [benzene-1,3-dicarboxylic acid (H_2L1), benzene-1,2-dicarboxylic acid (H_2L2), and biphenyl-4,4′-dicarboxylic acid (H_2L3)] has allowed the rational design of three novel Cd(II) coordination polymers, $[Cd_3(Dpq)_3(L1)_3]\cdot 4.5H_2O$ (1), $[Cd(Dpq)(L2)(H_2O)]$ (2), and $[Cd_2(Dpq)_2(L3)_2]\cdot 1.5H_2O$ (3), which were hydrothermally synthesized and structurally determined by X-ray analysis [238]. Compound 1 features a 1-D ribbonlike structure, compound 2 shows novel 2-D four-connected networks, and compound 3 possesses an interesting 6-connected 2-fold interpenetrated 3-D α-Po-related architecture. The Dpq ligand takes a chelating coordination mode while the other two nitrogen atoms did not coordinate to the Cd(II) ions. In these complexes, the three benzene-dicarboxylate ligands are able to link Cd(II) ions in various coordination modes, giving rise to 1-, 2-, and 3-dimensional Cd complexes,

respectively. In addition, complexes 1-3 exhibit blue/green emission in the solid state at room temperature.

The synthesis and spectroscopic properties of lanthanide nitrate complexes of 1,4-di(N,N-di-n-butyl-acetamido)-quinoxaline-2,3-dione (L), $[Ln(NO_3)_3L{\cdot}H_2O]$ (Ln = La, Nd, Eu, Gd, Tb, Er), have been studied by Song et al. [239]. The fluorescence property of the europium complex in solid state and in acetonitrile, acetone, ethylacetate and tetrahydrofuran was also evaluated.

A new solid-state pH sensor has been constructed based on a poly 3,4-dihydro-2-hydoxyquinoxaline (HOQ) thin film electrochemically deposited onto a Pt disc electrode whose surface had previously been modified with Pt nanoparticles by electrochemical depositing from $HPtCl_6$-H_2SO_4 solution at -0.2 V. The poly HOQ film was deposited from HAc-NaAc solution by cycling the potential between 0.4 V and 1.1 V [240].

5.3 Biological applications of quinoxalines

The quinoxaline moiety is widely distributed in nature. Also quinoxaline ring is part of a number of synthetic antibiotics such as echinomycin, leromycin, and actinomycin, which are known to inhibit the growth of gram-positive bacteria and are also active against various transplantable tumours [241-243]. The well known antibiotics echinomycin [244,245] and triostins [246] consist of two quinoxaline-2-carboxylic acid moieties attached to a cyclic octadepsipeptide containing a sulfur cross-linkage. Besides, quinoxaline structure is recognized in a great number of naturally occurring compounds such as riboflavin (vitamin B2), flavoenzymes, molybdopterines and antibiotics of streptomyces type that are implicated in considerable intra and interelectron transfer biochemical processes. The quinoxaline derivatives show antibacterial, antiviral, anticancer, antifungal, antihelmintic, insecticidal activity [247-264].

Mitsopoulou et al. reported the synthesis, characterization and DNA binding of mixed platinum(II) complexes containing quinoxaline and 1,2-dithiolate ligands [265]. Interactions of the metal complexes and free ligands with double stranded calf thymus DNA were studied. These studies suggest that both complexes form adducts with DNA and distort the double helix by changing the base stacking. A novel Ru(III) complex, mer-[$RuCl_3(CH_3CN)(dpq)$] (1), has been synthesized and characterized by X-ray diffraction, where dpq = dipyrido[3,2-d:2′,3′-f]quinoxaline [266]. Interactions of this complex with DNA have been investigated by DNA melting experiments, DNA competitive binding with ethidium bromide, plasmid DNA cleavage experiments and viscosity measurements. The interaction with bovine serum albumin has also been studied using fluorescent quenching method. A series of acyclonucleosides 6,7-disubstituted 1-(pent-4-enyl)quinoxalin-2-one derivatives and the O-analogs were synthesized by a one-step condensation of the corresponding quinoxaline bases with 5-bromo-1-pentene are shown to inhibit HIV-1 and HIV-2 in MT-4 cells [267].

A large number of quinoxaline-N-oxides are also associated with a wide spectrum of biological activity ranging from antiinfective [268-270], anticancer [260], antimycobacterium tuberculosis [271] and angiotensin II receptor antagonists [272]. The quinoxaline 1,4-di-N-oxide derivative, 3-(4-bromophenyl)-2-(ethylsulfonyl)-6-methylquinoxaline 1,4-dioxide, exhibits high anti-cancer activity in hypoxia [273]. Quinoxaline1,4-di-N-oxide derivative also induces DNA oxidative damage not attenuated by vitamin C and E treatment [274]. Potent antitumoral copper complexes of 3-aminoquinoxaline-2-carbonitrile N1,N4-dioxide derivatives were synthesized and characterized [266]. The hypoxic selective cytotoxicity towards V79 cells and the superoxide dismutase-like activity of the complexes were determined and related to physicochemical properties of the compounds.

The complexation of the quinoxaline-2-carbonitrile N1,N4-dioxide derivatives with vanadium improve their bioavailability [275]. The vanadyl

complex with the formula $VO(L1)_2$, where L1 = 3-amino-6(7)-chloroquinoxaline-2-carbonitrile N1, N4-dioxide, is more potent cytotoxins than the free ligand, and showed excellent selective cytotoxicity in hypoxia. Torre et al reported Cu(II) quinoxaline N1,N4-dioxide complexes as selective hypoxic cytotoxins for the first time [276].

5.4 Optoelectronic applications of quinoxalines

Fluorescent heterocyclic compounds are of interest as functional materials in the emitters of electroluminescence devices. In particular, fluorescent dye materials whose fluorescence emission occurs at a longer wavelength in the red light region are expected to play a leading role in full colour electroluminescence displays. Quinoxaline is known to emit both the (n, π*) fluorescence and the (π, π*) phosphorescence in the vapor phase, for which the relative fluorescence and phosphorescence quantum yields depend on the pressure as well as on the excitation energy [277-280]. A large number of quinoxaline derivatives find application as dyes and as electroluminescent materials.

Karastatiris et al. synthesised and characterised soluble poly(p-phenylenevinylene) derivatives containing one or two quinoxaline moieties per repeat unit and has studied their use as emissive and electron transport materials in polymer light-emitting diodes [281]. These poly(p-phenylenevinylene) derivatives of quinoxaline emits greenish-yellow electroluminescence with a brightness of up to 450 cd/m^2. The reaction of bis(1,2-diketone) chromophore monomer and a tetramine at room temperature resulted in the formation of second-order non-linear optical poly(phenylquinoxalines) with high glass transition temperatures [282]. Six new copolymers of 9,9′-dioctylfluorene and 2,3-bis(p-phenylene) quinoxaline were synthesized, characterized, and used as blue-emitting materials in light-emitting diodes [283]. Significant enhancements in LED brightness and external quantum efficiency by factors of up to 120 were observed in copolymers containing 15-50 mol % 2,3-bis(p-phenylene) quinoxaline when using bilayer LiF/Al cathodes.

The properties of the lowest excited triplet states of quinoxaline derivatives 2,3-dimethylquinoxaline and 2,3,6,7-tetramethylquinoxaline in acetonitrile have been investigated by using time-resolved laser flash photolysis at 266 nm [284]. New 6,7-bis-(3-methylbutoxyl)quinoxaline fluorescent dyes with groups of different electron-donating ability were synthesized by the condensation of [3-(diethoxyphosphoryl methyl)-6,7-bis-(3-methylbutoxy)-quinoxalin-2-ylmethyl]-phosphonic acid diethyl ester with arylaldehydes [285]. Three novel poly(aryl ether)s were synthesized from the reaction of three bisphenols with 2,3-bis(4-fluorophenyl)-quinoxaline via nucleophilic aromatic substitution [286]. In THF solutions the polymers showed absorption maxima at 349-354 nm and emission maxima at 417-454 nm, with quantum yields of 22-41%. Matsumura et al. reported the synthesis of 2,3-dimorpholino-6-aminoquinoxaline derivatives and their application as fluorescent probe [287].

Durmus et al. reported the synthesis of polymeric 3,4-ethylenedioxythiophene-bis-substituted quinoxalines and their potential use toward green polymeric materials [288]. Spectroelectrochemistry showed that both polymers reveal two distinct absorption bands as expected for a donor-acceptor polymer. The electrochromic properties of polymeric quinoxalines are employed in the manufacture of anode material for electrochromic devices [289]. Quinoxaline derivatives are used as photoinitiators in UV-cured coatings [290]. The iridium(III) complexes bearing 2,3-diphenylquinoxalines are shown to be highly efficient and pure-red emitting materials for electrophosphorescent organic light-emitting diodes and excellent quantum efficiencies for photoluminescence within the range of 50-79% were attained in dichloromethane solution at room temperature [291]. Hwang et al. synthesised and characterised four iridium complexes having substituted quinoxalines. One of the complexes was used to fabricate the red-emitting polymer light emitting diodes by blending it into a polymer mixture [292]. Porphyrins bearing quinoxaline derivatives were synthesized by the condensation reaction of 2,2′-(p-tolylmethylene)bis(1H-pyrrole) and a bisstyryl derivative containing 6,7-diisopentyloxyquinoxaline [293]. The chromophoric system of the fluorescent and

highly conjugated porphyrin macrocycles were studied from the viewpoint of protonation and deprotonation effects on their absorption and emission spectra in solution. The liquid crystalline properties and crystal structure of 5,6-didodecyloxyquinoxaline-2-(1H)-one oxime were studied using differential scanning calorimetry, optical polarizing microscopy and X-ray investigation [294]. The compound displayed a discotic mesophase over a large temperature interval. X-ray diffraction studies also revealed that this compound forms a discotic hexagonal ordered columnar mesophase and thus, has potential use as a colored liquid crystal.

6. Scope of the present work

A variety of Schiff base complexes derived from salicylaldehyde were found to have immense application in various fields. In the present investigation, we have used 3-hydroxyquinoxaline-2-carboxaldehyde in the place of salicylaldehyde and so what ever studies have been done in the case of Schiff base derivatives of salicylaldehyde, can be explored in the case of the Schiff base derivatives of 3-hydroxyquinoxaline-2-carboxaldehyde. Starting from this aldehyde one can prepare a large number of Schiff bases and their metal complexes and these compounds may find interesting applications in medicine, material science and catalysis. Indeed, to the best of our knowledge, not much work has been carried out to understand the catalytic behaviour of the Schiff base complexes derived from 3-hydroxyquinoxaline-2-carboxaldehyde. In this thesis, results of our studies on the synthesis and characterisation some new transition metal complexes derived from the above aldehyde and their catalytic activities in some oxidation and hydrogenation reactions are presented.

References

[1] H. Schiff. Annalen, 131 (1864) 118.

[2] P.A. Vigato, S. Tamburini. Coordination Chemistry Reviews, 248 (2004) 1717–2128.

[3] N.E. Borisova, M.D. Reshetova, Y.A. Ustynyuk. Chemical Reviews, 107 (2007) 46-79.

[4] P.G Cozzi. Chemical Society Reviews, 33 (2004) 410-421.

[5] M. Kojima, H. Taguchi, M. Tsuchimoto, K. Nakajima. Coordination Chemistry Reviews 237 (2003) 183-196

[6] J. Costamagna, J. Vargas, R. Latorre, A. Alvarado, G. Mena. Coordination Chemistry Reviews, 119 (1992) 67-88

[7] A. Syamal, M.R. Maurya. Coordination Chemistry Reviews, 95 (1989) 183-238

[8] C.W. Tang, S.A. VanSlyke. Applied Physics Letters, 51 (1987) 913-915.

[9] T. Yu, W. Su, W. Li, Z. Hong, R. Hua, B. Li. Thin solid Films, 515 (2007) 4080-4084.

[10] Y. Yi, X. Q. Wei, M.G. Xie, Z.Y. Lu. Chinese Chemical Letters, 15 (2004) 525-528.

[11] X. Q. Wei, Z.Y. Lu, P. Zou, M.G. Xie. Chinese Chemical Letters, 14 (2003) 263 –266.

[12] J. Xie, J. Qiao, L. Wang, J. Xie, Y. Qiu. Inorganic Chemica Acta, 358 (2005) 4451-4458.

[13] D.R. Kanis, M.A. Ratner, T.J. Marks. Chemical Reviews 94 (1994) 195-242.

[14] L.R. Dalton, A.W. Harper, R. Ghosn, W.H. Steier, M. Ziari, H. Fetterman, Y. Shi, R.V. Mustacich, A.K.Y. Jen, K.J. Shea. Chemistry of Materials, 7 (1995) 1060-1081.

[15] R.G. Benning. Journal of Material Chemistry, 5 (1995) 365-378.

[16] S.R. Marder, D.N. Beratan, L.T. Cheng. Science, 252 (1991) 103-106.

[17] T. Verbiest, S. Houbrechts, M. Kauranen, K. Clays, A. Persoons. Journal of Material Chemistry, 7 (1997) 2175-2189.

[18] N.J. Long. Angewandte Chemie International Edition, 34 (1995) 21-38.

[19] M. Bourgault, C. Mountassir, H. Le Bozec, I. Ledoux, G. Pucetti, J. Zyss. Journal of Chemical Society, Chemical Communication, (1993) 1623-1624.

[20] S. Di Bella, I. Fragata, I. Ledoux, M.A. Draz-Garcia, P.G. Lacroix, T.J. Marks. Chemistry of Materials, 6 (1994) 881-890.

[21] W.M. Laidlaw, R.G. Denning, T. Verbiest, E. Chauchard , A. Persoons. Nature, 363 (1994) 58-59.

[22] B.J. Coe, J.D. Foulon, T.A. Hamor, C.J. Jones, J.A. McCleverty, D. Bloor, G.H. Cross, T.L. Axon. Journal of Chemical Society, Dalton Transactions, (1994) 3427-3439.

[23] H.S. Nalwa. Applied Organometallic Chemistry, 5 (1991) 349-377.

[24] G.L. Geoffroy, M.S. Wrighton. Organometallic Photochemistry; Academic Press: New York, 1979.

[25] J.P. Collman, L.S. Hegedus. Principles and Applications of Organotransition Metal Chemistry; University Science Books: Mill Valley, CA, 1987.

[26] O. Kahn. Molecular Magnetism; VCH Publishers: New York, 1993.

[27] S. Di Bella. Chemical Society Reviews, 30 (2001) 355-366.

[28] P.G. Lacroix. European Journal of Inorganic Chemistry, (2001) 339-348.

[29] C.E. Powell, M.G. Humphrey. Coordination Chemistry Reviews, 248 (2004) 725-756.

[30] B.J. Coe, J.A. Harris, L.A. Jones, B.S. Brunschwig, K. Song, K. Clays, J. Garin, J. Orduna, S.J. Coles, M.B. Hursthouse. Journal of American Chemical Society, 127 (2005) 4845-4859.

[31] B.J. Coe, J.A. Harris, B.S. Brunschwig, I. Asselberghs, K. Clays, J. Garin, J. Orduna. Journal of American Chemical Society, 127 (2005) 13399-13410.

[32] B.J. Coe, J.A. Harris, L.A. Jones, B.S. Brunschwig. Dalton Transactions, (2003) 2384-2386.

[33] D.R. Kanis, M.A. Ratner, T.J. Marks. Chemical Reviews, 94 (1994) 195-242.

[34] S. Di Bella, I. Fragala, I. Ledoux, T.J. Marks. Journal of American Chemical Society, 117 (1995) 9481-9485.

[35] S. Di Bella, I. Fragala, T.J. Marks, M.A. Ratner. Journal of American Chemical Society, 118 (1996) 12747-12751.

[36] P.G. Lacroix , S. Di Bella , I. Ledoux. Chemistry of Materials, 8 (1996) 541-545.

[37] S. Di Bella, I. Fragala, I. Ledoux, M.A. Diaz-Garcia, T.J. Marks. Journal of American Chemical Society, 119 (1997) 9550-9557.

[38] G. Lenoble, P.G. Lacroix, J.C. Daran, S. Di Bella, K. Nakatani. Inorganic Chemistry, 37 (1998) 2158-2165.

[39] S. Di Bella, I. Fragala, A. Guerri, P. Dapporto, K. Nakatani. Inorganica Chimica Acta, 357 (2004) 1161-1167.

[40] F. Averseng, P.G. Lacroix, I. Malfant, G. Lenoble, P. Cassoux, K. Nakatani, I. Maltey-Fanton, J. A. Delaire, A. Aukauloo. Chemistry of Materials, 11 (1999) 995-1002.

[41] T. Shamspur, I. Sheikhshoaie, M.H. Mashhadizadeh. Journal of Analytical Atomic Spectrometry, 20 (2005) 476-478.

[42] S. Sadeghi, M. Eslahi, M.A. Naseri, H. Naeimi, H. Sharghi, A. Shameli. Electroanalysis, 15 (2003) 1327-1333.

[43] M. H. Mashhadizadeh, I. Sheikhshoaei, S. Saeid-Nia. Sensors and Actuators B chemical, 94, (2003) 241-246.

[44] R.K. Mahajan, I. Kaur, M. Kumar. Sensors and Actuators B chemical, 91 (2003) 26-31.

[45] M.H. Mashhadizadeh, I. Sheikhshoaei. Analytical and Bioanalytical Chemistry, 375 (2003) 51.

[46] L. P. Singh, J. M. Bhatnagar. Talanta, 64 (2004) 313-319.

[47] A.R. Fakhari, T.A. Raji, H. Naeimi. Sensors and Actuators B chemical, 104 (2005) 317-323.

[48] T. Jeong, H.K. Lee, D.C. Jeong, S. Jeon. Talanta, 65 (2005) 543-548.

[49] M. Shamsipur, M. Yousefi, M. Hosseini, M.R. Ganjali, H. Sharghi, H. Naeimi. Analytical Chemistry, 73 (2001) 2869-2874.

[50] M.R. Ganjali, T. Poursaberi, M. Hosseini, M. Salavati-Niasari, M. Yousefi, M. Shamsipur. Analytical Sciences, 18 (2002) 289-292.

[51] M.R. Ganjali, M.R. Pourjavid, M. Rezapour, T. Poursaberi, A. Daftari, M. Salavati-Niasari. Electroanalysis, 16 (2004) 922-927.

[52] V.K. Gupta, R.N. Goyal, A.K. Jain, R.A. Sharma. Electrochimica Acta, 54 (2009) 3218–3224.

[53] V.K. Gupta, A.K. Jain, G. Maheshwari. Talanta, 72 (2007) 49-53.

[54] J. Patole, D. Shingnapurkar, S. Padhye, C Ratledge. Bioorganic & Medicinal Chemistry Letters, 16 (2006) 1514-1517.

[55] V.T Dao, M.K Dowd, M.T Martin, C Gaspard, M Mayer, Michelot R.J. European Journal of Medicinal Chemistry, 39 (2004) 619-624

[56] Khan A, Sarkar S, Sarkar D. International Journal of Antimicrobial Agents, 32 (2008) 40-45

[57] M.S. Iqbal, A.H. Khan, B.A. Loothar, I.H. Bukhari. Medicinal Chemistry Research, 18 (2009) 31-42

[58] P.G. Kulkarni, G.B. Avaji, Bagihalli, S.A Patil, P.S. Badami. Journal of Coordination Chemistry 62 (2009) 481-492

[59] G. Puthilibai, S. Vasudevan, S.K. Rani, G. Rajagopal. Spectrochimica Acta - Part A: Molecular and Biomolecular Spectroscopy, 72 (2009) 796-800

[60] P.G Avaji, C.H.V Kumar, S.A Patil, K.N. Shivananda, C. Nagaraju. European Journal of Medicinal chemistry, (2009) doi:10.1016/j.ejmech.2009.03.032

[61] G.B. Bagihalli, P.G. Avaji, S.A. Patil, P.S. Badami. European Journal of Medicinal Chemistry 43 (2008) 2639-2649.

[62] N. Chitrapriya, V. Mahalingam, L.C. Channels, M. Zeller, F.R. Fronczek, K. Natarajan. Inorganica Chimica Acta, 361 (2008) 2841–2850.

[63] E. Keskioglu, A.B. Gunduzalp, S. Cete, F. Hamurcu, B. Erk. Spectrochimica Acta Part A, 70 (2008) 634–640.

[64] H. Katircioglu, Y. Beyatlı, B. Aslim, Z. Yuksekdag, T. Atici. Internet Journal of Microbiology, 2(2) (2006).

[65] V.P. Daniel, B. Murukan, B.S. Kumari, K. Mohanan. Spectrochimica Acta Part A, 70 (2008) 403–410.

[66] M.S. Nair, R.S. Joseyphus. Spectrochimica Acta Part A, 70 (2008) 749–753.

[67] A.S. El-Tabl, F.A. El-Saied, W. Plass, A.N. Al-Hakimi. Spectrochimica Acta Part A, 71 (2008) 90–99.

[68] D.E. Goldberg, V. Sharma, A. Oskaman, I.Y. Gluzman, T.E. Wellems, D.J. Piwnica-Worms. Biological Chemistry, 272 (1997) 6567-6572.

[69] V. Sharma, A. Beatty, D.E. Goldberg, D. Piwnica-Worms. Chemical Communication, (1997) 2223-2224.

[70] V. Sharma, D. Piwnica-Worms. Chemical Reviews, 99 (1999) 2545-2560.

[71] K.E. Erkkila, D.T. Odom, J.K. Barton. Chemical Reviews, 99 (1999) 2777–2796.

[72] C. Liu, M. Wang, T. Zhang, H. Sun. Coordination Chemistry Reviews, 248 (2004)147–168.

[73] D.S. Sigman, A. Mazumder, D.M. Perrin, Chemical Reviews. 93 (1993) 2295–2316.

[74] K.J. Humphreys, K.D. Karlin, S.E. Rokita. Journal of American Chemical Society, 124 (2002) 8055–8066.

[75] E.A. Kesicki, M.A. DeRosch, L.H. Freeman, C.L. Walton, D.F. Harvey, W.C. Trogler. Inorganic Chemistry, 32 (1993) 5851–5867.

[76] S.A. Tysoe, R. Kopelman, D. Schelzig. Inorganic Chemistry, 38 (23) (1999) 5196–5197.

[77] C. Liu, S. Yu, D. Li, Z. Liao, X. Sun, H. Xu. Inorganic Chemistry, 41 (4) (2002) 913–922.

[78] A.C. Lim, J.K. Barton. Biochemistry, 32 (41) (1993) 11029-11034.

[79] S. Dhar, M. Nethaji, A.R. Chakravarty. Inorganic Chemistry, 45 (2006) 11043–11050.

[80] M. Roy, S. Saha, A.K. Patra, M. Nethaji, A.R. Chakravarty. Inorganic Chemistry, 46 (2007) 4368–4370.

[81] A.T. Chaviara, E.E. Kioseoglou, A.A. Pantazaki, A.C. Tsipis, P.A. Karipidis, D.A. Kyriakidis, C.A. Bolos. Journal of Inorganic Biochemistry, 102 (2008) 1749–1764.

[82] E.V. Hackl, V.L. Galkin, Y.P. Blagoi. International Journal of Biological Macromolecules, 34 (2004) 303-308.

[83] K. Jiao, Q.X. Wang, W. Sun, F.F. Jian. Journal of Inorganic Biochemistry, 99 (2005) 1369-1375.

[84] S.K. Gupta, D.D. Agarwal, D. Raina. Indian Journal of Chemistry Section A: Inorganic, Bio-inorganic, Physical, Theoretical and Analytical Chemistry, 35A (1996) 995

[85] S.K. Gupta, D. Raina. Transition Metal Chemistry, 22 (1997) 372-374

[86] S.K. Gupta, D. Raina. Transition Metal Chemistry, 22 (1997) 225-228

[87] S.K. Gupta, K. Jain, Y.S. Kushwah. Indian Journal of Chemistry Section A: Inorganic, Bio-inorganic, Physical, Theoretical and Analytical Chemistry, 38A (1999) 506

[88] S.K. Gupta, Y.S. Kushwah. Polyhedron 20 (2001) 2019-2025

[89] S.K. Gupta, P.B. Hitchcock, Y.S. Kushwah, Journal of Coordination Chemistry, 55 (2002) 1401-1407

[90] S.K. Gupta, P.B. Hitchcock, Y.S. Kushwah, G.S. Argal. Inorganica Chimica Acta, 360 (2007) 2145–2152

[91] G. Barone, N. Gambino, A. Ruggirello, A. Silvestri, A. Terenzi, V.T. Liveri. Journal of Inorganic Biochemistry, 103 (2009) 731–737

[92] A. Silvestri, G. Barone, G. Ruisi, D. Anselmo, S. Riela, V.T. Liveri. Journal of Inorganic Biochemistry 101 (2007) 841–848

[93] Z-H Xu, F-J Chen, P-X Xi, X-H Liu, Z-Z Zeng. Journal of Photochemistry and Photobiology A: Chemistry 196 (2008) 77–83

[94] R. Vijayalakshmi, M. Kanthimathi, V. Subramanian, B.U Nair. Biochimica et Biophysica Acta, 1475 (2000) 157-162.

[95] R. Vijayalakshmi, M. Kanthimathi, R. Parthasarathi, B.U. Nair, Bioorganic & Medicinal Chemistry 14 (2006) 3300–3306

[96] Y. Kou, J Tian, D. Li, W. Gu, X. Liu, S. Yan, D. Liao, P. Cheng. Journal of the Chemical Society, Dalton Transactions. (2009) 2374–2382

[97] A. Silvestri, G. Barone, G. Ruisi, M.T. Lo Giudice, S. Tumminello. Journal of Inorganic Biochemistry 98 (2004) 589–594

[98] S. Niu, M. Zhao, R. Ren, S. Zhang. Journal of Inorganic Biochemistry, 103 (2009) 43–49

[99] T. Uchida, T. Katsuki. Tetrahedron Letters, 42 (2001) 6911-6914.

[100] A. Watanabe, T. Uchida, K. Ito, T. Katsuki. Tetrahedron Letters, 43 (2002) 4481-4485.

[101] D.R. Reddy, E.R. Thornton. Journal of Chemical Society, Chemical Communication, 1992, 172-173.

[102] A. Waldemar, T.F. Rainer, R.S. Veit, R.S.-M. Chantu. Journal of American Chemical Society, 120 (1998) 708-714.

[103] K. Nakajima, K. Kojima, T. Aoyama, J. Fujita. Chemistry Letters, (1986) 1483-1486.

[104] K. Nakjima, M. Kojima, K. Toriumi, K. Saito, J. Fujita. Bullettin of Chemical Society Japan, 62 (1989) 760-767.

[105] C. Bolm, F. Bienewald. Angewandte Chemie International Edition in English, 34 (1995) 2640-2642.

[106] A.H. Vetter, A. Berkessel. Tetrahedron Letters, 39 (1998) 1741-1744.

[107] C. Ohta, H. Shimizu, A. Kondo, T. Katsuki. Synlett, (2002) 161-163.

[108] Z. Flores-Lopez, M. Parra-Hake, R. Somanathan, P.J.Walsh. Organometallics, 19 (2000) 2153-2160.

[109] A. Gama, L.Z. Flores-Lopez, G. Aguirre, M. Parra-Hake, R. Somanathan, P.J. Walsh. Tetrahedron Asymmetry, 13 (2002) 149-154.

[110] B. Cabezon, A. Sastre, T. Torres, W. Schafer, J.J. Borras-Almenar, E.J. Coronado. Journal of Chemical Society, Dalton Transactions, (1995) 2305-2310.

[111] R.C. Matthews, D.K. Howell, W.J. Peng, S.G. Train, W.D. Treleaven, G.G. Stanley. Angewandte Chemie International Edition in English, 35 (1996) 2253-2256.

[112] N.O. Komatsuzaki, R. Katoh, Y. Himeda, H. Sugihara, H. Arakawa, K. Kasuga. Bullettin of Chemical Society Japan, 76 (2003) 977-984.

[113] E.K. Beuken, P.W.N.M. Leeuwen, P.H.M. Budzelaar, N. Veldman, A.L. Spek, B.L. Feringa. Journal of Chemical Society, Dalton Transactions, (1996) 3561-3569.

[114] M. Lubben, R. Hage, A. Meetsma, K. Bijma, B.L. Feringa. Inorganic Chemistry, 34 (1995) 2217-2224.

[115] A.G.J. Ligtenbarg, E.K. Beuken, A. Meetsma, N. Veldman, W.J.J. Smeets, A.L. Spek, B.L. Feringa. Journal of Chemical Society, Dalton Transactions, (1998) 263-270.

[116] J. Bozell, B. Hames, D. Dimmel. Journal of Organic Chemistry, 60 (1995) 2398-2404.

[117] L. Simandi. Advances in Catalytic Activation of Dioxygen by Metal Complexes, Kluwer Academic Publishers, Dordrecht, Chapter 6, 2003.

[118] T. Punniyamurthy, J. Iqbal. Tetrahedron Letters, 35 (1994) 4003-4006.

[119] Y-L. Zhang, W-J. Ruan, X-J. Zhao, H-G. Wang, Z-A. Zhu. Polyhedron, 22(12) (2003) 1535-1546.

[120] W.H. Leung, C.M. Che. Inorganic Chemistry, 28 (1989) 4619-4621

[121] E.M. McGarrigle, D.G. Gilheany. Chemical Reviews, 105 (2005) 1563-1602.

[122] N. Finnley, P.J. Pospil, S. Chang, M. Palucki , R. Konsler, K. Hansen, E. Jacobsen. Angewandte Chemie International Edition in English, 36 (1997) 1720-1723.

[123] E.N. Jacobsen. in Comprehensive Organometallic Chemistry II, Eds. E. W. Abel, F. G. A. Stone and E. Willinson, Pergamon, New York, vol. 12, p. 1097, 1995.

[124] H. Nishikori, C. Ohta, T. Katsuki. Synlett, (2000) 1557-1560.

[125] T. Takeda, R.Irie, T. Katsuki. Synlett, 7 (1999) 1166-1168.

[126] T. Katsuki. Chemical Society Reviews, 33 (2004) 437-444

[127] S.H. Zhao, P.R. Ortiz, B.A. Keys, K.G. Davenport. Tetrahedron Letters, 37 (1996) 2725-2728.

[128] I. Fernández, J.R. Pedro, R. Salud. Tetrahedron, 52 (1996) 12031-12038.

[129] V.R. de Souza, G.S. Nunes, R.C. Rocha, H.E. Toma. Inorganica Chimica Acta, 348 (2003) 50-56.

[130] R.I. Kureshy, N.H. Khan, S.H.R. Abdi, S.T. Patel, P.K. Iyer, R.V. Jasra. Journal of Catalysis, 209 (2002) 99-104.

[131] C-M Che, J-S Huang. Coordination Chemistry Reviews 242 (2003) 97-113.

[132] T. Takeda, R. Irie, Y. Shinoda. T. Katsuki, Synlett (1999) 1157-1159.

[133] K. Nakata, T. Takeda, J. Mihara, T. Hamada, R. Irie, T. Katsuki. Chemistry A European Journal 7 (2001) 3776-3782.

[134] R.M. Stoop, S. Bachmann, M. Valentini, A. Mezzetti. Organometallics 19 (2000) 4117-4126.

[135] C. Bonaccorsi, A. Mezzetti. Current Organic Chemistry, 10 (2006) 225-240.

[136] R.I. Kureshy, N.H. Khan, S.H.R. Abdi, P. Iyer. Journal of Molecular Catalysis A: Chemical, 124 (1997) 91-97.

[137] R. Drozdzak, B. Allaert, N. Ledoux, I. Dragutan, V Dragutan, F. Verpoort. Coordination Chemistry Reviews 249 (2005) 3055–3074.

[138] R.G. Cavell, K. Aparna, R.P. Kamalesh Babu, Q. Wang. Journal of Molecular Catalysis A. Chemical, 189 (2002) 137-143.

[139] G.J.P. Britovsek, V.C. Gibson, B.S. Kimberly, P.J. Maddox, S.J. McTavish, G.A. Solan, A.J.P. White, D.J. Williams. Chemical Communications, (1998) 849-850.

[140] G.J.P. Britovsek, V.C. Gibson, D.F. Wass. Angewandte Chemie International Edition, 38 (1999) 428-447.

[141] S. Matsui, T. Fujita. Catalysis Today, 66 (2001) 63-73.

[142] Y. Nakayama, H. Bando, Y. Sonobe, T. Fujita. Journal of Molecular Catalysis A. Chemical, 213 (2004) 141-150.

[143] R. Souane, F. Isel, F. Peruch, P.J. Lutz. Comptes Rendus Chimie, 5 (2002) 43-48.

[144] D.P. Knight, A.J. Clarke, B.S. Kimberley, R.A. Jackson, S. Peter. Chemical Communication. (2002) 352-353.

[145] M.A Mekewi. International Journal of Polymeric Materials, 55, (2006) 219- 234.

[146] Y. Nishibayashi, I. Takei, S.Vemara, M. Hidai. Organometallics, 18 (1999) 2291-2293.

[147] T. Langer, G. Helmchen. Tetrahedron Letters, 37 (1996) 1381-1386.

[148] J.W. Faller, A.R. Lavoie. Organometallics, 20 (2001) 5245-5247.

[149] D.J. Cross, J.A. Kenny, I. Houson, L. Campbell, T. Walsgrove, M. Wells. Tetrahedron Asymmetry, 12 (2001) 1801-1806.

[150] G. Venkatachalam, R. Ramesh. Inorganic Chemistry Communications, 8 (2005) 1009–1013.

[151] G. Venkatachalam, R. Ramesh. Inorganic Chemistry Communications, 9 (2006) 703–707.

[152] M. Costa, P. Pelagatti, C. Pelizzi, D. Rogolino. Journal of Molecular Catalysis A: Chemical 178 (2002) 21–26.

[153] E. Tas, A. Kilic, M. Durgun, I. Yilmaz, I. Ozdemir, N. Gurbuz. Journal of Organometallic Chemistry 694 (2009) 446–454.

[154] V.T. Kasumov, E. Tas, F. Koksal, S. Ozalp-Yaman. Polyhedron 24 (2005) 319–325.

[155] H. Dai, X. Hu, H. Chen, C. Bai, Z. Zheng. Tetrahedron: Asymmetry, 14 (2003) 1467–1472.

[156] I. Karame, M. Jahjah, A. Messaoudi, M.L. Tommasino, M. Lemaire. Tetrahedron: Asymmetry, 15 (2004) 1569–1581.

[157] S. Kano, H. Nakano, M. Kojima, N. Baba, K. Nakajima. Inorganica Chimica Acta, 349 (2003) 6-16.

[158] F.I. Zubkov, E.V. Boltukhina, K.F. Turchin, A.V. Varlamov. Tetrahedron 60 (2004) 8455-8463.

[159] A.V. Varlamov, F.I. Zubkov, E.V. Boltukhina, N.V. Sidorenko, R.S. Borisov. Tetrahedron Letters, 44 (2003) 3641-3643.

[160] S.E. Schaus, J. Branalt, E.N. Jacobsen. Journal of Organic Chemistry, 1998, 63, 403-405.

[161] D.A. Evans, J.M. Janey, N. Magomedov, J.S. Tedrow. Angewandte Chemie International Edition, 40 (2001) 1884-1888.

[162] M.H. Wu, E.N. Jacobsen. Tetrahedron Letters, 38 (1997) 1693-1696.

[163] B.D. Brandes, E.N. Jacobsen. Tetrahedron: Asymmetry, 8 (1997) 3927-3933.

[164] A. Miller, W. Jin, S.T. Nguyen. Angewandte Chemie International Edition, 2002, 41, 2953-2956.

[165] T. Katsuki. Synlett, 2003, 281-297.

[166] Z. Zhuo, Y. Xiaoquan, L. Chen, C. Huilin, H. Xinquan. Tetrahedron Letters, 42 (2001) 2847-2849.

[167] S. Iyer, G.M. Kulkarni, C. Ramesh. Tetrahedron, 60 (2004) 2163-2172.

[168] K. Sarkar, M. Nandi, M. Islam, M. Mubarak, A. Bhaumik. Applied Catalysis A: General, 352 (2009) 81-86.

[169] K.C. Gupta, A.K. Sutar, C.C. Lin. Coordination Chemistry Reviews, 253 (2009) 1926-1946.

[170] B. Bahramian, F.D. Ardejani, V. Mirkhani, K. Badii. Applied Catalysis A: General, 345 (2008) 97-103.

[171] M. Salavati-Niasari, S.N. Mirsattari. Journal of Molecular Catalysis A: Chemical, 268 (2007) 50-58.

[172] M. Salavati-Niasari, M. Hassani-Kabutarkhani, F. Davar. Catalysis Communications, 7 (2006) 955-962.

[173] M. Salavati-Niasari, P. Salemi, F. Davar. Journal of Molecular Catalysis A: Chemical, 238 (2005) 215-222.

[174] W-S Kim, Y-K Choi. Applied Catalysis A: General, 252 (2003) 163-172.

[175] C. Baleizo, H. Garcia. Chemical Reviews, 106 (2006) 3987-4043.

[176] T.C.O.M. Leod, D.F.C. Guedes, M.R. Lelo, R.A. Rocha, B.L. Caetano, K.J. Ciuffi, M.D. Assis. Journal of Molecular Catalysis A: Chemical, 259 (2006) 319-327.

[177] B.B. De, B.B. Lohray, S. Sivaram, P.K. Dhal. Journal of Polymer Science Part A: Polymer Chemistry, 35 (1997) 1809-1818.

[178] F. Minutolo, D. Pini, P. Salvadori. Tetrahedron: Asymmetry, 1996,7, 2293-2302.

[179] R.I. Kureshy, N.H. Khan, S.H.R. Abdi, P. Iyer. Reactive and Functional Polymers, 34 (1997) 153-160.

[180] D. Angelino-Mark, E. Laibinis-Paul. Macromolecules 31 (1998)7581-7587.

[181] L. Canali, D.C. Sherrington, H. Deleuze. Reactive and Functional Polymers, 40 (1999) 155-168.

[182] E. Minutolo, D. Pini, A. Petri, P. Salvadori. Tetrahedron Asymmetry, 7 (1996) 2293-2302.

[183] R.I. Kunesky, N.H. Khan, S.H.R. Abdi, P. Iyer, Reactive and Functional Polymers, 34 (1997) 153-160.

[184] C.E. Song, E.J. Roh, B.M. Yu, D.Y. Chi, S.C. Kim, K.J. Lee. Chemical Communication, (2000) 615-616.

[185] D. Brunel, N. Bellocq, P. Sutra, A. Cauvel, M. Lasperas, P. Moreau, F. Di Renzo, A. Galarneau, F. Fajula. Coordination Chemistry Reviews, 1085 (1998) 178–180.

[186] A.P. Deshmukh, V.G. Akerkar, M.M. Salunkhe. Journal of Molecular Catalysis A: Chemical, 153 (2000) 75-82.

[187] K.C. Gupta, H.K. Abdulkadir, S. Chand. Journal of Macromolecular Science A. Pure and Applied Chemistry, 39 (2002) 1451-1474.

[188] K.C. Gupta, H. K. Abdulkadir, S. Chand. Journal of Applied Polymer Science, 90 (2003) 1398-1411.

[189] K.C. Gupta, H.K. Abdulkadir, S. Chand. Journal of Macromolecular Science A. Pure and Applied Chemistry, 40 (2003) 475-500.

[190] S.B. Ogunwumi, T. Bein. Chemical Communications, (1997) 901-902.

[191] Y.F. Farzaneh, M. Majidian, M. Ghandi. Journal of Molecular Catalysis A: Chemical, 148 (1999) 227-233.

[192] A. Zsigmond, A. Horvath, F. Notheisz. Journal of Molecular Catalysis A: Chemical, 171 (2001) 95-102.

[193] A. Zsigmond, F. Notheisz, Z. Frater, J.E. Backvall. Studies in Surface Science and Catalysis, 108 (1997) 453-459.

[194] D. Chatterjee, A. Mitra. Journal of Molecular Catalysis A: Chemical, 144 (1999) 363-367.

[195] M.J. Sabater, A. Corma, A. Domenech, V. Fornes, H. Garcia. Chemical Communications, (1997) 1285-1286.

[196] F. Ding, Y. Sun, S. Monseaert, R. Drozdzak, I. Dragutan, V. Dragutan, F. Verpoort. Current Organic Synthesis, 5 (2008) 291-304.

[197] S.G. Telfer, R. Kuroda. Coordination Chemistry Reviews, 242 (2003) 33-46

[198] E. Ispir. Dyes and Pigments, 82 (2009) 13-19

[199] P.S. Chittilappilly, N. Sridevi, K.K.M. Yusuff. Journal of Molecular Catalysis A: Chemical, 286 (2008) 92–97.

[200] P.S. Chittilappilly, K.K.M. Yusuff. Indian Journal of Chemistry -Section A Inorganic, Physical, Theoretical and Analytical Chemistry, 47 (2008) 848-853.

[201] R. Sreekala, K.K. M. Yusuff. Reaction Kinetics & Catalysis Letters, 48 (1992) 575-581.

[202] S. Mayadevi, K.K.M. Yusuff. Synthesis and Reactivity in Inorganic and Metal-Organic Chemistry, 27 (1997) 319-330.

[203] S. Mayadevi, P.G. Prasad, K.K.M. Yusuff. Synthesis and Reactivity in Inorganic and Metal-Organic Chemistry, 33 (2003) 481-496.

[204] Vogel's Textbook of Practical Organic Chemistry, 5th ed., 1989.

[205] D.J. Brown, Quinoxalines: supplements II. In The Chemistry of Heterocyclic Compounds

[206] E. C. Taylor, Wipf, P., Eds.; John Wiley and Sons: New Jersey, 2004

[207] D.J. Brown, in: E.C. Taylor, P. Wipf (Eds.), The Chemistry of Heterocyclic Compounds, John Wiley and Sons, New Jersey, 2004.

[208] A.E.A. Porter, In Comprehensive Heterocyclic Chemistry; A.R. Katritsky, C.W. Rees, Eds.; Pergamon: Oxford, 1984, pp 157–197.

[209] G.H.C. Woo, J.K. Snyder, Z-K. Wan. Progress in Heterocyclic Chemistry, 14 (2002) 279-309.

[210] P. Thirumurugan, D. Muralidharan. P.T. Perumal, Dyes and Pigments 81 (2009) 245–253

[211] S. Ajaikumar, A. Pandurangan. Applied Catalysis A: General 357 (2009) 184–192

[212] L. Mao, H. Sakurai, T Hirao. Synthesis, 15 (2004) 2535-2539.

[213] X. Li, Q. P. Hu, X.G. Cui, D.H. Wang. Chinese Chemical Letters; 15 (2004) 1400-1402.

[214] V. Nair, R. Dhanya, C. Rajesh, M.M. Bhadbhade, K. Manoj. Organic Letters; 6 (2004) 4743-4745.

[215] V.A. Mamedov, A.A. Kalinin, A.T. Gubaidullin, O.G. Isaikina, I.A. Litvinov. Russian Journal of Organic Chemistry, 41 (2005) 599-606.

[216] Y. Gui, X-B. Tang, C-X. Shao, J-T. Li, W-H. Sun. Chinese Journal of Chemistry, 23(2005) 589-595.

[217] S.V. More, M.N.V. Sastry, C-C. Wang, C-F. Yao. Tetrahedron Letters, 46(37), 2005, 6345-6348.

[218] C.S. Cho, S.G. Oh. Tetrahedron Letters, 47 (2006) 5633-5636.

[219] C. S. Cho, W. X. Ren, S. C. Shim. Tetrahedron Letters, 48 (2007) 4665-4667.

[220] M. K. Nasar, R.R. Kumar, S. Perumal. Tetrahedron Letters, 48 (2007) 2155-2158.

[221] X. Hui, F. Schmidt, M.A. Fakhfakh, X. Franck, B. Figadère. Heterocycles, 72 (2007) 353-361.

[222] S. Ahmad, M. Ali. Chinese Journal of Chemistry, 25(2007) 818-821.

[223] X. Wu, A.E.V. Gorden. Journal of Combinatorial Chemistry, 9(2007) 601-608.

[224] J. Gris, R. Glisoni, L. Fabian, B. Fernandez, A.G. Moglioni. Tetrahedron Letters, 49 (2008) 1053-1056.

[225] F. Dong, G. Kai, F. Zhenghao, Z. Xinli, L. Zuliang. Catalysis Communications, 9 (2008) 317-320.

[226] W. Kaim, Angewandte Chemie International Edition, 22 (1983) 171-190

[227] Y.B Xie, X.J Wang, D. Wang. Acta Crystallographica Section E: Structure Reports Online; 61(10) (2005) m2086-m2087

[228] E. Rotondo, A. Rotondo, F. Nicolò, M.L Di Pietro, M.A Messina, M. Cusumano. European Journal of Inorganic Chemistry, 23 (2004) 4710-4717.

[229] Z. Popovic, G. Pavlović, B.M Kukovec. Acta Crystallographica Section C: Crystal Structure Communications, 63 (2007) m181-m183

[230] E.Y Lee, B.K Park, C. Kim, S.J. Kim, Y. Kim. Acta Crystallographica Section E: Structure Reports Online, 64(2) (2008) m286.

[231] K.F Konidaris, S.P Perlepes, G. Aromi, S.J Teat, A. Escuer, E. Manessi-Zoupa. Inorganic Chemistry Communications, 11(2) (2008) 186-191.

[232] B. Therrien, G. Suss-Fink. Acta Crystallographica Section E: Structure Reports Online, 63, (2007) m1627.

[233] K.K-W Lo, T.K.-M Lee. Inorganica Chimica Acta, 360 (2007) 293-302.

[234] K.K.-W Lo, K-S Sze, K.H-K Tsang, N. Zhu. Organometallics, 26 (2007) 3440-3447.

[235] B.M.E Markowitz, M.M. Turnbull, F.F Awwadi. Acta Crystallographica Section E: Structure Reports Online, 63 (2007) m2043.

[236] L. Wang, X-J Zhu, W-Y Wong, J-P Guo, W-K Wong, Z-Y Li. Dalton Transactions, 19 (2005) 3235-3240.

[237] B.M.E Markowitz, M.M Turnbull, F.F Awwadi. Acta Crystallographica Section E: Structure Reports Online, 62 (2006) m1278-m1280.

[238] X.-L Wang, Y.-F Bi, H-Y Lin, G.-C Liu. Crystal Growth and Design, 7 (2007) 1086-1091.

[239] X-Q Song, Y-W Wang, J-R Zheng, W-S Liu, M-Y Tan. Spectrochimica Acta-Part A: Molecular and Biomolecular Spectroscopy, 68 (2007) 701-704.

[240] X. Li, Z. Zhang, J. Zhang, Y. Zhang, K. Liu. Mikrochimica Acta, 154 (2006) 297-301.

[241] A. Dell, D.H William, H.R Morris, G.A Smith, J. Feeney, G.C.K Roberts. Journal of the American Chemical Society, 97 (1975) 2497-2502.

[242] C. Bailly, S. Echepare, F. Gago, M. Waring. Anti-Cancer Drug Design, 14 (1999) 291-303.

[243] S.Sato, O. Shiratori, K. Katagiri. Journal of Antibiotics, 20 (1967) 270.

[244] M.J. Waring, L.P.G Wakelin. Nature, 252 (1974) 653-657.

[245] M.J. Waring, L.P.G Wakelin. Biochemical Journal, 157 (1976) 721-740

[246] Addess K. J.; Feigon. Journal of Biochemistry, 33 (1994) 12397

[247] D. Catarzi, V. Colotta, F. Varano, O. Lenzi, G. Filacchioni, L. Trincavelli, C. Martini, C. Montopoli, S. Moro. Journal of Medicinal Chemistry, 48 (2005) 7932-7945

[248] A. Jaso, B. Zarranz, I. Aldana, A. Monge. Journal of Medicinal Chemistry, 48 (2005) 2019-2025.

[249] V.M. Lakshmi, F.F. Hsu, T.V. Zenser. Chemical Research in Toxicology, 18 (2005) 1038-1047

[250] R.J. Turesky, A.K. Goodenough, W. Ni, L. McNaughton, D.M. LeMaster, R.D. Holland, R.W. Wu, J.S. Felton. Chemical Research in Toxicology, 20 (2007) 520-530.

[251] G.S.M. Sundaram, B. Singh, C. Venkatesh, H. Ila, H. Junjappa. Journal of Organic Chemistry, 72 (2007) 5020 -5023.

[252] M.A Naylor, M.A Stephen, J. Nolan, B. Sutton, J.H Tocher, E.M Fielden, J.E Adams, I Strafford. Anti-Cancer Drug Design, 8 (1993) 439–461

[253] J. Harmenberg, A. Akesson-Johansson, A. Graslund, T. Malmfors, J. Bergman, B. Wahren, S. Akerfeldt, L. Lundblad, S. Cox. Antiviral Research, 15 (1991) 193–204

[254] A. Fournet, R. Mahieux, M.A Fakhfakh, X. Franck, R. Hocquemiller, B. Figadere. Bioorganic & Medicinal Chemistry Letters, 13 (2003) 891–894

[255] M-H Munos, J. Mayrargue, A. Fournet, J-C Gantier, R. Hocquemiller, H. Moskowitz. Chemical and Pharmaceutical Bulletin, 42 (1994) 1914–1916.

[256] R. Sarges, H.R Howard, R.C Browne, L.A Label, P.A Seymour. Journal of Medicinal Chemistry, 33 (1990) 2240-2254.

[257] G. Sakata, K. Makino, Y. Kurasawa. Heterocycles 27 (1998) 2481

[258] G. Arthur, K.B Elor, G.S Robert, Z.Z Guo, J.P Richard, D Stanley, R.K John, T.J Sean. Journal of Medicinal Chemistry, 48 (2005) 744.

[259] J. Andres, Z. Belen, A. Ibnacio, M. Antonio. Journal of Medicinal Chemistry, 48 (2005) 2019-2025

[260] B. Zarranz, A. Jaso, I. Aldana, A. Monge, Bioorganic and Medicinal Chemistry, 12 (2004) 3711

[261] V.K Tandon, D.B Yadav, H.K Maurya, A.K Chaturvedi, P.K Shukla. Bioorganic and Medicinal Chemistry, 14 (2006) 6120-6126

[262] M. Kushida, H. Wanibuchi, K. Morimura, A. Kinoshita, J.S Kang, R. Puatanachokckai, M. Wei, Y. Funae, S. Fukushima. Cancer Science, 96 (2005) 747-757

[263] E.R Kotb, M.A Anwar, M.S Soliman, M.A Salama. Phosphorus, Sulfur and Silicon and the Related Elements, 182 (2007) 1119-1130

[264] I.A.I Ali, I.A Al-Masoudi, N.M Aziz, N.A Al-Masoudi. Nucleosides, Nucleotides and Nucleic Acids, 27 (2008) 146-156

[265] C.A Mitsopoulou, C.E Dagas, C. Makedonas. Journal of Inorganic Biochemistry, 102 (2008) 77-86.

[266] C. Tan, J. Liu, H. Li, W. Zheng, S. Shi, L. Chen, L. Ji. Journal of Inorganic Biochemistry, 102 (2008) 347-358.

[267] I.A.I Ali, I.A Al-Masoudi, H.G. Hassan, N.A Al-Masoudi. Chemistry of Heterocyclic Compounds, 43 (2007) 1052-1059

[268] M. Loriga, A. Nuvole, G. Paglietti, G. Fadda, S. Zanetti. European Journal of Medicinal Chemistry, 25 (1990) 527–532

[269] G. Aguirre, H. Cerecetto, R.D. Maio, M. Gonzalez, M.E.M. Alfaro, A. Jaso, B. Zarranz, M.A Ortega, I. Aldana, A. Monge-Vega. Bioorganic and Medicinal Chemistry, 14 (2004) 3835–3839

[270] A. Carta, G. Paglietti, M.E.R Nikookar, P. Sanna, L. Sechi, S. Zanetti. European Journal of Medicinal Chemistry, 37 (2005) 355– 366

[271] A. Jaso, B. Zarranz, I. Aldana, A. Monge. European Journal of Medicinal Chemistry, 38 (2003) 791–800

[272] K.S Kim, L. Qian, J.E Bird, K.E Dickinson, S. Moreland, T.R Schaeffer, T.L Waldron, C.L Delaney, H.N Weller, A.V Miller. Journal of Medicinal Chemistry, 36 (1993) 2335–2342

[273] Q. Weng, D. Wang, P. Guo, L. Fang, Y. Hu, Q. He, B. Yang. European Journal of Pharmacology, 581 (2008) 262-269

[274] A. Azqueta, L. Arbillaga, G. Pachon, M. Cascante, E.E Creppy, A.L Cerain. Chemico-Biological Interactions, 168 (2007) 95-105

[275] M. Vieites, P. Noblía, M.H. Torre, H. Cerecetto, M. L. Lavaggi, A.J Costa-Filho, A. Azqueta, A.L de Cerain, A. Monge, B. Parajón-Costa, M. González, D. Gambino. Journal of Inorganic Biochemistry, 100 (2006) 1358-1367

[276] M.H Torre, D. Gambino, J. Araujo, H. Cerecetto, M. González, M.L Lavaggi, A. Azqueta, A. Lopez De Cerain, A.M. Vega, U. Abram, A.J. Costa-Filho. European Journal of Medicinal Chemistry, 40 (2005) 473-480

[277] B. Soep, A. Tramer. Chemical Physics, 7 (1975) 52-61

[278] J.E. Brus, J.R. McDonald, Chemical Physics Letters, 23 (1973) 87-92

[279] J.E. Brus, J.R. McDonald, Journal of Chemical Physics, 61 (1974) 3895-3904

[280] E.C. Lim, C.S. Huang, Journal of Chemical Physics, 58 (1973) 1247-1248

[281] P. Karastatiris, J.A Mikroyannidis, I.K Spiliopoulos, A.P Kulkarni, S.A Jenekhe. Macromolecules, 37 (2004) 7867-7878

[282] E. Gubbelmans, T. Verbiest, I. Picard, A. Persoons, C. Samyn. Polymer, 46 (2005) 1784-1795

[283] A.P Kulkarni, Y. Zhu, S.A Jenekhe. Macromolecules, 38 (2005) 1553-1563

[284] Y. Pan, Z. Sheng, X. Ye, Z. Ao, G. Chu, J. Dai, S. Yu. Journal of Photochemistry and Photobiology A: Chemistry, 174 (2005) 98-105

[285] J-Y Jaung. Dyes and Pigments, 71 (2006) 245-250

[286] V.P. Barberis, J.A. Mikroyannidis, I.K. Spiliopoulos. Synthetic Metals, 157 (2007) 475-480

[287] Y. Matsumura, A. Katoh. Journal of Luminescence, 128 (2008) 625-630

[288] A. Durmus, G.E. Gunbas, L. Toppare. Chemistry of Materials, 19 (2007) 6247-6251

[289] M. Ak, M.S Ak, M. Gullu, L. Toppare. Smart Materials and Structures, 16 (2007) 2621-2626

[290] D. K. Balta, S. Keskin, F. Karasu, N. Arsu. Progress in Organic Coatings, 60 (2007) 207-210

[291] K. Tani, H. Fujii, L. Mao, H. Sakurai, T. Hirao. Bulletin of the Chemical Society of Japan, 80 (2007) 783-788

[292] F-M Hwang, H-Y Chen, P-S Chen, C-S Liu, Y. Chi, C-F Shu, F-I Wu, P-T Chou, S-M Peng, G-H Lee. Inorganic Chemistry, 44 (2005) 1344-1353

[293] J-H Kim, J.Y. Jaung. Dyes and Pigments, 77 (2008) 474-477

[294] M. Durmus, F. Dincer, V. Ahsen. Dyes and Pigments, 77 (2008) 402-407

Chapter 2

Materials and methods
Synthesis and characterisation of the Schiff base ligands

Contents

This chapter is broadly divided into two sections. Part A which provides details of the reagents used and various analytical and physico-chemical techniques employed in the characterisation and catalytic activity studies. Part B which gives the details of the preparation and spectral characterisation of Schiff base ligands used in the present study

A) Materials and Methods

2.1 Chemicals

The important chemicals used in the present study are given in the Table 1. All chemicals employed in the present study were of analytical grade. Solvents employed were either of 99% purity or purified by known laboratory procedures [1].

Table 1: Important chemicals with specified make

Name of chemical	Manufacturer
o-Phenylenediamine	Loba Chemie
Sodium pyruvate, glacial acetic acid, benzene, toluene, cyclohexene	SRL
Bromine, precipitated calcium carbonate, 2-aminophenol, 4-aminoantipyrine, Cupric chloride, phenol	Merck
1,8-Diaminonaphthalene, trans-1,2-diaminocyclohexane, 2,3-diaminomaleonitrile, ruthenium chloride, vanadyl sulphate	Sigma Aldrich

2.2 Analytical methods

A variety of physico-chemical methods have been employed to characterise the structure of organic Schiff base ligands, their metal chelates and in catalytic activity studies. A brief account of these methods is given below.

2.2.1 Elemental analyses

CHN analyses of all the synthesized compounds were done on an Elementar model Vario EL III CHNS analyser at SAIF, Sophisticated Test and Instrumentation Centre, Kochi, India. Chlorine was estimated gravimetrically using the standard procedure after fusing the complex with sodium carbonate/sodium peroxide mixture [2]. The metal content of the complexes were determined by AAS after digestion with concentrated nitric acid. The analysis were done using Thermo Electron Corporation, M series Atomic Absorption Spectrophotometer.

2.2.2 Magnetic susceptibility measurements

The magnetic susceptibility measurements were done at room temperature on a Magway MSB Mk 1 Magnetic Susceptibility Balance. The Magnetic Scsceptibility Balance (MSB) is the result of collaboration with Professor D. F. Evans of Imperial College, London, and is designed as a replacement for a traditional Guoy balance system. The Evans method uses the same configuration as the Guoy method but, instead of measuring the force which a magnet exerts on the sample, the equal and opposite force which the sample exerts on a suspended permanent magnet is observed.

The MSB works on the basis of a stationary sample and moving magnets. The pairs of magnets are placed at opposite ends of a beam so placing the system in balance. Introduction of the sample between the poles of one pair of magnets produces a deflection of the beam that is registered by means of phototransistors. A current is made to pass through a coil mounted between the poles of the other pair of

magnets, producing a force restoring the system to balance. At the position of equilibrium, the current through the coil is proportional to the force exerted by the sample, and can be measured as a voltage drop.

The solid sample is tightly packed into weighed sample tube with a suitable length (*l*) and noted the sample weight (*m*). Then the packed sample tube was placed into tube guide of the balance and noted the reading (*R*) was noted. The mass susceptibility, χ_g, is calculated using:

$$\chi_g = \frac{C_{Bal} * l * (R - R_0)}{10^9 * m}$$

where: l = the sample length (cm)

m = the sample mass (g)

R = the reading for the tube plus sample

R_0 = the empty tube reading

C_{Bal} = the balance calibration constant

Then molar susceptibility $\chi_m = \chi_g \times$ molecular formula of the complex. The molar susceptibility is the corrected with diamagnetic contribution. The effective magnetic moment, $\mu_{eff,}$ is then calculated using the following expression:

$\mu_{eff} = 2.83\sqrt{T * X_A}$ where X_A is the corrected molar susceptibility.

2.2.3 Conductivity measurements

The molar conductivities of the complexes in dimethylformamide (DMF) solutions (10^{-3} M) at room temperature were measured using direct reading conductivity meter, Systronics conductivity bridge type 305.

2.2.4 NMR spectra

^{1}H NMR spectra of the Schiff bases, N,N'-bis(3-hydroxyquinoxaline-2-carboxalidene)trans(R,R')1,2-diaminocyclohexane and 3-hydroxyquinoxaline-2-

carboxalidene-2-aminophenol, were recorded in MeOD using Bruker AMX 400 FT-NMR Spectrometer using TMS as the internal standard at SAIF, Indian Institute of Science, Bangalore, India. ^{1}H NMR and ^{13}C NMR spectra of 3-hydroxyquinoxaline-2-carboxaldehyde and the ^{1}H NMR spectra of the Schiff bases, N,N'-bis(3-hydroxyquinoxaline-2-carboxalidene)1,8-diaminonaphthalene, N,N'-bis(3-hydroxyquinoxaline-2-carboxalidene)2,3-diaminomaleonitrile and 3-hydroxyquinoxaline-2-carboxalidene-4-aminoantipyrine, were also recorded in $CDCl_3$ and DMSO-d^6 on a Bruker Avance DRX 500 MHz NMR spectrometer at NIIST, Trivandrum, Kerala.

2.2.5 Infrared spectra

Room-temperature FT−IR spectra were recorded as KBr pellets with a JASCO FTIR 4100 Spectrophotometer in the 4000-400 cm^{-1} range. The far IR spectra of metal complexes were recorded using polyethylene pellets in the 500-100 cm^{-1} region on a Nicolet Magna 550 FTIR instrument at the SAIF, Indian Institute of Technology, Bombay, India.

2.2.6 Cyclic voltammetric studies

Cyclic voltammetric measurements of the all the synthesised complexes were carried out on a Bio-Analytical System (BAS) model CV-50 W electrochemical analyser. The three-electrode cell comprised a reference Ag/AgCl, a counter electrode as platinum wire and a working glassy carbon (GC) electrode with surface area of 0.7 cm^2. The GC was polished with 0.3 and 0.005 nm alumina before each experiment and when necessary the electrode was sonicated in distilled water for 10 min. Dissolved oxygen was removed by purging the solution with pure nitrogen for about 15 min before each experiment. Scanning the cyclic voltammogram for a blank solution was done to check the purity of the supporting electrolyte and the solvent.

Cyclic voltametric studies of the ligands were carried out in 1:1 tetrahydrofuran-methanol mixture with a BAS CV-27 Electrochemical Analyser using glassy-carbon working electrode. A Pt wire and Ag/AgCl were used as counter and reference electrodes, respectively.

2.2.7 Electronic spectra

Electronic spectra of the ligands and its complexes were recorded in various solvents on a Thermoelectron Nicolet evolution 300 UV-vis spectrophotometer. Diffuse reflectance spectra of the complexes were recorded at room temperature in a Jasco V 570 UV-Vis spectrophotometer in the wavelength range 200-1800 nm with a scanning rate 200 nm/minute. Absorbance spectra were obtained from the reflectance spectra by means of Kubelka–Munk transformations.

2.2.8 TG/DTA/DTG

TG-DTA-DTG analysis of the ligands and the complexes were carried out under air and nitrogen at a heating rate of 20 ºC min^{-1} using a Perkin Elmer Pyres Diamond TG/DTA analyser.

2.2.9 EPR spectra

X-band EPR spectra of the complexes were recorded in the solid state at RT, solid state at LNT and in DMF at LNT using Varian E-112 X/Q band spectrophotometer using TCNE as standard at the SAIF, IIT, Mumbai, India.

2.2.10 Catalytic studies

The hydrogenation reactions were carried out in a 100 mL Bench top Mini-Reactor (Figure 1) made of stainless steel 316 (Autoclave Engineers, Division of Snap-tite, Inc. Pennsylvania). Hydrogenation was performed by charging the reactor with known quantities of the catalyst and benzene. Air was flushed out of the reactor with low-pressure of hydrogen, after which the inlet valve was closed and

heating commenced with stirring at 600 rpm. When the designated temperature was reached, hydrogen was fed to the reactor at a predetermined pressure (time zero), which was maintained through out the reaction with the help of a mass flow meter. During the run, samples (about 0.5 mL each) were withdrawn periodically and analyzed using a Chemito 8510 Gas Chromatograph and the products of the reaction were identified by using Varian 1200 L Single Quadrupole GC-MS.

Figure 1: Bench top mini-reactor (100 mL)

Catalytic oxidations were performed in two necked stirred flasks fitted with a water condenser. All glassware was oven-dried prior to use. In a typical experiment an appropriate amount of the catalyst was dissolved in freshly distilled acetonitrile. The required amount of cyclohexene/phenol was then added to the reaction mixture followed by the requisite amount of oxidant (30% H_2O_2). The reaction mixture was refluxed with continuous stirring in an oil bath provided with a digital temperature controller. Samples were withdrawn from the reaction solution at appropriate times and analyzed by GC. The oxidation products were identified by comparison with

authentic samples (retention time in GC). The identities of various products were confirmed by GC-MS.

2.2.11 Gas Chromatography

The gas chromatograph used in the catalytic activity studies is a Chemito 8510 Gas Chromatograph with FID detector. The column used was Chromosorb W and nitrogen was used as the carrier gas. The GC-MS used was Varian 1200 L Single Quadrupole GC-MS with helium as the carrier gas and VF-5MS as column (SAIF, Sophisticated Test & Instrumentation Centre, Cochin University of Science and Technology, Cochin, India).

B) Synthesis and Characterisation of the Schiff base ligands

Schiff bases are generally synthesised by the condensation of aldehydes and amines. In the present investigation the aldehyde employed was 3-hydroxyquinoxaline-2-carboxaldehyde. The amines chosen were 1,8-diaminonaphthalene, 2,3-diaminomaleonitrile, trans-1,2-diaminocyclohexane, 2-aminophenol, 4-aminoantipyrine. The synthesis of Schiff bases involves two main stages: synthesis of 3-hydroxyquinoxaline-2-carboxaldehyde and condensation of this aldehyde with the above mentioned amines.

2.3 Synthesis of 3-hydroxyquinoxaline-2-carboxaldehyde (hqc)

The general reaction for the formation of quinoxaline derivatives involves the condensation of α-oxo acids with o-phenylenediamine [3-7]. Although a method was reported by Ohle and Noetzel [8] for the synthesis of 3-hydroxyquinoxaline-2-carboxaldehyde, it turned out to be inconvenient for the preparation of the Schiff base as the aldehyde could be obtained only in the hydrated from and undergoes some physical changes in the presence of light. Therefore a new procedure was employed for the synthesis. This procedure involves preparation of 3-hydroxy-2-dibromomethylquinoxaline form 3-hydroxy-2-methylquinoxaline and its conversion

to the aldehyde. 3-Hydroxy-2-methylquinoxaline was prepared by the condensation of pyruvic acid with o-phenylenediamine [9,10]. 3-Hydroxy-2-dibromomethylquinoxaline could also be prepared from $CHBr_2COCO_2H$ by the method of Bruckner [11].

2.3.1 Preparation of 3-hydroxy-2-methylquinoxaline (hmq)

Separate solutions of o-phenylenediamine (0.1 M; 10.81 g) and sodium pyruvate (0.1 M; 11.00 g) in 250 mL distilled water were prepared. The sodium pyruvate solution was converted to pyruvic acid using conc: HCl (8 mL). The pyruvic acid solution was taken in a 1 L beaker. To this solution, o-phenylenediamine was added drop by drop with constant stirring. The precipitated pale yellow compound (Scheme 1) was filtered, washed with water and dried over anhydrous calcium chloride. The crude sample was recrystallized from 50% absolute ethanol. Yield: 90%; Colour: pale yellow; No sharp melting point was observed and the compound decomposes with in the range 212-225 °C accompanied by a change in colour from pale yellow to light brown.

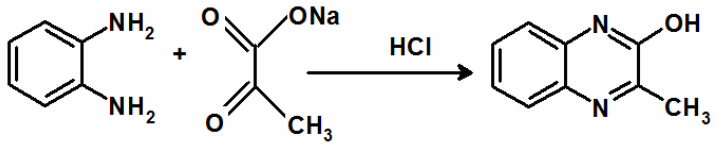

Scheme 1

2.3.2 Preparation of 3-hydroxy-2-dibromomethylquinoxaline (hdmq)

To a solution of 3-hydroxy-2-methylquinoxaline (0.1 M; 16.02 g) in glacial acetic acid (200 mL), 10% (v/v) bromine in glacial acetic acid (110 mL) was added with stirring. The mixture was then exposed to sunlight for 1 hr with occasional stirring. It was then diluted to 1 L with distilled water and the precipitated dibromo compound (Scheme 2) was filtered, washed with water and dried. The crude product was purified by recrystallisation form 50% absolute ethanol. Yield: 92%; Colour : pale yellow; No sharp melting point, but decomposes with in the range 210-222 °C with a change in colour from pale yellow to light brown.

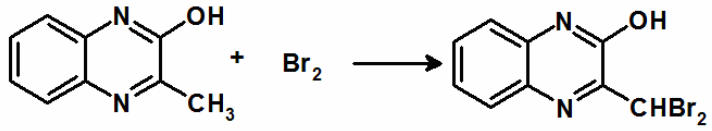

Scheme 2

2.3.3 Preparation of 3-hydroxyquinoxaline-2-carboxaldehyde (hqc)

The dibromo compound (5 g) was thoroughly mixed with precipitated calcium carbonate (20 g) using mortar and pestle. The mixture was refluxed with distilled water (500 mL) in a 1 L RB flask for 3 hrs with occasional shaking. The aldehyde (Scheme 3) remaining in the solution was collected by filtration. The yellow aqueous solution thus obtained is very stable and can be used for the preparation of Schiff base. The aldehyde was obtained as fine yellow powder by concentrating the aqueous solution using rotary evaporator, extracting the aldehyde with ether, drying the ether extract using anhydrous sodium sulphate and removing ether using a rotary evaporator. The yellow solid is not stable and changes its colour to light brown in air indicating oxidation/decomposition of the aldehyde. Therefore, it would be better to use the aldehyde solution for the synthesis of Schiff base. Yield: 50%; Colour: yellow; No sharp melting point, but decomposes with in the range 108-130 °C and the colour changes from yellow to light brown.

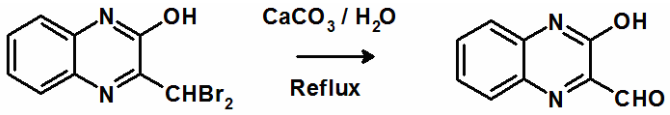

Scheme 3

2.4 Characterisation of 3-hydroxyquinoxaline-2-carboxaldehyde (hqc)

The aldehyde, 3-hydroxyquinoxaline-2-carboxaldehyde, was characterised by UV-visible, FT-IR, ^{1}H NMR and ^{13}C NMR spectra and the results are given below.

2.4.1 Elemental analyses

The analytical data for the hmq, hdmq and hqc are given in the Table 2. They are in good agreement with molecular formula.

Table 2: Analytical data a of hmq, hdmq and hqc

Compound	Molecular formula	Formula weight	Carbon (%)	Hydrogen (%)	Nitrogen (%)
hmq	$C_9H_{18}N_2O$	160.17	67.49 (67.38)	5.03 (4.98)	17.49 (17.37)
hdmq	$C_9H_6Br_2N_2O$	317.96	34.00 (33.93)	1.90 (1.86)	8.81 (8.77)
hqc	$C_9H_6N_2O_2$	174.16	62.07 (62.01)	3.47 (3.40)	16.09 (16.06)

[a] Calculated values in parentheses

2.4.2 Electronic spectra

The electronic spectra of hmq, hdmq and hqc are taken in methanol (10^{-4} mol l^{-1}) (Table 3 and Figures 2-4). In the UV-visible spectra of all these compounds the first three peaks are due to the $\pi \rightarrow \pi^*$ transitions of the heterocyclic quinoxaline ring and the fourth one is due to the $n \rightarrow \pi^*$ transition of the –C=N– group in quinoxaline ring [12].

Table 3: UV-visible spectral data of hmq, hdmq and hqc in methanol (10^{-4} mol l^{-1})

Compound	λ_{max}(nm) (ε_{max} x 10^{-4} (L mol^{-1} cm^{-1}))
hmq	210 (2.98), 229 (3.51), 278 (0.94), 335 (1.13)
hdmq	212 (2.98), 232 (2.65), 296 (1.04), 359 (0.98)
hqc	209 (2.78), 231 (2.17), 283 (0.67), 338 (0.75)

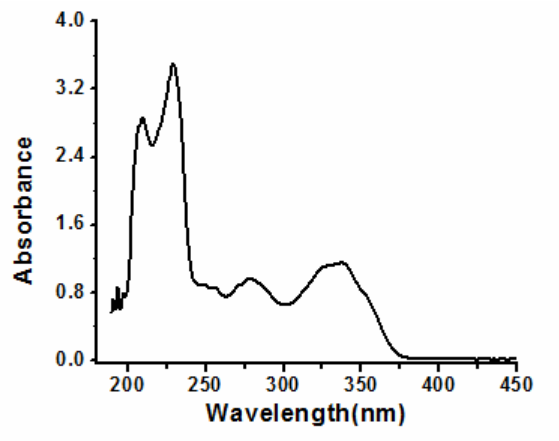

Figure 2: UV-visible spectrum of hmq

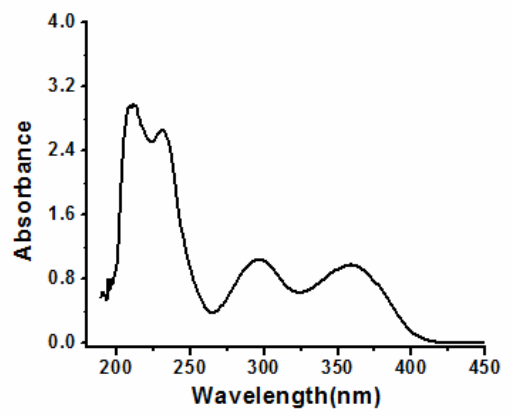

Figure 3: UV-visible spectrum of hdmq

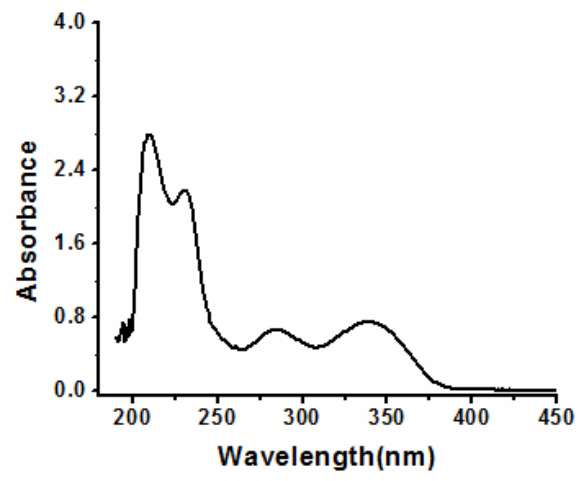

Figure 4: UV-visible spectrum of hqc

2.4.3 Infrared spectra

Table 4 lists the FT-IR spectral bands of hmq, hdmq and hqc and corresponding spectra are given in Figure 5 to 7.

Table 4: Infrared spectral bands (cm^{-1}) for hmq, hdmq and hqc

Schiff base	Spectral bands (cm^{-1})
hmq	3313, 3168, 3108, 3011, 2966, 2900, 2845, 2784, 2707, 1950, 1920, 1666, 1611, 1569, 1504, 1486, 1431, 1381, 1350, 1279, 1213, 1192, 1158, 1117, 1030, 1010, 974, 945, 929, 892, 852, 779, 755, 728, 692, 601, 585, 560, 468, 455, 416
hdmq	3314, 3156, 3104, 3009, 2969, 2888, 2836, 2775, 2715, 1662, 1612, 1557, 1502, 1480, 1433, 1398, 1350, 1281, 1225, 1158, 1131, 1103, 1069, 1022, 956, 943, 913, 895, 866, 825, 799, 761, 734, 714, 684, 618, 601, 563, 502, 476, 468, 447, 431
hqc	3483, 3164, 3095, 3012, 2965, 2906, 2836, 1721, 1670, 1600, 1568, 1541, 1497, 1420, 1394, 1345, 1260, 1218, 1160, 1072, 1025, 942, 900, 872, 825, 807, 762, 722, 647, 607, 587, 548, 526, 483, 432

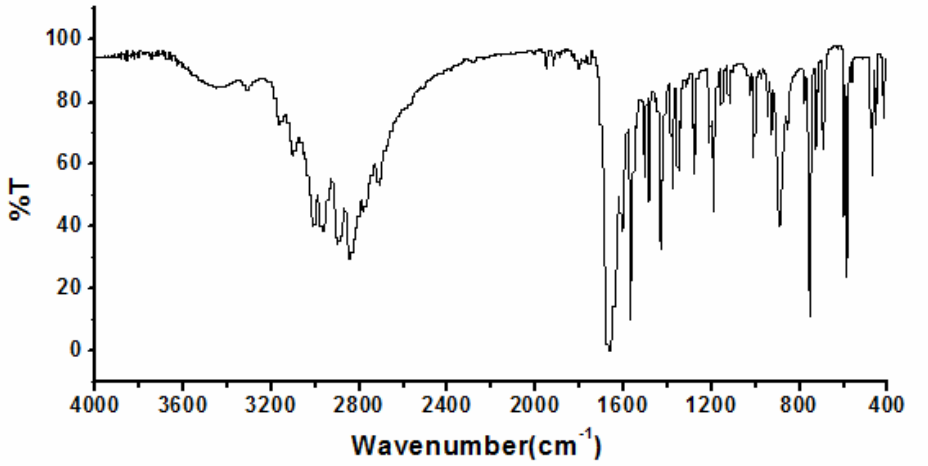

Figure 5: FT-IR spectrum of hmq

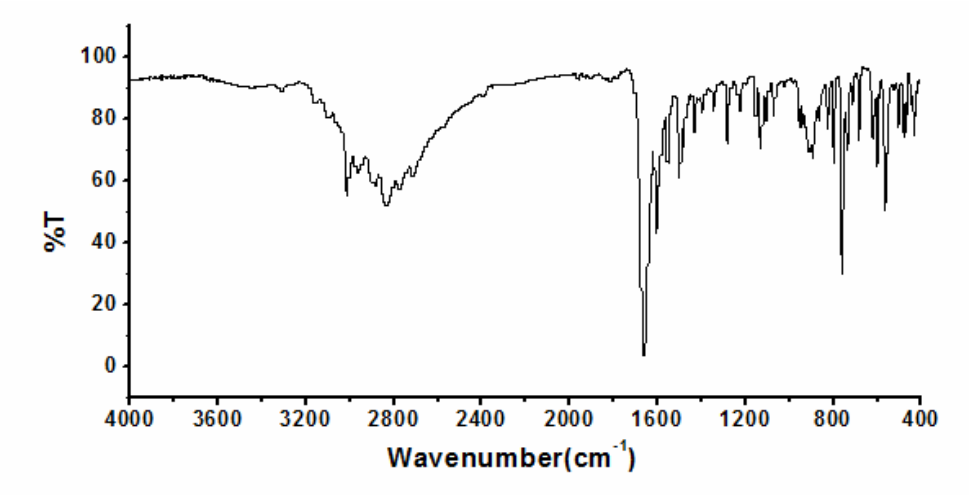

Figure 6: FT-IR spectrum of hdmq

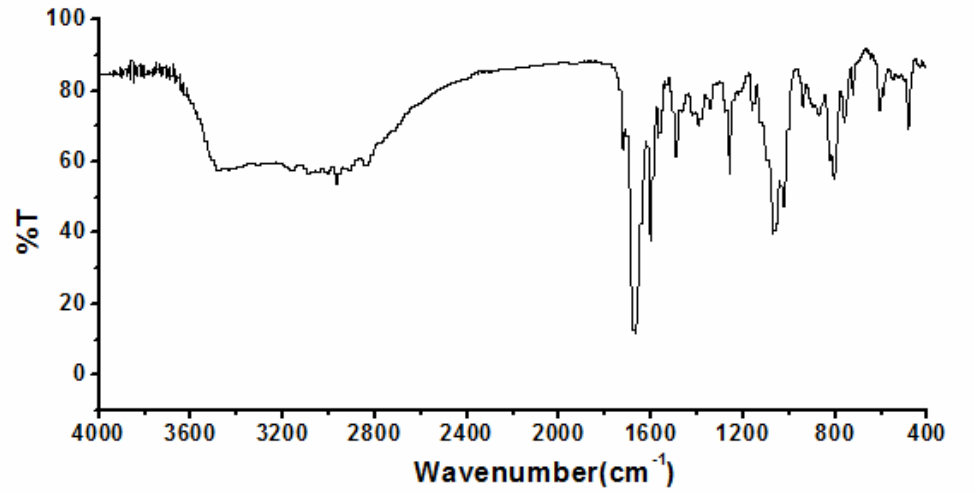

Figure 7: FT-IR spectrum of hqc

2.4.4 NMR spectra

The ^{1}H NMR and ^{13}C NMR data of the hmq, hdmq and hqc and their assignments are given in the Table 5. The ^{1}H NMR spectra of hmq, hdmq and hqc are given in Figures 8-10.

Table 5: ^{1}H NMR and ^{13}C NMR data of the hmq, hdmq and hqc

Compound	Assignments
hmq	^{1}H NMR δ p.p.m.: (500 MHz, DMSO-d^{6}, 295 K): δ = 2.40 (s, 3H, C—CH$_3$), 7.28, 7.27, 7.25 (t, 1H), 7.45, 7.46 (d, 1H), 7.47, 7.48, 7.49 (t, 1H), 7.69, 7.70 (d, 1H), 12.31 (s, 1H, Ar—OH or N—H). ^{13}C NMR (500 MHz, DMSO-d^{6}, 296 K) δ p.p.m.: 159.17, 154.88, 131.88, 131.61, 129.26, 127.82, 122.98, 115.17, 20.48.
hdmq	^{1}H NMR δ p.p.m.: (500 MHz, DMSO-d^{6}, 295 K): δ = 7.25 (s, 1H, CH—Br$_2$), 7.37, 7.38, 7.39 (t, 1H), 7.51, 7.53 (d, 1H), 7.61, 7.62, 7.63 (t, 1H), 7.85, 7.84 (d, 1H), 10.18 (s, 1H, Ar—OH or N—H). ^{13}C NMR (500 MHz, DMSO-d^{6}, 297 K) δ p.p.m.: 154.21, 151.23, 136.57, 131.87, 130.86, 128.96, 123.95, 115.61, 29.62.
hqc	^{1}H NMR δ p.p.m.: (500 MHz, DMSO-d^{6}, 296 K): δ 7.28-7.92 (m, 4H, aromatic quinoxaline ring), 10.25 (s, 1H, –CH=O), 12.40-13.00 (m, 1H, Ar—OH or N—H). ^{13}C NMR (500 MHz, DMSO-d^{6}, 297 K) δ p.p.m.: 188.88, 160.00, 153.89, 149.36, 134.37, 133.15, 131.75, 130.50, 115.51.

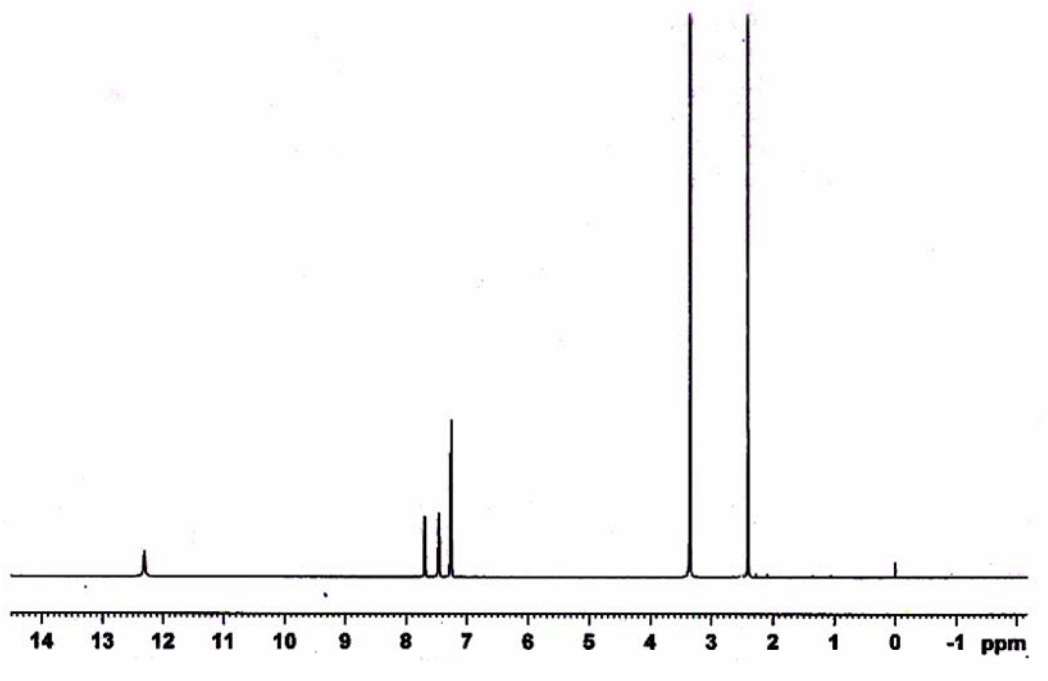

Figure 8: The ^{1}H NMR spectrum of hmq in DMSO-d^{6}

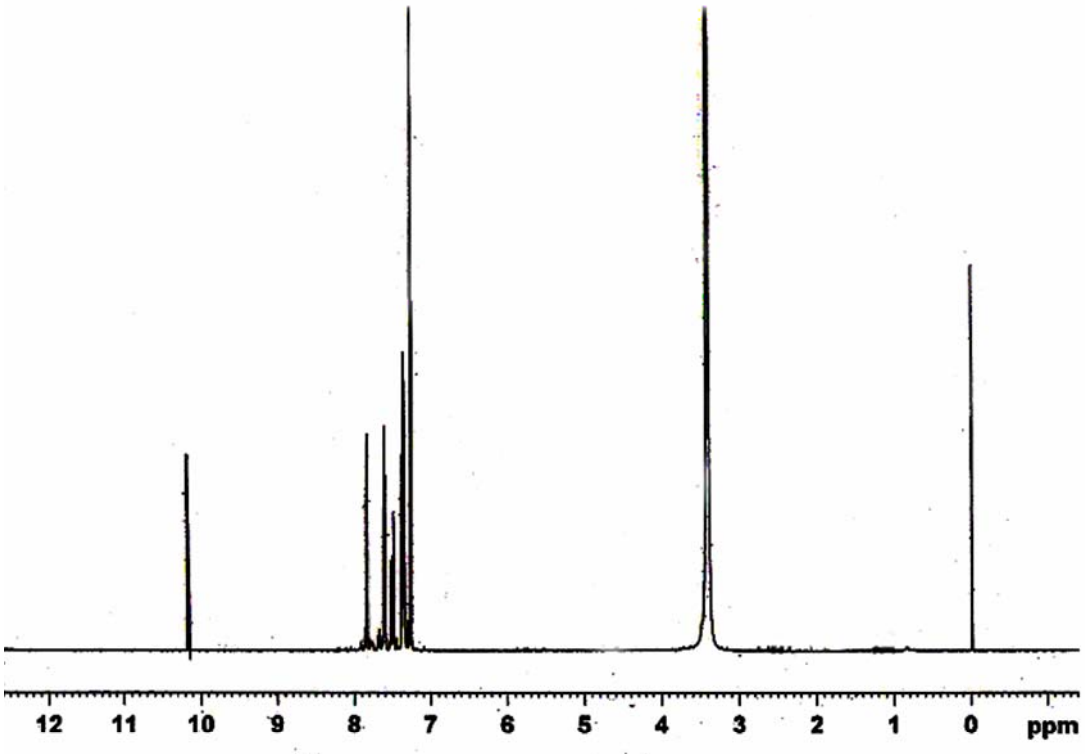

Figure 9: The ^{1}H NMR spectrum of hdmq in DMSO-d^{6}

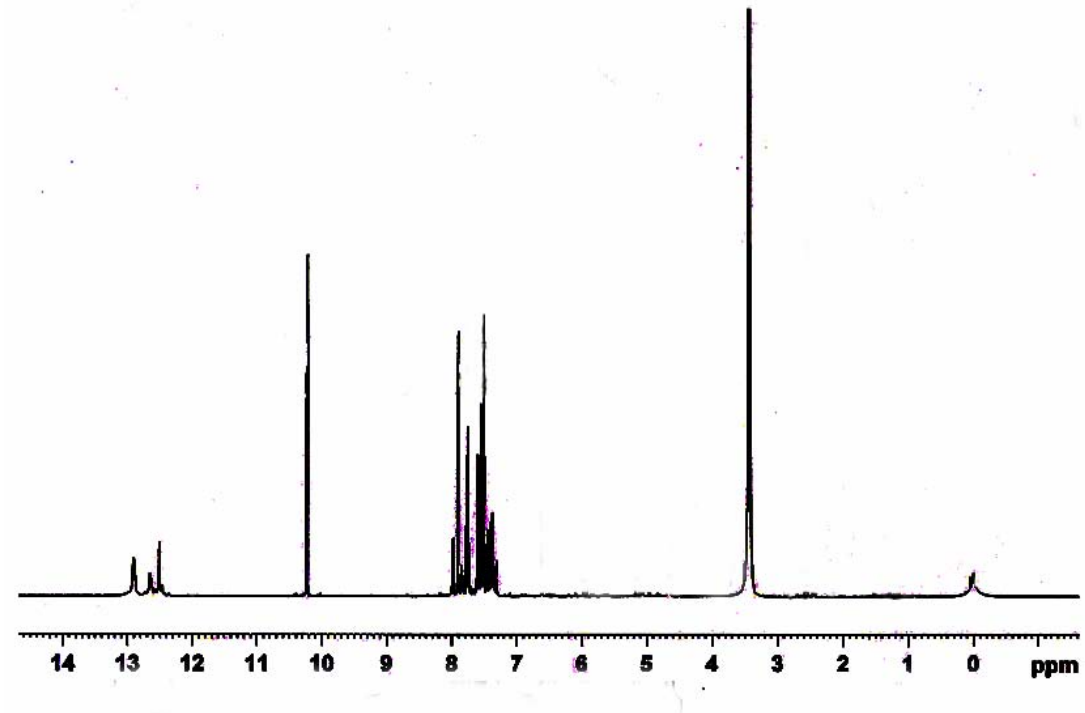

Figure 10: The ^{1}H NMR spectrum of hqc in DMSO-d^{6}

2.5 Synthesis of Schiff bases

2.5.1 Synthesis of N,N'-bis(3-hydroxyquinoxaline-2-carboxalidene)1,8-diaminonaphthalene (hqcdan-H_2)

To a solution of 3-hydroxyquinoxaline-2-carboxaldehyde (5 g, 28.7 mmol, in 500 mL distilled water), 3 to 4 drops of Con. HCl was added. An alcoholic solution of 1,8-diaminonaphthalene (2.3 g, 14.4 mmol) in methanol (20 mL) was added to this solution with constant stirring. The dark violet coloured Schiff base (Scheme 4) precipitated was filtered, washed with water and dried over anhydrous calcium chloride. Yield: 95%.

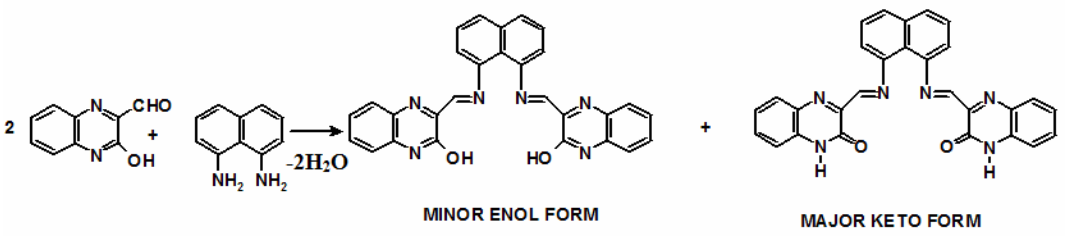

Scheme 4

2.5.2 Synthesis of N,N'-bis(3-hydroxyquinoxaline-2-carboxalidene)2,3-diaminomaleonitrile (hqcdmn-H_2)

To the solution of 3-hydroxyquinoxaline-2-carboxaldehyde (5 g, 28.7 mmol, in 500 mL distilled water), 3 to 4 drops of Con. HCl was added. An alcoholic solution of 2,3-diaminomaleonitrile (1.6 g, 14.4 mmol) in methanol (20 mL) was added to this solution drop by drop with constant stirring. The red coloured Schiff base (Scheme 5) precipitated was filtered, washed with water and dried over anhydrous calcium chloride. The crude product was recrystallised from absolute ethanol. Yield: (90%, 5.9 g)

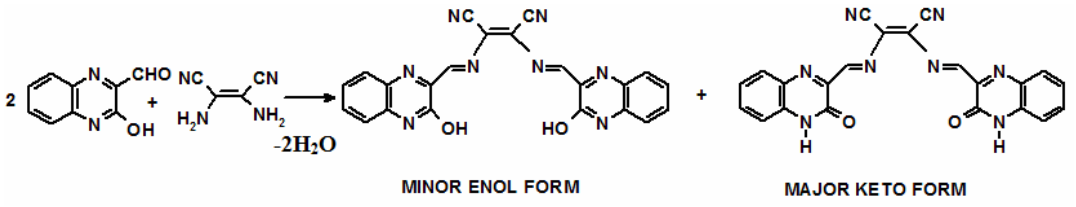

Scheme 5

2.5.3 Synthesis of N,N'-bis(3-hydroxyquinoxaline-2-carboxalidene)trans (R,R')1,2-diaminocyclohexane (hqcdac-H_2).

To the solution of 3-hydroxyquinoxaline-2-carboxaldehyde (5 g, 28.7 mmol, in 500 mL distilled water), 3 to 4 drops of Con. HCl was added. An alcoholic solution of trans(R,R')1,2-diaminocyclohexane (1.6 g, 14.4 mmol) in methanol (20 mL) was added to this solution by drop by drop with constant stirring. The yellow coloured Schiff base (Scheme 6) precipitated was filtered, washed with water and dried over anhydrous calcium chloride. The crude product was recrystallised from methanol. Yield: 70 %.

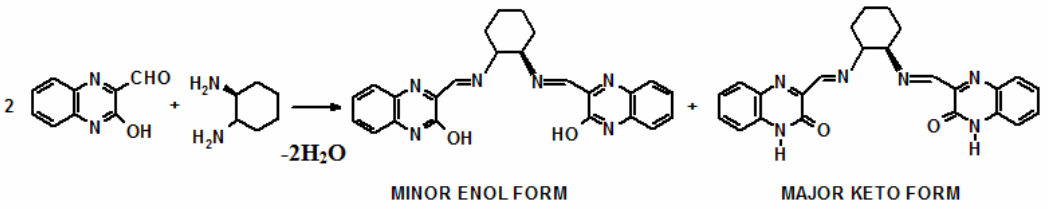

Scheme 6

2.5.4 Synthesis of 3-hydroxyquinoxaline-2-carboxalidene-2-aminophenol (hqcap-H_2)

To a solution of 3-hydroxyquinoxaline-2-carboxaldehyde (5 g, 28.7 mmol, in 500 mL distilled water), 3 to 5 drops of Con. HCl was added. An alcoholic solution of 2-aminophenol (3.1 g, 28.7 mmol) in methanol (20 mL) was added to this solution with constant stirring. The orange red Schiff base precipitated (Scheme 7) was filtered washed with water and dried over anhydrous calcium chloride in a desiccator. Yield: 90 %.

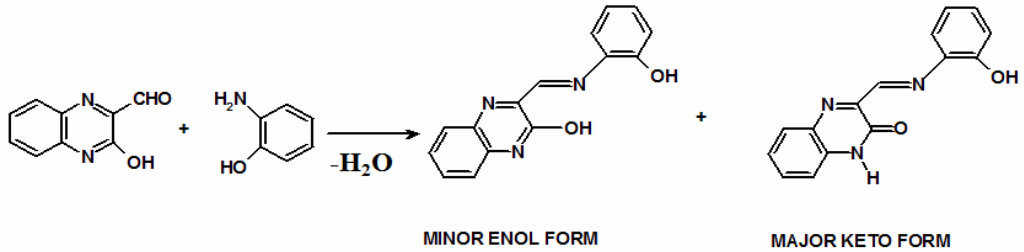

Scheme 7

2.5.5 Synthesis of 3-hydroxyquinoxaline-2-carboxalidene-4-aminoantipyrine (hqcaap-H)

To the solution of 3-hydroxyquinoxaline-2-carboxaldehyde (5 g, 28.7 mmol, in 500 mL distilled water), 3 to 5 drops of Con. HCl was added. An alcoholic solution of 4-aminoantipyrine (5.8 g, 28.7 mmol) in methanol (20 mL) was added to this solution with constant stirring. The orange red Schiff base (Scheme 8) precipitated was filtered, washed with water and dried over anhydrous calcium chloride. Yield: (90%, 9.3 g).

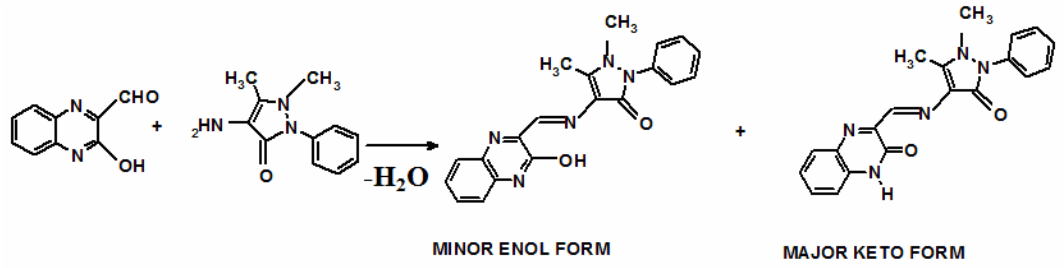

Scheme 8

2.6 Characterisation of the Schiff base ligands

Extensive spectroscopic investigations have been reported for 2-hydroxyquinoxalines and their derivatives but they have focused mainly on the prototropic equilibrium [13]. This amide-iminol tautomerism involves a fast hydrogen transfer between nitrogen and oxygen and they exist in the predominant amide form. The Schiff base ligands were characterised by elemental analysis, UV-visible spectra, diffuse reflectance spectra, FT-IR spectra and ^{1}H NMR spectra. The electrochemical behaviour and thermal stability of these Schiff bases were determined by cyclic voltammetry and TG-DTA analyses.

2.6.1 Elemental analyses

The analytical data of the Schiff base are in good agreement with molecular formula and are given in Table 6.

Table 6: Analytical data a of the Schiff base ligands

Schiff base	Molecular formula	Formula weight	Carbon (%)	Hydrogen (%)	Nitrogen (%)
hqcdan-H_2	$C_{28}H_{16}N_6O_2$	486.52	71.48 (71.41)	3.86 (3.83)	17.86 (17.84)
hqcdmn-H_2	$C_{22}H_{12}N_8O_2$	420.38	62.86 (62.78)	2.88 (2.72)	26.66 (26.42)
hqcdac-H_2	$C_{24}H_{22}N_6O_2$	426.47	67.59 (67.48)	5.20 (5.11)	19.71 (19.62)
hqcap-H_2	$C_{15}H_{11}N_3O_2$	265.27	67.92 (67.79)	4.18 (4.11)	15.84 (15.72)
hqcaap-H	$C_{20}H_{17}N_5O_2$	359.38	66.84 (66.68)	4.77 (4.65)	19.47 (19.32)

[a] Calculated values in parentheses

2.6.2 Electronic spectra

The electronic spectra of the Schiff bases in methanol exhibit three major peaks (Figure 11). The first two peaks are due to $\pi \rightarrow \pi^*$ transitions of the aromatic rings and $n \rightarrow \pi^*$ transitions in the quinoxaline ring of the Schiff bases [Table 7]. The $n \rightarrow \pi^*$ transitions of nonbonding electrons present on the nitrogen of azomethine group in the Schiff base appears as the third peak. Since the metal complexes of the Schiff bases are relatively less soluble in most of the solvents, we have recorded the electronic spectra in the diffuse reflectance mode also. Though the Schiff bases are soluble in almost all solvents their diffuse reflectance spectra (DRS) were also recorded with a view to compare them with that of the complexes. The diffuse reflectance spectra of all the Schiff bases also show three major bands (Table 8 and Figure 12). The first band in the range 243-253 nm is due to the $\pi \rightarrow \pi^*$ transitions of the aromatic rings and the second band in the range 315-361 nm is due to the $n \rightarrow \pi^*$ transition of the –C=N− group in quinoxaline ring [12]. The third band in the range 388-482 nm may be due to the azomethine $n \rightarrow \pi^*$ transition. All the absorption peaks are blue shifted in methanol with respect to the peaks in the

DRS spectrum. In solution, the ground state of Schiff bases is stabilized by hydrogen bonding with the solvent. In the excited state, the hydrogen bond of the molecule is almost completely broken or weakened to a larger extent. As a result the excited state is less stabilized and absorption is shifted to higher energy [14,15].

Table 7: UV-visible spectral data of Schiff base ligands in methanol (10^{-5} mol l^{-1})

Schiff base	λ_{max}(nm) ($\varepsilon_{max} \times 10^{-5}$ (L mol^{-1} cm^{-1}))
hqcdan-H_2	232(1.37), 323(0.43)
hqcdmn-H_2	223(1.14), 302(0.39), 448(0.67)
hqcdac-H_2	228(1.07), 318(0.35), 402(0.18)
hqcap-H_2	201(0.65), 206(0.54), 232(0.91), 276(0.29), 336(0.27), 465(0.21)
hqcaap-H	210(1.98), 224(1.90), 423(1.45)

Table 8: Diffuse reflectance spectral data of Schiff base ligands

Schiff base	λ_{max} (nm)
hqcdan-H_2	243, 326(sh), 355, 464(sh)
hqcdmn-H_2	246, 315, 415, 476
hqcdac-H_2	253, 319, 388
hqcap-H_2	248, 328(sh), 361, 417, 442(sh)
hqcaap-H	253, 354, 415(sh), 482, 625(sh)

Barium sulphate as the reference
sh = shoulder peak

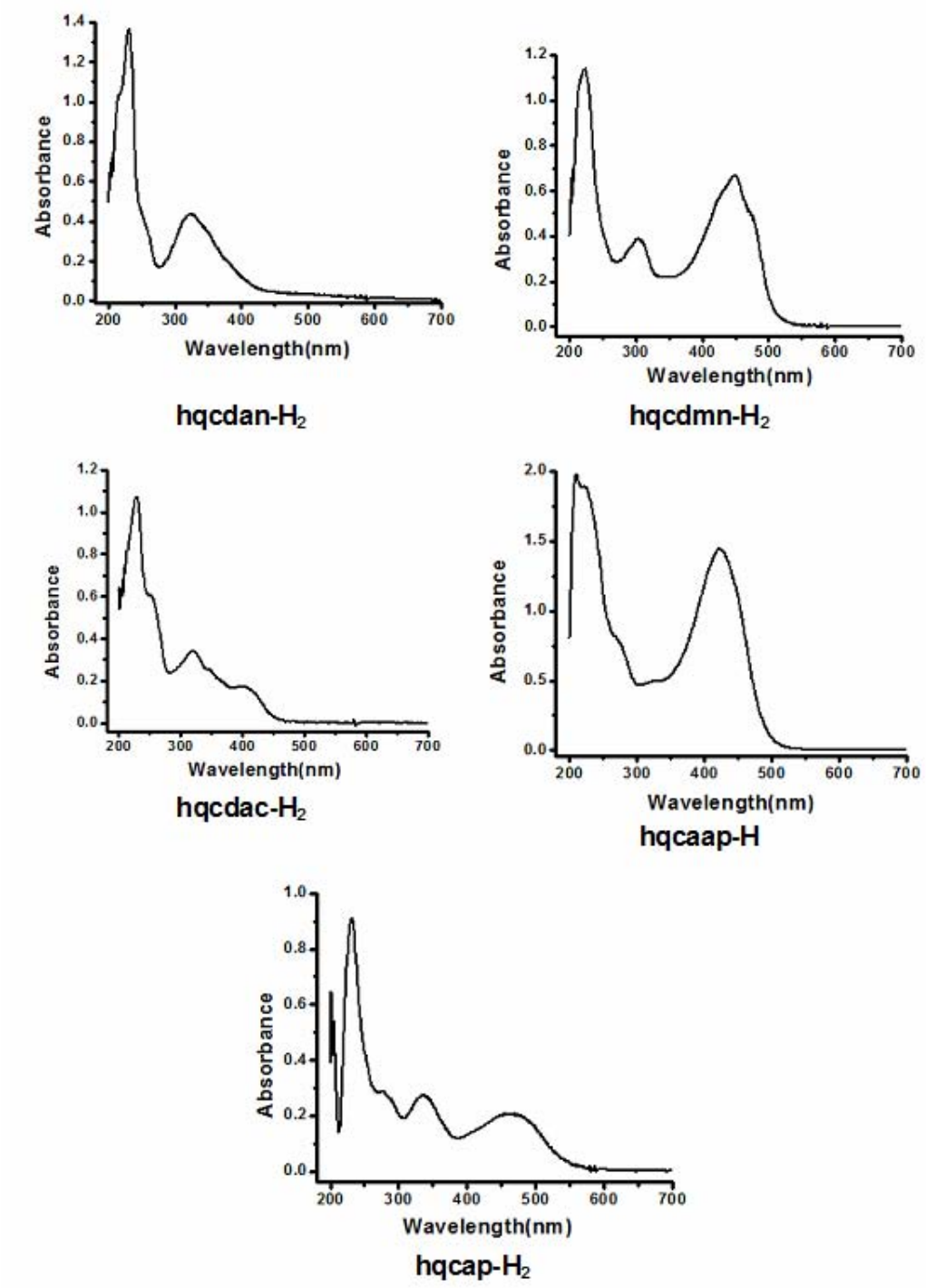

Figure 11: UV-visible spectra of Schiff base ligands in methanol (10^{-5} mol l^{-1})

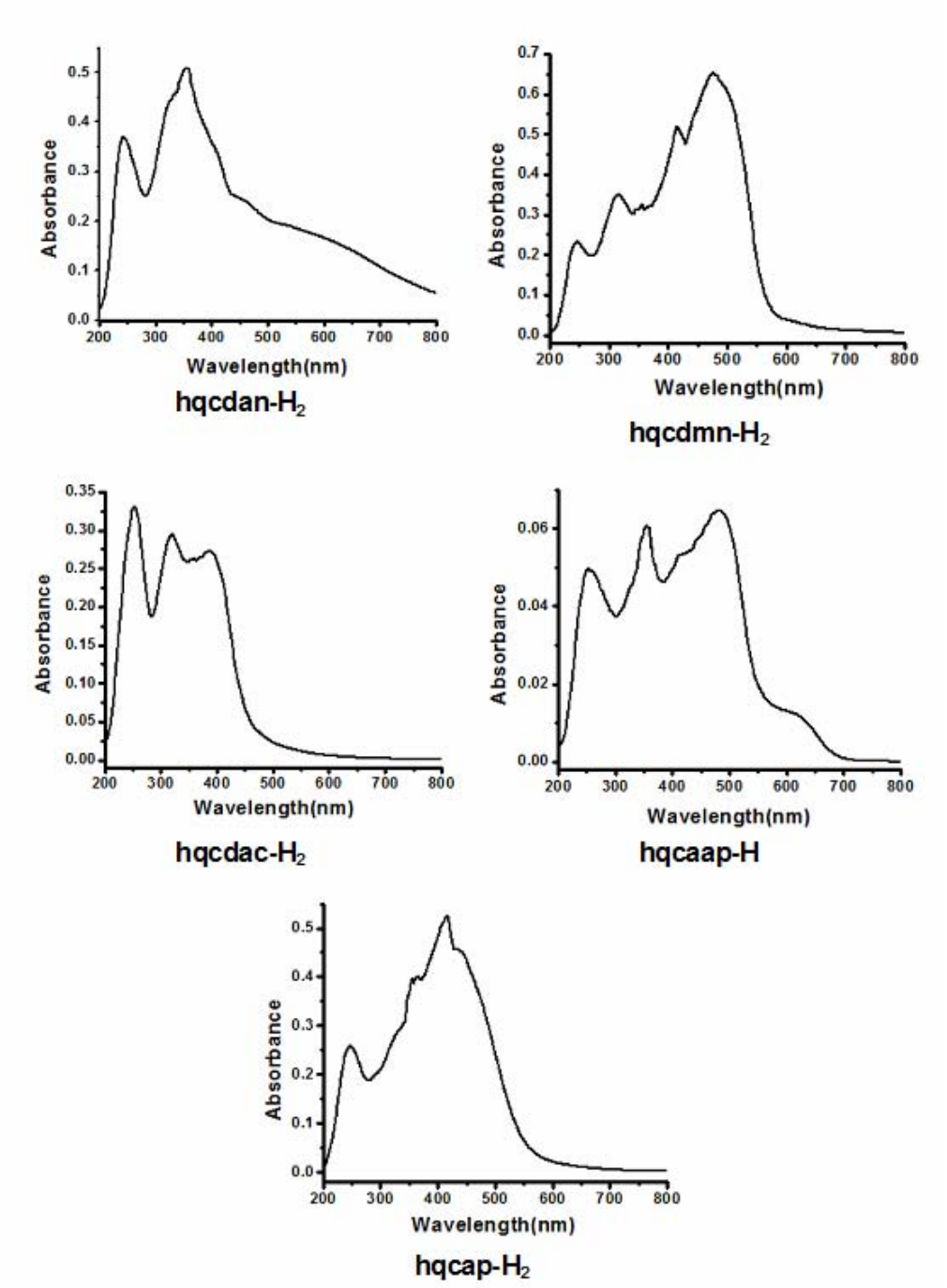

Figure 12: Diffuse reflectance spectra of Schiff base ligands

2.6.3 Infrared spectra

Infrared spectroscopy is identified to be an invaluable tool in the assessment of products obtained by the condensation of aldehyde and amines. Examination of the –NH2, –CH=O, and −C=N− regions of an infrared spectrum provided valuable structural information related to the structure of the Schiff bases. The IR spectra of all the Schiff bases (Figures 13-17) reveals a strong broad absorption band centered around 3410 cm^{-1}, which may be due to a hydrogen bonded $\nu_{(OH)}$ in the iminol tautomer or $\nu_{(NH)}$ in the amide tautomer. The medium intensity bands observed in the range 3168-2904 cm^{-1} correspond to asymmetric and symmetric stretching vibrations of the aromatic CH groups. In the case of tautomeric quinoxaline derivatives, particularly quinoxaline-2-ones, the IR stretching frequencies of the C=O and C=N (quinoxaline ring) vary from compound to compound and it is difficult to assign a particular range for these two types of stretching frequencies [16-27]. In the amide tautomeric form, these Schiff bases contain ketonic carbonyl groups which are evidenced by the presence of strong bands in the range 1633-1674 cm^{-1} [28]. Although these Schiff bases contain three different types of C=N bonds arising from the quinoxaline ring and azomethine linkage, they are not well resolved in the infrared spectrum of the ligand. In the spectra of all the Schiff bases, the azomethine –CH=N band is superimposed with the C=O group of the amide tautomer and appear as a weak band. The peaks that appear in the range 1597-1643 cm^{-1} may be due to stretching of the azomethine -CH=N group, whereas the bands in the range 1600-1525 cm^{-1} could be due to the ν(C=N) stretches of the quinoxaline ring (Table 9). A group of bands observed in the range 1215-930 cm^{-1} may be due to the aromatic in-plane deformation vibrations and fairly strong band near 820 cm^{-1} may be due to the =CH out-of-plane vibration. The medium intensity bands in the range 1306-1294 cm^{-1} may be due to the phenolic ν(C−O) stretch of the iminol form of the Schiff bases. The pyrazoline carbonyl stretch in the case of Schiff base, hqcaap-H, appears at 1656 cm^{-1} in good agreement with those derived from 4-aminoantipyrine and substituted salicylaldehydes [29]. The IR spectrum of hqcdmn-

H_2 may be easily fingerprinted by two very intense –C≡N bands at 2243 and 2202 cm^{-1} [30].

Table 9: Characteristic infrared spectral bands (cm^{-1}) for the Schiff base ligands

Schiff base	ν(O—H)[a]	ν(C=O)[b]	ν(C=N)[c]	ν(C=N)[d]	ν(C—O)[e]
hqcdan-H_2	3430	1633	1597	1540, 1524	1299
hqcdmn-H_2	3390	1674	1643	1598, 1554	1294
hqcdac-H_2	3434	1646	1625	1565, 1534	1290
hqcap-H_2	3412	1665	1606	1570, 1522	1300
hqcaap-H	3451	1670	1637	1591, 1545	1306

[a] ν(N−H)/ ν(O−H) of the free Schiff base, [b] C=O of the amide form of Schiff base, [c] −CH=N of azomethine group, [d] C=N of quinoxaline ring, [e] phenolic ν(C−O)

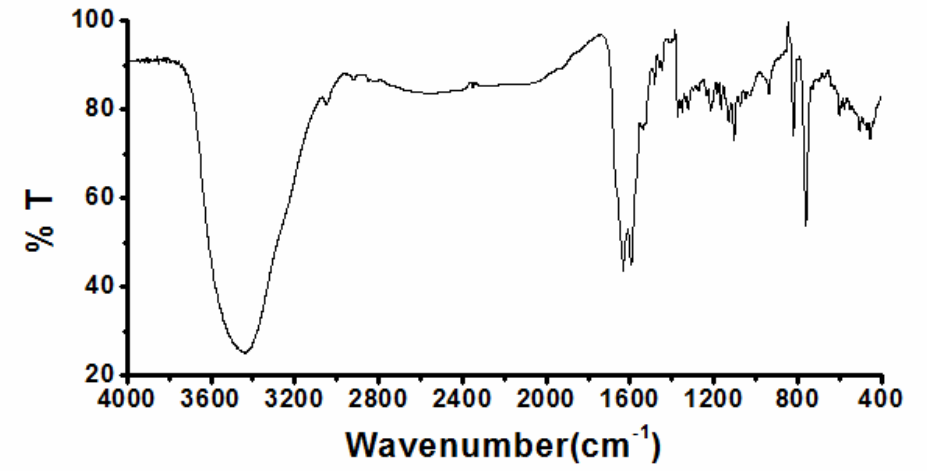

Figure 13: FT-IR spectrum of hqcdan-H_2

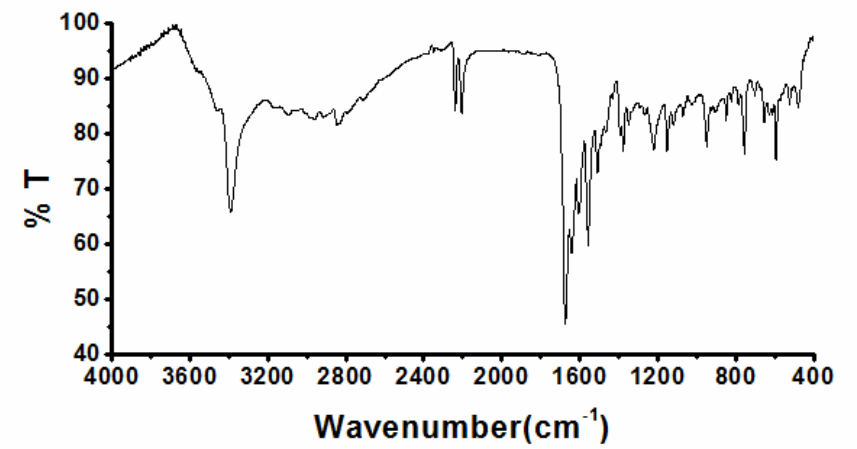

Figure 14: FT-IR spectrum of hqcdmn-H_2

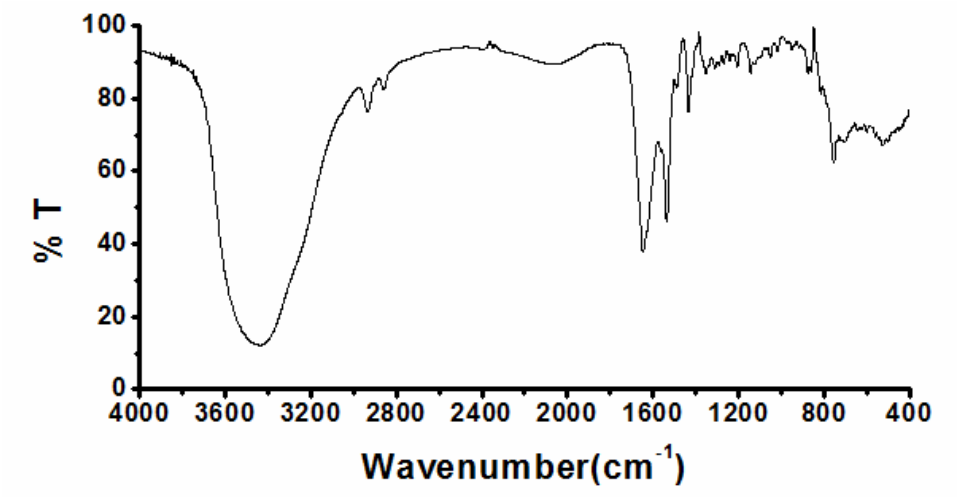

Figure 15: FT-IR spectrum of hqcdac-H_2

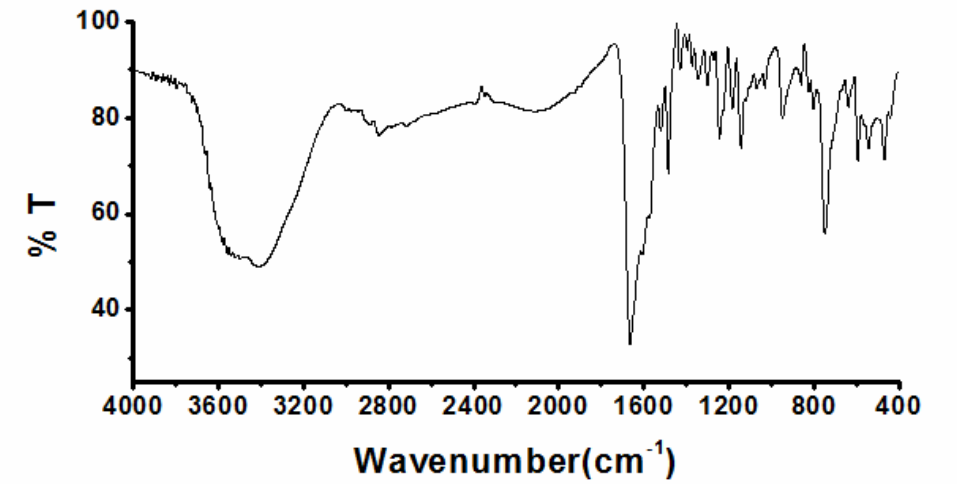

Figure 16: FT-IR spectrum of hqcap-H_2

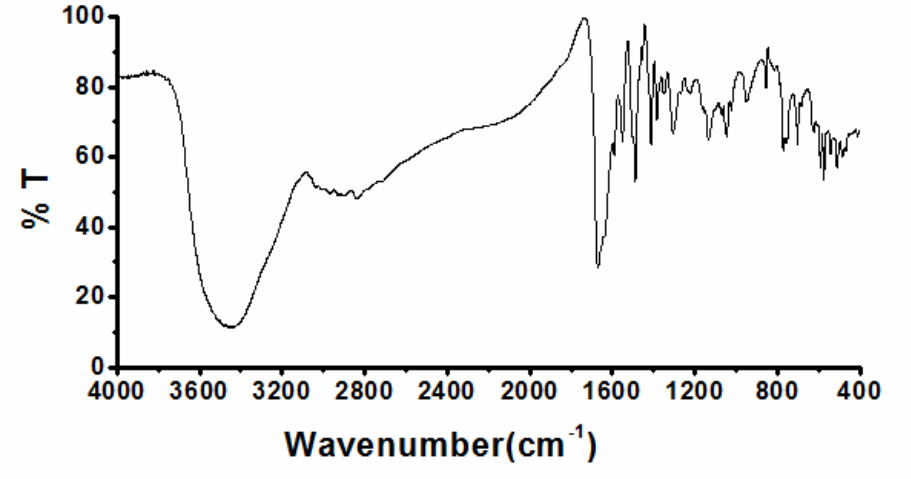

Figure 17: FT-IR spectrum of hqcaap-H

2.6.4 NMR spectra

The ^{1}H NMR spectra of Schiff bases (Figures 18-22) shows signals in confirmity with the tautomeric structure. The peaks observed in the range 12.2-13.4 ppm in these Schiff bases are assignable to the N—H proton of the amide tautomer or O—H of the iminol form [31]. The azomethine protons of the Schiff bases appear in the range 7.1-9.9 ppm. Multiplet signals observed in the 6.4-8.1 ppm range are due to the aromatic protons of the Schiff bases. The ^{1}H NMR data of the Schiff bases are given in Table 10.

Table 10: ^{1}H NMR data of the Schiff base

Schiff base	Assignments
hqcdan-H2	^{1}H NMR (500 MHz, $CDCl_3$, 298 K) δ p.p.m.: 6.43- 7.96 (aromatic protons), 7.14 (m, 1H, azomethine proton), 12.90 (s, 1H, Ar—OH or N—H).
hqcdmn-H2	^{1}H NMR (500 MHz, DMSO-d^6, 298 K) δ p.p.m.: 7.86-7.26 (aromatic protons), 8.98-8.53 (m, 2H, azomethine proton), 12.77, 12.67 (Ar—OH or N—H).
hqcdac-H2	^{1}H NMR δ p.p.m.: (500 MHz, MeOD, 296 K): δ = 0.5-3.5(protons of cyclohexane ring), 7.8-8.0 (aromatic protons), 8.5-8.7 (2H, azomethine protons), 12.2-12.4 (broad, Ar—OH or N—H).
hqcap-H2	^{1}H NMR δ p.p.m.: (500 MHz, MeOD, 296 K): δ = 7.1-8.1 (8H, Ar—H), 9.1-9.3 (1H, azomethine proton), 13.1-13.4 (broad, Ar—OH or N—H).
hqcaap-H	^{1}H NMR δ p.p.m.: (500 MHz, DMSO-d^6, 296 K): δ = 2.49 (s, 3H, C—CH_3), 3.27 (s, 3H, N—CH3), 7.28- 7.85 (9H, Ar—H), 9.98 (s, 1H, azomethine proton), 12.51 (s, 1H, Ar—OH or N—H).

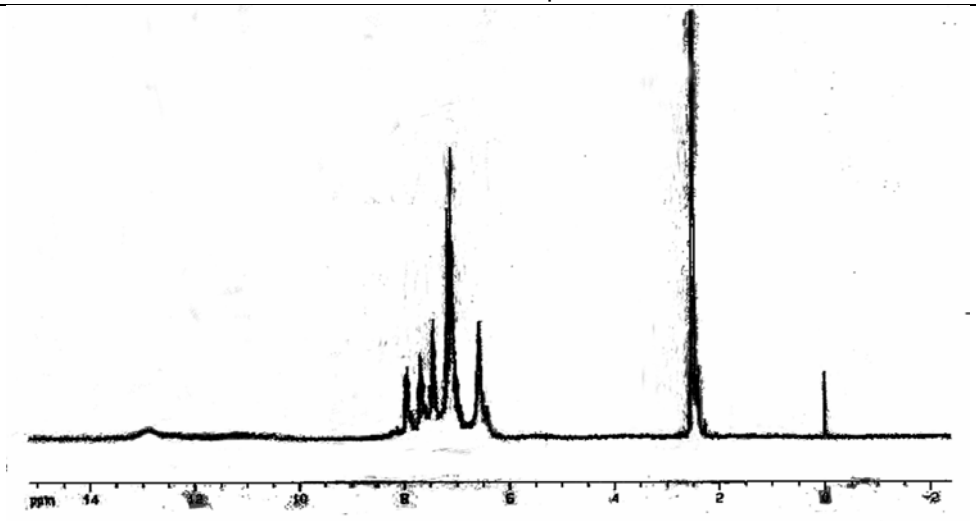

Figure 18. The ^{1}H NMR spectrum of hqcdan-H_2 in $CDCl_3$

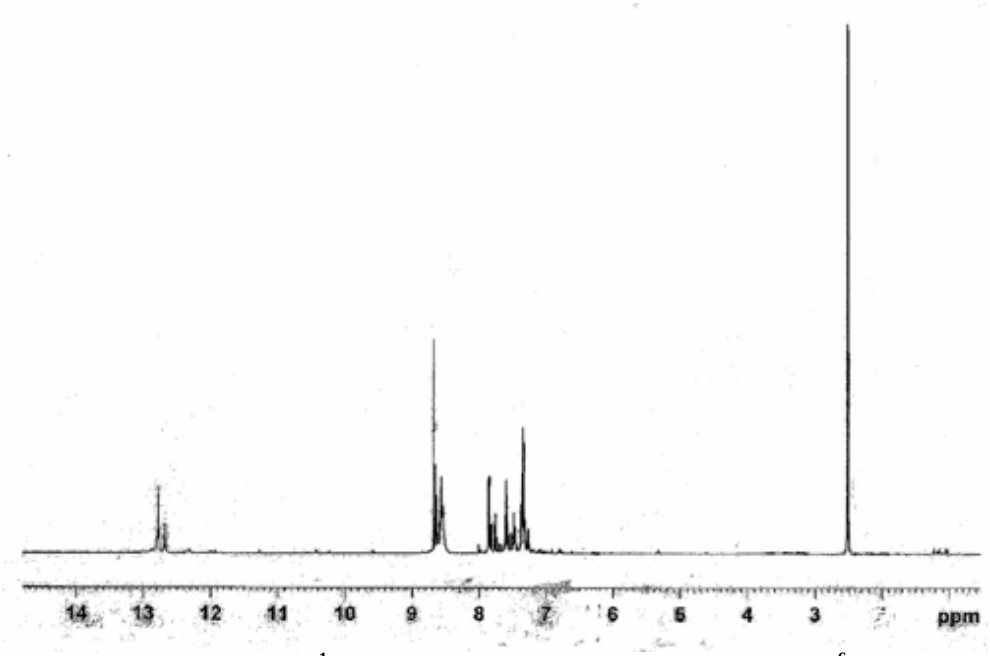

Figure 19: The ^{1}H NMR spectrum of hqcdmn-H_2 in DMSO-d^{6}

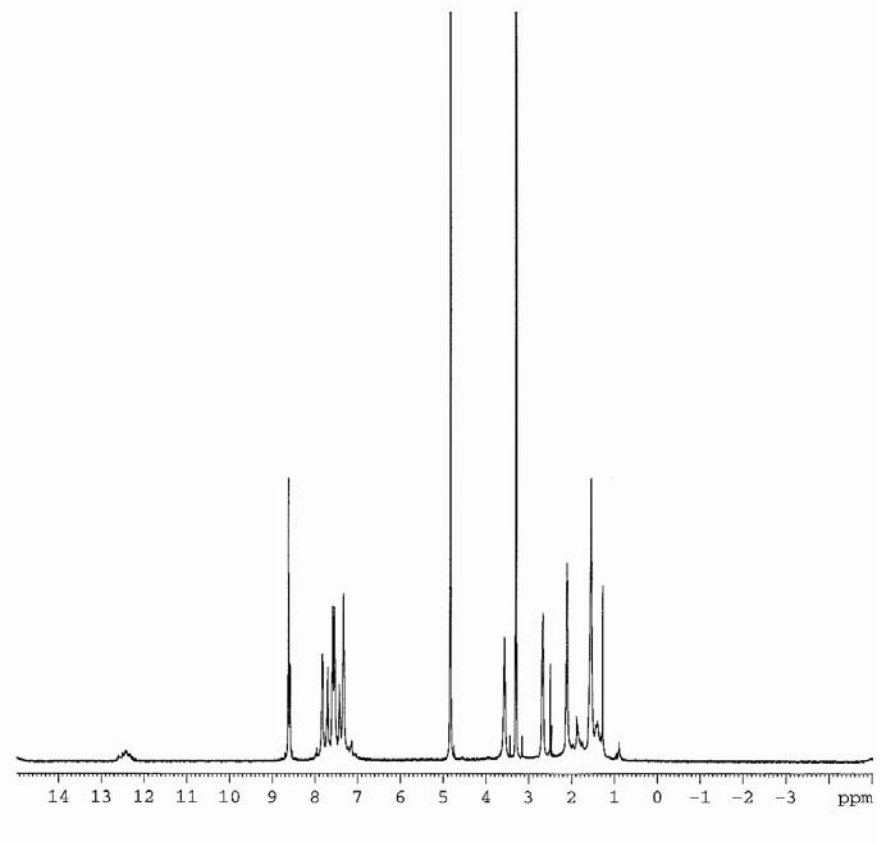

Figure 20: The ^{1}H NMR spectrum of hqcdac-H_2 in MeOD

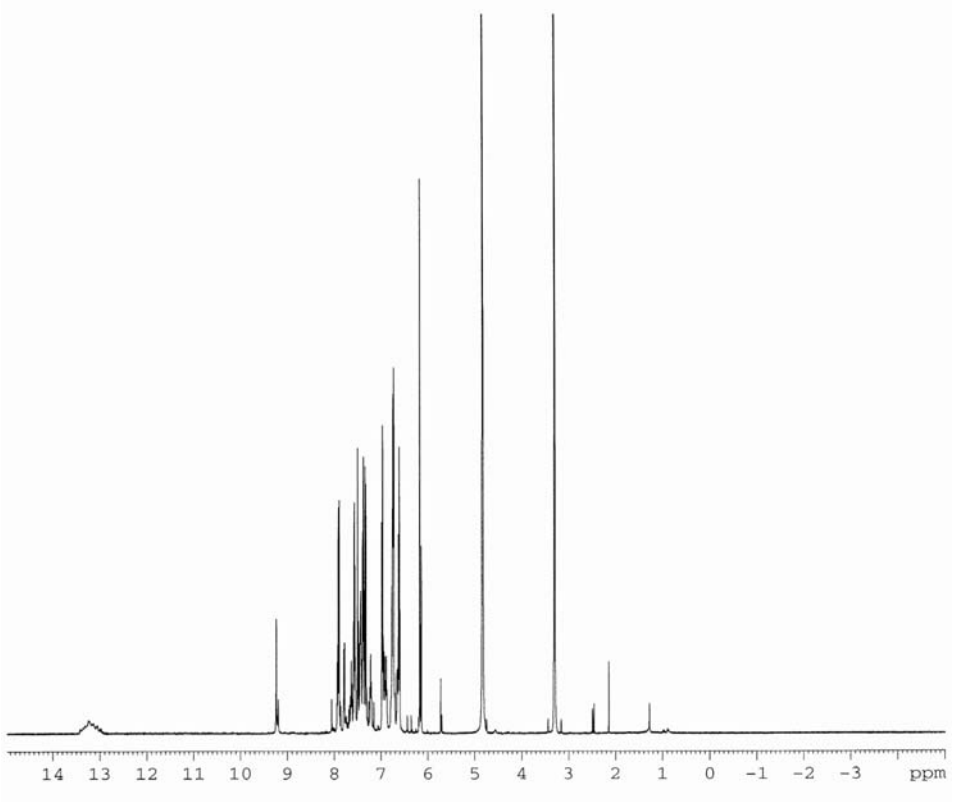

Figure 21: The ^{1}H NMR spectrum of hqcap-H_2 in MeOD

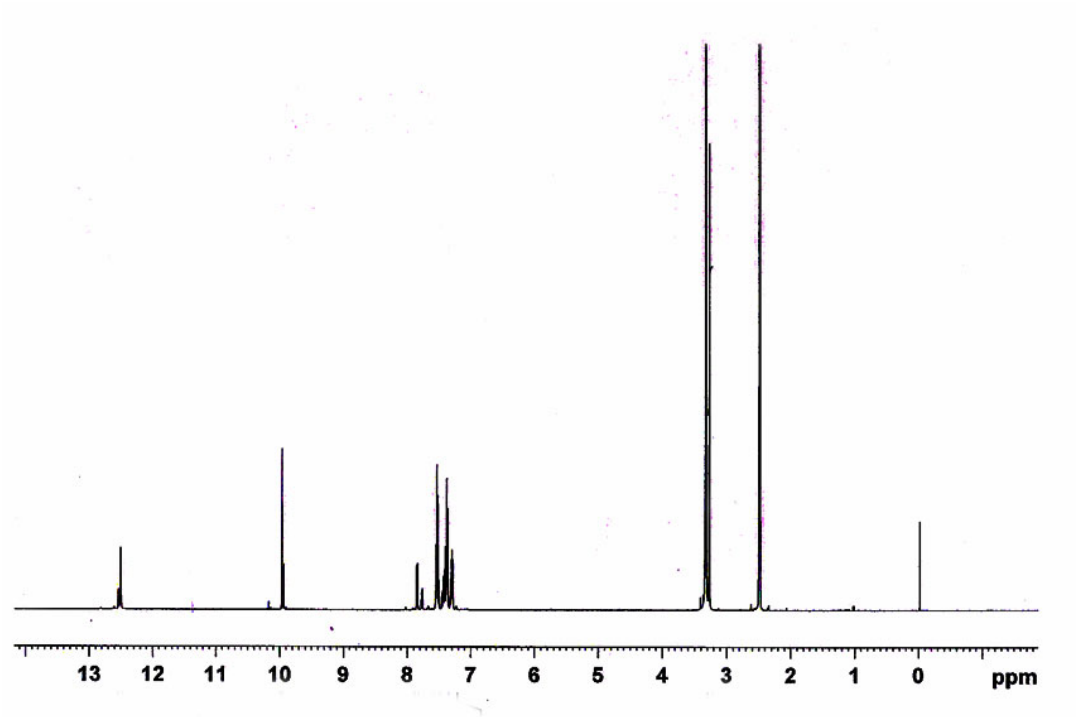

Figure 22: The ^{1}H NMR spectrum of hqcaap-H in DMSO-d^{6}

2.6.5 Cyclic voltammetric studies

The cyclic voltammetric behaviour of Schiff bases in a 1:1 mixture of methanol-tetrahydrofuran is characterised by one reduction peak and two oxidation peaks (Figure 23). The studies were done with Schiff base solutions (5×10^{-5} mol l^{-1}) and tetra n-butylammonium hexafluorophosphate (0.05 mol l^{-1}) as the supportimg electrolyte. The relatively less negative value of the reduction potential for these Schiff bases (Table 11) when compared to other pyrazine derivatives [32-34], could possibly be due to the presence of oxygen atoms bonded directly to the pyrazine ring of the ligand. The oxidation and reduction peaks appearing in the +1.5 to 0.0 V range in the cyclic voltammograms of all the Schiff bases are quasi-reversible and the E1/2 value for this redox couple falls in the range of 0.10 to 0.23 V. One electron transfer during the redox process is evident from the Ipc/Ipa values lying in the range 1.05 to 1.19 and further these observations point to the redox nature of the ligand. A comparative study of the cyclic voltammetric behaviour of the Schiff bases with its metal complexes could provide information on whether the redox reaction of the metal complexes is metal centered or ligand centered.

Table 11: Electrochemical data of Schiff bases in methanol-tetrahydrofuran at 298K

Schiff base	E_{pc} (mV)	E_{pa} (mV)	$E_{1/2}$ (mV)	I_{pc} (μV)	I_{pa} (μV)	No. of electrons (I_{pc}/I_{pa})
hqcdan-H_2	92	273; -906	183	6.64	6.32	1.05
hqcdmn-H_2	112	344; -898	228	4.17	3.79	1.10
hqcdac-H_2	116	96; -995	106	4.48	4.18	1.07
hqcap-H_2	165	179; -1009	172	2.73	2.73	1.19
hqcaap-H	191	8; -995	100	5.04	4.23	1.00

E_{pc} = anodic peak potential; E_{pa} = cathodic peak potential; I_{pc} = anodic peak current; I_{pa} = cathodic peak current; $E_{1/2} = 0.5 \times (E_{pa} + E_{pc})$; scan rate 50 mV

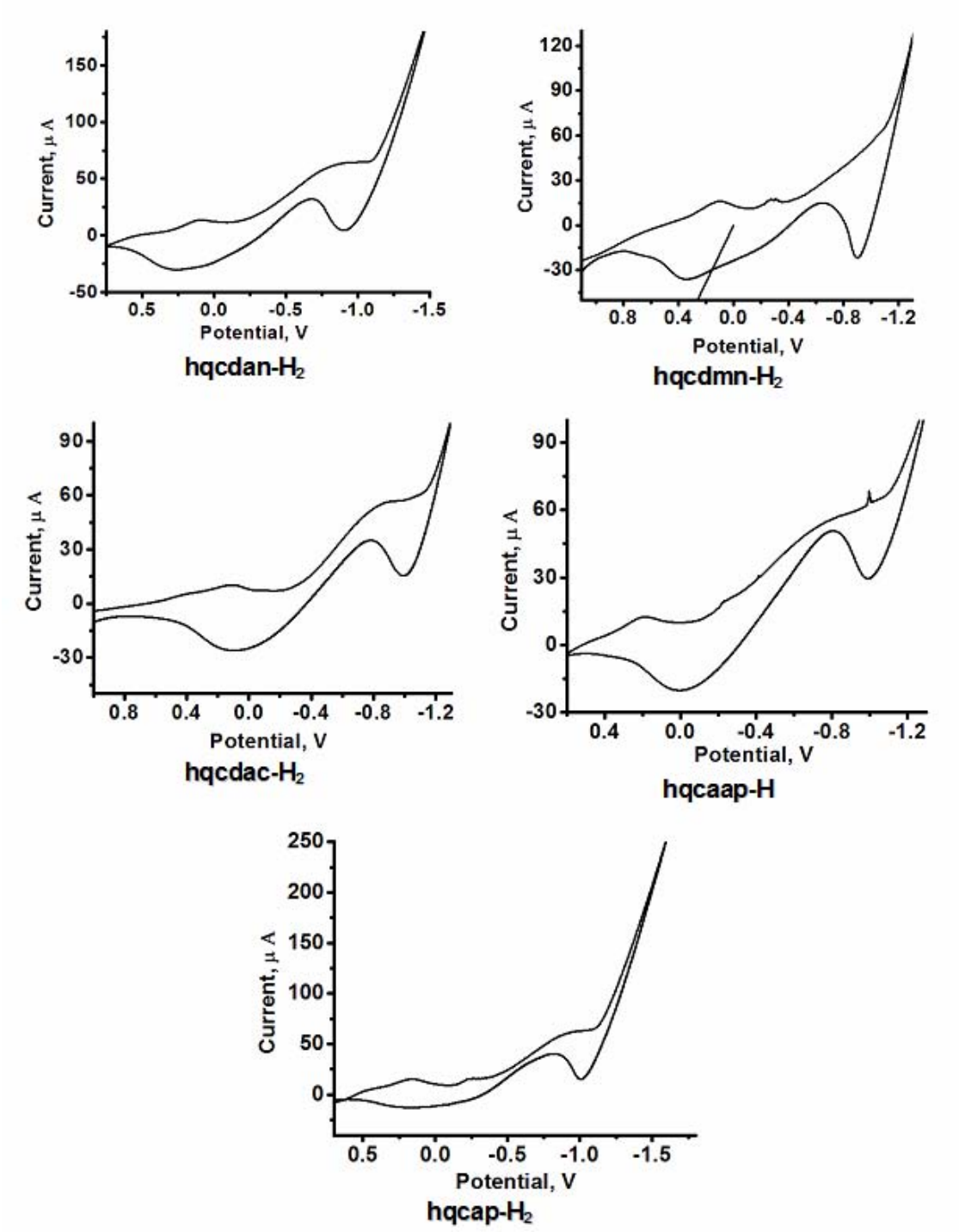

Figure 23: Cyclic voltammograms of the Schiff base ligands

2.6.6 Thermal studies

The thermal properties of Schiff bases and their metal complexes were investigated by TG-DTA measurements with a view to compare their thermal stabilities. The thermograms of the Schiff bases in nitrogen and air are given in Figures 24-28. The thermograms reveal that these compounds do not have a sharp melting point. The results of the thermal studies of the Schiff base metal complexes are presented in detail in the respective chapters.

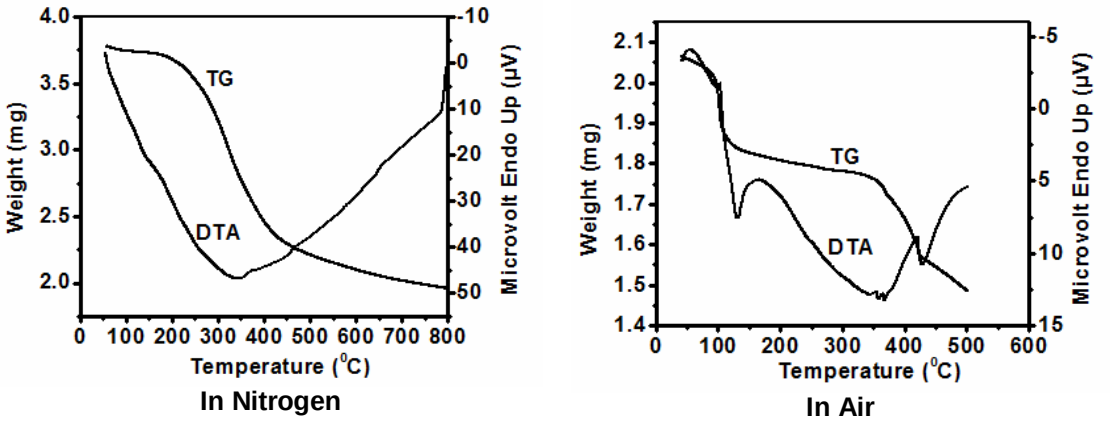

Figure 24: TG-DTA curves of hqcdam-H_2

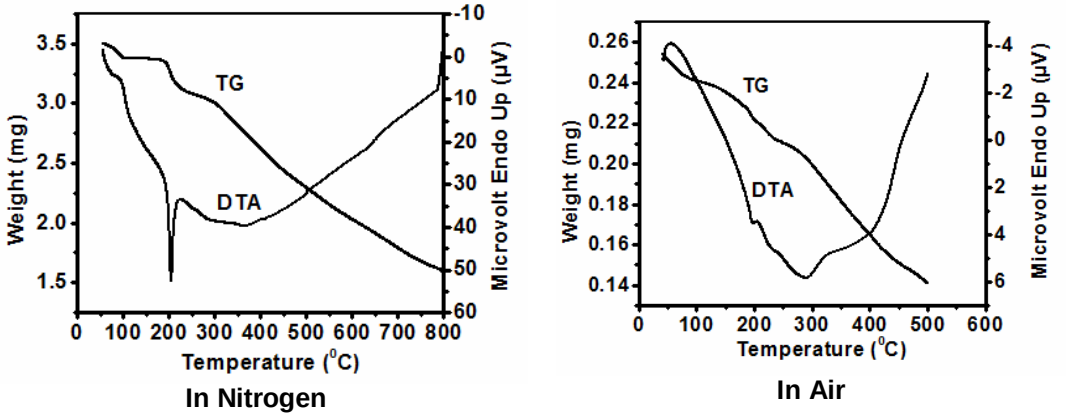

Figure 25: TG-DTA curves of hqcdmn-H_2

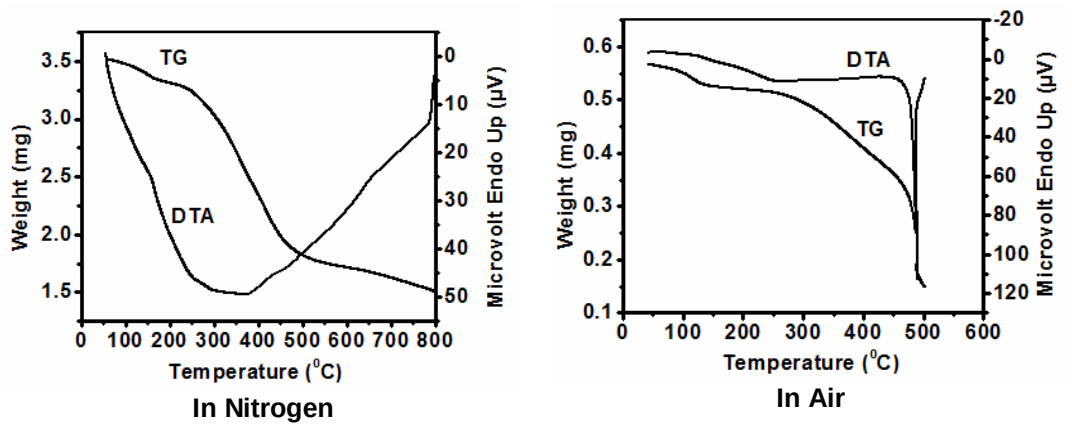

Figure 26: TG-DTA curves of hqcdac-H_2

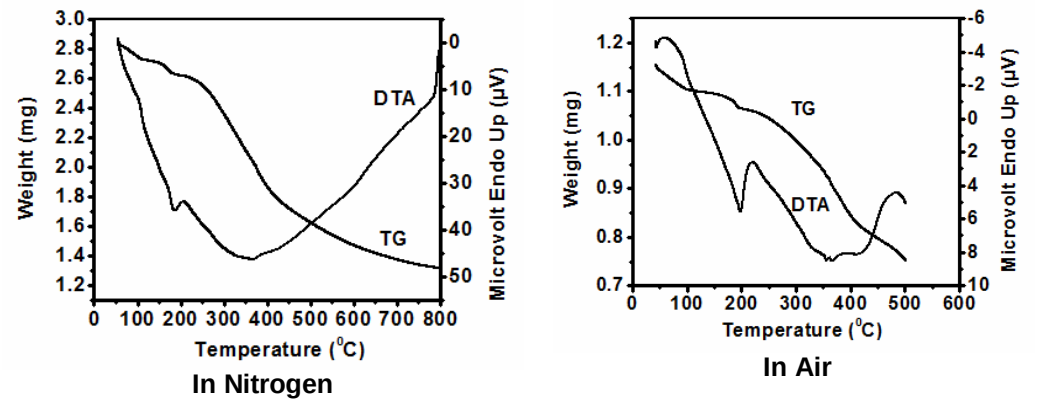

Figure 27: TG-DTA curves of hqcap-H_2

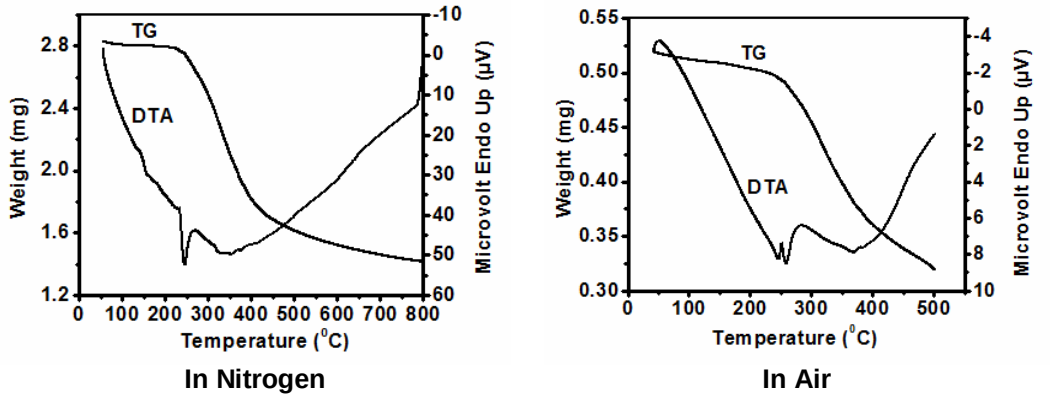

Figure 28: TG-DTA curves of hqcaap-H

Conclusions

This chapter deals with the details on various experimental and characterization techniques employed in the present study. The syntheses and characterization of the five new Schiff bases, N,N'-bis(3-hydroxyquinoxaline-2-carboxalidene)1,8-diaminonaphthalene (hqcdan-H_2), N,N'-bis(3-hydroxyquinoxaline-2-carboxalidene)2,3-diaminomaleonitrile (hqcdmn-H_2), N,N'-bis(3-hydroxyquinoxaline-2-carboxalidene)trans(R,R')1,2-diaminocyclohexane (hqcdac-H_2), 3-hydroxyquinoxaline-2-carboxalidene-2-aminophenol (hqcap-H_2) and 3-hydroxyquinoxaline-2-carboxalidene-4-aminoantipyrine (hqcaap-H), are also described in detail. The formation of these Schiff bases via the condensation of 3-hydroxyquinoxaline-2-carboxaldehyde with amines such as 1,8-diaminonaphthalene, 2,3-diaminomaleonitrile, trans-(R,R')1,2-diaminocyclohexane, 2-aminophenol and 4-aminoantipyrine have been confirmed with the aid of spectroscopic techniques such as FT-IR, UV-visible, NMR. The present organic Schiff bases, like other 2-hydroxyquinoxaline analogues, are found to exhibit prototropic tautomerism.

References

[1] D.D. Perrin, W.L.F Armarego, Purification of Laboratory Chemicals, Third Ed,; New York, Pergamon, 1998.

[2] A.I. Vogel, A Text Book of Quantitative Inorganic Analysis, Third Ed.; Longman, London, 1978.

[3] M. Goldweber, H.P. Schultz, Journal of American Chemical Society, 76 (1954) 287-288

[4] G. H. C. Woo, J. K. Snyder, Z. -K. Wan. Progress in Heterocyclic Chemistry, 14 (2002) 279-309.

[5] S. Ajaikumar, A. Pandurangan, Applied Catalysis A: General, 357 (2009) 184–192

[6] P. Thirumurugan, D. Muralidharan, P.T. Perumal, Dyes and Pigments, 81 (2009) 245–253

[7] H-J. Son, W-S. Han, D-H. Yoo, K-T. Min, S-N. Kwon, J. Ko, S.O. Kang, Journal of Organic Chemistry, 74 (2009) 3175–3178

[8] H. Ohle, G. Noetzel, Chemische Berichte, 76B (1943) 624

[9] O. Hinsberg, Annales de Chimie, 237 (1887) 340

[10] M.A. Verity, R. Gallagher, W.J. Brown, Biochemical Journal, 103 (1967) 375-381

[11] C. Bruckner, Chemische Berichte, 24 (1891) 3001

[12] Y.J. Seok, K.S. Yang, S.T. Kim, W.K. Huh, S.O. Kang, Journal of carbohydrate chemistry 15 (1996) 1085-1096

[13] G.W.H. Cheeseman, E.S.G. Werstiuk, Advances in Heterocyclic Chemistry, 22 (1978) 367-431

[14] M. Ahmed, Z.H. Khanl, Spectrochimica Acta Part A: Molecular and Biomolecular Spectroscopy, 56 (2000) 965-981

[15]Y. Hao, B. Xu, Z. Gao, H. Wang, H. Zhou, X. Liu, Journal of Materials Science and Technology, 22 (2006) 225-229

[16] R.M. Ramadan, M.S.A. Hamza, A.E.M. Salem, F.M. El-Zawawy, Transition Metal Chemistry, 24 (1999) 193-197

[17] S-K. Lin, Molecules, 1 (1996) 37-40

[18] R. Touzani, T. Ben-Hadda, S. Elkadiri, A. Ramdani, O. Maury, H. Le Bozec, L. Toupet, P.H. Dixneuf, New Journal of Chemistry, 25 (2001) 391-395

[19] A. Gazit, H. App, G. McMahon, J. Chen, A. Levitzki, F.D. Bohmer, Journal of Medicinal Chemistry, 39 (1996) 2170-2177

[20] V.L. Gein, A.V. Kataeva, L.F. Gein, Chemistry of Heterocyclic Compounds 43 (2007) 1385 - 1389

[21] V.A. Mamedov, A.A. Kalinin, A.T. Gubaidullin, O.G. Isaikina, I.A. Litvinov, Russian Journal of Organic Chemistry, 41 (2005) 599-606

[22] K.S. Bozdyreva, Z.G. Aliev, A.N. Maslivets, Russian Journal of Organic Chemistry, 44 (2008) 607-611

[23] V.A. Mamedov, A.A. Kalinin, A.T. Gubaidullin, T.K. Rizvanov, A.V. Chernova, G.M. Doroshkina, I.A. Litvinov, Y.A. Levin, Russian Journal of Organic Chemistry, 39 (2003) 131-140

[24] I. V. Mashevskaya, I. A. Tolmacheva, E. V. Voronova, T. F. Odegova, G. A. Aleksandrova, A. F. Goleneva, S. V. Koltsova, A. N. Maslivets, Pharmaceutical Chemistry Journal, 36(2) (2002) 86-88.

[25] M. Barbasiewicz, A. Szadkowska, R. Bujok, K. Grela, Organometallics, 25 (15) (2006) 3599-3604

[26] E.R. Kotb, M.A. Anwar, M.S. Soliman, M.A. Salama, Phosphorus, Sulfur, and Silicon and the Related Elements, 182 (2007) 1119-1130

[27] A. Cuenca, Langmuir, 16 (2000) 72-75

[28] V.A. Mamedov, A.A. Kalinin, N.M. Azancheev, Y.A. Levin. Russian Journal of Organic Chemistry, 39 (2003) 125-30

[29] P.M. Selvakumar, E. Suresh, P.S. Subramanian, Polyhedron, 26 (2007) 749-756

[30] M.J. MacLachlan, M.K. Park, L.K. Thompson, Inorganic Chemistry, 35 (1996) 5492-5499

[31] V.A. Mamedov, D.F. Saifina, E.A. Berdnikov, I. Kh. Rizvanov, Russian Chemical Bulletin, 56 (2007) 2127-2130

[32] S.M. Molnar, K.R. Neville, G.E. Jensen, K.J. Brewer, Inorganica Chimica Acta, 206 (1993) 69−76

[33] S. Roffia, M. Marcaccio, C. Paradisi, F. Paolucci, V. Balzani, G. Denti, S. Serroni, S. Campagna, Inorganic Chemistry, 32 (1993) 3003-3009

[34] D.L. Carlson, W.R. Murphy Jr, Inorganic Chimica Acta, 181 (1991) 61−64

Chapter 3

Synthesis and characterisation of oxovanadium(IV) complexes

Contents

3.1 Introduction

Vanadium is an element with a very rich chemistry. It forms large array of compounds in which the most important oxidation states are +3, +4, and +5 [1]. The oxovanadium ion (IV) (i.e. VO^{2+} or vanadyl ion) finds itself an important place among these ions. This is largely due to the increasing importance of the ion in biological systems and also due to the interesting fact that the coordination number and geometry of the metal ion is highly ligand dependent [2-5]. Its toxicity is also less as compared with the vanadate ion [6].

Oxovanadium(IV) salts are known to form stable complexes with bi, tri and tetradentate Schiff bases. In these complexes V(IV) could exists in a five or six coodinated state [7-10]. A square pyramidal or distorted trigonal bipyramidal structure is observed for five coordinated complexes [11] while distorted octahedral geometry are reported for the six coordinate ones [12]. Furthermore, polymeric structures have been proposed for some V(IV) complexes of tetradentate Schiff bases [9,13,14], with low values of V=O stretching frequencies. This lowering of the V=O stretching frequencies is considered to be an indication of the existence of oxygen-bridging units of the type V−O−V [15] in these complexes.

Recognition of the importance of metal complexes with Schiff base ligands in the field of catalysis has prompted researchers to give more attention to these ligands [16-20]. A number of tridentate and tetradentate Schiff-base

oxovanadium(IV) complexes were found to give quick response in the conversion of methyl phenyl sulfide to the corresponding sulfoxide [21,22]. In recent years several vanadium complexes of multidentate ligands containing O and N donor sites were tested for catalysis of bromide oxidation [23]. A number of reports have appeared on the Schiff base complexes of $VOSO_4$ containing salicyldehyde and several monoamines and diamines [24-33] but only little attention has been given to the complexes of $VOSO_4$ with heterocyclic Schiff bases [34-36]. Herein, we describe the synthesis and spectral characterisation of oxovanadium(IV) complexes of the Schiff bases derived from the heterocyclic 3-hydroxyquinoxaline-2-carboxaldehyde.

3.2 Experimental

3.2.1 Materials

The details of materials used for the syntheses of Schiff base ligands have been given in Chapter 2. The metal salt used is oxovanadyl sulphate.

3.2.2 Synthesis of Schiff base ligands

The syntheses of Schiff base ligands have been discussed in detail in Chapter 2

3.2.3 Synthesis of complexes

All the oxovanadium(IV) complexes were synthesised by the following general procedure. The complexes were prepared by mixing an aqueous solution (10 mL) of the salt $VOSO_4.2H_2O$ (5 mmol, 1.27 g) and an alkaline solution of the ligand, hqcdan-H_2 (5 mmol, 2.43 g), hqcdmn-H_2 (5 mmol, 2.10 g), hqcdac-H_2 (5 mmol, 2.13 g), hqcap-H_2 (5 mmol, 1.80 g) or hqcaap-H (5 mmol, 1.33 g) in distilled water (250 mL) with a ligand to metal molar ratio 1:1. Equivalent amounts of NaOH were added to deprotonate the phenolic OH group of the Schiff base ligand. The solid mass which precipitated out is collected, washed with 1: 9 methanol-water

followed by petroleum ether and dried over anhydrous calcium chloride in a desiccator.

3.3 Results and discussion

Oxovanadium(IV) complexes of all the five ligands have been synthesized by the reaction of $VOSO_4.2H_2O$ and the respective ligands in methanol–water (1:6) with stirring in the presence of equivalent amount of NaOH, in order to convert this keto form of the Schiff base to enolate form, which renders the coordination of enolate oxygen. All the complexes are brown, non-hygroscopic solids. They are soluble in acetonitrile, DMF, ethanol and nitrobenzene but insoluble in benzene. However, our attempts to grow single crystals suitable for X-ray crystal structure determination were not successful.

3.3.1 Elemental analyses

The analytical data suggest that all the complexes are binuclear with the deprotonated ligand coordinated to two vanadium(IV) ions. Formulae have been computed for the complexes and are given in Table 1. Complexes I, II, III and V contain one sulphate group, which is evidenced by the percentage of sulphur in these complexes.

Table 1: Analytical data a of the oxovanadium(IV) complexes

Compound	Molecular formula	Formula weight	V (%)	C (%)	H (%)	N (%)	S (%)
$[(VO)_2(hqcdan)SO_4].H_2O$ **I**	$C_{28}H_{18}N_6O_9SV_2$	716.43	14.17 (14.22)	46.88 (46.94)	2.48 (2.53)	11.65 (11.73)	4.42 (4.48)
$[(VO)_2(hqcdmn)SO_4].H_2O$ **II**	$C_{22}H_{12}N_8O_9SV_2$	666.33	15.20 (15.29)	39.59 (39.66)	1.77 (1.82)	16.77 (16.82)	4.75 (4.81)
$[(VO)_2(hqcdac)SO_4].H_2O$ **III**	$C_{24}H_{22}N_6O_9SV_2$	672.42	15.06 (15.15)	42.81 (42.87)	3.26 (3.30)	12.45 (12.50)	4.69 (4.77)
$[(VO)_2(hqcap)_2].H_2O$ **IV**	$C_{30}H_{20}N_6O_7V_2$	678.40	14.98 (15.02)	53.06 (53.11)	2.88 (2.97)	12.32 (12.39)	- -
$[(VO)_2(hqcaap)_2SO_4].2H_2O$ **V**	$C_{40}H_{36}N_{10}O_{12}SV_2$	982.72	10.33 (10.37)	48.84 (48.89)	3.63 (3.69)	14.19 (14.25)	3.22 (3.26)

[a] Calculated values in parentheses

3.3.2 Molar conductivity and magnetic susceptibility measurements

The observed molar conductance values (Table 2) in 10^{-3} M DMF indicate non-electrolytic nature of the complexes [37]. The room temperature magnetic moment (μ_{eff}) values of the five oxovanadium(IV) complexes are in the range of 0.98–1.62 B.M (Table 2). These values are much smaller than the spin-only moment for a d1 system. The subnormal magnetic moments can be considered as due to an exchange interaction between vanadium(IV) ions [38,39]. The values are in good agreement with the molecular formulae obtained from elemental analysis and the proposed binuclear structures. There are several reports on such binuclear structures proposed for a number of oxovanadium(IV) complexes with subnormal magnetic moments [40-47]

Table 2: Magnetic moment values and molar conductance data of the oxovanadium(IV) complexes.

Complex	μ_{eff} (BM) [a]	Molar conductance (ohm^{-1} cm^2 mol^{-1})
$[(VO)_2(hqcdan)SO_4].H_2O$ (I)	1.02	4.8
$[(VO)_2(hqcdmn)SO_4].H_2O$ (II)	1.62	4.2
$[(VO)_2(hqcdac)SO_4].H_2O$ (III)	1.44	5.2
$[(VO)_2(hqcap)_2].H_2O$ (IV)	0.98	5.4
$[(VO)_2(hqcaap)_2SO_4].2H_2O$ (V)	1.28	5.6

[a] Magnetic moment value per vanadium atom in the complex

3.3.4 Cyclic voltammetry

The electrochemical properties of complexes have been studied using cyclic voltammetry and results are tabulated in Table 3. The cyclic voltammograms for all the complexes in DMSO (Figure 1) consist of an irreversible reduction wave in the range −0.865 to −1.237 V. This irreversible reduction may be attributed to reduction of V^{IV} to V^{III}. The V^{IV} to V^{V} oxidation in these complexes occurred in the range +0.647 to +965 V (irreversible). Similar observations have been made by Rao et al

in the case of binuclear oxovanadium(IV) Schiff base complexes derived form aryl hydrazones [48]. Since the $E_{1/2}$ values for the free Schiff base ligands lies in the range +0.100 to +0.228 V (Chapter 2), the above oxidation and redox processes are not ligand centered, but metal centered. However, we can see a reversible redox wave at $E_{1/2}$ = +0.206 V (E_{pc} = +0.132; E_{pa} = +0.279 V) in the case of I, which is probably due to the oxidation-reduction of the ligand in the complex.

Table 3: Cyclic voltammetric data of oxovanadium(IV) complexes in DMSO.

Complex	$V^{IV,III}$ (V)	$V^{IV,V}$ (V)
$[(VO)_2(hqcdan)SO_4].H_2O$ (I)	-1.237	0.825
$[(VO)_2(hqcdmn)SO_4].H_2O$ (II)	-1.035	0.707
$[(VO)_2(hqcdac)SO_4].H_2O$ (III)	-1.117	0.965
$[(VO)_2(hqcap)_2].H_2O$ (IV)	-1.004	0.909
$[(VO)_2(hqcaap)_2SO_4].2H_2O$ (V)	-0.865	0.647

Supporting electrolyte: TBHP; concentration of the complexes: 1 mmol;
all the potentials are referenced to Ag/AgCl electrode.

3.3.5 Infrared spectra

The IR spectra of the complexes on comparison with that of the free ligands reveal remarkable changes. Selected vibrational bands of the free ligands and the oxovanadium complexes, which are useful for determining the mode of coordination of the ligands, are given in Table 4. The broad bands at 3000–3500 cm^{-1} due to the ν_{NH}/ ν_{OH} of free Schiff bases were not observed in the spectrum of the complexes suggesting the coordination of phenolic oxygen after enolisation and deprotonation of the Schiff base ligands. The appearance of a broad absorption band centered around 3400, 3504, 3410, 3424 and 3490 cm^{-1} respectively in the spectra of the complexes, I, II, III, IV and V indicates the presence of lattice/coordinated water. This fact is also indicated by the results of elemental analyses and TG-DTA-DTG of these complexes [49].

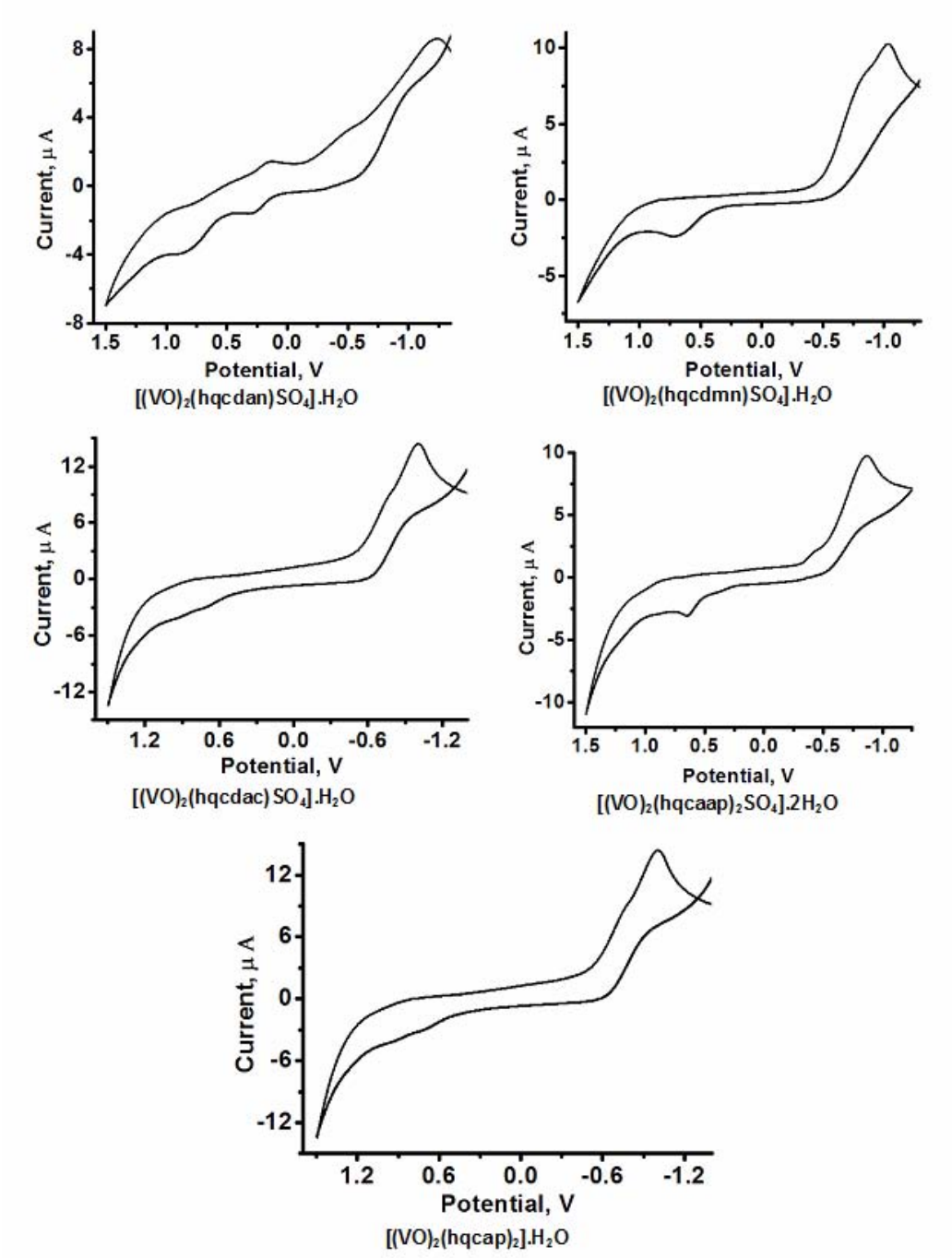

Figure 1: Cyclic voltammograms of the oxovanadium(IV) complexes in DMSO

Disappearance of the strong amide band and the formation of new bands in the range 1305−1323 cm^{-1} (corresponding to ν(C—O)) support the coordination of oxygen of the amide carbonyl to the metal through enolization and deprotonation

[50]. The stability of six membered chelate ring formed by the nitrogen atom of the imine group and the –OH group located at the quinoxaline ring rules out the possibility of coordinaton of the ring nitrogen of quinoxaline.

Table 4: Characteristic infrared spectral bands (cm^{-1}) for oxovanadium(IV) complexes.

Compound	ν(O—H)[a/b]	ν(C=N)[c]	ν(C—O)[d]	*ν*(V–O)	*ν*(V–N)	ν(V=O)	ν(SO_4^{2-})	
							ν_3	ν_1
hqcdan-H_2	3430[a]	1597	1299	-	-	-	-	-
I	3400[b]	1657	1323	531	434	976	1166, 1146, 1105	823
hqcdmn-H_2	3390[a]	1643	1294					
II	3504[b]	1656	1309	536	423	935	1156, 1140, 1115	826
hqcdac-H_2	3434[a]	1625	1290	-	-	-	-	-
III	3410[b]	1673	1310	536	436	962	1142, 1129, 1102	818
hqcap-H_2	3451[a]	1637	1306	-	-	-	-	-
IV	3424[b]	1688	1310	538	425	974	-	-
hqcaap-H	3412[a]	1606	1300	-	-	-	-	-
V	3490[b]	1687	1305	525	433	970	1153, 1141, 1073	855

[a] ν(N–H)/ ν(O–H) of the free Schiff base or ; [b] ν(O—H) of coordinated water molecule; [c] –CH=N of azomethine group; [d] phenolic ν(C–O).

The azomethine stretching frequencies of the free Schiff base ligands were found to increase in the case of complexes indicating the participation of the azomethine nitrogen in chelation (Table 4). This unexpected increase in azomethine stretching frequency on coordination might be due to the extensive delocalization of the π-electrons in fully conjugated Schiff base ligand. Furthermore, in these complexes, two non-ligand bands in the region 525–538 cm^{-1} and 423–436 cm^{-1} can be assigned to the stretching modes of the metal to ligands bonds, *ν*(V–O) and *ν*(V–N), respectively [51].

By comparing the infrared spectra of the vanadyl complexes with that of the corresponding free Schiff base ligands, in the 800–1100 cm^{-1} region, it was possible to identify the V=O stretching frequencies [52]. The V=O stretching frequencies of the complexes range from 935 to 976 cm^{-1} (Figure 2), which suggests the absence of –V=O—V=O– chain structure [53]. The relatively low V=O stretching frequencies compared to other penta-coordinated square-pyramidal oxovanadiun(IV) complexes [54] indicate that the V=O bond is weakened due to strong σ and π electron donation

by the electron rich Schiff base ligands to the antibonding orbital of the V=O group [55,56]. This is very much possible as the Schiff bases have phenolate oxygen and electron rich azomethine nitrogen in conjugation with the quinoxaline ring. The presence of alkoxy oxygen-bridged V−O−V bonds in complexes I, II, III and IV (Figure 2) are confirmed by the presence of prominent bands in the region 753−770 cm^{-1} [57,58]. The presence of chelating bidentate coordination of the SO_4^{2-} group in each complex is supported by the presence of triply degenerate ν_3 and single ν_1 bands (Table 4) in the IR spectra [51].

In addition to these changes, some other variations were also observed in the stretching frequencies of the Schiff bases on complexation to the metal. Coordination of hqcdmn-H_2 is further verified from the changes in the nature of the two very intense ν_{CN} bands at 2243 and 2202 cm^{-1}. This doublet appears as a major ν_{CN} stretch at 2200 cm^{-1} along with a weak band at 2236 cm^{-1} after complexation [59]. The band at 1656 cm^{-1} due to the C═O group of the antipyrine part of the hqcaap-H is shifted to 1646 cm^{-1} in complex, V, indicating the involvement of this group in coordination [60].

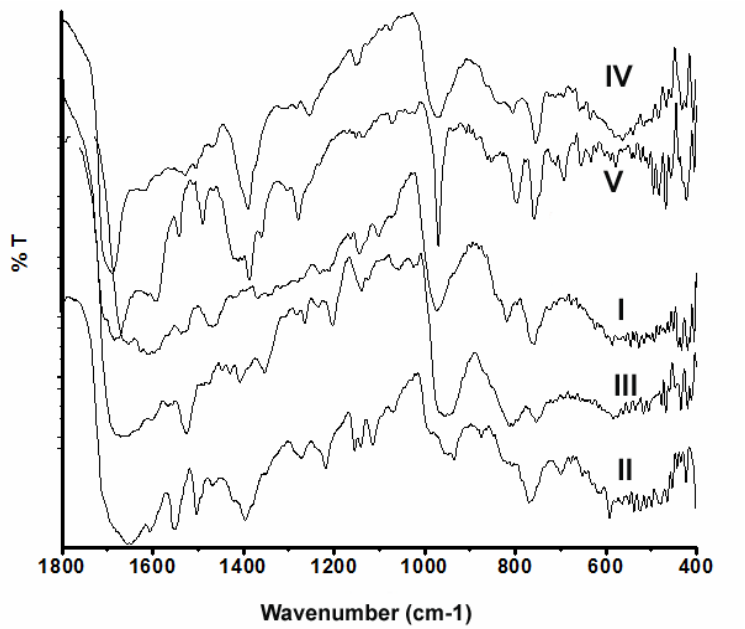

Figure 2: FT-IR spectra of the oxovanadium(IV) complexes

3.3.6 Electronic spectra

The electronic spectrum of the complexes in a saturated solution of acetonitrile (Figure 3) is dominated by ligand centered bands and shows three absorption peaks (Table 5). However, the diffuse reflectance spectrum of the complex (Table 5 and Figure 4) exhibits bands characteristics of a square pyramidal oxovanadium complex [61]. The d-d bands, which could not be observed in the solution spectrum, are seen in the diffuse reflectance spectra, due to the high concentration of the complex in the solid state.

Table 5: Electronic spectral assignments for oxovanadium(IV) complexes.

Complex	Electronic spectral bands; nm (cm^{-1})	Assignments
I	216 (46,290)[a], 231 (43,290)[a], 321 (31,150)[a]	Intra ligand transitiions
	519 (19,260)[as]	$^2B_2 \rightarrow {}^2A_1$ or CT
	216 (46,290)[bs], 264 (37,880)[bs], 343 (29,150)[bs]	Intra ligand transitiions
	560 (17,850)[b]	$^2B_2 \rightarrow {}^2A_1$
	683 (14,640)[bs]	$^2B_2 \rightarrow {}^2B_1$
	872 (11,460)[bs], 1180 (8,475)[b]	$^2B_2 \rightarrow {}^2E$
II	210 (47,620)[a], 304 (32,890)[a], 444 (22,520)[a]	Intra ligand transitiions
	515 (19,410)[as]	$^2B_2 \rightarrow {}^2A_1$ or CT
	216 (46,290)[b], 266 (37,590)[bs], 311 (32,150)[bs]	Intra ligand transitiions
	500 (20,000)[b]	$^2B_2 \rightarrow {}^2A_1$
	543 (18,410)[b]	$^2B_2 \rightarrow {}^2B_1$
	700 (14,280)[bs]; 1130 (8,850)[bs]	$^2B_2 \rightarrow {}^2E$
III	215 (46,510)[a], 312 (32,050)[a]	Intra ligand transitiions
	414 (24,150)[a]	$^2B_2 \rightarrow {}^2A_1$ or CT
	220 (45,450)[b], 264 (37,880)[bs], 321 (31,150)[bs], 412 (24,270)[b]	Intra ligand transitiions
	500 (24,270)[bs]	$^2B_2 \rightarrow {}^2A_1$
	750 (13,330)[bs]	$^2B_2 \rightarrow {}^2B_1$
	1180 (8,470)[b]	$^2B_2 \rightarrow {}^2E$
IV	212 (47,170)[a], 308 (32,460)[a], 408 (24,510)[a]	Intra ligand transitiions
	474 (21,090)[as]	$^2B_2 \rightarrow {}^2A_1$ or CT
	219 (45,660)[b], 266 (37,590)[bs], 316 (31,640)[bs]	Intra ligand transitiions
	509 (19,640)[b]	$^2B_2 \rightarrow {}^2A_1$
	688 (14,970)[bs]	$^2B_2 \rightarrow {}^2B_1$
	996 (10,040)[bs]	$^2B_2 \rightarrow {}^2E$
V	207 (48,310)[a], 306 (32,680)[a], 384 (26,040)[a]	Intra ligand transitiions
	461 (21,690)[as]	$^2B_2 \rightarrow {}^2A_1$ or MLCT Intra
	220 (45,450)[b], 265 (37,730)[bs], 336 (29,760)[b]	ligand transitiions
	501 (19,960)[b]	$^2B_2 \rightarrow {}^2A_1$
	776 (12,880)[b]	$^2B_2 \rightarrow {}^2B_1$
	1124 (8,890)[bs]	$^2B_2 \rightarrow {}^2E$

[a] Saturated solution spectrum in acetonitrile; [b] Diffuse reflectance spectrum in the solid state;
[s] Shoulder band

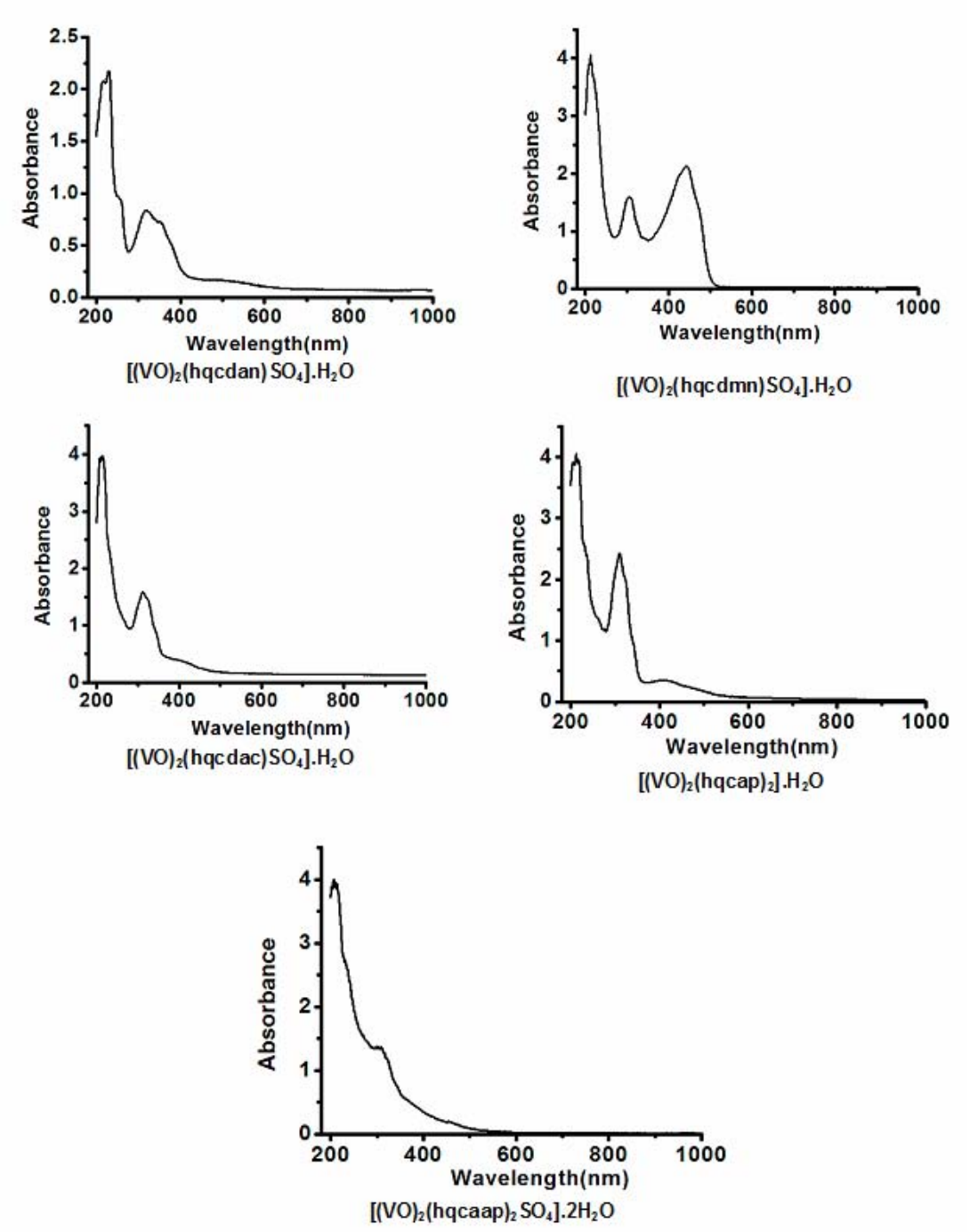

Figure 3: Electronic spectra of the oxovanadium(IV) complexes in acetonitrile

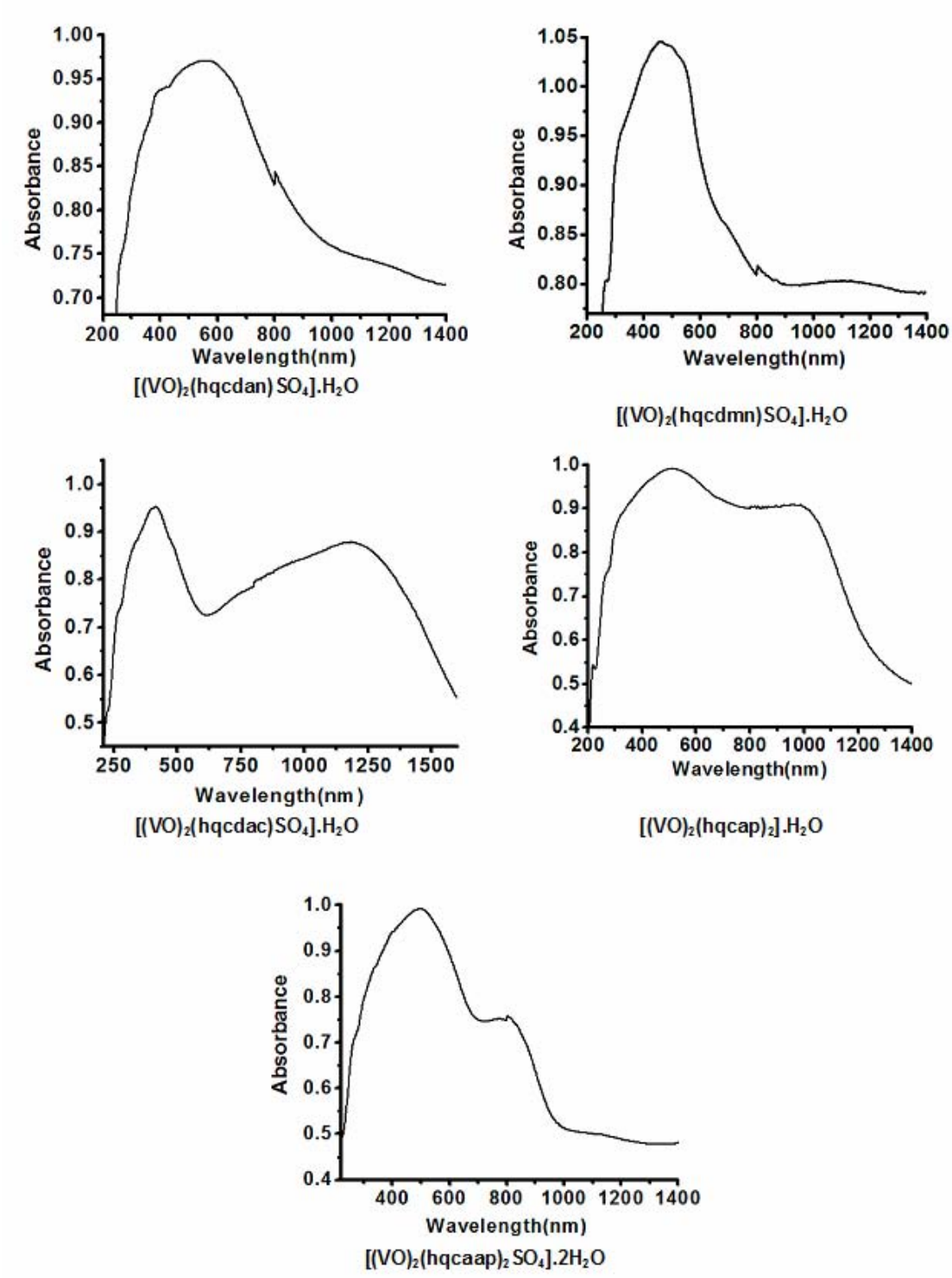

Figure 4: Diffuse reflectance spectra of the oxovanadium(IV) complexes

3.3.7 Thermal Analysis

In the present investigation, heating rates were suitably controlled at 20 °C min $^{-1}$ under a nitrogen atmosphere/static air and the weight loss was measured from ambient temperature up to 1000 °C. The TG/DTA/DTG curves are represented in Figures 5-9. All the oxovanadium complexes decompose at higher temperature compared to the free Schiff base ligands (see Chapter 2) suggesting coordination of the Schiff bases to vanadium. The initial weight loss upto 130 °C in all these complexes corresponds to the loss of hydrated water molecules [62]. This is followed by the decomposition of the complex. In nitrogen atmosphere the decomposition was not completed even after 1000 °C. However in air the complexes decompose completely. In these cases the metal percentages calculated from the metal oxide residues were found to agree with data obtained from the analytical metal content determination.

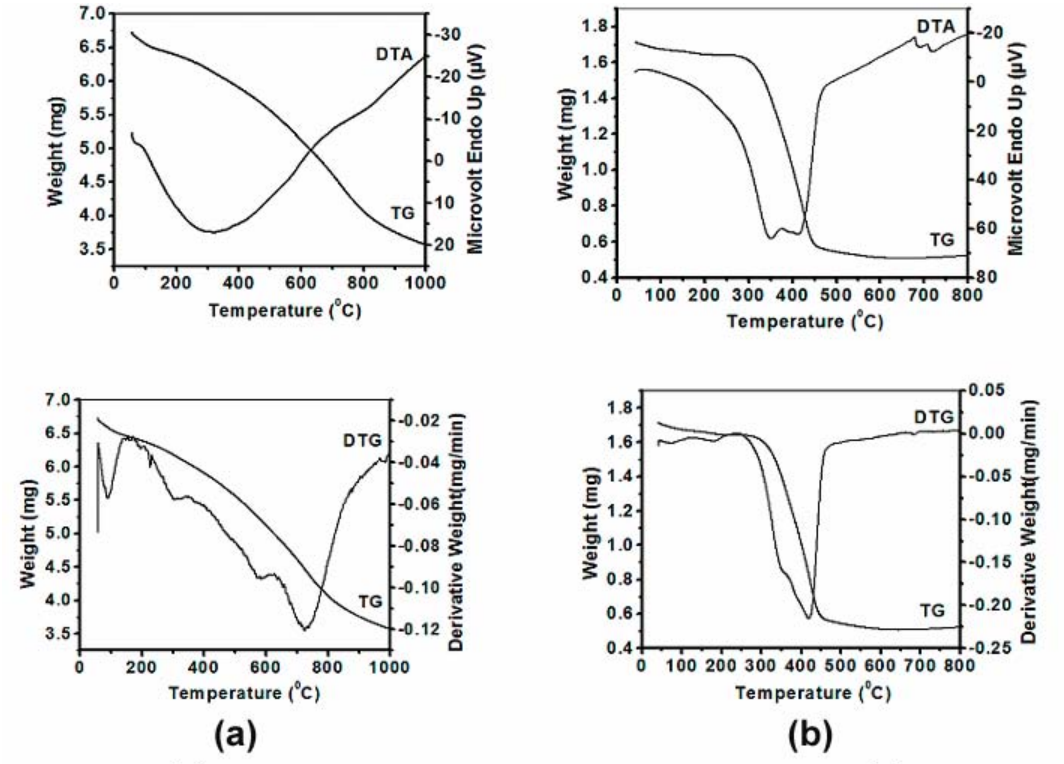

Figure 5: TG-DTA-DTG curves of $[(VO)_2(hqcdan)SO_4].H_2O$: in nitrogen (a) and in air (b)

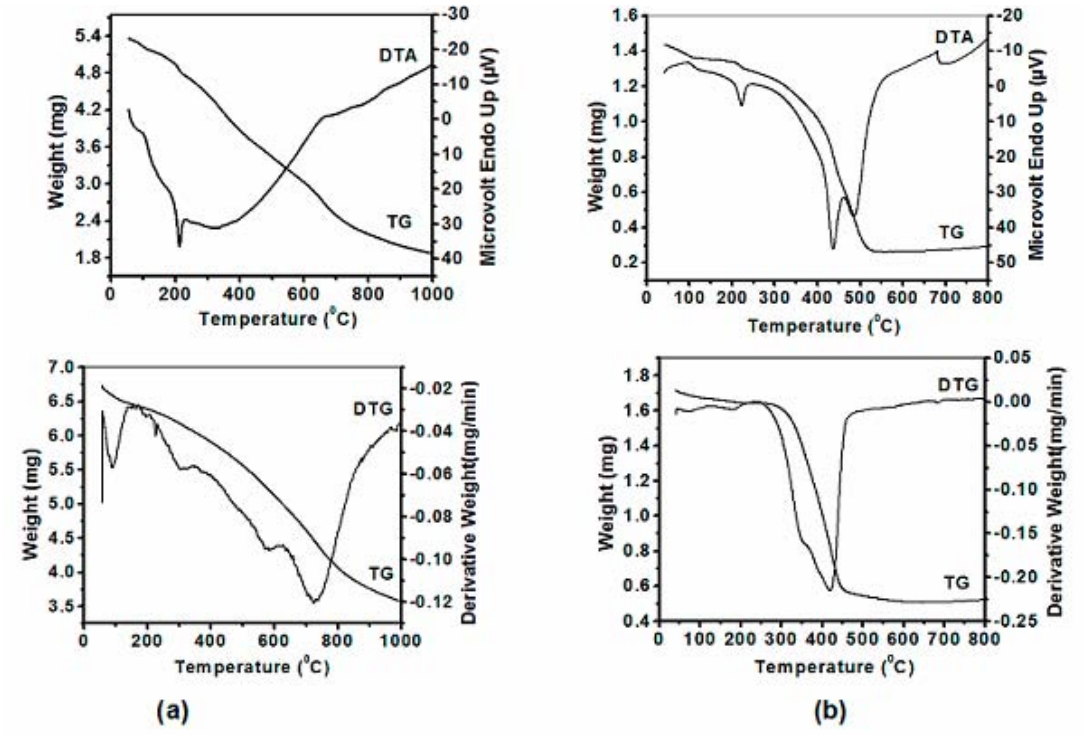

Figure 6: TG-DTA-DTG curves of $[(VO)_2(hqcdmn)SO_4].H_2O$: in nitrogen (a) and in air (b)

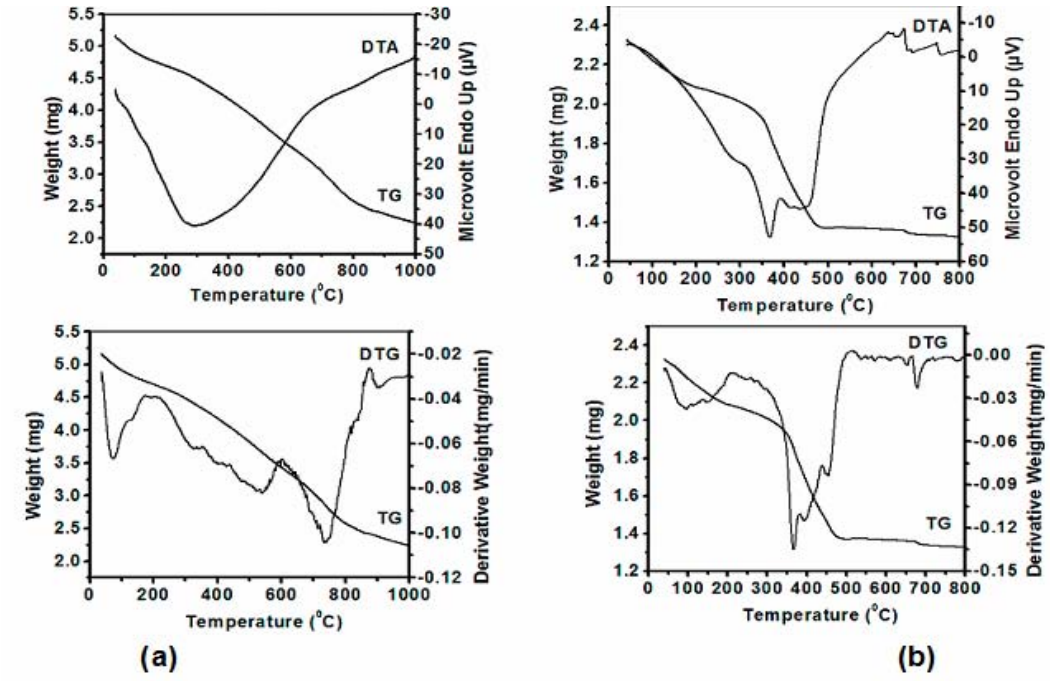

Figure 7: TG-DTA-DTG curves of $[(VO)_2(hqcdac)SO_4].H_2O$: in nitrogen (a) and in air (b)

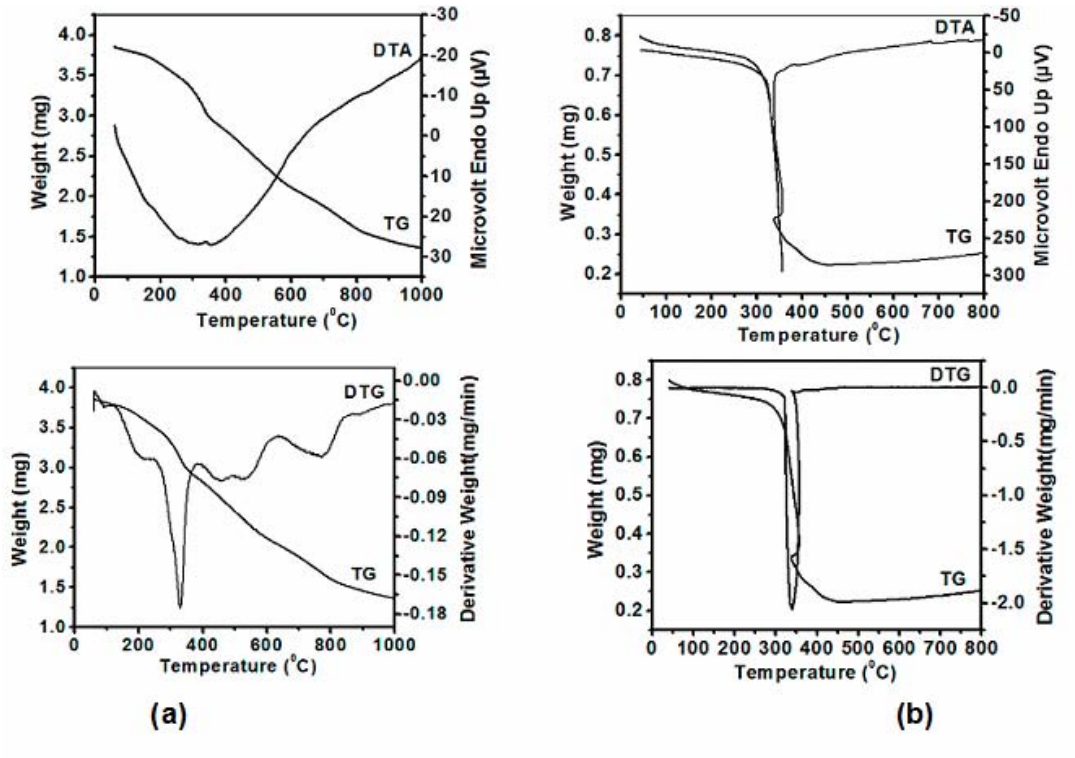

Figure 8: TG-DTA-DTG curves of $[(VO)_2(hqcap)_2].H_2O$: in nitrogen (a) and in air (b)

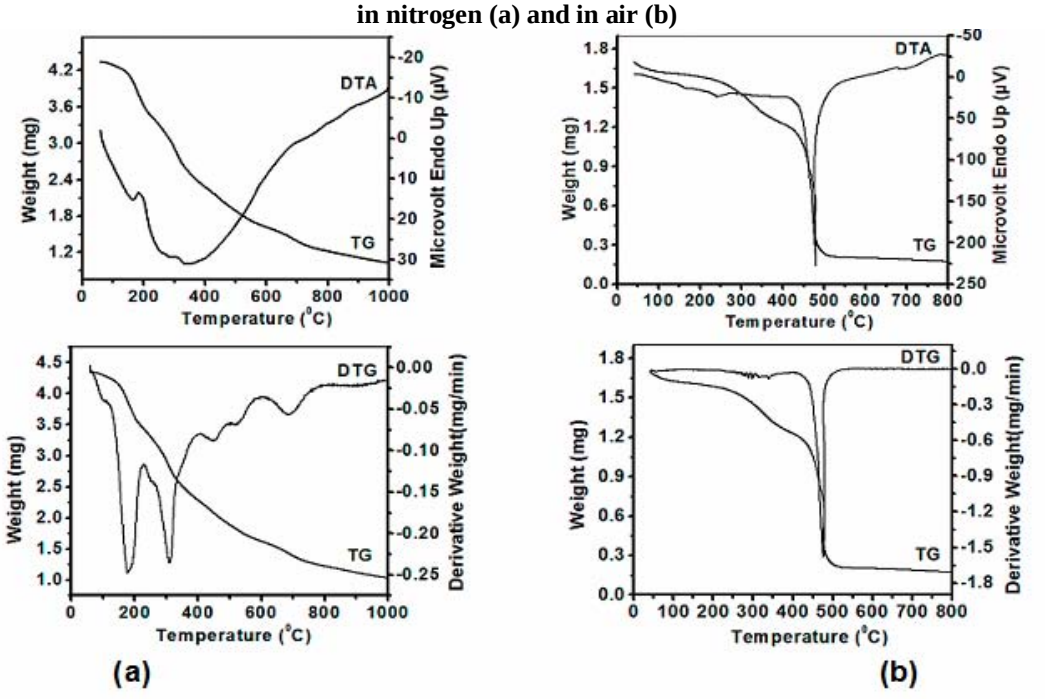

Figure 9: TG-DTA-DTG curves of $[(VO)_2(hqcaap)_2SO_4].2H_2O$: in nitrogen (a) and in air (b)

3.3.8 EPR spectra

EPR spectra of all the oxovanadium(IV) complexes were recorded in polycrystalline state at 298 K and in DMF solution at 77 K using 100 KHz field modulation and the g values were calculated relative to the standard marker TCNE (g = 2.00277). In polycrystalline state at 298 K, all the complexes are more or less isotropic (Figures 11, 13, 15, 17 and 19). Even though hyperfine splittings are observed in complexes I, II and V, they are not clear. The calculated g values for these binuclear oxovanadium complexes lie with in the range 1.902-1.913 [63] and are given in Table 6.

The EPR spectrum of all the oxovanadium complexes in DMF at 77K shows typical eight-line splitting pattern, as expected for ^{51}V (I = 7/2; n = 2I+1) (Figures 10, 12, 14, 16 and 18). The absence of any ligand nitrogen hyperfine lines in the $g_{\|}$ region indicates that the unpaired electron, for most of the times stays in the d_{xy} orbital localized on the metal, thus excluding the possibility of its direct interaction with the ligand [64-68]. Corresponding parameters (Table 6) are characteristics of square pyramidal oxovanadium(IV) complexes with C_{4V} symmetry, the V=O bond along z and the other four donor atoms are along the *x*, *y* axes, exhibiting two *g* ($g_z = g_{\|} < g_{\perp} = g_x = g_y$) and two *A* ($Az = A_{\|} > A_{\perp} = A_x = A_y$) values [69].

Table 6: EPR spectral parameters of oxovanadium(IV) complexes in polycrystalline state at 298K and DMF solution at 77K

Complex	Polycrystalline state (298 K); g_{iso}	DMF solution (77K)			
		$A_{\|}$	$A_{\perp}$	$g_{\|}$	$g_{\perp}$
$[(VO)_2(hqcdan)SO_4].H_2O$	1.913	100.55	65.39	1.933	1.981
$[(VO)_2(hqcdmn)SO_4].H_2O$	1.907	97.25	63.32	1.945	1.999
$[(VO)_2(hqcdac)SO_4].H_2O$	1.902	91.92	58.22	1.955	2.007
$[(VO)_2(hqcap)_2].H_2O$	1.907	141.70	65.07	1.897	1.991
$[(VO)_2(hqcaap)_2SO_4].2H_2O$	1.902	142.68	63.83	1.895	1.994

The $A_{\|}$ and $A_{\perp}$ values are expressed in units of cm^{-1} multiplied by a factor of 10^{-4}.

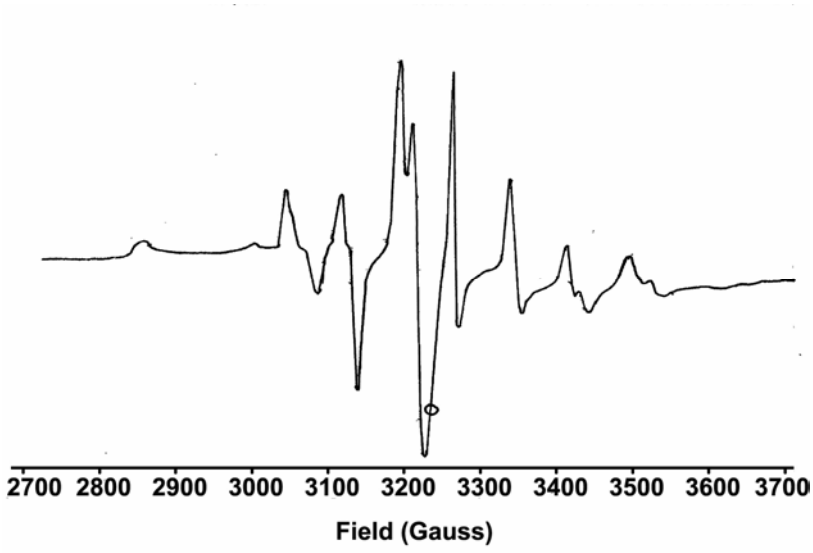

Figure 10: EPR spectrum of $[(VO)_2(hqcdan)SO_4].H_2O$ (I) in DMF LNT

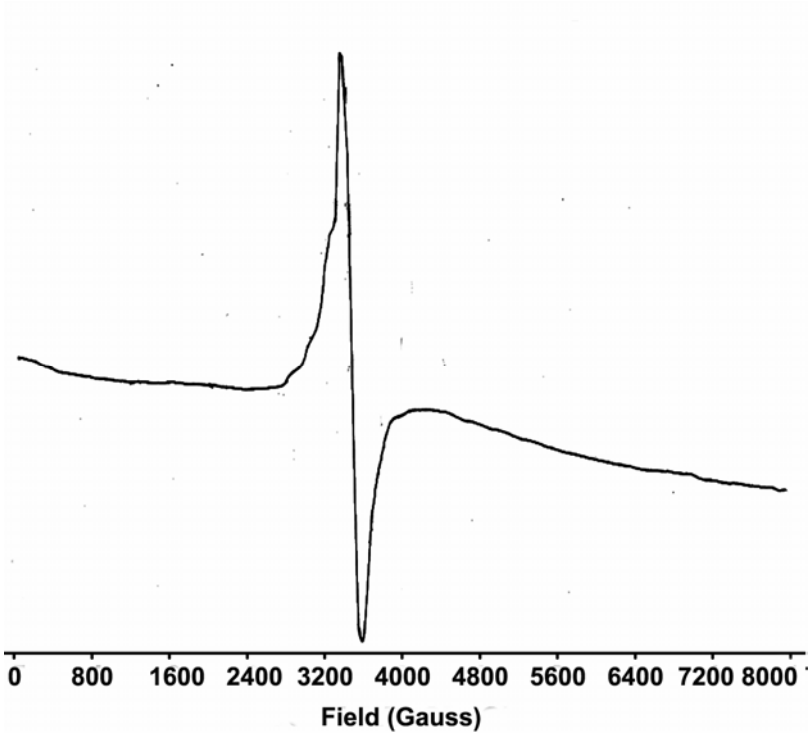

Figure 11: EPR spectrum of $[(VO)_2(hqcdan)SO_4].H_2O$ (I) in solid RT

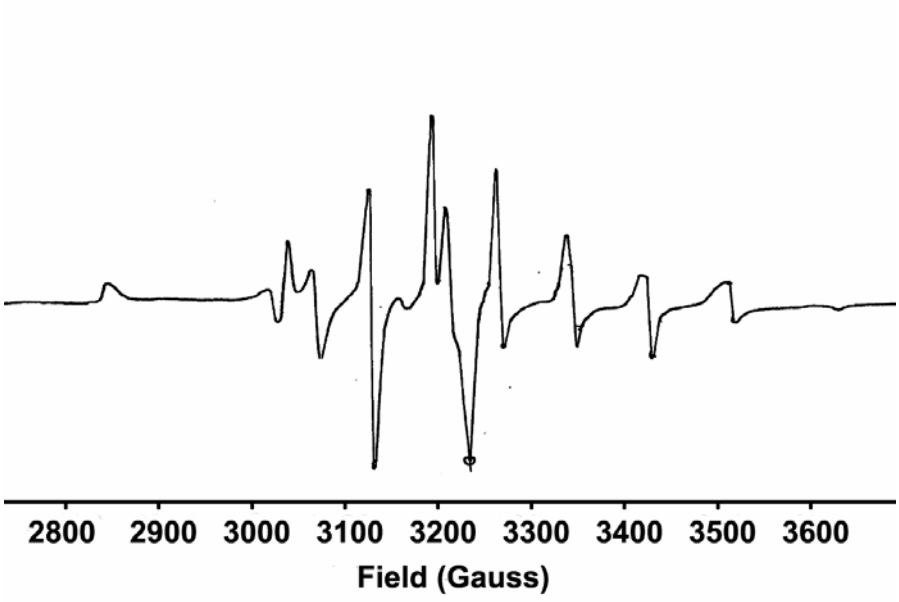

Figure 12: EPR spectrum of $[(VO)_2(hqcdmn)SO_4].H_2O$ (II) in DMF LNT

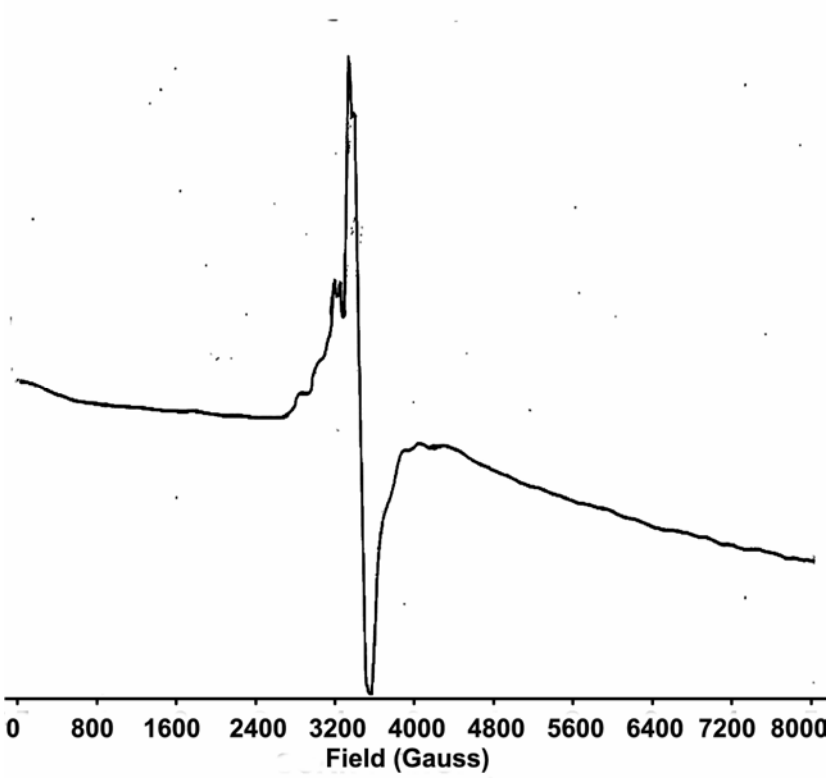

Figure 13: EPR spectrum of $[(VO)_2(hqcdmn)SO_4].H_2O$ (II) in solid RT

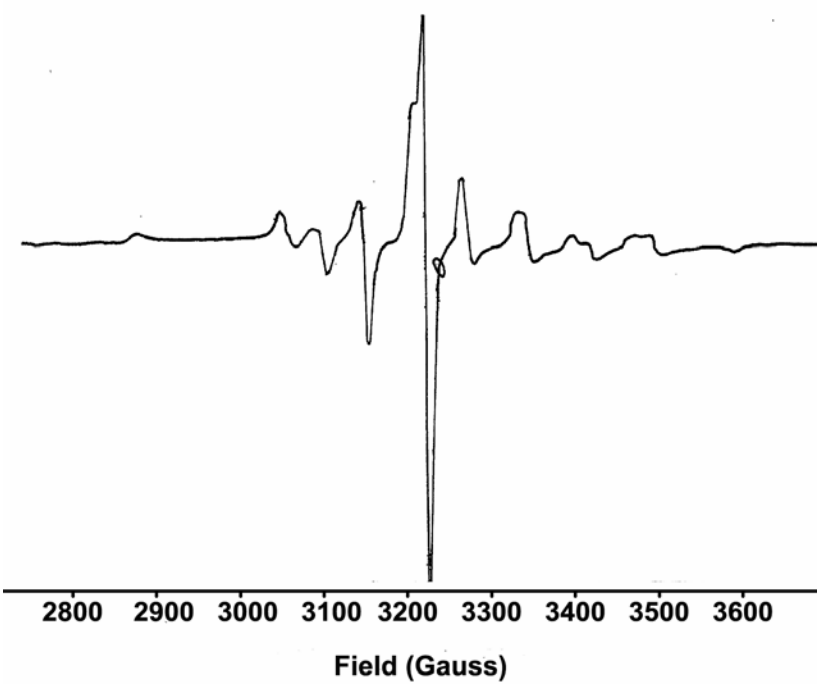

Figure 14: EPR spectrum of $[(VO)_2(hqcdac)SO_4].H_2O$ (III) in DMF LNT

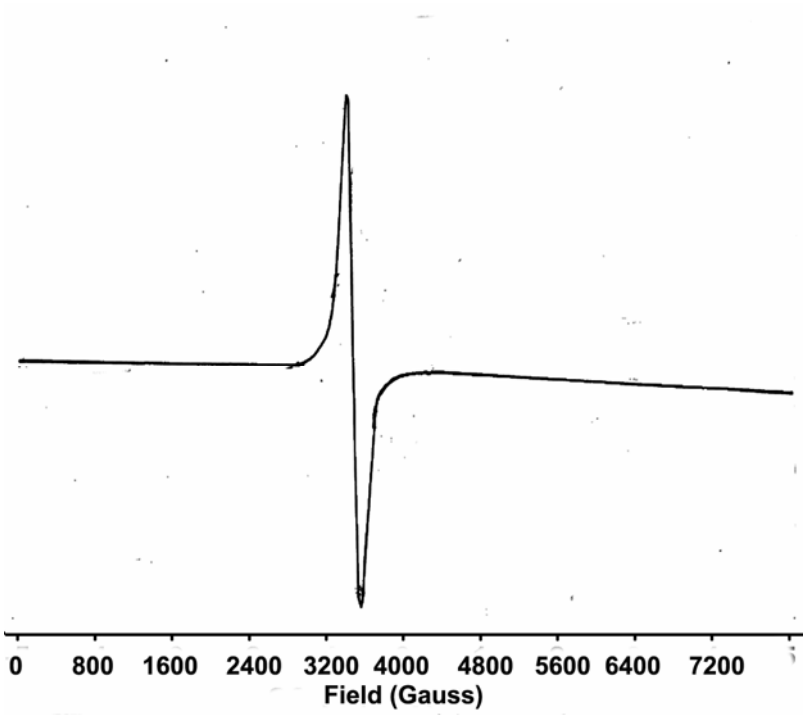

Figure 15: EPR spectrum of $[(VO)_2(hqcdac)SO_4].H_2O$ (III) in solid RT

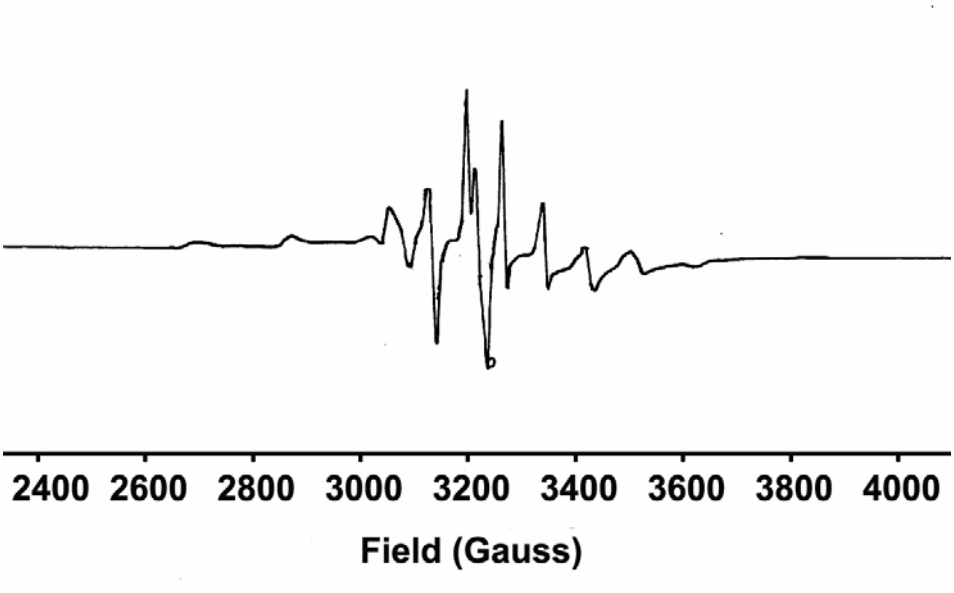

Figure 16: EPR spectrum of $[(VO)_2(hqcap)_2].H_2O$ (IV) in DMF LNT

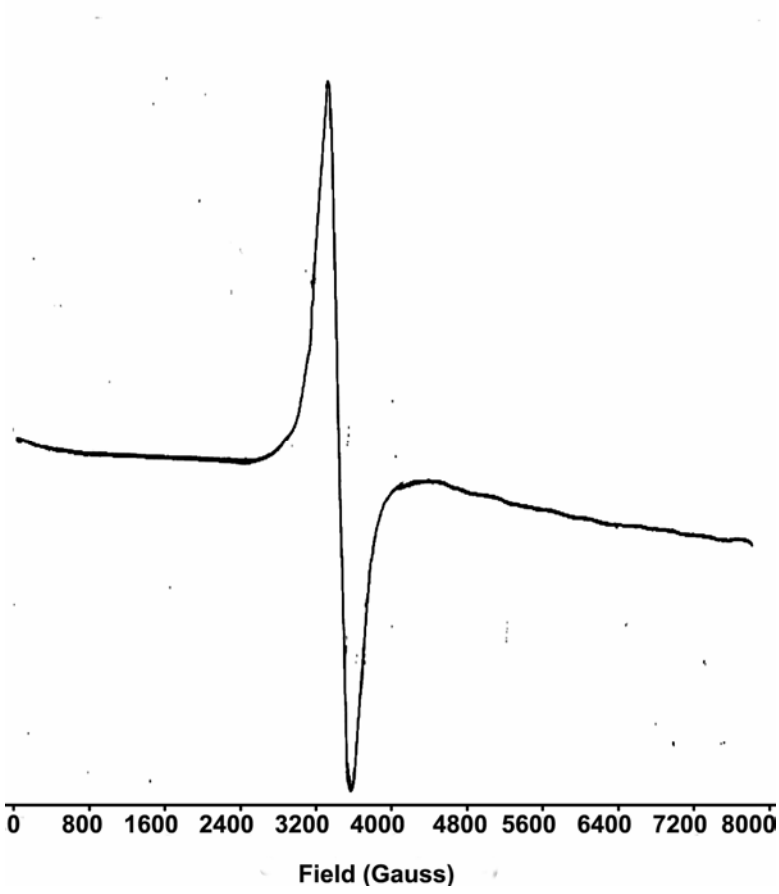

Figure 17: EPR spectrum of $[(VO)_2(hqcap)_2].H_2O$ (IV) in solid RT

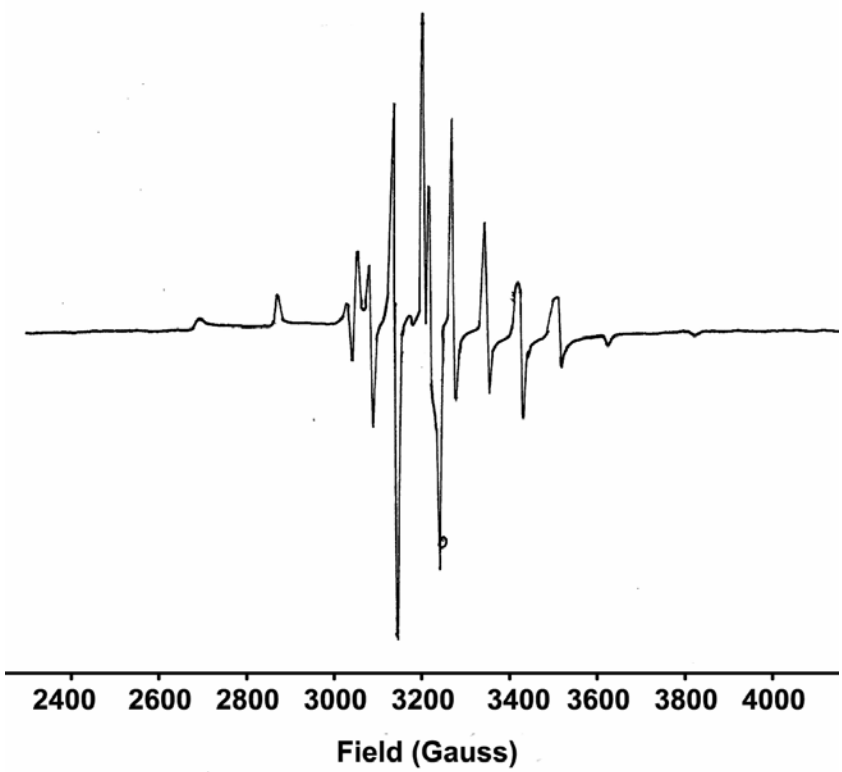

Figure 18: EPR spectrum of $[(VO)_2(hqcaap)_2SO_4].2H_2O$ (V) in DMF LNT

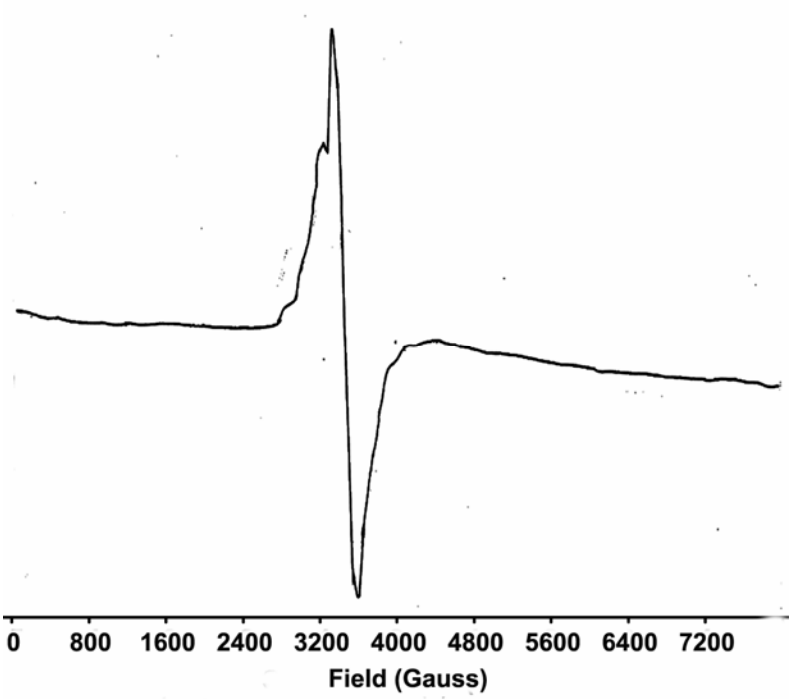

Figure 19: EPR spectrum of $[(VO)_2(hqcaap)_2SO_4].2H_2O$ (V) in solid RT

Conclusions

The vanadium complexes synthesised in this study have a binuclear structure as suggested by elemental analysis and cyclic voltammetric data. The values of infrared stretching frequencies corresponding to the V=O band are in good agreement with penta-coordinated oxovanadium(IV) complexes and the solid state diffuse reflectance spectra of these complexes also exhibit spectral bands corresponding to the electronic transitions characteristic of square-pyramidal oxovanadium complex. The square pyramidal structure is again confirmed by the EPR spectra, which display well resolved axial anisotropy with typical eight-line patterns. The presence of the SO_4^{2-} group in complexes I, II, III and V is evidenced by the presence of a triply degenerate ν_3 and single ν_1 bands in the IR spectra. The presence of lattice/coordinated water molecules is also indicated by thermal and IR studies. Based on the above observations we have proposed the following structures for complexes (Figure 20).

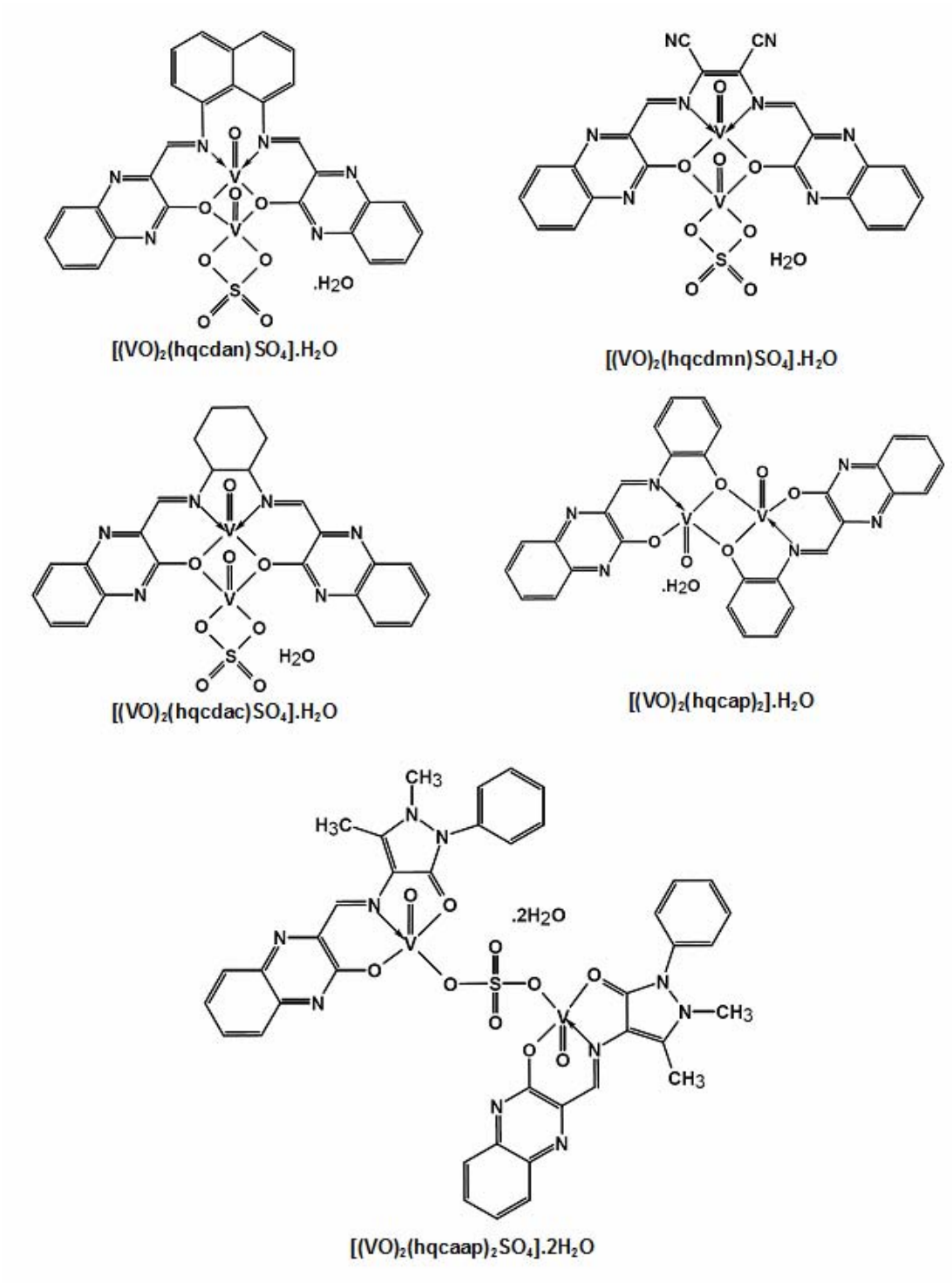

Figure 20: Proposed binuclear structure for the oxovanadium(IV) complexes

References

[1] D.C. Crans, J.J. Smee, E. Gaidamauskas, L. Yang. Chemical Reviews, 104 (2004) 849-902

[2] H. Sakurai, A. Tamura, J. Fugono, H. Yasui, T. Kiss. Coordination Chemistry Reviews, 245 (2003) 31-37

[3] H. Sakurai, T. Inohara, Y. Adachi, K. Kawabe, H. Yasui, J. Takada. Bioorganic and Medicinal Chemistry Letters, 14 (2004) 1093-1096.

[4] T.S. Smith, R. Lo Brutto, V.L. Pecoraro. Coordination Chemistry Reviews, 228 (2002) 1-18

[5] C.E. Holloway, M. Melnik. Reviews in Inorganic Chemistry, 7 (1985) 75-159

[6] F.T.G. Hudson. Vanadium Toxicology and Biological Significance, Elsevier, New York, (1996) 140

[7] J. Selbin. Chemical Reviews, 65 (1965) 153–175

[8] J. Selbin. Coordination Chemistry Reviews, 1 (1966) 293-314

[9] A.P. Ginsberg, E. Koubek, H.J. Williams. Inorganic Chemistry, *5* (1966) 1656–1662

[10] R.L. Carlin, F. Ann Walker. Journal of the American Chemical Society, 87 (1965) 2128–2133

[11] M. Pasquali, F. Marchetti, C. Floriani, S. Merlino. Journal of the Chemical Society, Dalton Transactions, (1977) 139 – 144

[12] R.L. Carlin, F. Ann Walker, Journal of the American Chemical Society, 87 (1965) 2128–2133

[13] M. Mathew, A.J. Carty, G.J. Palenik. Journal of the American Chemical Society, 92 (1970) 3197–3198

[14] G.A. Kolawole, K.S. Patel. Journal of the Chemical Society, Dalton Transactions, (1981) 1241 – 1245

[15] G.A. Kolawole, K.S. Patel. J. Chem. Soc., Dalton Trans.**,** 1981, 1241 – 1245

[16] S. Mukherjee, S. Samanta, B. Chandra, A. Bhaumik. Applied Catalysis A: General, 301 (2006) 79-88

[17] S. Mukherjee, S. Samanta, A. Bhaumik, B. Chandra. Applied Catalysis B: Environmental, 68 (2006) 12-20

[18] E.N. Jacobsen, E.W. Abel, F.G.A. Stone, E. Willinson. Comprehensive Organometallic Chemistry II, 12 (1995) 1097

[19] C. Yuan, L. Lu, X. Gao, Y. Wu, M. Guo, Y. Li, X. Fu, M. Zhu. Journal of Biological Inorganic Chemistry, (2009) DOI: 10.1007/s00775-009-0496-6

[20] L. Canali, D.C. Sherington. Chemical Society Reviews, 28 (1999) 85-93

[21] R. Ando, S. Mori, M. Hayashi, T. Yagyu, M. Maeda. Inorganica Chimica Acta, 357 (2004) 1177–1184

[22] R. Ando, H. Ono, T. Yagyu, M. Maeda. Inorganica Chimica Acta, 351 (2003) 107-113

[23] A. Butler, J. Reedijk, E. Bouwman. Bioinorganic Catalysis, 68 (1999) 407-408

[24] M. Tsuchimoto, G. Hoshina, R. Uemura, K. Nakajima, M. Kojima, S. Ohba. Bulletin of the Chemical Society of Japan, 73 (2000) 2317-2323

[25] M. Sakamoto, M, Ohsaki, K, Yamamoto, Y. Nakayama, A. Matsumoto, H. Okawa. Bulletin of the Chemical Society of Japan, 65 (1992) 2514-2519

[26] A. Bezaatpour, M. Behzad, D.M Boghaei. Journal of Coordination Chemistry 62 (2009) 1127-1133

[27] S. Rayati, M. Koliaei, F. Ashouri, S. Mohebbi, A. Wojtczak, A. Kozakiewicz. Applied Catalysis A: General, 346 (2008) 65-71

[28] R. Rajavel, M.S. Vadivu, C. Anitha. European Journal of Chemistry, 5 (2008) 620-626

[29] N Raman, E Jesintha, J. Joseph, K. rajasekaran. Asian Journal of Spectroscopy, 12 (2008) 99-105

[30] B.T. Thaker, K.R. Surati, C.K. Modi. Russian Journal of Coordination Chemistry, 34 (2008) 25-33

[31] P.K. Sasmal, A.K. Patra, M. Nethaji, A.R. Chakravarty. Inorganic Chemistry, 46 (2007) 11112-11121

[32] A. Syarnal, K.S. Kale. Journal of Molecular Structure, 38 (1977) 195-202

[33] D.K. Rastogi, P.C. Pachauri. Journal of Inorganic and Nuclear Chemistry, 39 (1977) 151-153

[34] E.B. Seena, N. Mathew, M. Kuriakose and M.R.P. Kurup. Plyhedron, 27(2008) 1455-1462

[35] M. Athar, N. Ahmad. Synthesis and Reactivity in Inorganic, Metal-Organic, and Nano-Metal Chemistry, 17 (1987) 723-745

[36] B.T Thaker, J Lekhadia, A Patel, P Thaker. Transition Metal Chemistry. 19 (1994) 623-631

[37] W.J. Geary. Coordination Chemistry Reviews, 7 (1971) 81-122

[38] S.N. Rao, D.D. Mishra, R.C. Maurya, N.N. Rao. Polydedron, 16 (1997) 1825-1829

[39] J.A. Jahagirdar, B.R. Havinale. Transition Metal Chemistry, 17 (1992) 539-542

[40] J.A. Bertrand, J.A. Kelley, J.L. Breece. Inorganica Chimica Acta, 4 (1970) 247-250

[41] U.V. Zelentsov. Russian Journal of Inorganic Chemistry, 7 (1962) 670

[42] H. Okawa, I. Ando, S. Kida. Bulltin of chemical society of Japan, 47 (1974) 3041-3044

[43] A.P. Ginsberg, E. Koubek, H.J. Williams. Inorganic Chemistry, 5 (1966) 1656-1662

[44] R.L. Belford, N.D. Chasteen, H. So, R.E. Tapscott. Journal of the American Chemical Society, 91 (1969) 4675-4680

[45] Y-T Li, C-W Yan, C-S Xu. Synthesis and Reactivity in Inorganic and Metal-Organic Chemistry, 29 (1999) 995-1007

[46] A. El-Dissouky, A.K. Shehata, G. El-Mahdey, Polyhedron, 16 (1997) 1247−1253

[47] M. Tumer, H. Koksal, M.K. Sener, S. Serin. Transition Metal Chemistry, 24 (1999) 414-420

[48] S.N. Rao, D.D. Mishra, R.C. Maurya, N.N. Rao. Polyhedron, 16 (1997)1825-1829

[49] S.A. Sallam. Transition Metal Chemistry, 30 (2005)341–351

[50] B.V. Patel, K. Desai, T. Thaker. Synthesis and Reactivity in Inorganic and Metal-Organic Chemistry, 19 (1989) 391-412

[51] K. Nakamoto, Coordination Compounds In Infrared and Raman Spectra of Inorganic and Coordination Compounds, 4th Ed.; John Wiley and Sons, Inc.: New York, 1986

[52] A.P. Ginsberg, E. Koubek, H.J. Williams. Inorganic Chemistry, 5 (1966) 1656-1662

[53] R.L. Farmer, F.L. Urbach. Inorganic Chemistry, 13 (1974) 587-592

[54] J. Selbin, Chemical Reviews 65 (1965) 153-175

[55] T.M. Dewey, J.D. Bois, K.N. Raymond. Inorganic Chemistry, 32 (1993) 1729-1738

[56] S.R. Cooper, Y.B. Koh, K.N. Raymond. Journal of the American Chemical Society, 104 (1982) 5092-5102

[57] R. Ando, M. Nagai, T. Yagyu, M. Maeda. Inorganica Chimica Acta, 351 (2003) 107-113

[58] I. Cavaco, J.C. Pessoa, M.T. Duarte, R.T. Henriques, P.M. Matias, R.D. Gillard. Journal of the Chemical Society, Dalton Transactions, (1996) 1989

[59] M.J. MacLachlan, M.K. Park, L.K. Thompson. Inorganic Chemistry, 35 (1996) 5492−5499

[60] R.M. Issa, A.M. Khedr, H.F. Rizk. Spectrochimica Acta Part A, 62 (2005) 621–629

[61] A. El-Dissouky, A.K. Shehata, G. El-Mahdey. Polyhedron, 16 (1997) 1247−1253

[62] G.G. Mohamed. Spectrochimica Acta Part A: Molecular and Biomolecular Spectroscopy, 64 (2006) 188-195

[63] R.C. Maurya, H. Singh, A. Pandey. Synthesis and Reactivity in Inorganic and Metal-Organic Chemistry, 32 (2002) 231-246

[64] H. Kon, E. Sharpless. Journal of Chemical Physics, 42 (1965) 906-907

[65] D. Kivelson, S.K. Lee. Journal of Chemical Physics, 41 (1964) 1896

[66] N.A. Mangalam, M.R.P. Kurup. Spectrochimica Acta Part A, 71 (2009) 2040–2044

[67] T. Ghosh, S. Bhattacharya, A. Das, G. Mukherjee, M.G.B. Drew. Inorganica Chimica Acta, 358 (2005) 989-996

[68] N. Raman, J.D. Raja, A. Sakthivel. Journal of Chemical Sciences, 119 (2007) 303-310

[69] E. Garribba, G. Micera, A. Panzanelli, D. Sanna. Inorganic Chemistry, 42 (2003) 3981-3987

Synthesis and characterisation of copper(II) complexes

Contents

4.1 Introduction

Copper being an essential trace element, is present in parts per million concentration range in biological systems. The element functions as a key cofactor in a diverse array of biological oxidation reduction reactions [1]. Copper containing proteins (hemocyanin, tyrosinase, chatecol oxidase etc.) are involved in various processes in living systems [2-5]. Copper(II) is known to form complexes with a variety of molecular geometries and in these complexes the d^9 configuration makes the structure distort in octahedral and tetrahedral symmetries (Jahn-Teller effect). The distortion is usually seen as axial elongation, consistent with the lability and geometric flexibility of the complex. Therefore, typical Cu(II) complexes have square planar or square pyramidal geometries with weakly associated ligands in the axial position(s). Trigonal bipyramidal coordinations are also known for Cu(II) complexes. In some cases bridged complexes in which two or more Cu(II) ions are linked by hydroxo or other anionic ligands are also reported [6,7].

The transition metal complexes having oxygen and nitrogen donor Schiff bases possess unusual configurations and structural lability and are sensitive to the molecular environment. Four coordinated copper(II) complexes usually form a square planar coordination geometry that may be distorted to pseudo tetrahedral geometry depending on the ligand environment [8-10]. Several model systems, including those with bidentate Schiff base ligands, have been reported correlating the molecular structure with the electronic ground state of blue copper proteins [11].

Binucleating ligands that contain a bridging phenoxo group have been widely used owing to their abilities to form stable complexes [12]. Many copper(II) Schiff base complexes are known to be useful reagents for oxidative and hydrolytic cleavage of DNA [13]. In addition to the biological properties a large number of copper(II) Schiff base complexes have been used as catalysts in the aziridination [14] and cyclopropanation of olefins [15] and also in the peroxidative oxidation of phenol to dihydroxy benzenes [16], in which they act as models for catalase enzymes.

In this chapter, a report on the synthesis and characterization of some novel mono and binuclear Cu(II) complexes of the Schiff bases derived from the heterocyclic aldehyde, 3-hydroxyquinoxaline-2-carboxaldehyde has been presented.

4.2 Experimental

4.2.1 Materials

The details of materials used for the syntheses of the Schiff base ligands and their copper complexes are given in chapter 2. The metal salt used was copper chloride.

4.2.2 Synthesis of complexes

All the copper(II) complexes were prepared by mixing an aqueous solution (10 mL) of the salt $CuCl_2.2H_2O$ (10 mmol, 1.7 g) and an alkaline solution of the ligand, hqcdan-H_2 (5 mmol, 2.43 g), hqcdmn-H_2 (5 mmol, 2.10 g), hqcdac-H_2 (5 mmol, 2.13 g), hqcaap-H (10 mmol, 1.80 g) or hqcap-H_2 (5 mmol, 1.33 g) in 1:5 methanol-distilled water (250 mL) with a ligand to metal molar ratio 1:1. Equivalent amounts of NaOH were added to deprotonate the phenolic OH group of the Schiff base ligands. The solid mass was collected, washed with 1:5 methanol-water and petroleum ether and dried over anhydrous calcium chloride in a desiccator.

4.3 Results and discussion

All the complexes are brown, non-hygroscopic solids. They are soluble in acetonitrile, DMF and DMSO and sparingly soluble in ethanol, methanol and chloroform and insoluble in benzene.

The organic Schiff base ligands predominantly exist in the keto tautomeric form in the solid state. During complexation step an equivalent amount of NaOH in 1:6 methanol-distilled water was added to the ligands, in order to achieve this keto to enolate form. This renders the coordination to enolate oxygen.

4.3.1 Elemental analyses

The analytical data indicate that the complexes have the formulae given in Table 1 and further that the complexes I, II, III and IV are binuclear and the complex V is mononuclear. The percentage of copper in the complexes was estimated using AAS and the chlorine content was estimated using standard procedures.

Table 1: Analytical data a of the copper(II) complexes

Compound	Molecular formula	Formula weight	Cu (%)	C (%)	H (%)	N (%)	Cl (%)
$[Cu_2(hqcdan)Cl_2].H_2O$ **(I)**	$C_{28}H_{18}N_6O_3Cl_2Cu_2$	684.48	18.50 (18.57)	49.08 (49.13)	2.62 (2.65)	12.24 (12.28)	10.27 (10.36)
$[Cu_2(hqcdmn)Cl_2]$ **(II)**	$C_{22}H_{10}N_8O_2Cl_2Cu_2$	616.37	20.51 (20.62)	42.72 (42.87)	1.56 (1.64)	18.11 (18.18)	11.41 (11.50)
$[Cu_2(hqcdac)Cl_2].H_2O$ **(III)**	$C_{24}H_{22}N_6O_3Cl_2Cu_2$	640.47	19.77 (19.84)	44.96 (45.01)	3.41 (3.46)	12.08 (13.12)	10.98 (11.07)
$[Cu_2(hqcap)_2]$ **(IV)**	$C_{30}H_{18}N_6O_4Cu_2$	653.59	19.38 (19.45)	55.09 (55.13)	2.70 (2.78)	12.80 (12.86)	-
$[Cu(hqcaap)Cl(H_2O)_2]$ **(V)**	$C_{20}H_{20}N_5O_4ClCu$	493.40	12.82 (12.88)	48.60 (48.69)	4.02 (4.09)	14.13 (14.19)	7.10 (7.19)

[a] Calculated values in parentheses

4.3.2 Molar conductivity and magnetic susceptibility measurements

The molar conductance values of the complexes (Table 2) in DMF indicate non-electrolytic nature [17]. The room temperature magnetic moments (μ_{eff}) values of the copper(II) complexes are seen to range from 1.17 to l. 76 BM (Table 2). These subnormal values of the magnetic moments support a binuclear structure for the complexes I, II, III and IV [18]. These values are far below the calculated spin only value of 1.73 BM for Cu(II) and the experimentally determined moments of magnetically discrete Cu(II) complexes (1.8-2.0 BM) [19] and they do indicate a high degree of antiferromagnetic interaction between the metal centers. These values further indicate a square planar geometry around each Cu(II) for the binuclear complexes and a degree of association. The monomeric nature of V was confirmed by a magnetic moment value of 1.76 BM and this value permit the assignment of a distorted octahedral structure about the copper(II) ion for the complex [20,21].

Table 2: Magnetic moment values and molar conductance data of the copper(II) complexes.

Complex	μ_{eff} (BM) [a]	Molar conductance (10^{-3} mol ohm^{-1} cm^2 mol^{-1})
$[Cu_2(hqcdan)Cl_2].H_2O$ (I)	1.35	4.8
$[Cu_2(hqcdmn)Cl_2]$ (II)	1.52	5.6
$[Cu_2(hqcdac)Cl_2].H_2O$ (III)	1.17	3.2
$[Cu_2(hqcap)_2]$ (IV)	1.26	4.6
$[Cu(hqcaap)Cl(H_2O)_2]$ (V)	1.76	4.4

[a] Magnetic moment value per copper atom in the complex

4.3.3 Cyclic voltammetry

Cyclic voltammetric studies of the copper(II) complexes were investigated in DMSO (10^{-3} mol l^{-1}) at a scan rate of 0.025 V in the potential range +1.5 to −1.5 V. The cyclic voltammograms of the copper complexes are shown in Figure 1 and the

redox potentials are summarized in Table 3. All complexes show two redox couple in the +1.5 to +0.5 V and −0.2 to −1.5 V range under the experimental conditions.

The redox properties of binuclear copper complexes have received much attention, particularly with respect to studies endeavoring to understand and mimic the redox functions of copper proteins [22]. It was recognized in the early literature that the two copper(II) ions could be reduced to copper(I) at the same potential or at different potentials [23-26]. In either case the reduction requires a two electron process and if the *E*° values are well separated a two peaked cyclic voltammogram is obtained [27,28]. Nevertheless care has to be taken in interpreting a two-stepped cyclic voltammogram because the same two-stepped behaviour also could be observed in systems involving a two electron reduction of Cu(III) to Cu(I) [29].

Table 3: Redox potentials for copper(II) complexes in DMSO solution at 298 K.

Complex	Redox couple	E_{pc} (mV)	E_{pa} (mV)	ΔE_p (mV)	$E^1_{1/2}$/ ($E^2_{1/2}$) (mV)	I_{pc} (μV)	I_{pa} (μV)	I_{pc}/I_{pa}
I	$Cu_2^{II,II}/Cu_2^{II,I}$	141	654	513	398	0.28	0.30	0.93
	$Cu_2^{II,I}/Cu_2^{I,I}$	−1361	−667	694	(−1014)	0.40	0.34	1.18
II	$Cu_2^{II,II}/Cu_2^{II,I}$	146	726	580	436	0.21	0.23	0.91
	$Cu_2^{II,I}/Cu_2^{I,I}$	−827	−328	499	(−578)	0.06	0.07	0.85
III	$Cu_2^{II,II}/Cu_2^{II,I}$	195	831	636	513	0.44	0.43	1.02
	$Cu_2^{II,I}/Cu_2^{I,I}$	−899	−597	302	(−748)	4.30	4.23	1.02
IV	$Cu_2^{II,II}/Cu_2^{II,I}$	41	1223	1182	632	0.45	0.52	0.86
	$Cu_2^{II,I}/Cu_2^{I,I}$	−1246	−578	668	(−912)	0.81	0.68	1.19
V	Cu^{III}/Cu^{II}	96	928	832	512	0.56	0.56	1.00
	Cu^{II}/Cu^{I}	−1039	−563	476	(−801)	1.89	1.75	1.08

E_{pc} = anodic peak potential; E_{pa} = cathodic peak potential; I_{pc} = anodic peak current; I_{pa} = cathodic peak current; I_{pc}/I_{pa} = number of electrons; $\Delta E_p = E_{pa} - E_{pc}$; $E^1_{1/2}/ E^2_{1/2} = 0.5 \times (E_{pa} + E_{pc})$; scan rate 25 mV

In the present binuclear copper(II) complexes we observe two-stepped cyclic voltammograms. The first redox peak appearing in the positive potential range +1.5 to +0.25 V corresponds to $Cu_2^{II,II}/Cu_2^{II,I}$ redox couple where as the second redox couple appearing in the negative potential range −0.5 to −1.2 V is attributable to the

$Cu_2^{II,I}/Cu_2^{I,I}$ redox processes. Here the measured ΔE_p values for both redox couples range from 0.30 to 1.20 V. In each redox couple the I_{pc}/I_{pa} falls in the range 0.86–1.19, which is a clear indication of one electron transfer for redox process. The $E_{1/2}$ values for the first and second redox couples, $E^1_{1/2}$ and $E^2_{1/2}$, fall in the range +0.39 to +0.64 V and −1.02 to −0.74 V respectively. Since the $E_{1/2}$ values for the free Schiff base ligands lies in the range of 0.10 to 0.23 V (see Chapter 2) we could expect the above redox process to be metal centered [30]. From the above observations, it is very well clear that the binuclear copper complexes undergo two one-electron reductions as follows:

$$Cu_2^{II,II} + e^- \rightarrow Cu^{II,I} + e^- \rightarrow Cu^{I,I}.$$

Similar sequential one electron transfer redox couples have also been observed for a number of binuclear Cu(II) complexes [31-38]. The electrochemical data is thus found to confirm the proposed binuclear structures of the prepared complexes I, II, III and V. Cyclic voltammogram of the mononuclear copper(II) complex, $[Cu(hqcaap)Cl(H_2O)_2]$, also exhibit two reversible one-electron waves under the same experimental conditions (Figure 1 and Table 3). The redox peaks in the range +1.5 to +0.25 V is due to the Cu^{III}/Cu^{II} couple and in the range −0.5 to −1.2 V is due to the Cu^{II}/Cu^{I} couple [39].

The electrochemical data shows that in all the complexes the first reduction observed at a relatively higher positive potential and second reduction is at relatively higher negative potential. The redox properties of the copper are influenced by coordination, stereochemistry and the hard/soft character of the ligand donor atoms. Oxygen, nitrogen, and sulfur centers have all been considered as possible donors in copper proteins [40-42]. However, due to inherent difficulties in relating coordination number and stereochemistry of the species present in solution, the redox process is generally described in terms of the nature of the ligands present [43]. Patterson and Holm [41], have shown that softer ligands tend to give more positive $E°$ values, while hard acids give rise to more negative $E°$ values. Here the

complexes are formed from the Schiff bases having phenolic oxygen and quinoxaline ring in conjugation with azomethine group. The higher positive value for the first reduction may be due to the soft donor nature of the azomethine group in the Schiff base and the higher negative value for the second reduction due to the "hard acid" character of the phenolato oxygen of the Schiff base.

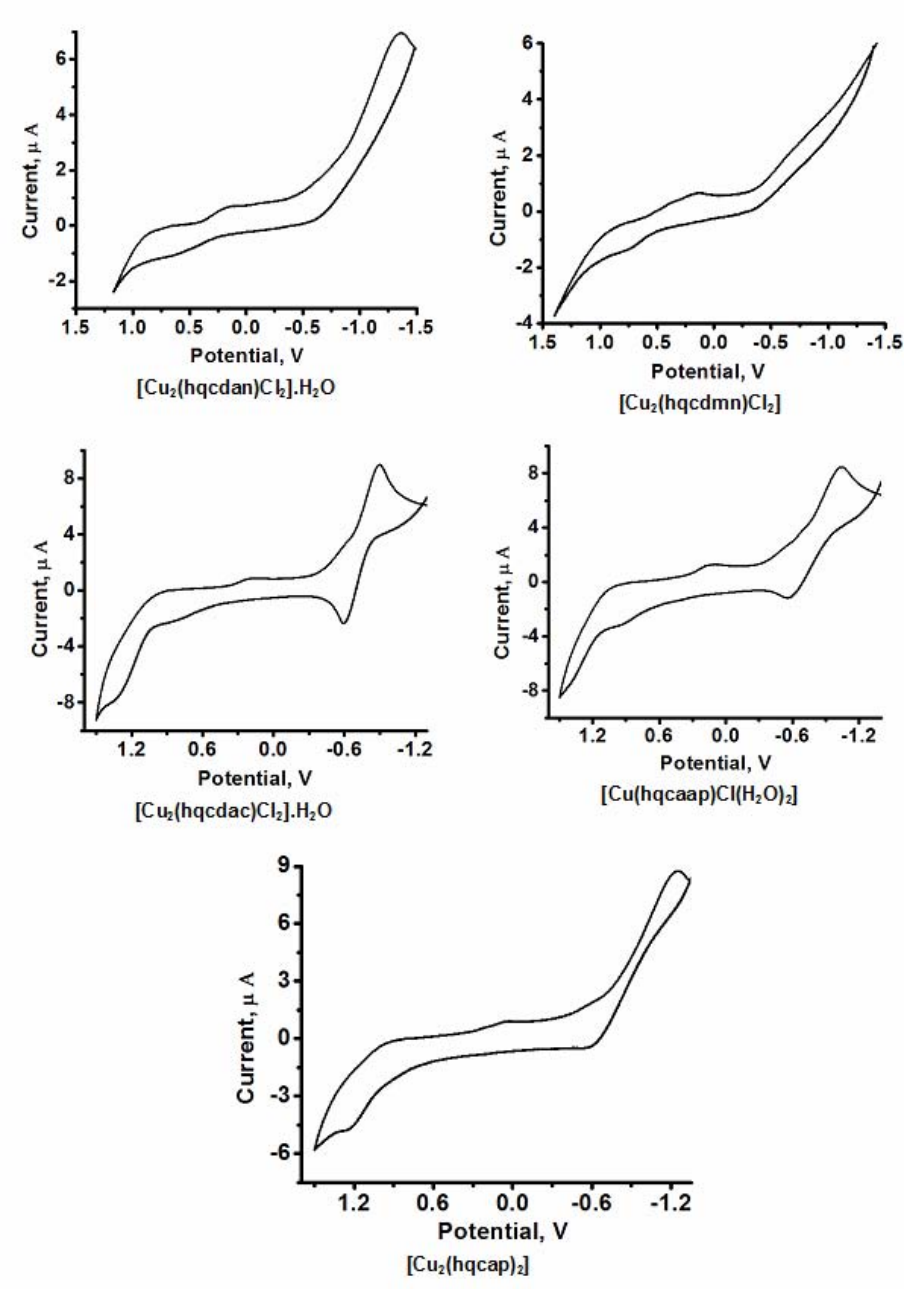

Figure 1: Cyclic voltammograms of the copper(II) complexes

4.3.5 Infrared spectra

The IR spectra of the complexes (Figures 2-6) when compared with that of the free ligands show remarkable differences. Selected vibrational bands of the free ligands and the copper complexes, useful for determining the mode of coordination of the ligands, are given in Table 4. The broad band at 3000–3500 cm^{-1} due to the the ν_{NH}/ ν_{OH} of the free Schiff base was not observed in the spectrum of the complex, which suggest that the coordination of phenolic oxygen takes place after enolisation and deprotonation. The appearance of a broad absorption band centered around 3514, 3442 and 3437 cm^{-1} in the spectra of the complexes, I, III, and IV respectively indicate the presence of lattice/coordinated water. The presence of two coordinated water molecules in the complex V is evidenced by the formation of two new bands at 1162 and 1186 cm^{-1} corresponding to δ(O—H) of the coordinated water [44]. Disappearance of the strong amide band and the formation of new bands in the range 1306−1318 cm^{-1} corresponding to ν(C—O) support the coordination of oxygen of the amide carbonyl to the metal through enolization and deprotonation [45]. The nitrogen of the quinoxaline ring is not involved in coordination because of stable six-membered chelate ring formed by the –OH group located at the ortho-position of the quinoxaline ring and azomethine unit.

The azomethine stretching frequencies of the free ligands were found to be increased in the complexes indicating the participation of the azomethine nitrogen in chelation. This unexpected increase in azomethine stretching frequency, which is observed in the case of vanadyl complexes also, might be due to the extensive delocalization of the π-electrons in fully conjugated Schiff base ligand. Furthermore, in these complexes, the bands in the regions 509−540 cm^{-1} and 421−435 cm^{-1} can be assigned to the stretching modes of the metal to ligand bonds, *ν*(Cu–O) and *ν*(Cu–N), respectively [46]. The groups of bands observed in the range 300−350 cm^{-1} in the far-IR spectra of the complexes might be due to the various ν(Cu—Cl) bonds of the complexes [47].

Coordination of the hqcdmn-H_2 is also evidenced from the changes in the nature of the two very intense ν_{CN} bands at 2243 and 2202 cm^{-1} of the free Schiff base. This doublet appears as a major ν_{CN} stretch at 2187 cm^{-1} along with a weak band at 2238 cm^{-1} after complexation. Similar observations have been made in the case of binuclear copper(II) complexes of the Schiff base derived from salicylaldehyde and 2,3 diaminomaleonitrile [48]. The band at 1656 cm^{-1} due to the C═O group of the antipyrine part of the hqcaap is shifted to 1646 cm^{-1} for the complex, V, indicating the involvement of this group in coordination [49].

Table 4: Characteristic infrared spectral bands (cm^{-1}) for copper(II) complexes

Compound	ν(O—H)[a/b]	ν(C=N)[c]	ν(C—O)[d]	ν(Cu–O)	ν(Cu–N)	ν(Cu—Cl)	δ(O–H)[e]
hqcdan-H_2	3430[a]	1597	1299	-	-	-	-
I	3514[b]	1658	1318	528	423	325	-
hqcdmn-H_2	3390[a]	1643	1294	-	-	-	-
II	-	1661	1309	540	421	336	-
hqcdac-H_2	3434[a]	1625	1290	-	-	-	-
III	3422[b]	1644	1306	532	435	318	-
hqcap-H_2	3412[a]	1606	1300	-	-	-	-
IV	-	1645	1317	509	425	-	-
hqcaap-H	3451[a]	1637	1306	-	-	-	-
V	3437[b]	1650	1312	510	422	338	1162, 1186

[a] ν(N−H)/ ν(O−H) of the free Schiff base or ; [b] ν(O—H) of coordinated water molecule;

[c] −CH=N of azomethine group; [d] phenolic ν(C−O); [e] δ(O–H) of coordinated water molecule.

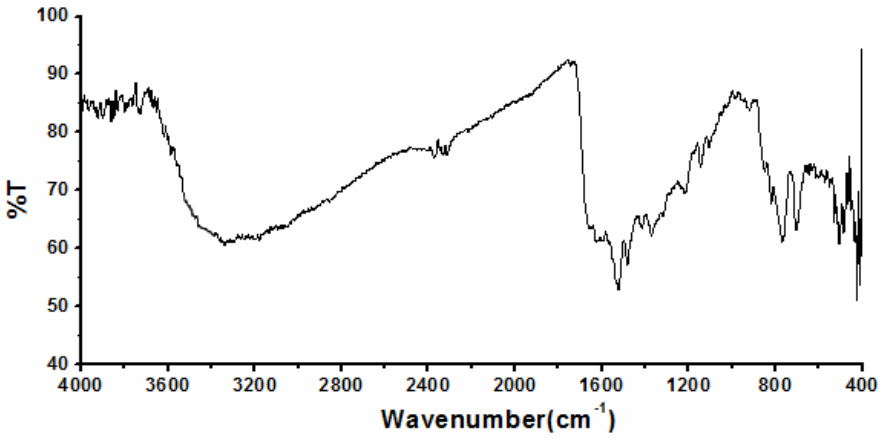

Figure 2: FT-IR spectrum of [Cu_2(hqcdan)Cl_2].H_2O (I)

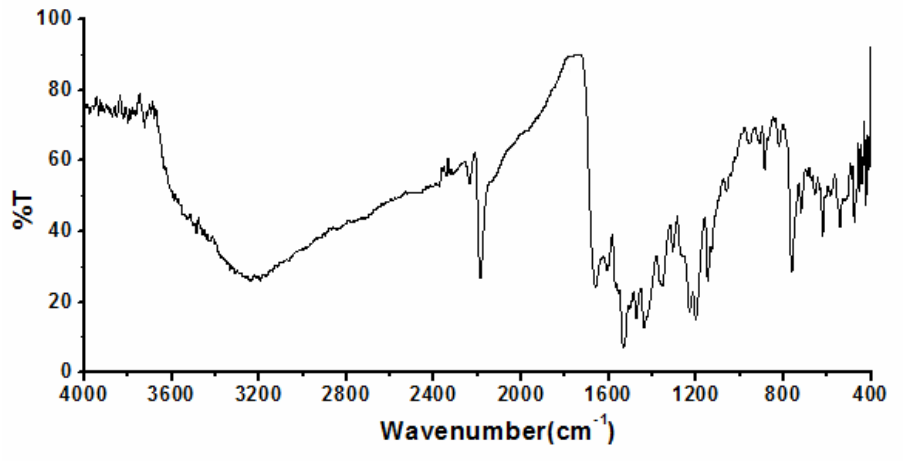

Figure 3: FT-IR spectrum of $[Cu_2(hqcdmn)Cl_2]$ (II)

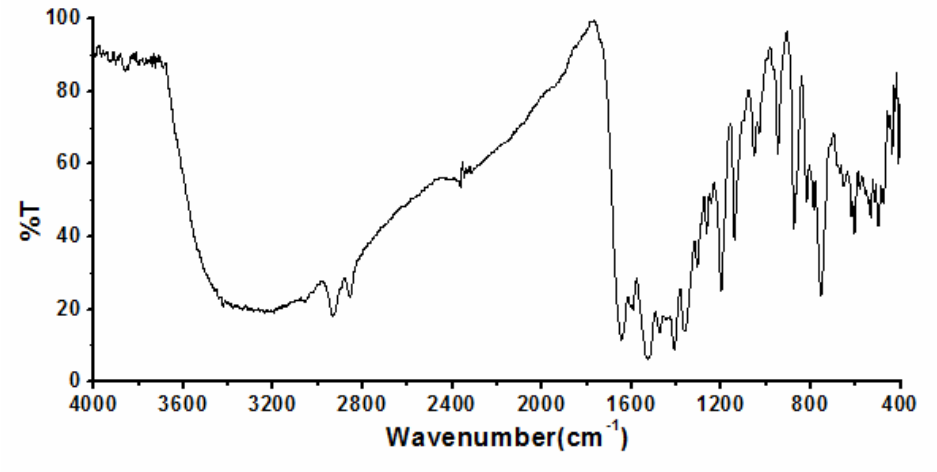

Figure 4: FT-IR spectrum of $[Cu_2(hqcdac)Cl_2].H_2O$ (III)

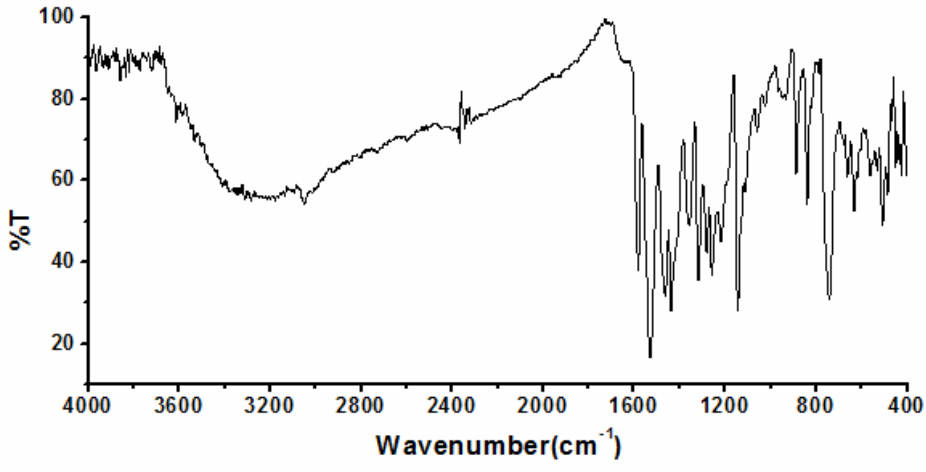

Figure 5: FT-IR spectrum of $[Cu_2(hqcap)_2]$ (IV)

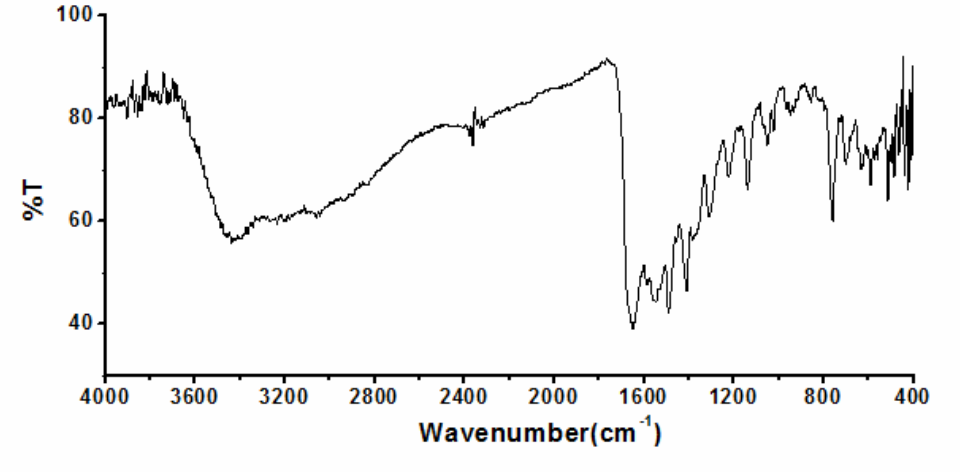

Figure 6: FT-IR spectrum of [Cu(hqcaap)Cl(H_2O)$_2$] (V)

4.3.6 Electronic spectra

The electronic spectrum of a saturated solution of the complexes I, II, III and IV in DMSO (Figure 7) shows three major absorption peaks in the range 315-340 nm, 385-490 nm and 500-530 nm. The first peak is assigned to $\pi \rightarrow \pi^*$ intraligand transitions. This band is at some what the same frequency in the Schiff base, which tells us that these transitions are not significantly affected by chelation. The extensive π conjugation present in these ligand systems clearly creates an environment for this type of intraligand $\pi \rightarrow \pi^*$ transitions [50]. On the other hand the band corresponding to azomethine showed a slight shift to longer wavelength on going from ligand to complex, indicating coordination of ligand to metals through the azomethine moiety [51,52]. The second peak could be due to Cu(II) → ligand charge transfer (MLCT) transitions [53]. For square planar complexes with d_{x2-y2} ground state, three spin allowed transitions are possible viz., $^2B_{1g} \rightarrow {}^2A_{1g}$ ($d_{x2-y2} \rightarrow d_{z2}$), $^2B_{1g} \rightarrow {}^2B_{2g}$ ($d_{x2-y2} \rightarrow d_{xy}$) and $^2B_{1g} \rightarrow {}^2E_g$ ($d_{x2-y2} \rightarrow d_{xz}$, d_{yz}) but it is often difficult to resolve into three bands since the four lower orbitals are so close together in energy that individual transfer from these to the upper d level cannot be distinguished. The third peak in the wavelength range 500–530 nm corresponds to d–d transition of this type as expected for square planar copper(II) complexes [54-58]. However, in the case of diffuse reflectance spectra (Figure 8), the d-d bands are

seen due to the high concentration of the complex in the solid state. The spectral bands and their assignments are given in Table 5. As no bands are observed above 1000 nm, the complex might have a square planar or close to square planar structure [59].

Electronic spectrum of the complex, V, in DMSO shows one d-d band at 504 nm (Figure 7) which can be assigned to $^2E_g \rightarrow {}^2T_{2g}$ transition of an octahedral geometry. Though in cases where the ^2E_g and $^2T_{2g}$ states of the octahedral Cu(II) ion (d^9) split under the influence of the tetragonal distortion the three transitions ^{2}B1g → ^{2}Eg, $^2B_{1g} \rightarrow {}^2B_{2g}$, and $^2B_{1g} \rightarrow {}^2A_{1g}$ are expected [60], their very close energies could have made them appear in the form of one broad band envelope. The reflectance spectrum of V (Figure 8) consists of three d-d bands at 492 nm (20,320 cm^{-1}), 688 nm (14,530 cm^{-1}) and a shoulder band at 954 nm (10,480 cm^{-1}) corresponding to the above said transitions, $^2B_{1g} \rightarrow {}^2E_g$, $^2B_{1g} \rightarrow {}^2B_{2g}$ and $^2B_{1g} \rightarrow {}^2A_{1g}$ respectively in a distorted octahedral geometry (Table 5).

Table 5: Electronic spectral assignments for copper(II) complexes

Complex	Electronic spectral bands; nm (cm^{-1})	Assignments
I	328 (30,480)[a], 441 (22,670)[a]	Intra ligand transitiions
	530 (18,860)[as]	$d_{xy} \rightarrow d_{yz}, d_{xz}, d_{z2}$
	219 (45,660)[b], 258 (38,760)[bs], 342 (29,240) [bs], 381 (26,240) [bs]	Intra ligand transitiions
	572 (17,480)[b]	$^2B_{1g} \rightarrow {}^2E_g$ ($d_{x2-y2} \rightarrow d_{xz}, d_{yz}$)
	680 (14,700)[b]	$^2B_{1g} \rightarrow {}^2B_{2g}$ ($d_{x2-y2} \rightarrow d_{xy}$)
	868 (11,560)[bs]	$^2B_{1g} \rightarrow {}^2A_{1g}$ ($d_{x2-y2} \rightarrow d_{z2}$)
II	316 (31,640)[a], 485 (20,610)[a]	Intra ligand transitiions
	517 (19,340)[a]	$d_{xy} \rightarrow d_{yz}, d_{xz}, d_{z2}$
	215 (46,510)[b], 266 (37,590)[b], 308 (32,460)[bs]	Intra ligand transitiions
	465 (21,500)[b]	$^2B_{1g} \rightarrow {}^2E_g$ ($d_{x2-y2} \rightarrow d_{xz}, d_{yz}$)
	600 (16,660)[b]	$^2B_{1g} \rightarrow {}^2B_{2g}$ ($d_{x2-y2} \rightarrow d_{xy}$)
	830 (12,040)[bs]	$^2B_{1g} \rightarrow {}^2A_{1g}$ ($d_{x2-y2} \rightarrow d_{z2}$)
III	325 (30,770)[a], 386 (25,900)[a], 437 (22,880)[a]	Intra ligand transitiions
	497 (20,120)[as]	$d_{xy} \rightarrow d_{yz}, d_{xz}, d_{z2}$
	217 (46,830)[b], 262 (38,160)[b], 355 (29,850)[bs]	Intra ligand transitiions
	420 (23,810)[b]	$^2B_{1g} \rightarrow {}^2E_g$ ($d_{x2-y2} \rightarrow d_{xz}, d_{yz}$)
	535 (18,690)[b]	$^2B_{1g} \rightarrow {}^2B_{2g}$ ($d_{x2-y2} \rightarrow d_{xy}$)
	874 (11,440)[bs]	$^2B_{1g} \rightarrow {}^2A_{1g}$ ($d_{x2-y2} \rightarrow d_{z2}$)
IV	345 (28,980)[as], 439 (22,770)[a]	Intra ligand transitiions
	532 (18,790)[as]	$d_{xy} \rightarrow d_{yz}, d_{xz}, d_{z2}$
	220 (45,450)[b], 263 (38,220)[bs], 317 (31,540)[bs]	Intra ligand transitiions
	478 (20,920)[b]	$^2B_{1g} \rightarrow {}^2E_g$ ($d_{x2-y2} \rightarrow d_{xz}, d_{yz}$)
	586 (17,600)[b]	$^2B_{1g} \rightarrow {}^2B_{2g}$ ($d_{x2-y2} \rightarrow d_{xy}$)
	836 (11,960)[bs]	$^2B_{1g} \rightarrow {}^2A_{1g}$ ($d_{x2-y2} \rightarrow d_{z2}$)
V	341 (29,320)[a], 439 (22,770)[as]	Intra ligand transitiions
	504 (19,840)[a]	$^2E_g \rightarrow {}^2T_{2g}$
	215 (46,510)[b], 260 (38,460)[bs], 336 (29,760)[b]	Intra ligand transitiions
	492 (20,320)[b]	$^2B_{1g} \rightarrow {}^2E_g$
	688 (14,530)[b]	$^2B_{1g} \rightarrow {}^2B_{2g}$
	954 (10,480)[bs]	$^2B_{1g} \rightarrow {}^2A_{1g}$

[a] Saturated solution spectrum in DMSO; [b] Diffuse reflectance spectrum in the solid state;
[s] Shoulder band

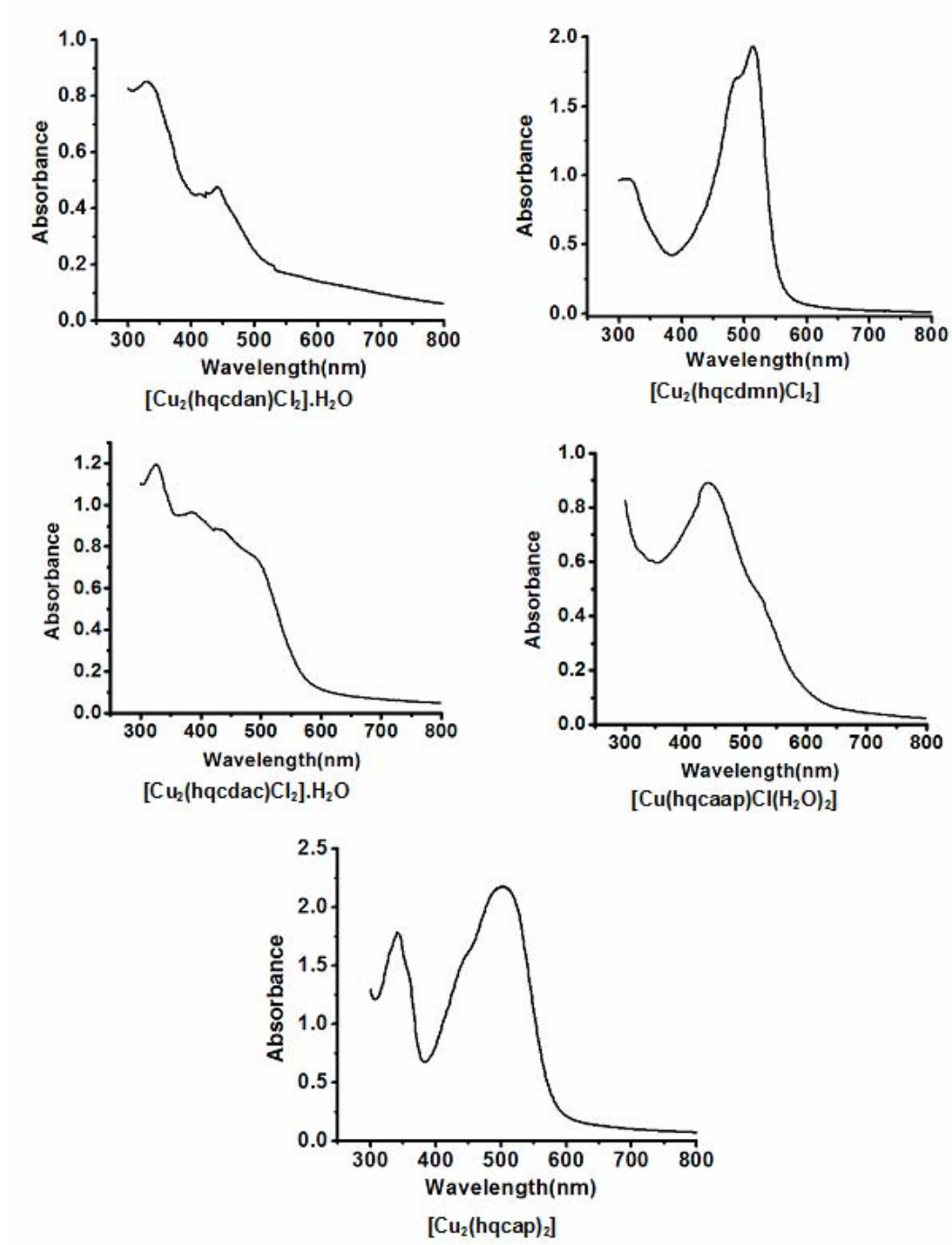

Figure 7: Electronic spectra of the copper(II) complexes in DMSO

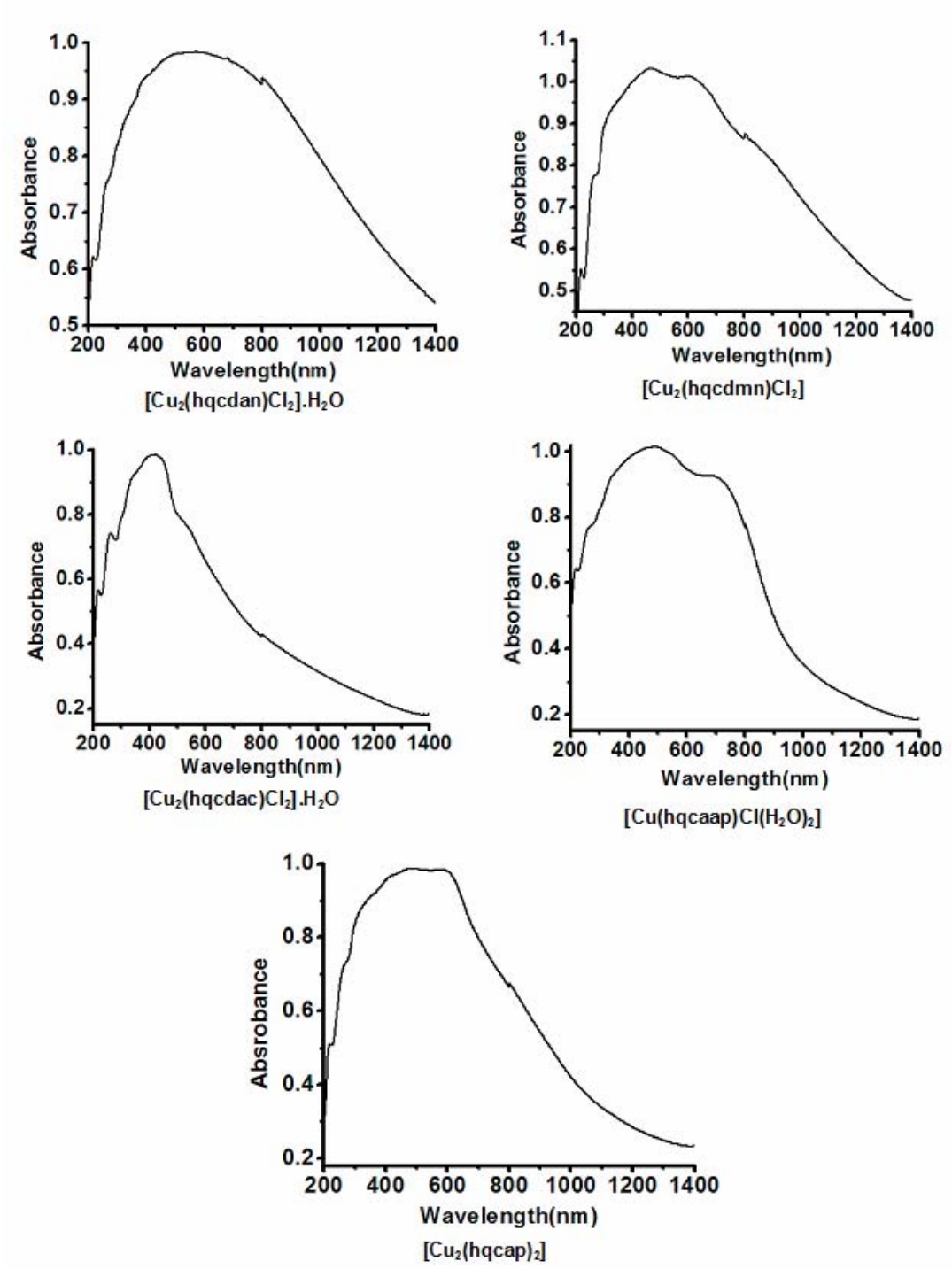

Figure 8: Diffuse reflectance spectra of the copper(II) complexes

4.3.7 Thermal Analysis

Thermal analyses of the complexes were carried out under nitrogen atmosphere/static air at a heating rate of 20 °C min^{-1} from ambient temperature up to 1000 °C. The TG/DTA/DTG curves are represented in Figures 9-13. With TG/DTA/DTG analysis it is often possible to check whether there is coordinated or lattice water in the complexes [61]. The molecular formulae of the complexes 1, III and IV deduced from elemental analysis indicates the presence of lattice/coordinated water. In the case of complexes II, IV and V there is no significant weight loss below 130 °C suggesting the absence of lattice water molecules.

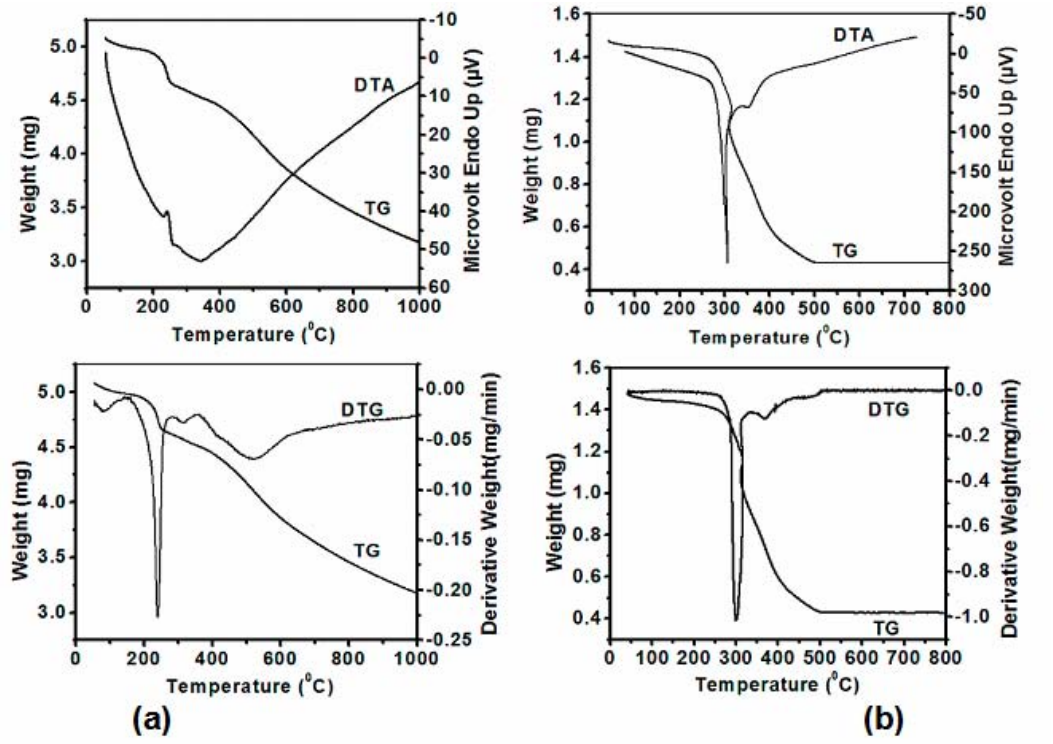

Figure 9: TG-DTA-DTG curves of $[Cu_2(hqcdan)Cl_2].H_2O$: in nitrogen (a) and in air (b)

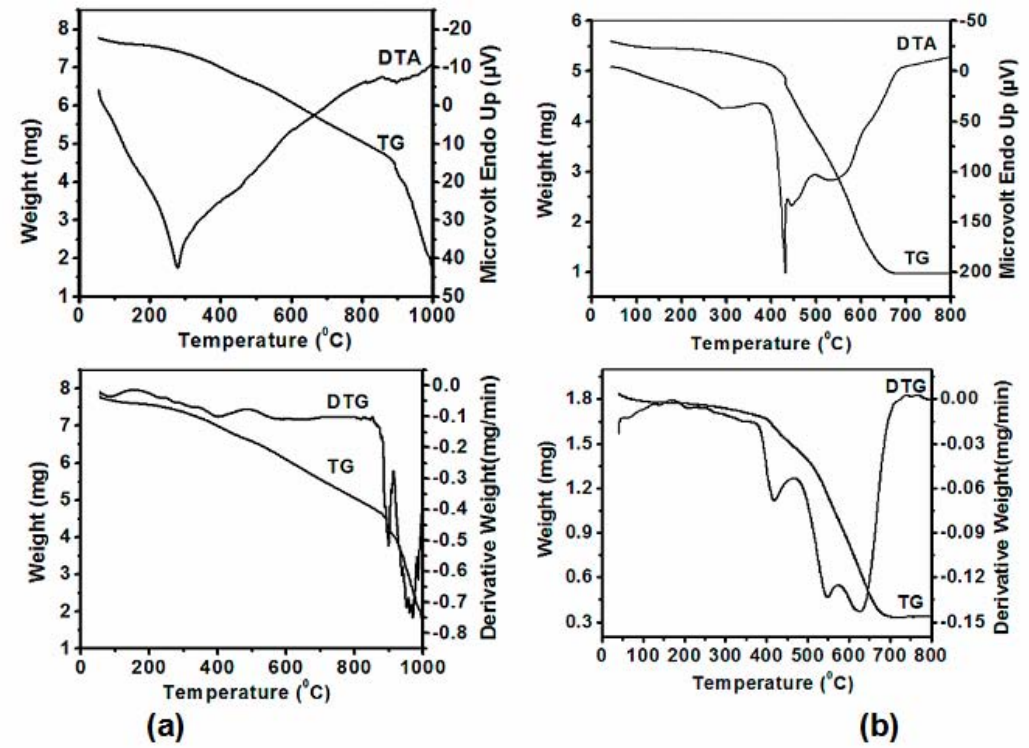

Figure 10: TG-DTA-DTG curves of $[Cu_2(hqcdmn)Cl_2]$: in nitrogen (a) and in air (b)

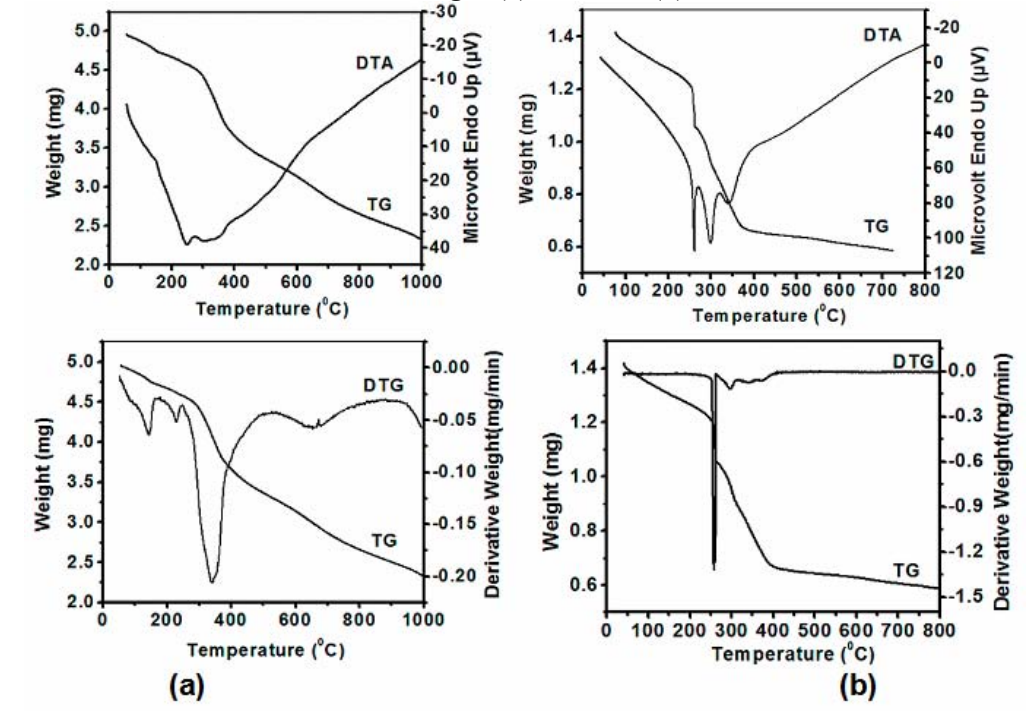

Figure 11: TG-DTA-DTG curves of $[Cu_2(hqcdac)Cl_2].H_2O$: in nitrogen (a) and in air (b)

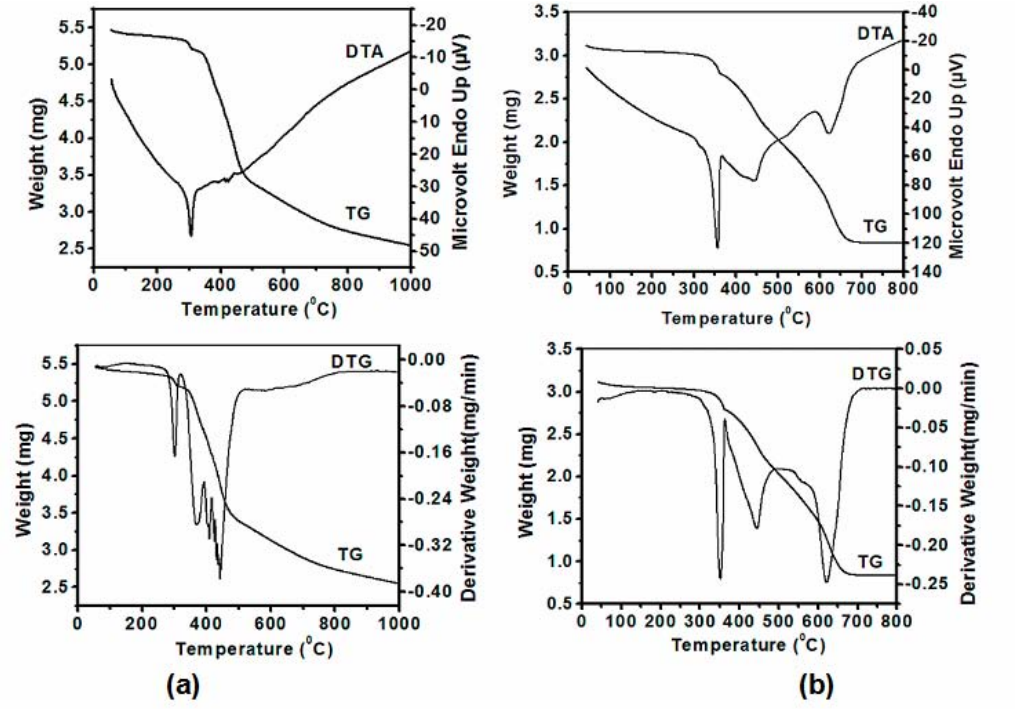

Figure 12: TG-DTA-DTG curves of $[Cu_2(hqcap)_2]$: in nitrogen (a) and in air (b)

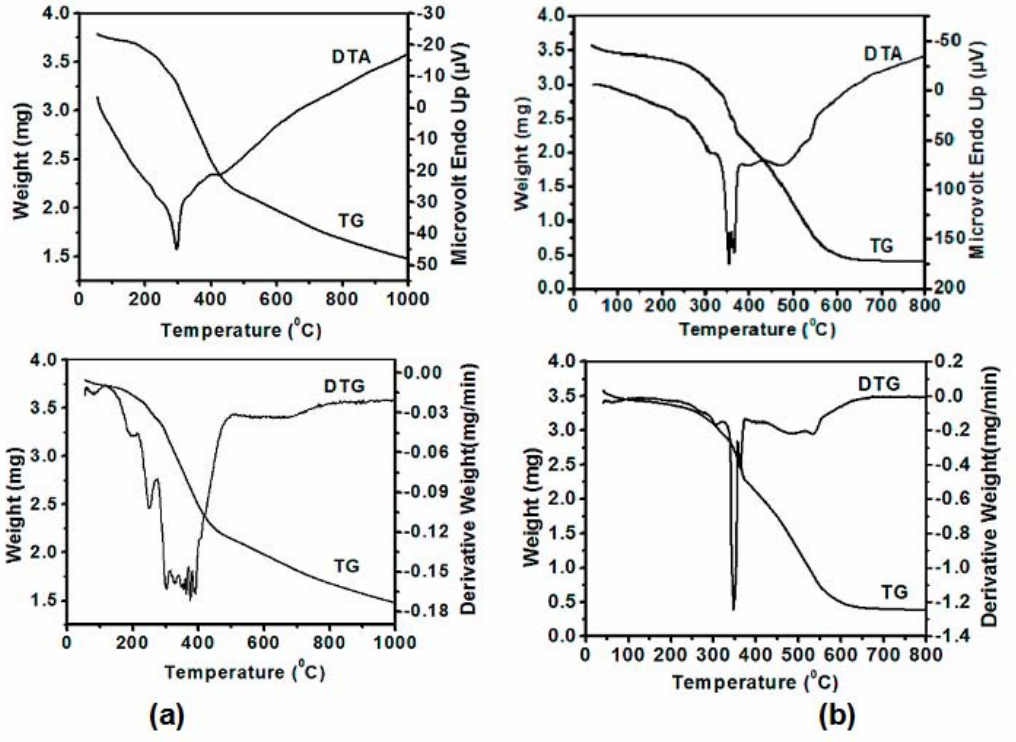

Figure 13: TG-DTA-DTG curves of $[Cu(hqcaap)Cl(H_2O)_2]$: in nitrogen (a) and in air (b)

But in complexes I and III weight loss corresponding to one water molecule is observed at a temperature below 130 °C which in turn implies that one molecule of water of hydration is associated with the complex. Mass loss in the temperature range 130−220 °C in the complex, V, corresponds to the presence of two coordinated water molecules [62-64]. This is followed by the decomposition of the anhydrous complexes in two or three steps. In nitrogen atmosphere the decomposition was not seen to be completed even after 1000 ºC. In air atmosphere the decomposition takes place at lower temperatures and ended with oxide formation.

4.3.8 EPR spectra

The EPR spectra of the complexes in the polycrystalline state at 298 and 77 K and that in DMF solution at 77 K were recorded in the X-band region, using 100 KHz field modulation and the g factors were quoted relative to the standard marker TCNE (g = 2.00277). The EPR spectra of all the complexes in the polycrystalline state at room temperature (298 K) show only one broad signal (Figure 14). Such an isotropic spectrum consisting of a broad signal and hence only one g value arises due to extensive exchange coupling through misalignment of the local molecular axes between different molecules in the unit cell and enhanced spin lattice relaxation. The g value varies in the range 2.099−2.124 (Table 6). This type of spectra unfortunately give no information on the electronic ground state of the copper(II) ion present in the complexes.

Table 6: EPR spectral parameters of the copper(II) complexes in polycrystalline state at 298 K

Parameters	I	II	III	IV	V
g_{iso}	2.103	2.110	2.099	2.124	2.113

Where (I) $[Cu_2(hqcdan)Cl_2].H_2O$; (II) $[Cu_2(hqcdmn)Cl_2]$; (III) $[Cu_2(hqcdac)Cl_2].H_2O$; (IV) $[Cu_2(hqcap)_2]$; (V) $[Cu(hqcaap)Cl(H_2O)_2]$.

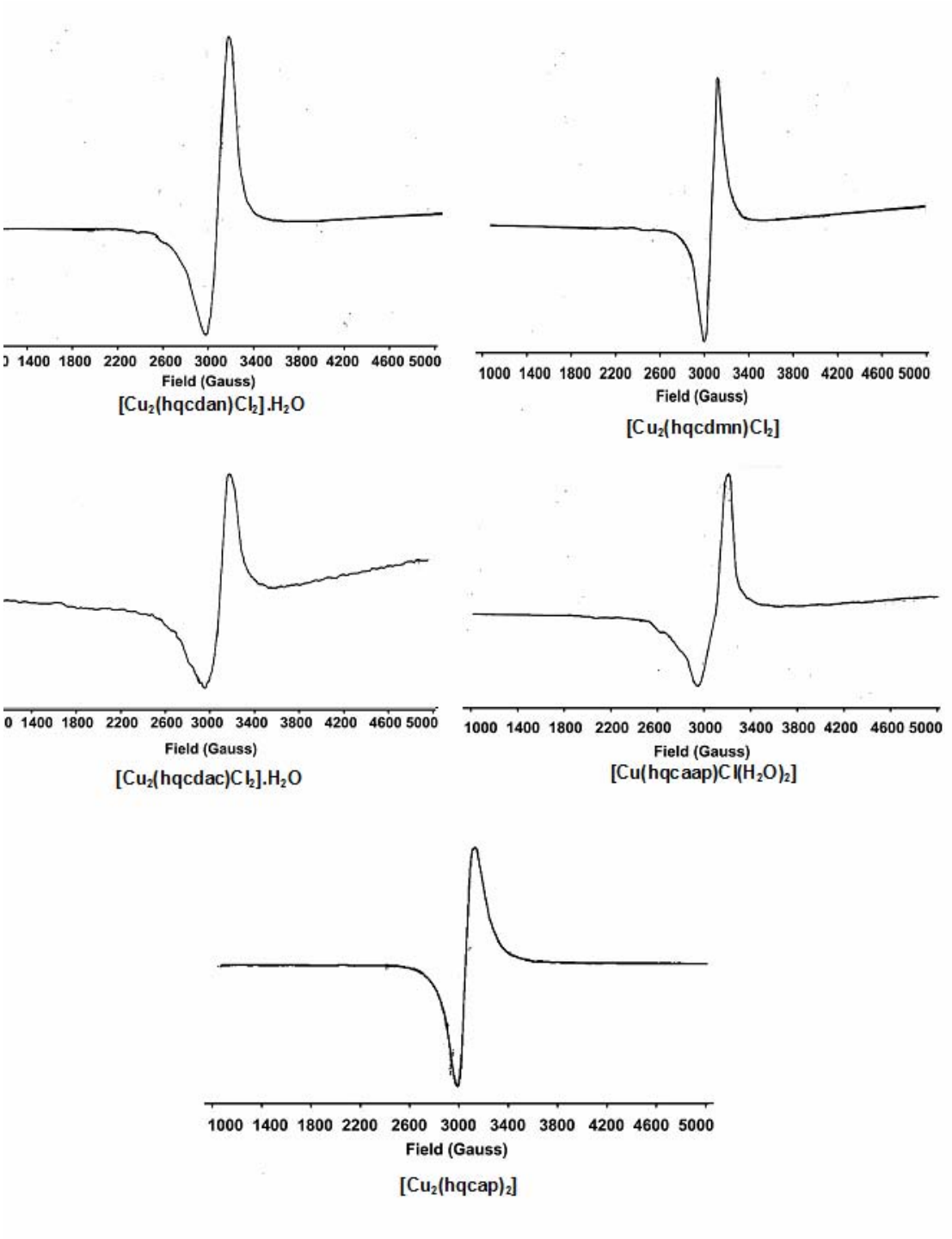

Figure 14: EPR spectra of copper(II) complexes in polycrystalline state at 298K

In the case of complexes, I and IV, half-field signals could not be observed in the spectrum recorded in polycrystalline state or in DMF at LNT. The solid state LNT spectra were similar to that recorded at RT. However, the spectra of these complexes in DMF at LNT (Figures 15,16) were found to be anisotropic and the corresponding $g_{\|}$ and $g_{\perp}$ values are given in Table 7.

Table 7: EPR spectral parameters of the copper(II) complexes in polycrystalline state at 77 K

Parameters	I	II	III	IV	V
$g_{\|}$	-	2.257		-	
$g_{\perp}$	-	2.110		-	
g_{iso} or g_1, g_2, g_3	-	-	2.015, 2.135, 2.238	-	1.727, 1.901, 2.129
$A_{\|}$ or A_1, A_2, A_3	-	-	-	-	204, 134, 169
$A_{\perp}$	-	-	-	-	-
G	-	2.36	3.24	-	-
Half field (Gauss)	-	-	1560	-	-

Where (I) $[Cu_2(hqcdan)Cl_2].H_2O$; (II) $[Cu_2(hqcdmn)Cl_2]$; (III) $[Cu_2(hqcdac)Cl_2].H_2O$; (IV) $[Cu_2(hqcap)_2]$; (V) $[Cu(hqcaap)Cl(H_2O)_2]$. The '*A*' values are expressed in units of cm^{-1} multiplied by a factor of 10^{-4}.

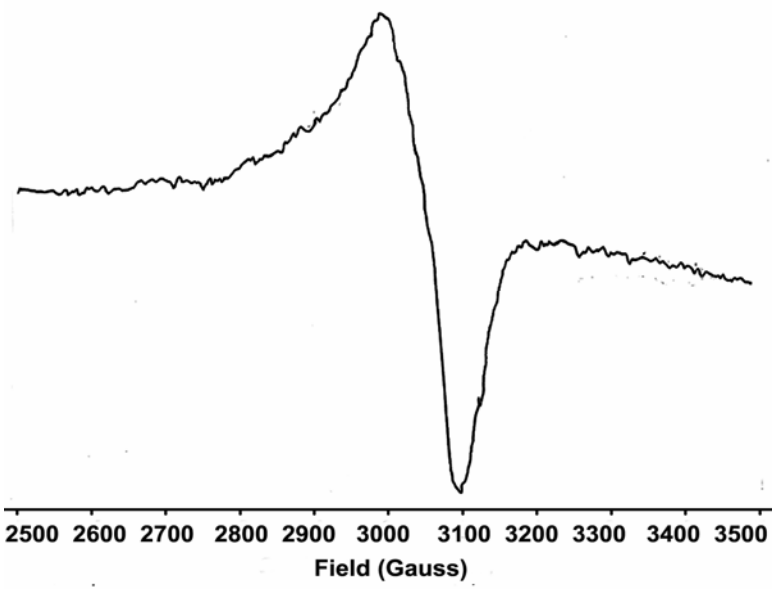

Figure 15: EPR spectrum of $[Cu_2(hqcdan)Cl_2].H_2O$ (I) in DMF at LNT

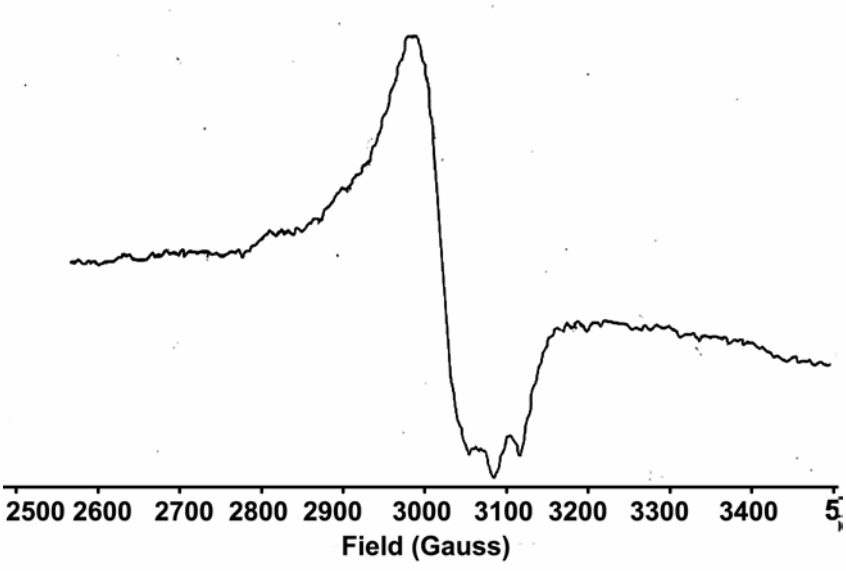

Figure 16: EPR spectrum of $[Cu_2(hqcap)_2]$ (IV) in DMF at LNT

The solid state EPR spectrum of complex, II, recorded at LNT (77 K) was found to be anisotropic with g-values, $g_{\|}$ = 2.257 and $g_{\perp}$ = 2.110 (Figure 17). The spectrum is axial in nature and $g_{\|} > g_{\perp} > 2.0023$, indicating $d_{x^2-y^2}$ ground state, which is characteristic of a square planar geometry [65]. The g_{av} value calculated from the relation: $g_{av} = 1/3(g_{\|} + 2g_{\perp})$ was found to be equal to 2.159. The deviation of the g_{av} from that of the free electron (2.0023) is due the covalent nature [66]. This covalent planar bonding like other complexes of N_2O_2 donor ligands is supported by a $g_{\|}$ value of 2.257 as suggested by Kivelson and Neiman [67]. Further, there exists considerable exchange interaction in the complex, II, which is evidenced by a G value ($G = (g_{\|} - 2.0023)/(g_{\perp} - 2.0023)$) of 2.36 [68].

The nature of the ESR spectrum of II recorded in DMF at LNT (Figure 18) shows rhombic spectral features with three 'g' values g_1, g_2 and g_3 at 2.049, 2.133 and 2.179 respectively [69]. Here the g_3 value is less than 2.3, which is in agreement with the covalent character of M−L bonds [67]. The hyperfine splitting

was not found. The anisotropic rhombic g-tensors with G < 4.0 (G = (g_3 − 2.0023)/ ($g_\perp$ − 2.0023); $g_\perp$ = ($g_1 + g_2$)/2); G = 1.99) suggest exchange coupling interactions in the complex [70]. The presence of a half-field signal (Figure 18) at 1570 G further substantiates the binuclear nature of the complex [69].

Table 8: EPR spectral parameters of the copper(II) complexes in DMF at 77 K

Parameters	I	II	III	IV	V
$g_\parallel$	2.233	-	-	2.237	-
$g_\perp$	2.109	-	-	2.131	-
g_{iso} or g_1, g_2, g_3	-	2.049, 2.133, 1.179	2.145	-	1.903, 1.976, 2.255
A or $A_\parallel$	-	166.9	131.7	-	-
$A_\perp$	-	-		-	-
G	-	1.99		-	-
Half field (Gauss)	-	1570		-	-

Where (I) $[Cu_2(hqcdan)Cl_2].H_2O$; (II) $[Cu_2(hqcdmn)Cl_2]$; (III) $[Cu_2(hqcdac)Cl_2].H_2O$; (IV) $[Cu_2(hqcap)_2]$; (V) $[Cu(hqcaap)Cl(H_2O)_2]$. The '*A*' values are expressed in units of cm^{-1} multiplied by a factor of 10^{-4}.

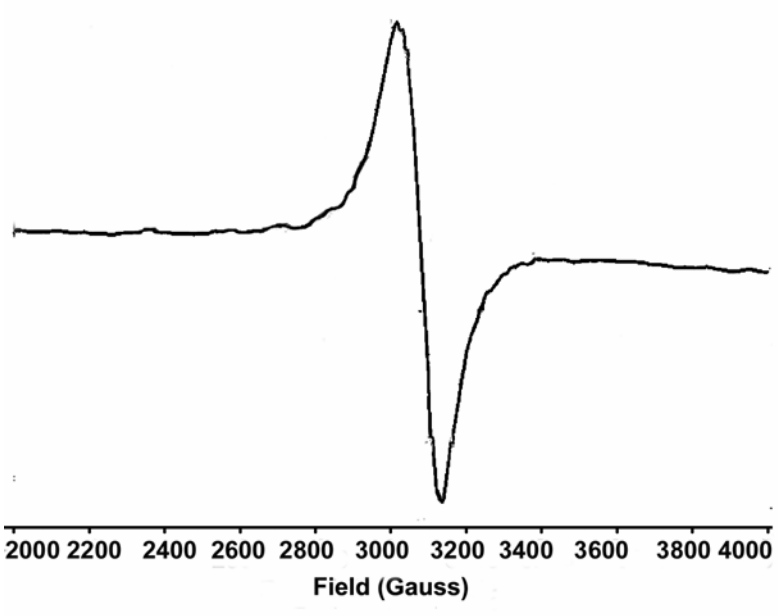

Figure17: EPR spectrum of $[Cu_2(hqcdmn)Cl_2]$ (II) in solid at LNT

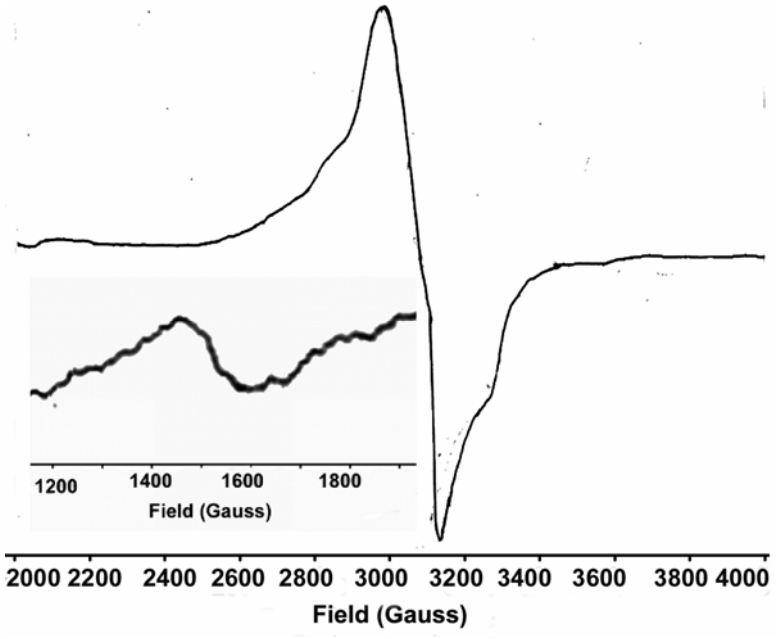

Figure 18: EPR spectrum of [Cu_2(hqcdmn)Cl_2] (I) in DMF at LNT

The EPR spectrum of complex III in the polycrystalline state at LNT (Figure 19) shows rhombic spectral features with three 'g' values g_1, g_2 and g_3 at 2.015, 2.135 and 2.238 respectively [69]. Here also the g_3 value is less than 2.3, indicating the covalent character of M−L bonds [67]. The hyperfine splitting was not found. The anisotropic rhombic g-tensors with G < 4.0 (G = (g_3 − 2.0023)/ ($g_\perp$ − 2.0023); $g_\perp$ = (g_1 + g_2)/2); G = 3.24) again suggest exchange coupling interactions in this complex also [70]. As in the case of complex II, half-field signal at 1560 G in the solid state EPR of III (Figure 19) at LNT confirms its binuclear nature [69]. The ESR spectrum of III recorded in DMF at LNT (Figure 20) shows seven hyperfine lines due to the two nearly Cu(II) centres with g = 2.145 and A = 131.9 × 10^{-4} cm^{-1}. Here the half field signal could not be observed.

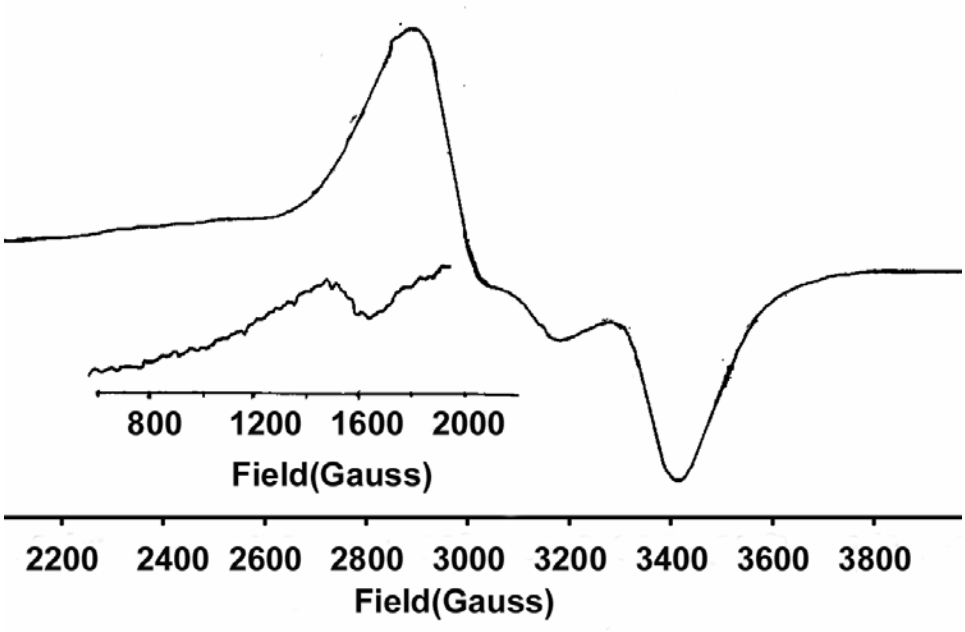

Figure 19: EPR spectrum of $[Cu_2(hqcdac)Cl_2].H_2O$ (III) in solid LNT

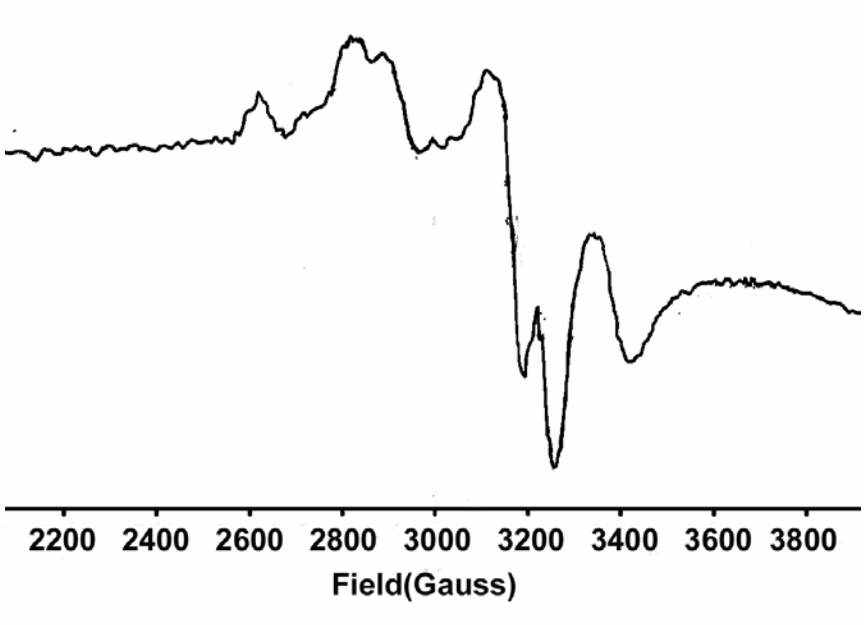

Figure 20: EPR spectrum of $[Cu_2(hqcdac)Cl_2].H_2O$ (III) in DMF LNT

The EPR spectrum of the mononuclear copper(II) complex, V, (Figure 21) in solid state at LNT gives three g values, g_1 = 1.727, g_2 = 1.901 and g_3 = 2.129, indicating a rhombic distortion in the symmetry. Each peak corresponding to the g values is splitted into four well resolved hyperfine lines [71]. The hyperfine lines is due to the interaction of the electron spin with copper nuclear spin (^{63,65}Cu, I = 3/2). The corresponding A values are $A_1 = 204 \times 10^{-4}$ cm^{-1}, $A_2 = 134 \times 10^{-4}$ cm^{-1} and $A_3 = 169 \times 10^{-4}$ cm^{-1}. The spectrum of V in DMF at LNT, (Figure 22) is significantly different from that in the solid state. Here also the spectrum gives three 'g' values, g_1 = 1.903, g_2 = 1.976 and g_3 = 2.255, but without any hyperfine lines. This may be due to the reason that in DMF the geometry of the complex may change from octahedral to square planar with the removal of two coordinated water molecules.

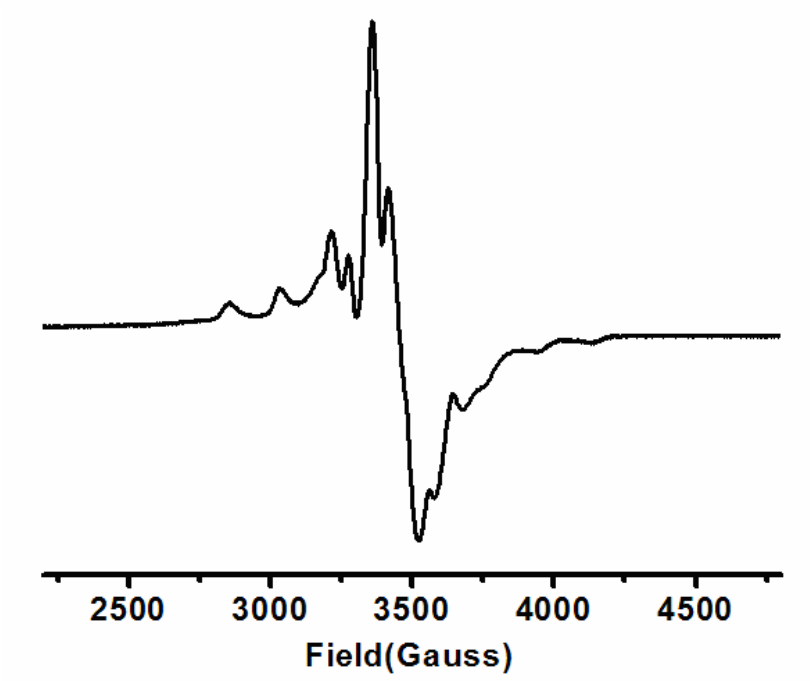

Figure 21: EPR spectrum of [Cu(hqcaap)Cl(H_2O)$_2$] (V) in solid at LNT

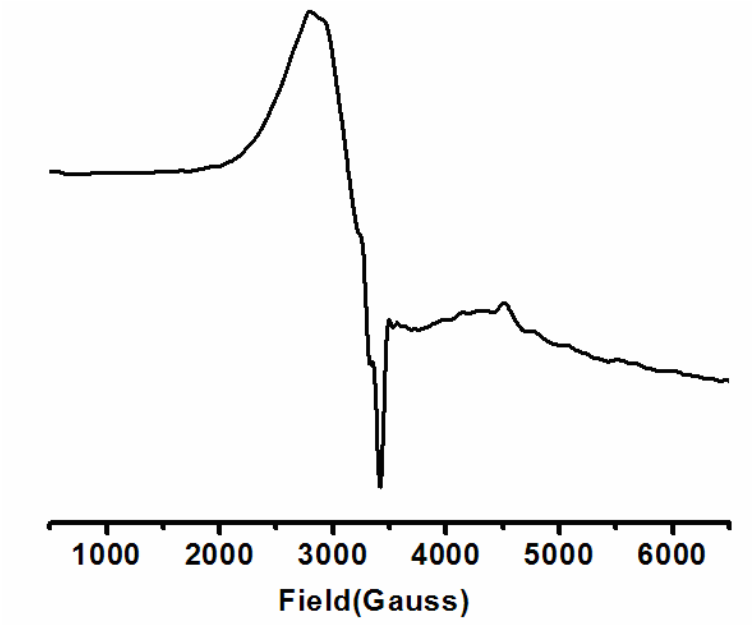

Figure 22: EPR spectrum of [Cu(hqcaap)Cl(H_2O)$_2$] (V) in DMF at LNT

Conclusions

The molecular formulae of the complexes were calculated from the elemental analyses data and found to be [Cu_2(hqcdan)Cl_2].H_2O, [Cu_2(hqcdmn)Cl_2], [Cu_2(hqcdac)Cl_2].H_2O, [Cu_2(hqcap)$_2$] and [Cu(hqcaap)Cl(H_2O)$_2$]. The subnormal magnetic moment values and cyclic voltammetric data substantiate a binuclear structure for all the complexes except for the last one. In this case a magnetic moment of 1.76 BM indicates the monomeric nature. The EPR spectral data also favours the binuclear structures with half-field signals. Square-planar geometry for the binuclear complexes and octahedral geometry for the mononuclear complex were further confirmed by DRS studies. Based on these evidences the following structures (Figure 23) have been proposed for the complexes.

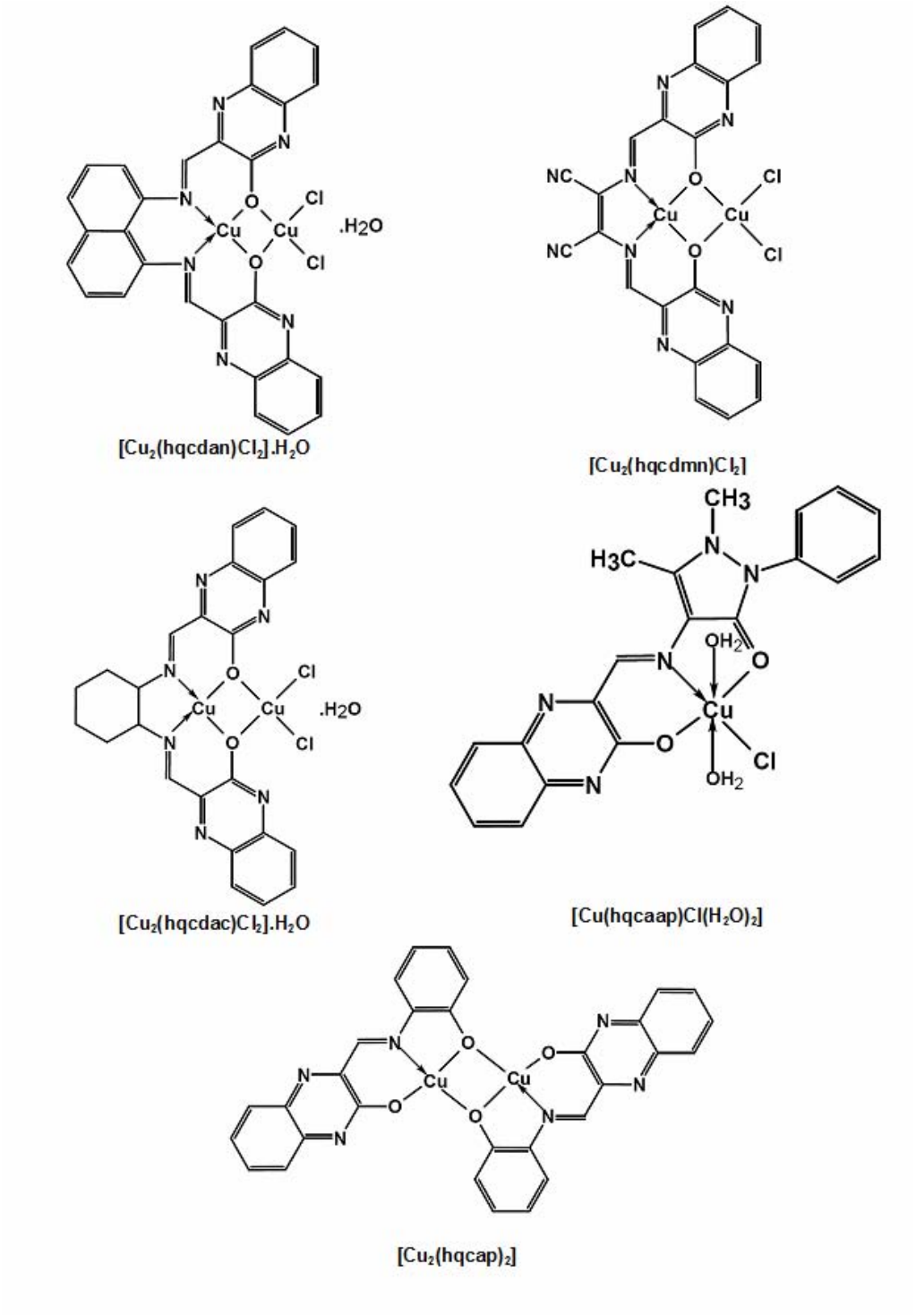

Figure 23: Proposed structures for the copper(II) complexes

References

[1] E.I. Solomon, U.M. Sundaram, T.E. Machonkin. Chemical Reviews, 96 (1996) 2563-2606

[2] K. Selmeczi, M .Giorgi, M. Reglier, G. Speier. Coordination Chemistry Reviews, 245 (2003) 191–201

[3] Y. Wang, J.L. DuBois, B. Hedman, K.O. Hodgson, T.D.P. Stack. Science 279 (1998) 537–540

[4] S. Dhar, D. Senapati, P.K. Das, P. Chattopadhyay, M. Nethaji, A.R. Chakravarty. Journal of the American Chemical Society, 125 (2003) 12118–12124

[5] M. Gonzalez-Alvarez, G. Alzuet, J. Borras, M. Pitie, B. Meunier. Journal of Biological Inorganic Chemistry, 8 (2003) 644–652

[6] L.M. Mirica, X. Ottenwaelder, T.D.P. Stack. Chemical Reviews, 104 (2004) 1013-1046

[7] F. Cotton, G. Wilkinson, C. Murillo, M. Bochmann. Advanced Inorganic Chemistry, 6th ed., John Wiley & Sons, (1999) 855-876

[8] R. Knock, A. Wilk, K.J. Wannowius, D. Reinen, H. Elias. Inorganic Chemistry, 29 (1990) 3799-3805

[9] E.C. Lingafelter, G.L. Simmons, B. Morosin, C. Scheringer, C. Freiburg. Acta Crystallographica Section C: Crystal Structure Communications, 14 (1961) 1222-1225

[10] T.P. Cheeseman, D. Hall, T.N. Waters. Journal of the Chemical Society, A (1966) 685-693

[11] I. Bertini, G. Canti, R. Grassi. Inorganic Chemistry, 19 (1980) 2198-2200

[12] S. Torelli, C. Belle, I. Gautier-Luneau, J.L. Pierre, E. Saint-Aman, J.M. Latour, L. Le Pape, D. Luneau. Inorganic Chemistry, 39 (2000) 3526-3536

[13] S. Dhar, M. Nethaji, A.R. Chakravarty. Inorganica Chimica Acta, 358 (2005) 2437–2444

[14] Z. Li, K.R. Conser, E.N. Jacobsen. Journal of the American Chemical Society, 115 (1993) 5326-5327

[15] Z. Li, Z. Zheng, B. Wan, H. Chen. Journal of Molecular Catalysis A: Chemical, 165 (2001) 67-71

[16] C.R. Jacob, S.P. Varkey, P. Ratnasamy. Microporous and Mesoporous Materials, 22 (1998) 465-474

[17] W.J. Geary. Coordination Chemistry Reviews, 7 (1971) 81-122

[18] J.J. Grzybowski, P.H. Merrell, F.L. Urbach. Inorganic Chemistry, 17 (1978) 3078-3082

[19] B.J. Hathaway, D.E. Billing. Coordination Chemistry Reviews, 5 (1970) 143-207

[20] F.A. Cotton, G. Wilkinson, C.A. Murillo, M. Bochmann. Advanced Inorganic Chemistry, 6th edn. Wiley, New York, (1999)

[21] J. Kohout, M. Hvastijova, J. Kozisek, J.G. Diaz, M. Valko, L. Jager, I. Svoboda. Inorganica Chimica Acta, 287 (1999) 186-192

[22] E.I. Solomon, U.M. Sundaram, T.E. Machonkin. Chemical Reviews, 96 (1996) 2563-2606

[23] R.C. Long, D.N. Hendrickson. Journal of the American Chemical Society, 105 (1983)1513-1521

[24] P. Zanello, P.A. Vigato, G.A. Mazzocchin. Transition metal Chemistry, 7 (1982) 291-293

[25] S.K. Mandel, K. Nag. Journal of the Chemical Society, Dalton transactions, (1983) 2429

[26] S. Harmalker, S.E. Jones, D.T. Sawyer. Inorganic Chemistry, 22 (1983) 2790-2794

[27] J.B. Flanagan, S. Margel, A.J. Bard, F.C. Anson. Journal of the American Chemical Society, 100 (1978) 4248-4253

[28] A.M. Bond, M. Haga, I.S. Creece, R. Robson, J.C. Wilson. Inorganic Chemistry, 28 (1989) 559-566

[29] A.R. Hendrcikson, R.L. Martin, N.M. Rohde. Inorganic Chemistry, 15 (1976) 2115-2119

[30] S. Theil, R. Yerande, R. Chikate, F. Dahan, A. Bousseksou, S. Padhye, J-P. Tuchagues. Inorganic Chemistry, 36 (1997) 6279-6286

[31] S. Torelli, C. Belle, I. Gautier-Luneau, J.L. Pierre, E. Saint-Aman, J.M. Latour, L. Le Pape, D. Luneau. Inorganic Chemistry, 39 (2000) 3526-3536

[32] R. Mahalakshmy, R. Venkatesan, P.S. Rao, R. Kannappan, T.M. Rajendiran, Transition Metal Chemistry 29 (2004) 623–629

[33] R.C. Long, D.N. Hendrickson. Journal of the American Chemical Society, 105 (1983) 1513-1521

[34] C. Pater, Journal of Coordination Chemistry, 28 (1992) 297

[35] T.M. Rajendiran, R. Mahalakshmy, R. Kannappan, J. Rajeswari, R. Venkatesan, P. Rao. Transition Metal Chemistry, 28 (2003) 280–287

[36] S-Z. Zhan, Y. Miao, P. Li, C-W. Yuan. Transition Metal Chemistry, 24 (1999) 311-316

[37] S. Sujatha, T.M. Rajendiran, R. Kannappan, R. Venkatesan, P.S. Rao. Proc. Indian Acad. Sci. (Chem. Sci.), 112 (2000) 559–572.

[38] M. Bera, P.K. Nanda, U. Mukhopadhyay, D. Ray. Journal of Chemical Sciences, 116 (2004) 151–158

[39] P. Zanello, P.A. Vigato, G.A. Mazzocchin. Transition Metal Chemistry, 7, (1982), 291-293

[40] N. Makino, P. McMahill, H.S. Mason, T.H. Moss. Journal of Biological Chemistry, 249 (1974) 6062-6066

[41] G.S. Patterson, R.H. Holm. J. Bioinorg. Chem. 4 (1975) 257.

[42] S. Dutta, P. Basu, A. Chakravorthy. Inorganic Chemistry, 30 (1991) 4031-4037

[43] B.J. Hathaway, G. Wilkinson, R.D. Gillard, J.A. Mc Cleverty. Comprehensive Coordination Chemistry, 5 (1987)

[44] S.M.E. Khalil, M.M. Mashaly, A.A.A. Emara. Synthesis and Reactivity in Inorganic and Metal-Organic Chemistry, 25 (1995) 1373−1389.

[45] B.V. Patel, K. Desai, T. Thaker. Synthesis and Reactivity in Inorganic and Metal-Organic Chemistry, 19 (1989) 391

[46] K. Nakamoto, Coordination Compounds. In Infrared and Raman Spectra of Inorganic and Coordination Compounds, 4th Ed.; John Wiley and Sons, Inc.: New York, 1986.

[47] W.E. Estes, J.R. Wasson, J.W. Hall, W.E. Hatfield. Inorganic Chemistry, 17 (1978) 3657−3664.

[48] M.J. MacLachlan, M.K. Park, L.K. Thompson. Inorganic Chemistry, 35 (1996) 5492−5499

[49] R.M. Issa, A.M. Khedr, H.F. Rizk. Spectrochimica Acta Part A, 62 (2005) 621–629.

[50] M.J. MacLachlan, M.K. Park, L.K. Thompson. Inorganic Chemistry, 35 (1996) 5492-5499

[51] M.M.H. Khalil, M. M. Aboaly, R. M. Ramadan. Spectrochimica Acta Part A, 61 (2005) 157–161

[52] O.A.M. Ali, M.M.H. Khalil, G.M. Attia, R.M. Ramadan. Spectroscopy Letters, 36 (2003) 71-82

[53] M. M. H. Khalil, S. A. Ali, R. M. Ramadan. Spectrochimica Acta 57A (2001) 1017-1024

[54] R.S. Downing, F.L. Urbach. Journal of the American Chemical Society, 91 (1969) 5977–5983

[55] T. Tanaka. Journal of the American Chemical Society, 80 (1958) 4108–4110

[56] T.N. Waters, D. Hall. Journal of the Chemical Society, (1959) A: 1200–1203

[57] A. Sreekanth, M.R.P. Kurup. Polyhedron, 22 (2003) 3321–3332

[58] E.M. Gouge, J.F. Geldard. Inorganic Chemistry, 17 (1978) 270−275

[59] A.B.P. Lever. Inorganic Electronic Spectroscopy, 2nd ed.; Elsevier: New York, 1984

[60] A.D. Harrish, B. Josasses, R.D. Archer. Inorganic chemistry, 4 (1965) 147-149

[61] S.A. Sallam. Transition Metal Chemistry, 30 (2005) 341–351

[62] S.M Annigeri, M.P Sathisha, V.K Revankar. Transition Metal Chemistry, 32 (2007) 81-87

[63] Y. M. Issa, H. M. Abdel Fattah, A. A. Soliman. Journal of Thermal Analysis and Calorimetry, 42 (1994) 1175-1184

[64] N. T. Abdel-Ghani, O. E. Sherif. Thermochimica Acta, 156 (1989) 69-83

[65] M.J. Bew, B.J. Hathaway, R.R. Fereday. Journal of the Chemical Society, Dalton Transactiions, (1972) 1229-1237.

[66] J.E. Wertz, J.R. Bolton. Electron Spin Resonance, McGraw. Hill Book Company, New York, 1972.

[67] D. Kivelson, R. Neiman. Journal of Chemical Physics, 35 (1961) 149-155.

[68] B.J. Hathaway, D.E. Billing. Coordination Chemistry Reviews, 5 (1970) 143–207

[69] P.F. Rapheal, E. Manoj, M.R.P. Kurup. Polyhedron, 26 (2007) 818–828

[70] S-Z. Zhan, Y. Miao, P. Li, C-W. Yuan. Transition Metal Chemistry, 24 (1999) 311-370.

[71] B.L. Silver, D. Getz, Journal of Chemical Physics, 61 (1974) 638-650

Chapter 5

Synthesis and characterisation of ruthenium(II) complexes

Contents

5.1 Introduction

Ruthenium, the heavier homologue of iron, has been of great significance in coordination chemistry because of the fascinating electron transfer and energy transfer properties displayed by the complexes of this metal [1]. Due to these characteristics a large variety of ruthenium complexes have found applications in diverse types of research areas. These include artificial photosynthesis, photomolecular devices, elucidation of structural and electron transfer properties of proteins and DNA, catalytic oxidation of water and organic substrates, and stoichiometric as well as catalytic reactions for organic synthesis [2-9]. A large number of transition metal complexes of ruthenium have proved to be useful catalysts in many reactions, such as oxidation, hydrogenation, carbonylation and hydroformylation, by virtue of the accessibility of ruthenium in different oxidation states and ease of coordination with different ligands [10-12].

As the coordination environment around the central metal ion directs properties of the complexes, complexation of ruthenium by ligands of different types has been of significant importance. Schiff bases have been found to be among the most convenient and attractive ligands for ruthenium complexes due to the following reasons [13]. Steric and electronic effects around the Ru core can be finely tuned by an appropriate selection of bulky and/or electron withdrawing or donating substituents incorporated into the Schiff bases. The two donor atoms, N

and O, of the chelated Schiff base exert two opposite electronic effects: the phenolate oxygen is a hard donor known to stabilize the higher oxidation state of the ruthenium atom whereas the imine nitrogen is a softer donor and, accordingly, will stabilize the lower oxidation state of the ruthenium.

In the present chapter the synthesis and spectral characterisation of five Schiff base complexes have been discussed. The complexes are synthesised by the reaction of the Schiff base ligands, N,N'-bis(3-hydroxyquinoxaline-2-carboxalidene)1,8-diaminonaphthalene (hqcdan-H_2), N,N'-bis(3-hydroxyquinoxaline-2-carboxalidene)2,3-diaminomaleonitrile (hqcdmn-H_2), N,N'-bis(3-hydroxyquinoxaline-2-carboxalidene)trans(R,R')1,2-diaminocyclohexane (hqcdac-H_2), 3-hydroxyquinoxaline-2-carboxalidene-2-aminophenol (hqcap-H_2) and 3-hydroxyquinoxaline-2-carboxalidene-4-aminoantipyrine (hqcaap-H), with Ru(III) chloride.

5.2 Experimental

5.2.1 Materials

The details of materials used for the syntheses of the Schiff base ligands are given in Chapter 2. The metal salt used was ruthenium trichloride trihydrate.

5.2.2 Synthesis of Schiff base ligands

The syntheses of the Schiff base ligands have been discussed in detail in Chapter 2

5.2.3 Synthesis of complexes

All the ruthenium(II) complexes were prepared by mixing an aqueous solution (10 mL) of the salt $RuCl_3.3H_2O$ (10 mmol, 2.6 g) and an alkaline solution of the ligand, hqcdan-H_2 (5 mmol, 2.43 g), hqcdmn-H_2 (5 mmol, 2.10 g), hqcdac-H_2 (5 mmol, 2.13 g), hqcaap-H (10 mmol, 1.80 g) or hqcap-H_2 (5 mmol, 1.33 g) in 1:5 methanol-distilled water (250 mL) with a ligand to metal molar ratio 1:1. The

complex separated out was washed with 1:5 methanol-water to remove salts, and then with petroleum ether and dried over anhydrous calcium chloride in a desiccator.

5.3 Results and discussion

All the complexes are brown, non-hygroscopic solids. They are soluble in acetonitrile, DMF, ethanol and nitrobenzene and are insoluble in benzene.

The ligands predominantly exist in the keto tautomeric form in the solid state. During complexation step an equivalent amount of NaOH in 1:6 methanol-distilled water was added to the ligands to convert this keto form to enolate form. This renders the coordination of enolate oxygen.

5.3.1 Elemental analyses

The analytical data (Table 1) suggest that the complexes I, II, III and IV are binuclear and the complex, V is mononuclear.

Table 1: Analytical data a of the ruthenium(II) complexes

Compound	Molecular formula	Formula weight	Cu (%)	C (%)	H (%)	N (%)	Cl (%)
$[Ru_2(hqcdan)Cl_2].H_2O$ **(I)**	$C_{28}H_{18}N_6O_3Cl_2Ru_2$	759.53	26.55 (26.61)	44.22 (44.28)	2.32 (2.39)	11.01 (11.06)	9.27 (9.34)
$[Ru_2(hqcdmn)Cl_2].H_2O$ **(II)**	$C_{22}H_{12}N_8O_3Cl_2Ru_2$	709.43	24.42 (28.49)	37.18 (37.25)	1.62 (1.70)	15.71 (15.79)	9.91 (9.99)
$[Ru_2(hqcdac)Cl_2].H_2O$ **(III)**	$C_{24}H_{22}N_6O_3Cl_2Ru_2$	715.52	28.12 (28.25)	40.21 (40.29)	3.02 (3.10)	11.66 (11.75)	9.85 (9.91)
$[Ru_2(hqcap)Cl_2(H_2O)].H_2O$ **(IV)**	$C_{15}H_{13}N_3O_4Cl_2Ru_2$	572.33	35.26 (35.32)	31.28 (31.48)	2.20 (2.29)	7.26 (7.34)	12.32 (12.39)
$[Ru(hqcaap)Cl(H_2O)_2].H_2O$ **(V)**	$C_{20}H_{22}N_5O_5ClRu$	548.94	17.99 (18.41)	43.70 (43.76)	3.98 (4.04)	12.71 (12.76)	6.41 (6.46)

[a] Calculated values in parentheses

5.3.2 Molar conductivity and magnetic susceptibility measurements

The molar conductance values of the complexes (Table 2) in DMF indicate non-electrolytic nature of the complexes [14]. All the complexes were found to be diamagnetic in nature although we used $RuCl_3.3H_2O$ for the synthesis. Further more all the complexes were found to be EPR silent.

Table 2: Molar conductance data (in 10^{-3} mol DMF) of the ruthenium(II) complexes

Complex	Molar conductance (ohm^{-1} cm^2 mol^{-1})
$[Ru_2(hqcdan)Cl_2].H_2O$ (I)	5.8
$[Ru_2(hqcdmn)Cl_2].H_2O$ (II)	5.1
$[Ru_2(hqcdac)Cl_2].H_2O$ (III)	5.4
$[Ru_2(hqcap)Cl_2(H_2O)].H_2O$ (IV)	5.7
$[Ru(hqcaap)Cl(H_2O)_2].H_2O$ (V)	4.2

5.3.3 Cyclic voltammetry

The electrochemical activity of the ruthenium complexes was studied in DMSO (10^{-3} mol l^{-1}) at a scan rate of 0.025 V in the potential range +1.5 to −1.5 V by cyclic voltammetry. The cyclic voltammograms of the ruthenium complexes are shown in Figure 1 and the voltammetric data are summarized in Table 3.

All the ruthenium(II) complexes exhibit two-stepped cyclic voltammograms under the experimental conditions. Qualitatively, it is expected that, for a dinuclear complex, the $Ru^{III/II}$ couple forming the [III,II] complex should be at more positive potential, while the $Ru^{III/II}$ couple forming the [II,II] complex should be at more negative potential [15]. The first redox peak appearing in the positive potential range corresponds to $Ru_2^{III,III}/Ru_2^{III,II}$ couple where as the second redox couple appearing in the negative potential range is attributable to the $Ru_2^{III,II}/Ru_2^{II,II}$ redox process [16].

For the mononuclear complex, V, the redox peak occurring at a positive potential corresponds to Ru^{IV}/Ru^{III} couple where as the second one occurring at higher negative potential is assigned to Ru^{III}/Ru^{II} redox process [17]. In all the ruthenium(II) complexes the ratio, I_{pc}/I_{pa}, falls in the range 0.91- 1.36, clearly confirming one electron transfer for redox processes.

Cyclic voltammograms of the Schiff base ligands display a quasi-reversible redox process (see Chapter 2). Therefore the ligand is susceptible to easy oxidation and reduction, which might be the reason for the formation of the diamagnetic and EPR silent ruthenium(II) complexes [18].

Table 3: Redox potentials for ruthenium(II) complexes in DMSO solution at 298K

Complex	Redox couple	E_{pc} (mV)	E_{pa} (mV)	$E^1_{1/2}$/ ($E^2_{1/2}$) (mV)	I_{pc} (μV)	I_{pa} (μV)	I_{pc}/I_{pa}
I	$Ru_2^{III,III}/Ru_2^{III,II}$	−0.138	0.752	0.307	0.24	0.20	1.20
	$Ru_2^{III,II}/Ru_2^{II,II}$	−1.142	−0.584	−0.863	0.62	0.48	1.29
II	$Ru_2^{III,III}/Ru_2^{III,II}$	−0.258	0.530	0.272	1.55	1.52	1.02
	$Ru_2^{III,II}/Ru_2^{II,II}$	−0.827	−0.559	−0.693	1.49	1.37	1.08
III	$Ru_2^{III,III}/Ru_2^{III,II}$	0.999	1.233	1.116	0.55	0.54	1.02
	$Ru_2^{III,II}/Ru_2^{II,II}$	−0.982	−0.604	−0.793	2.25	1.79	1.29
IV	$Ru_2^{III,III}/Ru_2^{III,II}$	−0.258	0.862	0.302	0.50	0.54	0.93
	$Ru_2^{III,II}/Ru_2^{II,II}$	−0.986	−0.613	−0.800	1.15	0.84	1.36
V	Ru^{IV}/Ru^{III}	−0.203	0.665	0.231	0.59	0.45	1.31
	Ru^{III}/Ru^{II}	−1.022	−0.614	−0.818	1.60	1.75	0.91

E_{pc} = anodic peak potential; E_{pa} = cathodic peak potential; I_{pc} = anodic peak current; I_{pa} = cathodic peak current; I_{pc}/I_{pa} = number of electrons; $E^1_{1/2}$/ $E^2_{1/2} = 0.5 \times (E_{pa} + E_{pc})$; scan rate 25 mV

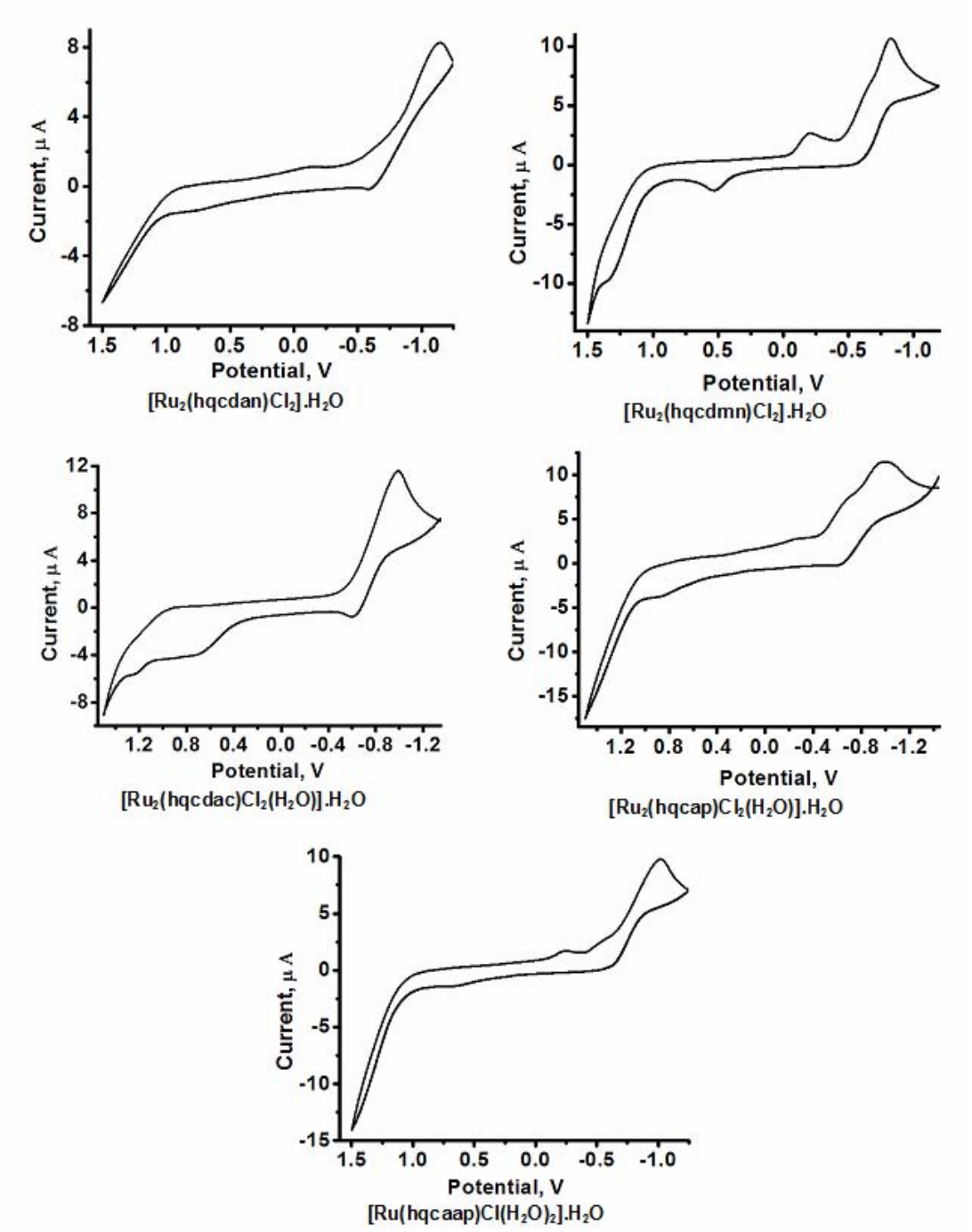

Figure 1: Cyclic voltammograms of the ruthenium(II) complexes

5.3.5 Infrared spectra

Selected infrared vibrational stretching frequencies of the free Schiff base ligands and the ruthenium complexes, which are useful for determining the mode of coordination of the ligands, are given in Table 4. The FT-IR spectra of the ruthenium(II) complexes are given Figures 2-6. In all these spectra there is a broad band in the range 3509-3413 cm^{-1} assignable to coordinated water or uncoordinated water molecules associated with the complex [19]. This fact is also indicated by the results of elemental analyses and TG-DTA-DTG of these complexes [20]. The presence of two coordinated water molecules in the complexes, IV and V, is evidenced by two new bands in their spectra (Table 4) corresponding to δ(O—H) of the coordinated water [21]. The bands due to ν_{NH}/ ν_{OH} of the free Schiff bases were not observed in the spectra of the complexes, suggesting the involvement of phenolic oxygen in coordination to Ru after enolisation and deprotonation. Disappearance of the strong amide band and the formation of new bands in the range 1306−1320 cm^{-1} (due to ν(C—O)) support the coordination of oxygen of the amide carbonyl to the metal through enolization and deprotonation. The participation of azomethine nitrogen atom of the Schiff bases in coordination is evidenced by an increase in their stretching frequency, which might be due to the extensive delocalization of the π-electrons in fully conjugated Schiff base ligand. This coordination stabilizes the lower oxidation state of ruthenium due to the high soft donor character of the imine (C=N) conjugated to two quinoxaline rings. The coordination of phenolic oxygen of the Schiff bases is supported by the appearance of new bands in 440-486 cm^{-1} range due to Ru—O stretching in the ruthenium complexes [22]. In addition, these complexes exhibit one strong band in the range 416-426 cm^{-1}, which may be due to ν(Ru—N) stretching [22] suggesting coordination of azomethine nitrogen atoms. The bands observed in the range 312-336 cm^{-1} in the far-IR spectrum of the complexes might be due to the ν(Ru—Cl) stretching [19].

Table 4: Characteristic infrared spectral bands (cm^{-1}) for ruthenium(II) complexes

Compound	ν(O—H)[a/b]	ν(C=N)[c]	ν(C—O)[d]	*ν*(Ru–O)	*ν*(Ru–N)	ν(Ru—Cl)	*δ*(O–H)[e]
hqcdan-H_2	3430[a]	1597	1299	-	-	-	-
I	3413[b]	1656	1320	486	421	336	-
hqcdmn-H_2	3390[a]	1643	1294	-	-	-	-
II	3509[b]	1655	1309	440	420	330	-
hqcdac-H_2	3434[a]	1625	1290	-	-	-	-
III	3420[b]	1687	1306	467	416	312	-
hqcap-H_2	3412[a]	1606	1300	-	-	-	-
IV	3450[b]	1692	1309	484	425	322	1112, 1150
hqcaap-H	3451[a]	1637	1306	-	-	-	-
V	3442[b]	1670	1312	448	426	325	1162, 1185

[a] ν(N−H)/ ν(O−H) of the free Schiff base or ; [b] ν(O—H) of coordinated water molecule; [c] −CH=N of azomethine group; [d] phenolic ν(C−O); [e] *δ*(O–H) of coordinated water molecule.

Some other changes were also observed in the stretching frequencies of the Schiff bases after complexation to the metal. In the case of complexes, I and IV, the coordination of the azomethine nitrogen atom results in the formation of a group of medium intensity bands in the range 1648-1515 cm^{-1}, that might be due to the C=N stretches of the quinoxaline ring. Coordination of the hqcdmn-H_2 is also evidenced from the changes in the nature of the two very intense ν_{CN} bands at 2243 and 2202 cm^{-1} of the free Schiff base (see Chapter 2). This doublet appears as a major ν_{CN} stretch at 2201 cm^{-1} along with a weak band at 2237 cm^{-1} after complexation [23]. The band at 1656 cm^{-1} due to the C═O group of the antipyrine part of the hqcaap-H is shifted to 1650 cm^{-1} for the complex, V, indicating the involvement of this group in coordination [21].

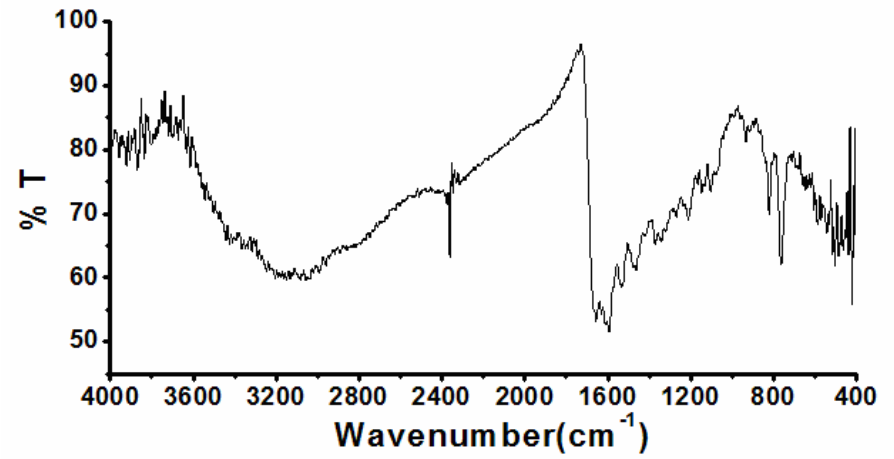

Figure 2: FT-IR spectrum $[Ru_2(hqcdan)Cl_2].H_2O$ (I)

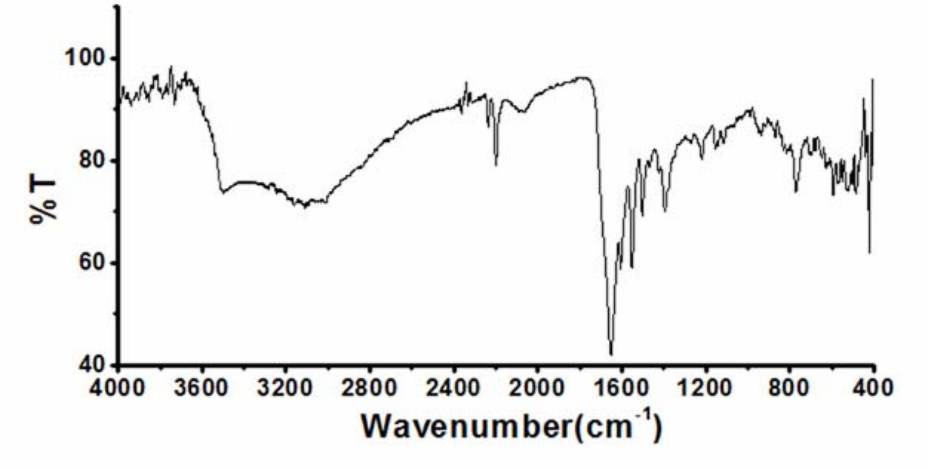

Figure 3: FT-IR spectrum of $[Ru_2(hqcdmn)Cl_2].H_2O$ (II)

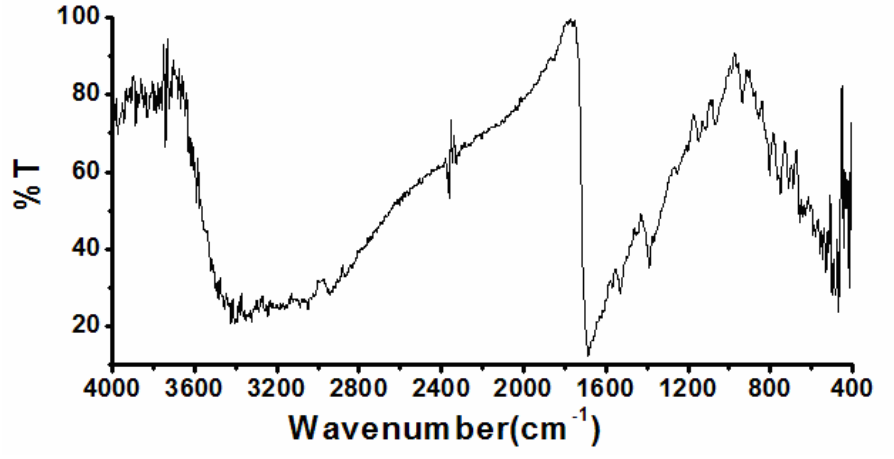

Figure 4: FT-IR spectrum of $[Ru_2(hqcdac)Cl_2].H_2O$ (III)

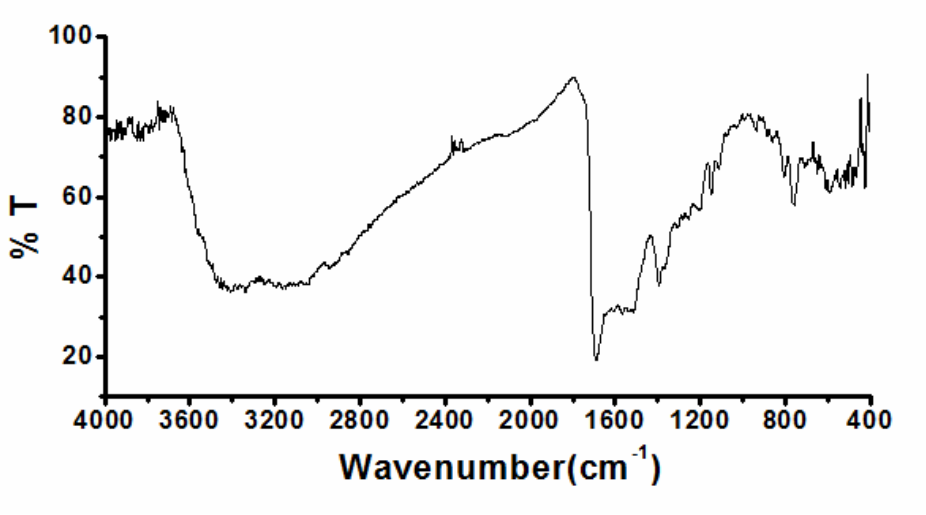

Figure 5: FT-IR spectrum of $[Ru_2(hqcap)Cl_2(H_2O)].H_2O$ (IV)

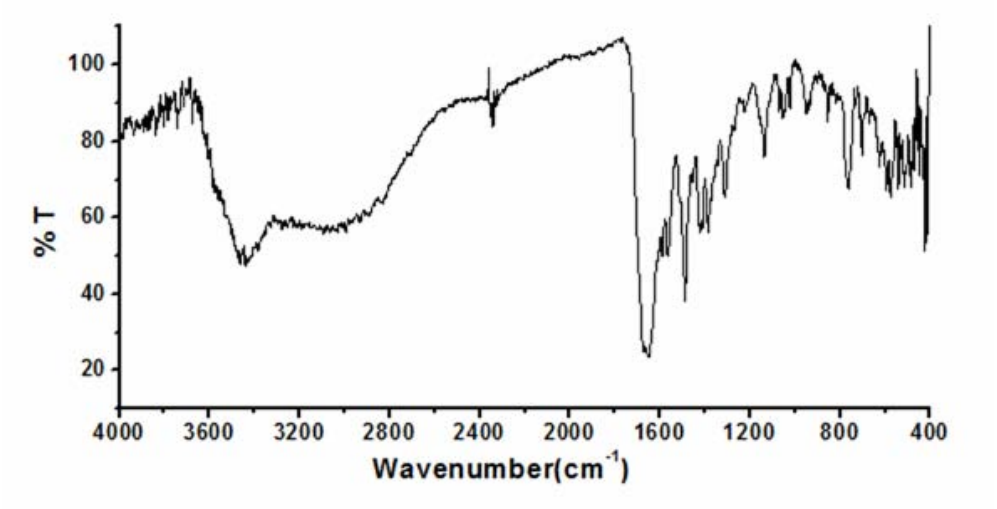

Figure 6: FT-IR spectrum of $[Ru(hqcaap)Cl(H_2O)_2].H_2O$ (V)

5.3.6 Electronic spectra

The electronic spectra of the complexes were recorded in DMSO solution and in the solid state. In solution spectrum (Figure 4), the ligand-centered bands obscure the d-d bands of the metal and therefore the latter could not be observed. However in the solid state diffuse reflectance spectra (Figure 5) the d-d bands, which could not be observed in the solution spectrum, are seen due to the high concentration of the complex.

Majority of divalent ruthenium complexes are 6-coordinate and octahedral and few are 5-coordinate and square pyramidal, while four coordinate Ru(II) complexes are rare [24-27]. The molecular formulae obtained in the case of complexes I, II, III and IV are in agreement with a four coordinate geometry. Since these complexes are diamagnetic, a low spin d^6 configuration is possible with the electrons getting paired in the d_{yz}, d_{xz} and d_{z2} orbitals leaving the two other orbitals (d_{xy} and d_{x2-y2}) empty. This might happen if the separation between d_{z2} and d_{xy} is larger in square planar geometry. We expect such a situation for the present complexes. Comparison of the solid state diffuse reflectance spectra of the Schiff bases (see Chapter 2) with that of the complexes, three new bands are seen in the spectrum of the complexes, which might be due to the transitions, $^1A_{1g} \rightarrow {}^1E_g$, $^1A_{1g} \rightarrow {}^1B_{1g}$ and $^1A_{1g} \rightarrow {}^1A_{2g}$ respectively (Table 5) in a square planar geometry.

The molecular formula suggests that the complex, V, is mononuclear and octahedral. The ground state of ruthenium(II) in an octahedral environment is $^1A_{1g}$, arising from the t_{2g}^6 configuration. The excited states corresponding to the $t_{2g}^5e_g^1$ configuration are $^3T_{1g}$, $^3T_{2g}$, $^1T_{1g}$ and $^1T_{2g}$. Hence, four bands corresponding to the transitions $^1A_{1g} \rightarrow {}^3T_{1g}$, $^1A_{1g} \rightarrow {}^3T_{2g}$, $^1A_{1g} \rightarrow {}^1T_{1g}$ and $^1A_{1g} \rightarrow {}^1T_{2g}$ are possible in the order of increasing energy. The transition $^1A_{1g} \rightarrow {}^1T_{2g}$ is not observed in the present complex, as it might have been masked by the charge transfer band at 486 nm (20570 cm^{-1}). The shoulder bands observed at 645 nm (15 500 cm^{-1}), 840 nm (11900 cm^{-1}) and 1422 nm (7030 cm^{-1}) might be due to $^1A_{1g} \rightarrow {}^1T_{1g}$ and spin forbidden $^1A_{1g} \rightarrow {}^3T_{2g}$ and $^1A_{1g} \rightarrow {}^3T_{1g}$ transitions respectively.

Table 5: Electronic spectral assignments for ruthenium(II) complexes

Complex	Electronic spectral bands; nm (cm^{-1})	Assignments
I	303 (30,300)[a], 442 (23,690)[as]	Intra ligand transitions
	591 (16,920)[as]	$^1A_{1g} \rightarrow {}^1E_g$ or CT
	223 (44,840)[bs], 261 (38,314)[bs], 322 (31,050)[bs], 398 (25,120)[bs]	Intra ligand transitiions
	582 (17,180)[b]	$^1A_{1g} \rightarrow {}^1E_g$
	652 (15,330)[b]	$^1A_{1g} \rightarrow {}^1B_{1g}$
	827 (12,090)[bs]	$^1A_{1g} \rightarrow {}^1A_{2g}$
II	306 (32,680)[a], 439 (22,780)[a],	Intra ligand transitions
	515 (19,410)[as]	$^1A_{1g} \rightarrow {}^1E_g$ or CT
	219 (45,660)[b], 263 (38,020)[b], 320 (31,250)[bs], 386 (25,900)[bs]	Intra ligand transitiions
	517 (19,340)[b]	$^1A_{1g} \rightarrow {}^1E_g$
	686 (14,570)[b]	$^1A_{1g} \rightarrow {}^1B_{1g}$
	879 (11,370)[bs]	$^1A_{1g} \rightarrow {}^1A_{2g}$
III	256 (39,060)[a], 313 (31,940)[a]	Intra ligand transitions
	473 (21,140)[as]	$^1A_{1g} \rightarrow {}^1E_g$ or CT
	217 (46,080)[b], 258 (38,760)[bs], 325 (30,770)[bs]	Intra ligand transitions
	422 (23,690)[b]	$^1A_{1g} \rightarrow {}^1E_g$ or CT
	685 (14,590)[b]	$^1A_{1g} \rightarrow {}^1B_{1g}$
	856 (11,680)[bs]	$^1A_{1g} \rightarrow {}^1A_{2g}$
IV	432 (23,140)[a],	Intra ligand transitions
	592 (16,890)[as]	$^1A_{1g} \rightarrow {}^1E_g$ or CT
	219 (45,600)[b], 263 (38,020)[b], 330 (30,300)[bs]	Intra ligand transitiions
	482 (20,740)[b]	$^1A_{1g} \rightarrow {}^1E_g$
	691 (14,470)[b]	$^1A_{1g} \rightarrow {}^1B_{1g}$
	838 (11,930)[b]	$^1A_{1g} \rightarrow {}^1A_{2g}$
V	311 (32,150)[a], 428 (23,360)[a]	Intra ligand transitions
	589 (16,970)[as]	$^1A_{1g} \rightarrow {}^1T_{2g}$ or MLCT
	218 (45,870)[b], 261 (38,310)[bs], 335 (29,850)[b], 393 (25,440)[bs]	Intra ligand transitions
	486 (20,570)	$^1A_{1g} \rightarrow {}^1T_{2g}$ or MLCT
	645 (15,500)[bs]	$^1A_{1g} \rightarrow {}^1T_{1g}$
	840 (11,900)[bs]	$^1A_{1g} \rightarrow {}^3T_{2g}$
	1422 (7,030)	$^1A_{1g} \rightarrow {}^3T_{1g}$

[a] Saturated solution spectrum in DMSO; [b] Diffuse reflectance spectrum in the solid state; [s] Shoulder band

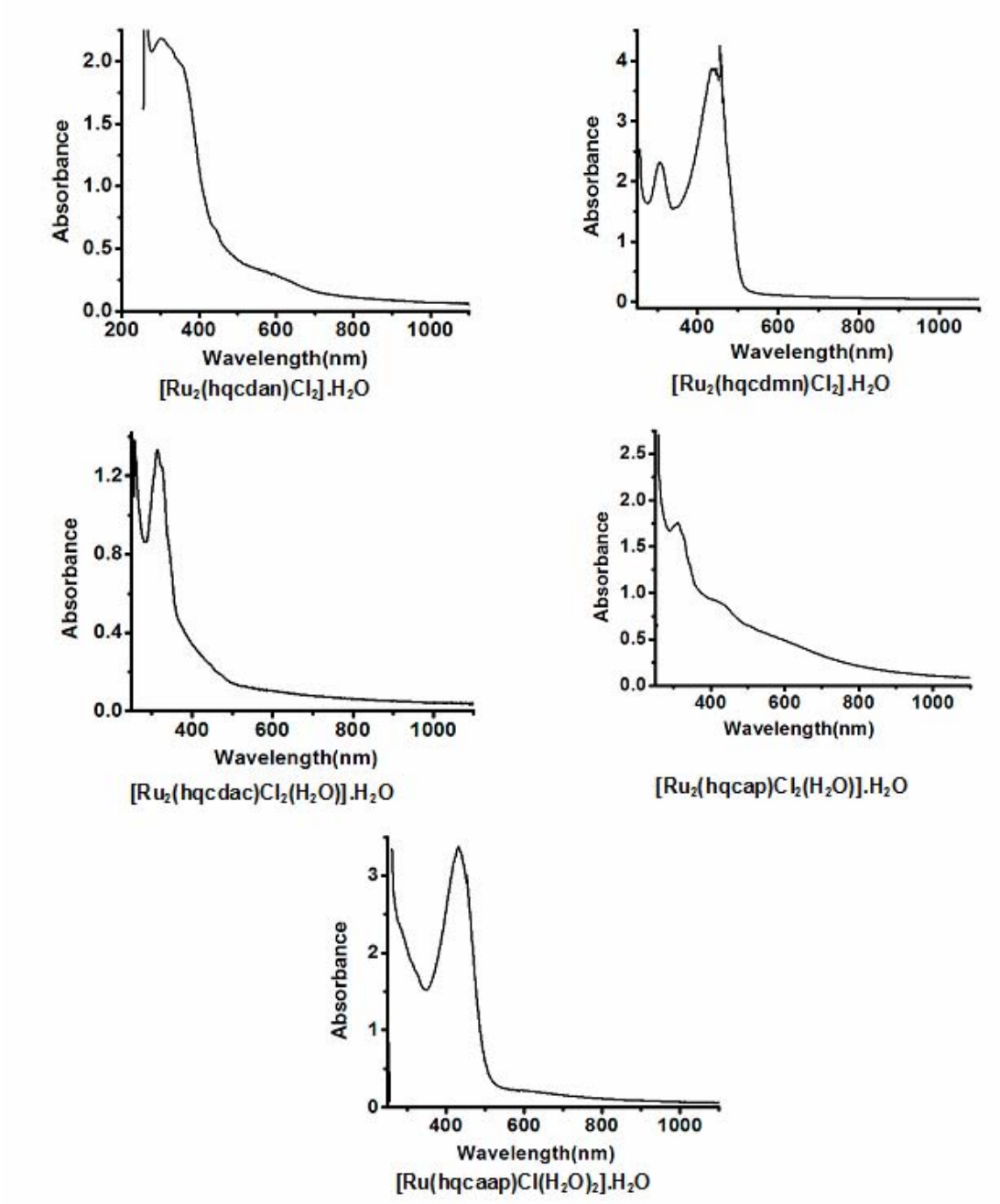

Figure 7: Electronic spectra of the ruthenium(II) complexes in DMSO

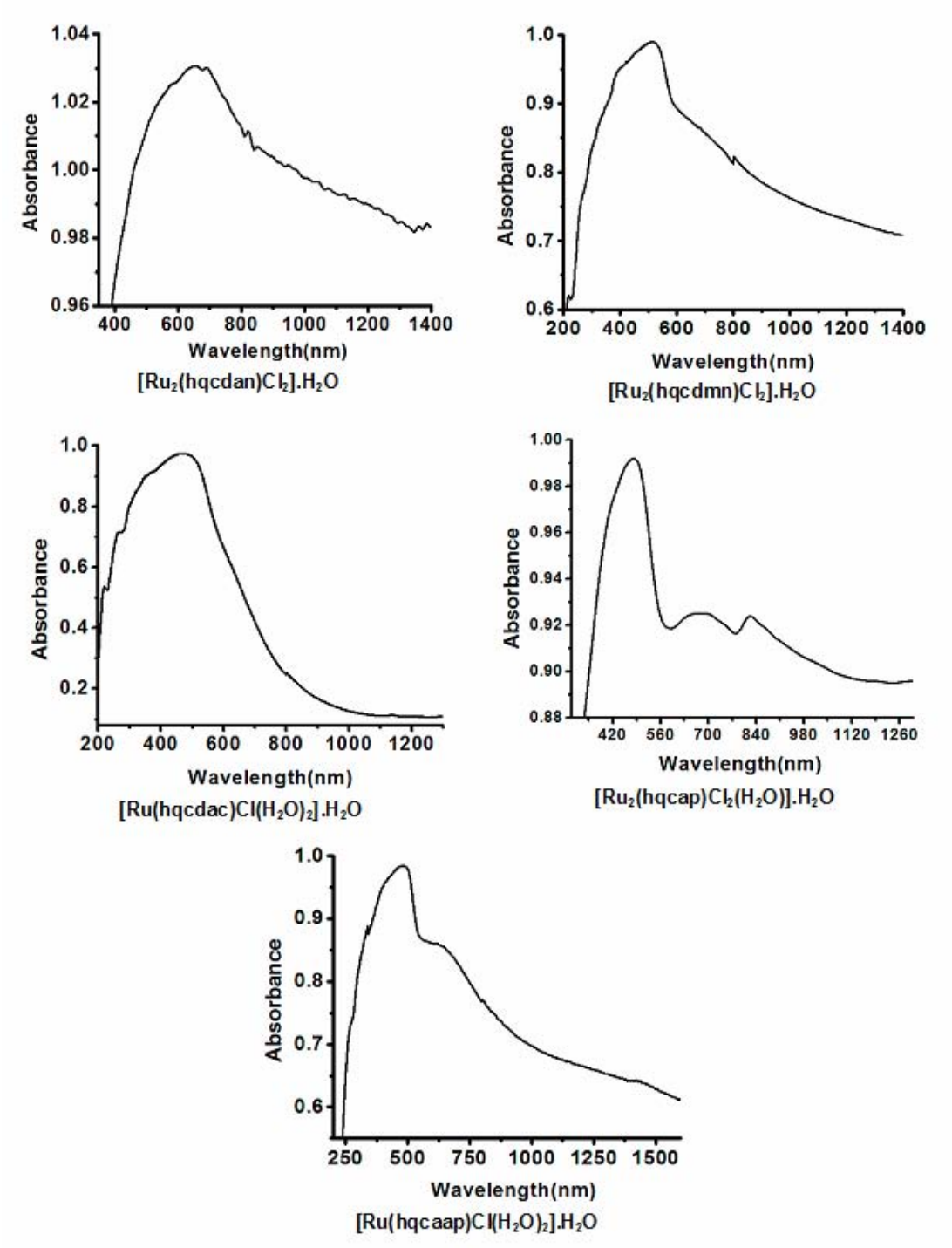

Figure 8: Diffuse reflectance spectra of the ruthenium(II) complexes

5.3.7 Thermal Analysis

Thermal stability of the complexes were investigated using TG-DTA-DTG at a heating rate of 20 ºC /min in nitrogen/air over a temperature range of 40-1000ºC. TG-DTA-DTG curves of the complexes are given in Figures 9-13. The initial weight loss below 130 °C in the thermograms of all the complexes is attributed to the removal of lattice water molecules associated with the complex. This is followed by two or three stage decompositions leading to the removal of other ligands. In nitrogen atmosphere the decomposition was incomplete even after 1000 ºC. However in air the decomposition takes place at lower temperatures with the formation of RuO as the residue.

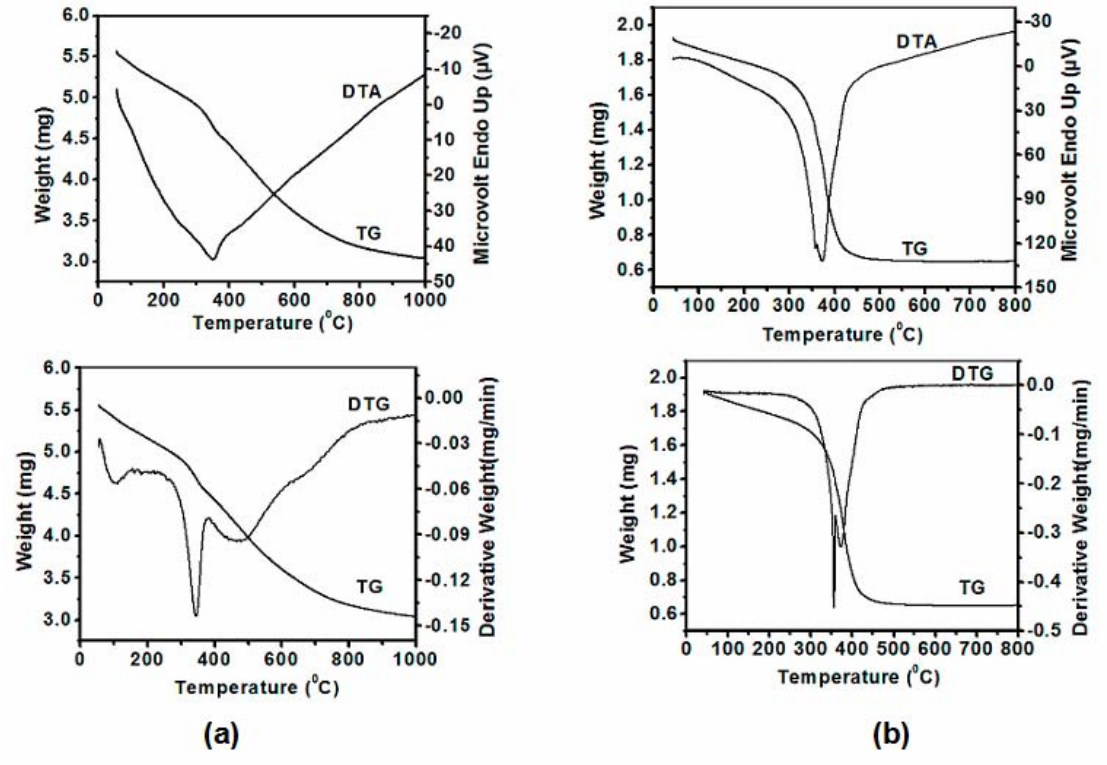

Figure 9: TG-DTA-DTG curves of $[Ru_2(hqcdan)Cl_2].H_2O$ (II): in nitrogen (a) and in air (b)

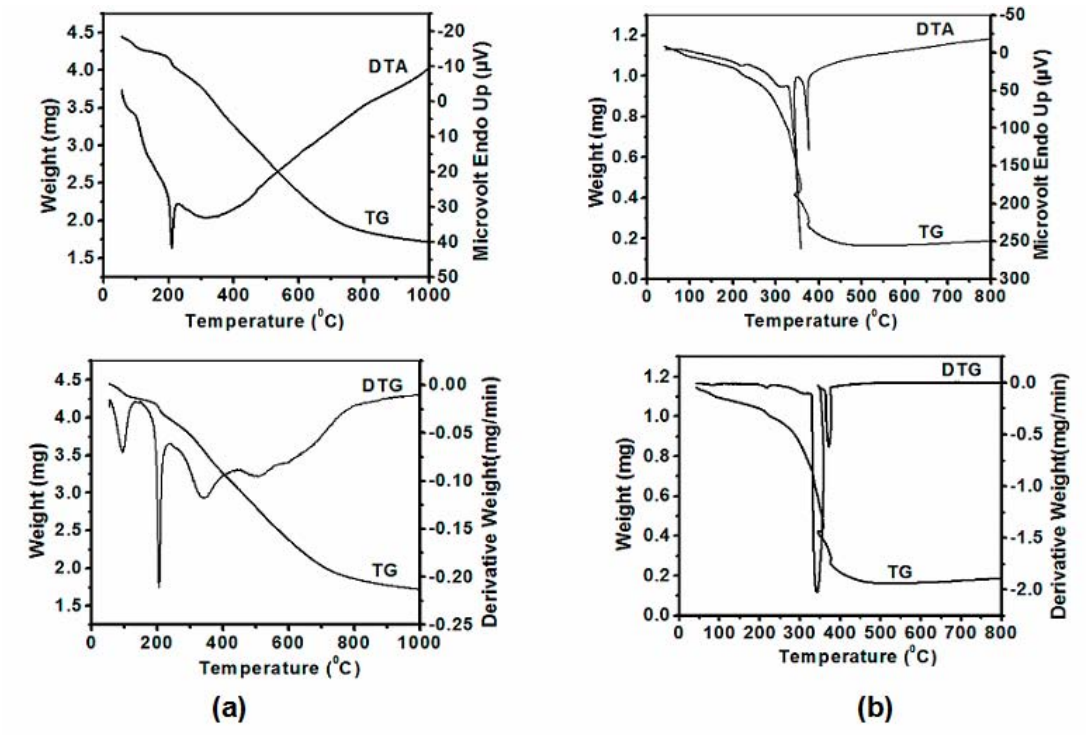

Figure 10: TG-DTA-DTG curves of $[Ru_2(hqcdmn)Cl_2].H_2O$ (II): in nitrogen (a) and in air (b)

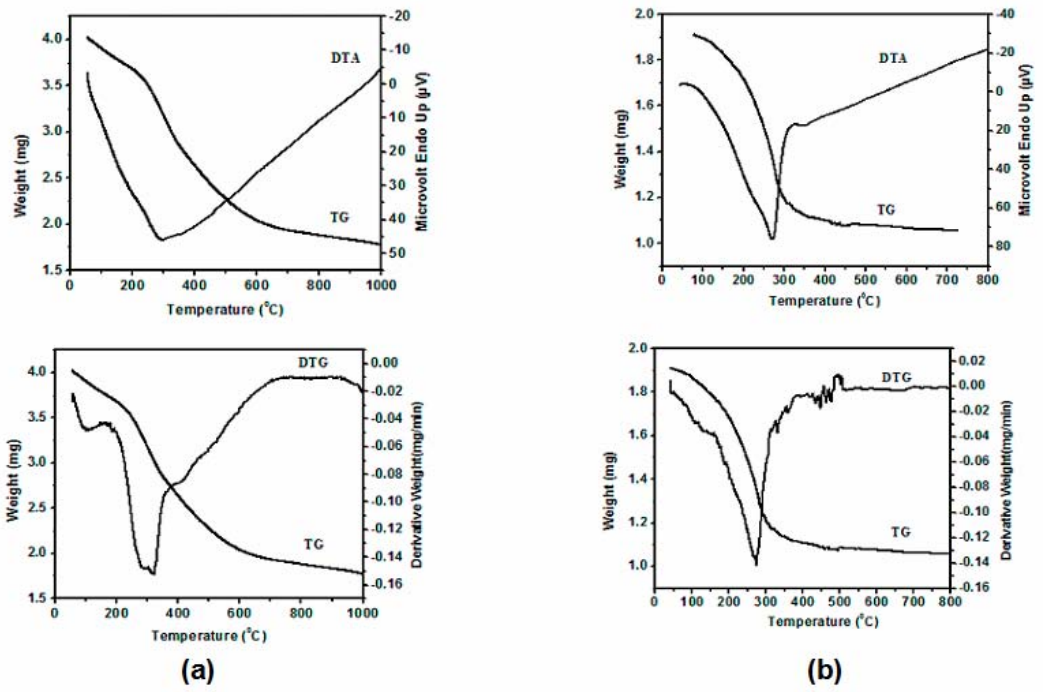

Figure 11: TG-DTA-DTG curves of $[Ru_2(hqcdac)Cl_2].H_2O$ (III): in nitrogen (a) and in air (b)

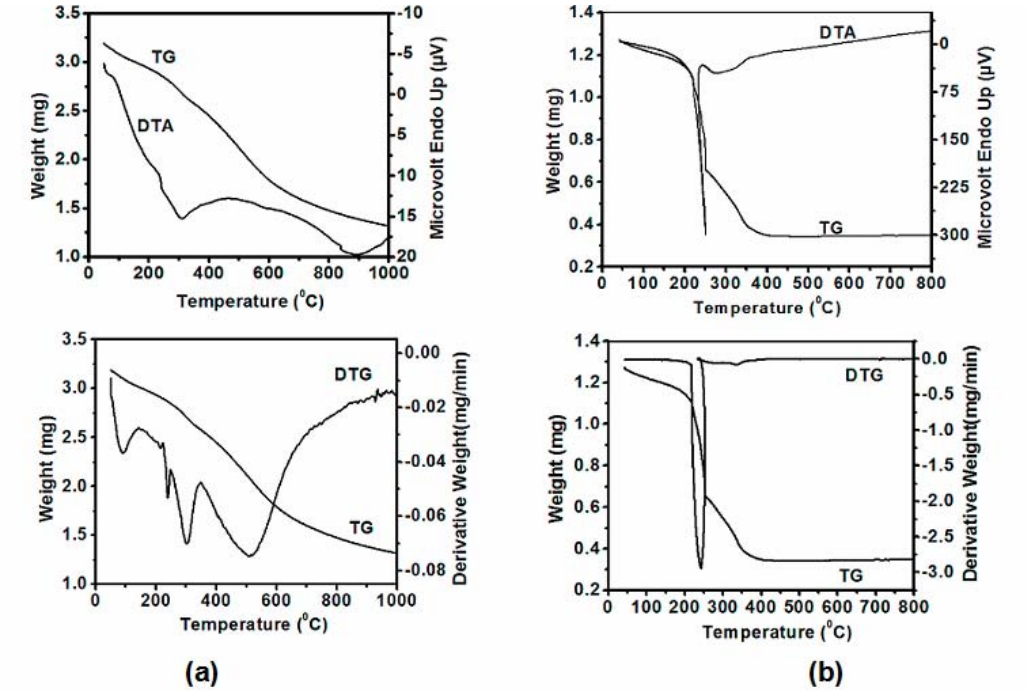

Figure 12: TG-DTA-DTG curves of $[Ru_2(hqcap)Cl_2(H_2O)].H_2O$ (IV): in nitrogen (a) and in air (b)

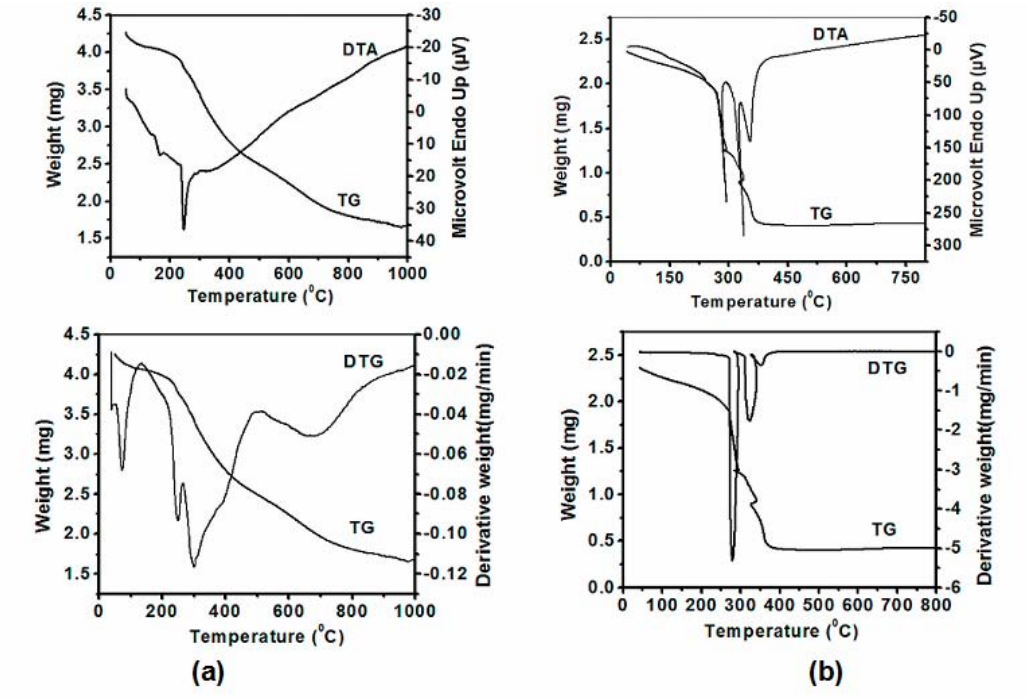

Figure 13: TG-DTA-DTG curves of $[Ru(hqcaap)Cl(H_2O)_2].H_2O$ (V): in nitrogen (a) and in air (b)

Conclusions

The elemental analyses and magnetic moment measurements suggest the metal ion in all the complexes to be in the +2 oxidation state with molecular formulae, $[Ru_2(hqcdan)Cl_2].H_2O$, $[Ru_2(hqcdmn)Cl_2].H_2O$, $[Ru_2(hqcdac)Cl_2].H_2O$, $[Ru_2(hqcap)Cl_2(H_2O)].H_2O$ and $[Ru(hqcaap)Cl(H_2O)_2].H_2O$. The two-stepped cyclic voltammograms observed for all the complexes also confirm these formulae. Coordination of the azomethine nitrogen and phenolate oxygen is evidenced by IR data, while electronic spectral data suggests a square-planar geometry for the binuclear complexes and octahedral geometry for the mononuclear species. That coordinated/lattice water are present in the complexes is evidenced by weight loss in the TG and presence of characteristic stretching bands in the IR spectrum. In the light of these findings, probable structures have been proposed for the complexes which are given below (Figure 14).

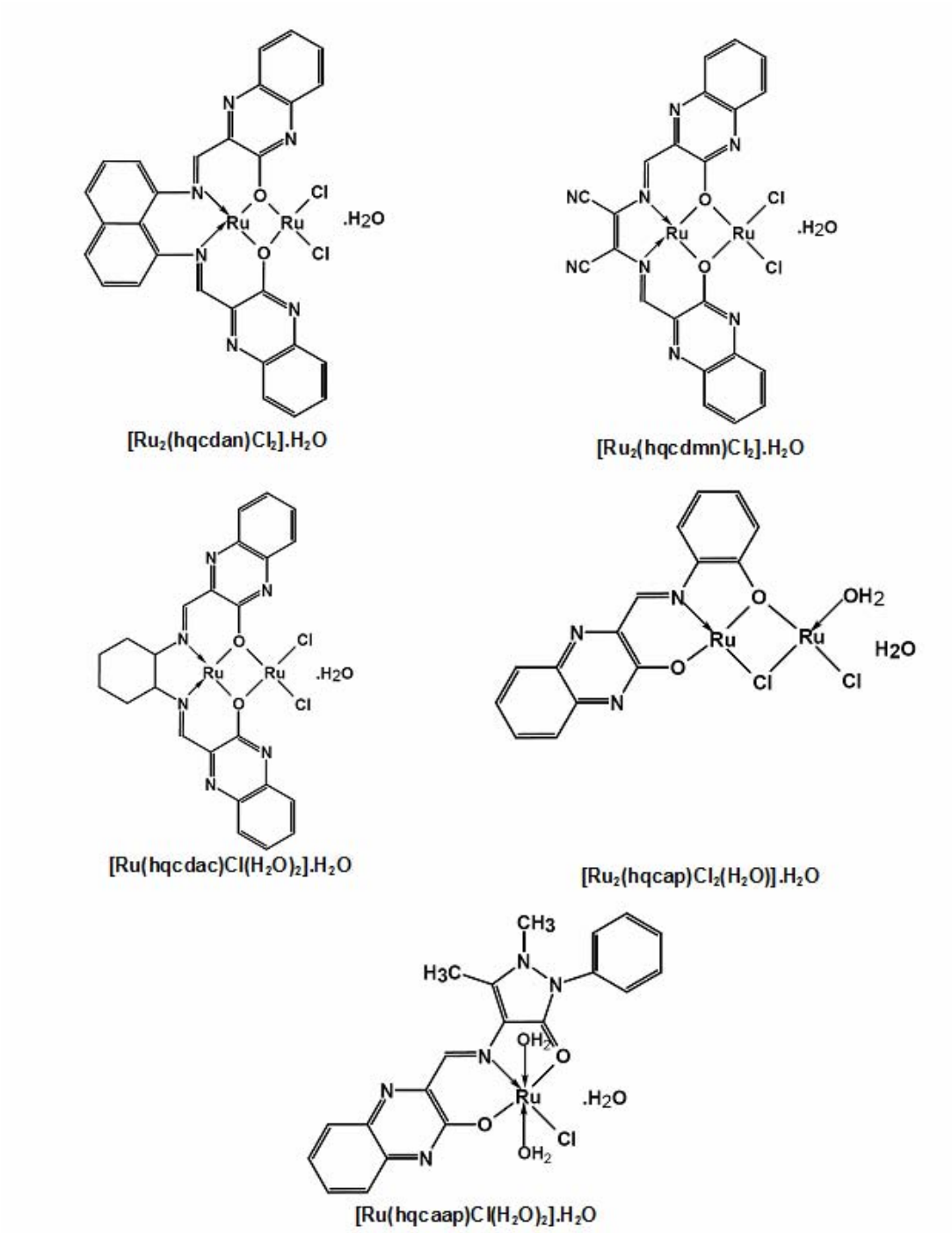

Figure 14: Proposed structures of the ruthenium(II) complexes

References

[1] D.R. Prasad, G. Ferraudi. Journal of Physical Chemistry, 86 (1982) 4037-4040.

[2] L. Sun, L. Hammarstrom, B. Akermark, S. Styring. Chemical Society Reviews, 30 (2001) 36-49.

[3] C. Joachim, J.K. Gimzewski, A. Aviram. Nature, 408 (2000) 541-548.

[4] N. Sardesai, S.C. Lin, K. Zimmermann, J.K. Barton. Bioconjugate Chemistry, 6 (1995) 302-312.

[5] H.B. Gray, J.R. Winkler, Annual Review of Biochemistry, 65 (1996) 537-561.

[6] P. Lincoln, E. Tuite, B. Norden, Journal of the American Chemical Society, 119 (1997) 1454-1455.

[7] S. Goswami, A.R. Chakravarty, A. Chakravorty. Journal of Chemical Society, Chemical Communication, (1982) 1288-1289.

[8] J.A. Gilbert, D. S. Eggleston, W.R. Murphy Jr., D.A. Geselowitz, S.W. Gersten, D.J. Hodgson, T.J. Meyer. Journal of the American Chemical Society, 107 (1985) 3855-3864.

[9] C-M Che. Pure and Applied Chemistry, 67 (1995) 225-232.

[10] K-M Sung, S. Huh, M-J Jun. Polyhedron, 18 (1999) 469-480.

[11] D. Chatterjee, A. Mitra, B.C. Roy. Journal of Molecular Catalysis, 161 (2000) 17-21.

[12] A.S. Goldstein, R.H. Beer, R.S. Drago. Journal of American Chemical Society, 116 (1994) 2424-2429.

[13] R. Drozdzak, B. Allaert, N. Ledoux, I. Dragutan, V. Dragutan, F. Verpoort. Coordination Chemistry Reviews, 249 (2005) 3055–3074.

[14] W.J. Geary. Coordination Chemistry Reviews, 7 (1971) 81-122.

[15] P.J. Mosher, G.P.A. Yap, R.J. Crutchley. Inorganic Chemistry, 40 (2001) 1189-1195.

[16] S. Chellamma, M. Lieberman. Inorganic Chemistry, 40 (2001) 3177-3180

[17] J. Chakaravarty, S. Bhattacharya. Polyhedron, 5 (1996) 1047-1055.

[18] S. Ghumaan, B. Sarkar, S. Patra, J. van Slageren, J. Fiedler, W. Kaim, G.K. Lahiri. Inorganic Chemistry, 44 (2005) 3210-3214.

[19] M.M. Taqui Khan, N.H. Khan, R.I. Kureshy, A.B. Boricha, Z.A. Shaikh. Inorganica Chimica Acta, 170 (1990) 213−223.

[20] S.A. Sallam. Transition Metal Chemistry, 30 (2005) 341–351.

[21] R.M. Issa, A.M. Khedr, H.F. Rizk, Spectrochimica Acta: Part A 62 (2005) 621−629.

[22] K. Nakamoto, Infrared and Raman Spectra of Inorganic and Coordination Compounds, 4th Edn, John Wiely and Sons, Inc.: New York, 1986.

[23] M.J. MacLachlan, M.K. Park, L.K. Thompson. Inorganic Chemistry, 35 (1996) 5492−5499.

[24] L.A. Watson, O.V. Ozerov, M. Pink, K.G. Caulton. Journal of the American Chemical Society, 125 (2003) 8426−8427.

[25] D. Huang, W.E. Streib, J.C. Bollinger, K.G. Caulton, R.F. Winter, T. Scheiring. Journal of the American Chemical Society, 121 (1999) 8087−8097.

[26] J.P. Lee, Z. Ke, M.A. Ramirez, T. Gunnoe, T.R. Cundari, P.D. Boyle, J.L. Petersen. Organometallics, 28 (2009) 1758-1775.

[27] J. Cirera, E. Ruiz, S. Alvarez. Inorganic Chemistry, 47 (2008) 2871-2889.

Oxidation of cyclohexene with hydrogen peroxide catalysed by oxovanadium(IV) complexes

Contents

6.1 Introduction

Transition metal Schiff base complexes, in particular N_2O_2 Schiff base complexes, have been extensively studied because of their potential use as catalysts in a wide range of oxidation reactions [1,2]. One of the attractive features of the N_2O_2 Schiff base complexes is that it is possible to tune the electronic and steric properties of the complexes by making alterations in the Schiff base portion. The introduction of bulky substituent near the coordination sites may lead to low symmetry complexes and enhanced catalytic properties. Furthermore, by suitable incorporation of donating/accepting groups, it may be possible to tune the electronic environment around the metal centre and alter the catalytic properties. A variety of Schiff base complexes of oxovanadium(IV) ion have been shown to catalyze a wide range of oxidation reactions [3-9].

Oxovanadium(IV) ion can readily coordinate four, five and six donor atoms to form VOL_4, VOL_5 and VOL_6-type of complexes. Most of the oxovanadium(IV) complexes with N_2O_2 Schiff base ligands are reported to have mononuclear structures having square pyramidal geometries whereas very few have binuclear structure [10-12]. During our investigations we have been able to synthesize and characterize new binuclear oxovanadium(IV) Schiff base complexes derived from 3-hydroxyquinoxaline-2-carboxaldehyde and investigate the catalytic activities in the

oxidation of cyclohexene using an environmentally friendly oxidant, H_2O_2 [13]. The results of these studies are presented in this chapter.

6.2 Experimental

6.2.1 Materials

The details of the materials and instruments used for the synthesis and characterisation of oxovanadium Schiff base complexes and their catalytic studies towards the oxidation of cyclohexene are given in Chapter 2.

6.2.2 Methods

The details of the syntheses Schiff bases and their vanadyl complexes are given in Chapters 2 and 3.

6.2.3 Catalytic activity measurements

Catalytic oxidation was carried out in a two-necked glass reactor (50 ml) fitted with a condenser and a septum. Hydrogen peroxide (30% w/v) was added through the septum to the magnetically stirred solution of cyclohexene and the complex in acetonitrile kept at the desired reaction temperature. The reaction mixture was refluxed with continuous stirring in an oil bath provided with a digital temperature controller. The course of the reaction was monitored by periodically withdrawing small samples (about 0.5 mL each) which were analyzed by gas chromatography fitted with OV−17 packed column (4 m × 4 mm id). Quantification was done after considering the response factors of the reagents and products obtained using standard mixtures.

6.3 Results and discussion

The spectral characterisation of the Schiff base ligands and their vanadyl complexes are given in Chapters 2 and 3.

6.3.2 Catalytic activity towards the oxidation of cyclohexene

Oxidation of cyclohexene generally yields various products such as cyclohexene peroxide, cyclohexenol, cyclohexenone and cyclohexene oxide etc [14]. However, the selectivity towards these products depends on various parameters like reaction conditions, central metal ion, solvent, oxidant agent, nature of the catalyst etc. Hydrogen peroxide was chosen in this work as a clean oxidant agent, since it is inexpensive, environmentally friendly and generates water as by product [15]. We carried out a blank experiment without catalyst under identical conditions. Only very low amount of substrate was converted in the blank reaction (below 2%) suggesting that our complex is functioning as a catalyst for cyclohexene oxidation reaction [16]. Allylic oxidation products such as cyclohexenol and cyclohexenone were formed as the major products along with cyclohexene oxide as the minor product, indicating the involvement of Fenton-type oxidation reactions [17]. Major formation of the allylic oxidation products shows the preferential attack of the activated C−H bond over the C=C bond [18]. The conversion and selectivity were calculated using the following relations [19].

$$X_{\text{cyclohexene}}\ (\%) = 100 \times ([\text{cyclohexene}]_i - [\text{cyclohexene}]_f)/[\ \text{cyclohexene}]_i,$$

where $X_{\text{cyclohexene}}$ is the conversion of cyclohexene, $[\text{cyclohexene}]_i$ is the molar concentration of cyclohexene before reaction, and $[\text{cyclohexene}]_f$ is the molar concentration of cyclohexene after sampling.

$$S_{\text{cyclohexene}}\ (\%) = 100 \times ([OX]_f + [OL]_f + [ONE]_f)/([\text{cyclohexene}]_i - [\text{cyclohexene}]_f),$$

where $S_{\text{cyclohexene}}$ is the selectivity for cyclohexene oxidation, and $[OX]_f$, $[OL]_f$, and $[ONE]_f$ are the molar concentration of cyclohexene oxide, cyclohexenol, and cyclohexenone, respectively, after reaction.

$$\text{Product distribution}\ (\%) = 100 \times [\text{product}]_f/([\ \text{cyclohexene}]_i - [\text{cyclohexene}]_f),$$

where $[product]_f$ is the molar concentration of product (cyclohexene oxide, cyclohexenol, or cyclohexenone) after reaction.

$$H_2O_{2eff}\ (\%) = 100 \times ([OX]_f + [OL]_f + [ONE]_f)/[H_2O_2]_{add},$$

where H_2O_{2eff} is the effective conversion of H_2O_2, and $[H_2O_2]_{add}$ is the molar concentration of the total added H_2O_2 in the reaction mixture.

All the oxovanadium(IV) complexes were screened for their activity in the oxidation of cyclohexene. The results of the screening studies are given in Table 1. Among these the complexes, $[(VO)_2(hqcdmn)SO_4].H_2O$ was found to be the most active. So a detailed catalytic activity study of the $[(VO)_2(hqcdmn)SO_4].H_2O$ in the oxidation of cyclohexene using aqueous 30% H_2O_2 as the oxidant was done and effect of varying the parameters like amount of catalyst, temperature, amount of solvent and time was investigated.

Table 1: The influence of catalyst on conversion and selectivity of cyclohexene oxidation [a]

Complex (5 mg)	$X_{cyclohexene}$ (%)	$S_{cyclohexene}$ (%)	Product distribution (%) [b]			H_2O_{2eff} (%)	TOF
			OX	OL	ONE		
I	44.2	11.5	0.7	6.0	4.8	5.5	275
II	50.7	20.9	1.3	6.6	13.0	11.2	266
III	45.6	13.7	2.3	5.5	5.8	6.6	318
IV	43.2	9.8	1.4	4.9	7.2	4.5	217
V	45.4	13.5	0.7	5.6	3.6	6.4	454

[a] Reaction conditions: acetonitrile (30 ml), temperature (80 °C), reaction time (2 h), H_2O_2 (18.70×10^{-3} mol), cyclohexene (1.97×10^{-2} mol).
[b] Here OX = cyclohexene oxide, OL = cyclohexenol and ONE = cyclohexenone.
TOF = mol of cyclohexene converted per mol of catalyst per hour. Here I, II, III, IV and V are $[(VO)_2(hqcdan)SO_4].H_2O$, $[(VO)_2(hqcdmn)SO_4].H_2O$, $[(VO)_2(hqcdac)SO_4].H_2O$, $[(VO)_2(hqcap)_2].H_2O$ and $[(VO)_2(hqcaap)_2SO_4].2H_2O$ respectively.

6.3.2.1 Influence of the catalyst

The influence of catalyst on the oxidation of cyclohexene was studied at 80 °C by varying the amount of catalyst from 1.50×10^{-6} mol to 7.50×10^{-6} mol keeping the amount of solvent, oxidant and substrate constant and the results are

given in Table 2. With increase in the amount of catalyst, an increase was observed in the percentage conversion, selectivity for cyclohexene oxidation and H_2O_2 efficiency increases. It is also found that by increasing the amount of catalyst, the cyclohexene oxide formation decreases whereas the distribution of allylic oxidation products enhances.

Table 2: The influence of catalyst on conversion and selectivity of cyclohexene oxidation [a]

Catalyst (10^{-6} mol)	$X_{cyclohexene}$ (%)	$S_{cyclohexene}$ (%)	Product distribution (%) [b]			H_2O_{2eff} (%)
			OX	OL	ONE	
1.50	42.4	8.4	1.8	2.1	4.6	3.8
3.00	43.7	10.6	1.7	2.7	6.2	4.9
4.50	45.1	12.9	1.6	3.6	7.8	6.1
6.00	47.7	16.8	1.4	5.2	10.2	8.5
7.50	50.7	20.9	1.3	6.6	13.0	11.2

[a] Reaction conditions: acetonitrile (30 ml), temperature (80 °C), reaction time (2 h), H_2O_2 (18.70×10^{-3} mol), cyclohexene (1.97×10^{-2} mol).
[b] Here OX = cyclohexene oxide, OL = cyclohexenol and ONE = cyclohexenone.

6.3.2.2 Influence of the oxidant H_2O_2

Cyclohexene oxidation was carried out by adding the H_2O_2 to the reaction mixture in one-lot at the reaction temperature. To study the effect of varying the amount of H_2O_2, the reaction was carried out with 7.50×10^{-6} mol of catalyst and the amounts of H_2O_2 from 9.35×10^{-3} mol to 28.05×10^{-3} mol while keeping other conditions as in the case above. The results are tabulated in Table 3. Percentage conversion, selectivity for cyclohexene oxidation and H_2O_2 efficiency increases to a maximum value with 18.70×10^{-3} mol of H_2O_2 and then decreases. The distribution of allylic oxidation products shows the same trend but the cyclohexene oxide percentage shows a gradual increase. The lower values of H_2O_2 efficiency for this reaction might be due to the higher efficiency of the complex to catalyze the hydrogen peroxide decomposition.

Table 3: The influence of oxidant on conversion and selectivity of cyclohexene oxidation [a]

H_2O_2 (10^{-3} mol)	X cyclohexene (%)	S cyclohexene (%)	Product distribution (%) [b]			H_2O_{2eff} (%)
			OX	OL	ONE	
9.35	42.7	9.0	1.1	4.3	3.6	8.1
14.03	46.7	15.4	1.2	5.3	8.9	10.1
18.70	50.7	20.9	1.3	6.5	13.0	11.2
23.36	46.9	15.8	1.6	4.2	10.0	6.2
28.05	45.2	13.4	1.7	3.0	8.4	4.2

[a] Catalyst (7.50×10^{-6} mol) and other conditions are the same as those in Table 2.

6.3.2.3 Influence of solvent

It is seen that variation of solvents has little influence on the conversion of cyclohexene and decreases in the order: dichloromethane (52.4 %) > chloroform (51.6 %) > methanol (51.0 %) > acetonitrile (50.7 %). However we chose acetonitrile as the solvent for common runs as the complex is more soluble in this solvent. Influence of the amount of acetonitrile on the oxidation of cyclohexene was studied by varying its volume from 10 to 40 ml while keeping the amount of catalyst, oxidant and substrate constant (Table 4). The amount of acetonitrile has a profound influence on the product distribution. With lower amounts of acetonitrile the three products are somewhat equally distributed whereas at higher amounts the percentage of epoxide decreases and that of the other two increases. An increase of the amount of solvent is also found to increase the percentage conversion, selectivity and H_2O_2 efficiency.

Table 4: The influence of solvent on conversion and selectivity of cyclohexene oxidation [a]

Acetonitrile (ml)	X cyclohexene (%)	S cyclohexene (%)	Product distribution (%) [b]			H_2O_{2eff} (%)
			OX	OL	ONE	
10	41.8	7.3	2.8	1.5	3.0	3.2
15	43.9	11.0	2.7	2.6	5.9	5.1
20	45.7	13.9	2.3	3.7	7.9	6.7
25	48.5	17.9	1.9	5.4	10.8	9.2
30	50.7	20.9	1.3	6.5	13.0	11.2
35	51.4	21.8	1.0	7.0	13.8	11.8
40	53.2	23.9	0.8	7.9	15.0	13.4

[a] Catalyst (7.50×10^{-6} mol) and other conditions are the same as those in Table 2.

6.3.2.4 Influence of reaction temperature

The reaction was studied over a wide range of temperature in 30 ml acetonitrile from 40 to 80 °C keeping the amount of catalyst, oxidant and substrate as constant (Table 5). Selection of this particular temperature range is due to the reason that at higher temperatures the decomposition of H_2O_2 predominates [20]. As the temperature increases, percentage conversion, selectivity for cyclohexene oxidation, H_2O_2 efficiency and percentage product distribution increases.

Table 5: The influence of temperature on conversion and selectivity of cyclohexene oxidation [a]

Temperature (°C)	$X_{cyclohexene}$ (%)	$S_{cyclohexene}$ (%)	Product distribution (%) [b]			H_2O_{2eff} (%)
			OX	OL	ONE	
40	42.2	7.9	1.0	1.4	5.5	3.5
50	44.6	12.1	1.1	3.0	8.0	5.7
60	46.8	15.5	1.2	4.3	9.9	7.6
70	48.7	18.3	1.3	5.5	11.6	9.4
80	50.7	20.9	1.4	6.5	13.0	11.2

[a] Catalyst (7.50×10^{-6} mol) and other conditions are the same as those in Table 2.

6.3.2.5 Influence of reaction time

The influence of reaction time on the oxidation of cyclohexene was probed by carrying out the reaction with 7.50×10^{-6} mol of catalyst in 30 ml of acetonitrile, 1.97×10^{-2} mol of cyclohexene, 18.70×10^{-3} mol of H_2O_2 and a temperature of 80 °C (Table 6). The conversion, selectivity, product distribution and H_2O_2 efficiency are found to increase with time. We studied the effects of various parameters on the hydroxylation of phenol for period of 2 h because a longer reaction time would lead to oxidation of dihydroxybenzenes to quinones and further to tar formation [21].

Table 6: Effect of reaction time in the catalytic activity and selectivity of cyclohexene oxidation [a]

Time (hrs)	$X_{cyclohexene}$ (%)	$S_{cyclohexene}$ (%)	Product distribution (%) [b]			H_2O_{2eff} (%)
			OX	OL	ONE	
1	46.4	14.9	1.1	4..3	9.5	7.3
2	50.7	20.9	1.3	6.5	13.0	11.2
3	51.7	22.1	1.3	7.2	13.5	12.0
4	52.7	23.4	1.4	7.9	14.0	12.9
5	53.5	24.3	1.4	8.6	14.2	13.7
6	54.5	25.3	1.5	9.2	14.7	14.6

[a] Catalyst 5 mg, acetonitrile 5 ml and other reaction conditions are the same as those in Table 2.

Conclusions

In this study, the catalytic activity of the synthesized oxovanadium(IV) complexes in the oxidation of cyclohexene were tested. The oxovanadium(IV) complex of the Schiff base, N,N'-bis(3-hydroxyquinoxaline-2-carboxalidene)2,3-diaminomaleonitrile exhibit better catalytic activity. A detailed investigation was carried out by varying the amount of this complex, temperature, amount of solvent and time. With aqueous 30% H_2O_2 as the oxidant, the complex was found to catalyze the oxidation with more selectivity for allylic oxidation products than that for the epoxide. The lower H_2O_2 efficiency observed for this reaction might be due to the greater catalytic activity of the complex towards the decomposition of hydrogen peroxide.

References

[1] L. Canali, D.C. Sherrington. Chemical Society Reviews, 28 (1999) 85-93.

[2] T. Katsuki. Coordination Chemistry Reviews, 140 (1995) 189−214.

[3] S. Rayati, N. Torabi, A. Ghaemi, S. Mohebbi, A. Wojtczak, A. Kozakiewicz. Inorganica Chimica Acta, 361 (2008) 1239–1245.

[4] M.R. Maurya, A. Kumar. Journal of Molecular Catalysis A: Chemical, 250 (2006) 190−198.

[5] M.R. Maurya, M. Kumar, A. Kumar, J. C. Pessoa. Dalton Transactions (2008) 4220–4232.

[6] R. Ando, S. Mori, M. Hayashi, T. Yagyu, M. Maeda, Inorganica Chimica Acta, 357 (2004) 1177–1184.

[7] G. Santoni, D. Rehder. Journal of Inorganic Biochemistry, 98 (2004) 758−764.

[8] D.M. Boghaei, S. Mohebi. Journal of Molecular Catalysis A: Chemical, 179 (2002) 41−51.

[9] P. Plitt, H. Pritzkow, T. Oeser, R. Kraemer. Journal of Inorganic Biochemistry,99 (2005) 1230–1237.

[10] L. Leelavathy, S. Anbu, M. Kandaswamy, N. Karthikeyan, N. Mohan. Polyhedron, 28 (2009) 903-910.

[11] H. Yue, D. Zhang, Z. Shi, S. Feng. Inorganica Chimica Acta, 360 (2007) 2681-2685.

[12] S. Rayati, N. Sadeghzadeh, H. R. Khavasi, Inorganic Chemistry Communications, 10 (2007) 1545-1548.

[13] F.S. Vinhado, P.R. Martins, A.P. Masson, D.G. Abreu, E.A. Vidoto, O.R. Nascimento, Y. Iamamoto, Journal of Molecular Catalysis A: Chemical, 188 (2002) 141–151.

[14] S.M. Mahajani, M.M. Sharma, T. Sridhar, Chemical Engineering Science 54 (1999) 3967−3976.

[15] F.S. Vinhado, P.R. Martins, A.P. Masson, D.G. Abreu, E.A. Vidoto, O.R. Nascimento, Y. Iamamoto, Journal of Molecular Catalysis A: Chemical, 188 (2002) 141–151.

[16] A.A. Costa, G.F. Ghesti, J.L. de Macedo, V.S. Braga, M.M. Santos, J.A. Dias, S.C.L. Dias. Journal of Molecular Catalysis A: Chemical, 282 (2008) 149–157.

[17] R.A. Sheldon, J.K. Kochi. Metal catalyzed oxidations of organic compounds, Academic Press, New York, 1981.

[18] M. Salavati-Niasari, P. Salemi, F. Davar. Journal of Molecular Catalysis A: Chemical, 238 (2005) 215–222.

[19] J. Wang, J-N Park, H-C Jeong, K-S Choi, X-Y Wei, S-I Hong, C.W. Lee. Energy and Fuels, 18 (2004) 470−476.

[20] A. Dubey, V. Rives, S. Kannan. Journal of Molecular Catalysis A: Chemical, 181 (2002) 151−160.

[21] J.S. Reddy, S. Sivasanker, P. Ratnasamy. Journal of Molecular Catalysis A: Chemical, 71 (1992) 373-381.

Chapter 7

Hydroxylation of phenol with hydrogen peroxide catalysed by copper(II) complexes

Contents

7.1 Introduction

Catalytic hydroxylation of phenol to catechol and hydroquinone using environmentally friendly oxidants such as dioxygen, hydrogen peroxide and alkyl hydroperoxide is an active area of research, especially in the fine chemicals industry [1,2]. Among these oxidants, hydrogen peroxide is easy to handle and ecofriendly as it produces only water as the by-product [3]. Over the past few decades, numerous reports have appeared on the hydroxylation of phenol with hydrogen peroxide as oxidant [4-13].

Schiff base transition metal complexes have been extensively studied because of their potential as catalysts in a wide range of reactions [7, 11, 14-15]. However, not all complexes are catalytically active. The formation of octahedral complexes with no vacant coordination sites or absence of labile ligands could be a possible reason. In this study, of the five copper(II) complexes synthesised from the bulky Schiff base ligands, four were found to have square planar geometry while one had an octahedral geometry with two coordinated water molecules. This favourable geometry could render the complexes catalytically active and hence we have made an attempt to study the efficiency of these mononuclear and binuclear copper(II) complexes towards the hydroxylation of phenol with H_2O_2 as an oxidant

7.2 Experimental

7.2.1 Materials

The materials used for the preparation Schiff base ligands, their copper complexes and their catalytic hydroxylation of phenol are presented in Chapter 2.

7.2.2 Methods

The synthesis of Schiff base ligands and their copper(II) complexes are given in Chapters 2 and 4.

7.2.3 Catalytic activity measurements

Hydroxylation of phenol was carried out in a two-necked glass reactor (50 ml) fitted with a condenser and a septum. Hydrogen peroxide (30% w/v) was added through the septum to the magnetically stirred solution of phenol containing catalyst and solvent (30 ml acetonitrile) kept at the desired reaction temperature. The reaction mixture was refluxed with continuous stirring in an oil bath provided with a digital temperature controller. The progress of the reaction was monitored by periodically withdrawing small samples (about 0.5 mL each) which were analyzed by using a gas chromatograph. Quantification was done after considering the response factors of the reagents and products obtained using standard mixtures.

7.3 Results and discussion

Details of the spectral characterisation of the Schiff base ligands and their copper(II) complexes are given in Chapters 2 and 4 respectively.

7.3.2 Catalytic activity towards the hydroxylation of phenol

The liquid-phase catalytic hydroxylation of phenol generally gives two major products, catechol and hydroquinone. These are the expected products, as the –OH group on phenol is ortho and para directing. Sometimes *p*-benzoquinone is also observed as a minor product due to further oxidation of hydroquinone [16]. In the

case of the present complex, only catechol and hydroquinone are observed. The conversion and selectivity were calculated using the following relations [17].

X_{phenol} (%) = 100 × ([phenol]$_i$ − [phenol]$_f$)/[phenol]$_i$,

where X_{phenol} is the conversion of phenol, [phenol]$_i$ is the molar concentration of phenol before reaction, and [phenol]$_f$ is the molar concentration of phenol after sampling.

S_{phenol} (%) = 100 × ([CAT]$_f$ + [HQ]$_f$)/([phenol]$_i$ − [phenol]$_f$),

where S_{phenol} is the selectivity for phenol hydroxylation, and [CAT]$_f$, and [HQ]$_f$ are the molar concentration of catechol and hydroquinone, respectively, after the reaction.

Product distribution (%) = 100 × [product]$_f$/([phenol]$_i$ - [phenol]$_f$),

where [product]$_f$ is the molar concentration of product (catechol or hydroquinone) after reaction.

H_2O_{2eff} (%) = 100 × ([CAT]$_f$ + [HQ]$_f$)/[H_2O_2]$_{add}$,

where H_2O_{2eff} is the effective conversion of H_2O_2, and [H_2O_2]$_{add}$ is the molar concentration of the total added H_2O_2 in the reaction mixture.

A comparison of the activity of the different copper(II) complexes towards the hydroxylation of phenol showed [Cu_2(hqcdmn)Cl_2] to be the most active. So a detailed investigation aimed at studying the influence of various parameters was carried out. A turnover frequency (mol of phenol converted per mol of catalyst per hour) of 460 h^{-1} has been found for the reaction using this complex as catalyst at 80 ^oC with 0.81 × 10^{-5} mol catalyst, 2.28 × 10^{-2} mol phenol and 18.70 × 10^{-3} mol H_2O_2.

Table 1: Catalytic activity and selectivity of copper(II) complexes in the hydroxylation of phenol [a]

Complex (5 mg)	X_{phenol} (%)	S_{phenol} (%)	Product distribution (%) [b]		H_2O_{2eff} (%)	TOF
			CAT	HQ		
I	61.0	8.0	7.5	3.2	10.7	616
II	61.9	8.9	8.2	3.5	11.8	629
III	61.3	8.3	8.2	2.8	11.1	603
IV	61.4	8.3	7.3	3.9	11.2	627
V	61.6	8.5	7.4	4.0	11.4	483

[a] Reaction conditions: acetonitrile (5 ml), temperature (80 °C), time (2 h), H_2O_2 (18.70×10^{-3} mol), phenol (2.28×10^{-2} mol).
[b] CAT = catechol, HQ = hydroquinone. The expected other products such as benzoquinone and tar is not formed. TOF = mol of phenol converted per mol of catalyst per hour.
Here I, II, III, IV and V are $[Cu_2(hqcdan)Cl_2].H_2O$, $[Cu_2(hqcdmn)Cl_2]$, $[Cu_2(hqcdac)Cl_2].H_2O$, $[Cu_2(hqcap)_2]$ and $[Cu(hqcaap)Cl(H_2O)_2]$ rescpectively.

7.3.2.1 Influence of the catalyst

The reaction when carried out in the absence of catalyst did not yield any products. The effect of varying the catalyst on the hydroxylation of phenol was studied at 80 °C by varying the amount of catalyst from 0.81×10^{-5} mol to 12.15×10^{-5} mol keeping the amount of solvent, oxidant and substrate constant and the results of which are given in Table 2. Percentage phenol conversion and H_2O_2 efficiency increased to a maximum with 1.62×10^{-5} mol of catalyst and then decreased with further increase in the amount of catalyst. This as explained earlier might be due to the decomposition of H_2O_2 with large amount of catalyst [9]. A similar trend was observed in the selectivity and product distribution.

Table 2: Effect of $[Cu_2(hqcdmn)Cl_2]$ in the catalytic activity and selectivity of phenol hydroxylation [a]

Catalyst (10^{-5} mol)	X_{phenol} (%)	S_{phenol} (%)	Product distribution (%) [b]		H_2O_{2eff} (%)
			CAT	HQ	
0.81	58.4	7.4	6.9	0.4	5.2
1.62	60.7	10.3	7.9	2.3	7.6
2.43	59.4	8.7	6.8	2.0	6.3
3.25	59.2	8.4	6.5	1.9	6.1
12.15	58.7	7.7	6.0	1.8	5.5

[a] Reaction conditions: acetonitrile (10 ml), temperature (80 °C), time (2 h), H_2O_2 (18.70×10^{-3} mol), phenol (2.28×10^{-2} mol).
[b] CAT = catechol, HQ = hydroquinone. The expected other products such as benzoquinone and tar is not formed.

7.3.2.2 Influence of the oxidant H_2O_2

The mode of addition of H_2O_2 to the reaction mixture is very important in the hydroxylation of phenol [5]. In the present case, H_2O_2 was added in one-lot at reaction temperature of 80 °C. With increase in the amount of the oxidant, H_2O_2, percentage phenol conversion, selectivity for phenol hydroxylation and percentage product distribution increases (Table 3). The H_2O_2 efficiency reaches a maximum at 14.03×10^{-3} mol of H_2O_2.

Table 3: Effect of 30 % H_2O_2 in the catalytic activity and selectivity of phenol hydroxylation [a]

H_2O_2 (10^{-3} mol)	X_{phenol} (%)	S_{phenol} (%)	Product distribution (%)		H_2O_{2eff} (%)
			CAT	HQ	
9.35	57.3	5.9	5.4	0.5	8.2
14.03	60.9	10.5	7.8	2.7	10.4
18.70	61.9	11.8	8.2	3.5	8.9
23.36	63.4	13.5	9.1	4.4	8.3
28.05	65.4	15.7	10.3	5.4	8.3

[a] Catalyst 0.81×10^{-5} mol, acetonitrile 5 ml and other reaction conditions are the same as those in Table 2.

7.3.2.3 Influence of solvent

It has been reported that solvents have a profound influence on the phenol conversion and on the ratio of catechol to hydroquinone [18]. To study the effect of solvent we carried out the hydroxylation in acetonitrile. An increase of the amount of acetonitrile from 0 to 30 ml decreases the percentage phenol conversion, selectivity for phenol hydroxylation, percentage product distribution and H_2O_2 efficiency (Table 4). It was further observed that the complex gives maximum conversion and selectivity without the solvent and hence the use of different solvents has no significance.

Table 4: Effect of the solvent in the catalytic activity and selectivity of phenol hydroxylation [a]

Acetonitrile (ml)	X $_{phenol}$ (%)	S $_{phenol}$ (%)	Product distribution (%)		H_2O_{2eff} (%)
			CAT	HQ	
0	68.7	19.0	11.9	7.2	15.9
5	61.9	11.8	8.2	3.5	8.9
10	58.4	7.4	7.0	0.4	5.2
15	57.1	5.6	5.3	0.3	3.9
20	55.9	3.8	3.6	0.2	2.6
25	55.3	2.9	2.8	0.1	2.0
30	54.0	1.0	1.0	0.0	0.7

[a] Catalyst 0.81 × 10^{-5} mol, acetonitrile 5 ml and other reaction conditions are the same as those in Table 2.

7.3.2.4 Influence of reaction temperature

The effect of temperature on the conversion of phenol was studied in the temperature range 40 to 80 °C. Selection of this particular temperature range is to avoid the enhanced H_2O_2 decomposition [10] and further oxidation of dihydroxybenzene to quinones and then to tar formation [5]. Phenol conversion, selectivity for phenol hydroxylation and H_2O_2 efficiency increases with elevation of temperature (Table 5). The percentage distribution of the catechol reaches a maximum at 60 °C and then decreases where as the percentage distribution of hydroquinone showed a gradual increase.

Table 5: Effect of temperature in the catalytic activity and selectivity of phenol hydroxylation [a]

Temperature (°C)	X $_{phenol}$ (%)	S $_{phenol}$ (%)	Product distribution (%)		H_2O_{2eff} (%)
			CAT	HQ	
40	56.0	3.9	3.9	0	2.7
50	59.2	8.4	8.1	0.3	6.1
60	60.2	9.7	8.9	0.8	7.1
70	61.3	11.1	8.4	2.6	8.3
80	61.9	11.8	8.2	3.5	8.9

[a] Catalyst 0.81 × 10^{-5} mol, acetonitrile 5 ml and other reaction conditions are the same as those in Table 2

7.3.2.4 Influence of reaction time

The influence of reaction time on the hydroxylation of phenol was studied with 0.81×10^{-5} mol of catalyst in 5 ml of acetonitrile at 80 °C with 2.28×10^{-2} mol of phenol, 18.70×10^{-3} mol of H_2O_2 (Table 6). The conversion, selectivity, product distribution and H_2O_2 efficiency were found to increase with reaction time. The reaction time was varied from 0 to 5 hours. Since a longer reaction time is not beneficial for this reaction, we studied the effects of various parameters except the effect of reaction time for period of 2 h. This is because a longer reaction time would lead to oxidation of dihydroxybenzenes to quinones and further to tar formation [9].

Table 6: Effect of reaction time in the catalytic activity and selectivity of phenol hydroxylation [a]

Time (hrs)	X_{phenol} (%)	S_{phenol} (%)	Product distribution (%)		H_2O_{2eff} (%)
			CAT	HQ	
1	59.5	8.8	6.8	2.0	6.4
2	61.9	11.8	8.2	3.5	8.9
3	63.1	13.1	8.7	4.4	10.1
4	63.7	13.8	8.9	4.9	10.7
5	64.5	14.8	9.5	5.3	11.6

[a] Catalyst 0.81×10^{-5} mol, acetonitrile 5 ml and other reaction conditions are the same as those in Table 2.

Conclusions

The catalytic activity of the copper(II) complexes were studied in the liquid-phase hydroxylation of phenol using H_2O_2 as an oxidant. Catechol and hydroquinone are the sole products of the reaction. All the complexes were screened for their activity towards the hydroxylation of phenol. Detailed study of the catalytic activity of the complex, $[Cu_2(hqcdmn)Cl_2]$, that gave maximum conversion in the screening studies was carried out by changing the different parameters like catalyst amount, reaction time, reaction

temperature, amount of oxidant, and the amount of solvent. It was also found that there exists an optimum value for the amount of catalyst as well as temperature and time, after which conversion decreases. Increase in the amount of H_2O_2 has a positive effect on the reaction while the quantity and nature of solvent have no significant effect.

References

[1] R.A. Sheldon, R.A. van Santen. Catalytic Oxidation: Principles and Applications, World Scientific, Singapore, 1995.

[2] Industrial Organic Chemical: Starting Materials and Intermediates: An Ullamann's Encyclopedia, vol. 6, Wiley/VCH, New York, 1999.

[3] J.O. Edwards, R. Curci. in: G. Strukul (Ed.), Catalytic Oxidations with Hydrogen Peroxide as Oxidant ,Kluwer Academic Publishers, Dordrecht, 1992.

[4] A. Tuel, S. Moussa-Khouzami, Y. B. Taarit, C. Naccache. Journal of Molecular Catalysis A: Chemical, 68 (1991) 45-52.

[5] J.S. Reddy, S. Sivasanker, P. Ratnasamy. Journal of Molecular Catalysis A: Chemical, 71 (1992) 373-381.

[6] L. Forni, C. Oliva, A.V. Vishniakov, A.M. Ezerets, I.E. Mukovozov, F.P. Vatti, V.N. Zubkovskaja. Journal of Catalysis, 145 (1994) 194-203.

[7] M.R. Maurya, M. Kumar, S.J.J. Titinchi, H.S. Abbo, S. Chand. Catalysis Letters, 86 (2003) 97-105.

[8] S. Jiang, Y. Kong, J. Wang, X. Ren, Q. Yan. Journal of Porous Materials, 13 (2006) 341-346.

[9] F.S. Xiao, J.M. Sun, X.J. Meng, R.B. Yu, H.M. Yuan, J.N. Xu, T.Y. Song, D.Z. Jiang, R.R. Xu. Journal of Catalysis, 199 (2001) 273-281.

[10] A. Dubey, V. Rives, S. Kannan. Journal of Molecular Catalysis A: Chemical, 181 (2002) 151-160.

[11] M. Salavati-Niasari, M.R. Ganjali, P. Norouzi. Journal of Porous Materials, 14 (2007) 423-432.

[12] M.E.L. Preethi, S. Revathi, T. Sivakumar, D. Manikandan, D. Divakar, A.V. Rupa, M. Palanichami. Catalysis Letters, 120 (2008) 56-64.

[13] M.V. Barmatova, I.D. Ivanchikova, O.A. Kholdeeva, A.N. Shmakov, V.I. Zaikovskii, M.S. Melgunov, Catalysis Letters, 127 (2009) 75-82.

[14] L. Canali, D.C. Sherrington. Chemical Society Reviews, 28 (1999) 85-93.

[15] T. Katsuki. Coordination Chemistry Reviews, 140 (1995) 189-214.

[16] R. Raja, P. Ratnasamy. Applied Catalysis A: General, 143 (1996) 145-158.

[17] J. Wang, J-N Park, H-C Jeong, K-S Choi, X-Y Wei, S-I Hong, C.W. Lee. Energy and Fuels 18 (2) (2004) 470-476.

[18] A. Tuel, S. Moussa-Khouzami, Y. Ben Taarit and C. Naccache, Journal of Molecular Catalysis A: Chemical, 68 (1991) 45-52.

Hydrogenation of benzene and toluene catalysed by ruthenium(II) complexes

Contents

8.1 Introduction

The design and synthesis of transition metal complexes of Schiff base having oxygen and nitrogen donor atoms is an active area of research, as they offer opportunity for including substrate chirality, tuning metal centered electronic factor, and enhancing solubility and stability of either homogeneous or heterogeneous catalyst [1-3]. Schiff base complexes of transition metals including ruthenium are found to be effective catalysts for various chemical transformations [4-8]. A number of ruthenium complexes have been prepared earlier and extensively used as catalysts in hydrogenation reactions [9-17]. The hydrogenation of aromatic compounds to cyclic products is an important reaction in chemical industry [18-22]. Even though a lot of success has been achieved with regard to transition metal complex catalyzed hydrogenation of olefins [23-26], there are only a few reports on studies involving hydrogenation of arenes using homogeneous metal complex catalysts [27-34]. The catalytic activity of transition metal Schiff base complexes in a given process is highly dependent on the enviornment about the metal centre and their conformational flexibility [35]. By small changes in the ligand frame work it is possible to enhance the steric and electronic effects in homogeneous metal complexes [36]. In most of the transition metal catalyzed hydrogenation reactions, involvement of hydride complexes as the intermediate species or as starting materials was suggested [37]. A crucial step in the hydrogenation reaction is the cleavage of the dihydrogen molecule. Presence of an electron-rich atmosphere

around the metal centre facilitates breaking of the H−H bond by the interaction of the filled metal d orbital with the empty sigma antibonding molecular orbital of H2 [37]. An increase in the N-basicity of the Schiff base ligand is found to increase the catalytic performance towards the metal catalyzed dehydrogenation/hydrogenation through such an interaction [38, 39]. Therefore increased interactions are expected in the case of Schiff bases derived from 3-hydroxyquinoxaline-2-carboxaldehyde, which have more basic donor nitrogen atoms. The presence of quinoxaline ring may build a favourable steric topography and electronic environment in the immediate coordination sphere of the metal and thus allowing fine tuning of various catalytic and biological properties of its complexes. With this in view, we have synthesized new complexes derived from 3-hydroxyquinoxaline-2-carboxaldehyde, containing ruthenium in +2 oxidation state. These ruthenium(II) complexes exhibited excellent catalytic activity towards hydrogenation of benzene and toluene. Details of the synthesis and characterization of these metal complexes are presented in Chapter 5. In this chapter, the results of our studies on the catalytic activity of these complexes towards hydrogenation of benzene and toluene are presented.

8.2 Experimental

8.2.1 Materials

Details regarding the materials used for the preparation of ruthenium complexes and the catalytic hydrogenation of benzene and toluene are given in Chapter 2. Hydrogen gas with >99.8% purity supplied by Sterling Gases Ltd. (Cochin, India), was used as such for hydrogenation reactions.

8.2.2 Methods

The syntheses of the Schiff base ligands and their ruthenium(II) complexes are given in Chapters 2 and 5.

8.2.3 Catalytic activity measurements

Details regarding the hydrogenation experiments are given in Chapter 2.

8.3 Results and discussion

The spectral characterisation of the Schiff base ligands and their metal(II) complexes of ruthenium are discussed in Chapters 2 and 5.

8.3.1 Catalytic hydrogenation of benzene and toluene

Generally partial and complete reduction of benzene or alkyl benzene takes place with the major formation of fully reduced product. The activity of some common metals towards the hydrogenation of benzene and alkyl benzene decreases in the order: Rh > Ru > Pt >Ni > Pd >Co [40]. The five ruthenium complexes, $[Ru_2(hqcdan)Cl_2].H_2O$, $[Ru_2(hqcdmn)\ Cl_2].H_2O$, $[Ru_2(hqcdac)Cl_2].H_2O$, $[Ru_2(hqcap)Cl_2(H_2O)].H_2O$ and $[Ru(hqcaap)Cl(H_2O)_2].H_2O$, were screened for its activity towards the hydrogenation of benzene and toluene. The reactions were carried out under solvent free conditions with 0.34 mol benzene/ 0.28 mol toluene, 80 °C temperature, 30 bar dihydrogen pressure, 600 rpm stirring speed and 2 mg catalyst. The percentage conversion of benzene/toluene was noted after two hours of reaction. The percentage conversion obtained with the complexes along with their turnover frequencies (TOF is the mol of benzene/toluene transformed per mole of the catalyst per hour) are given in Table 1.

Table 1: Activity of ruthenium complexes in the hydrogenation of benzene and toluene [a]

[catalyst]	Conversion (%)		TOF (h^{-1})	
	Benzene	Toluene	Benzene	Toluene
$[Ru_2(hqcdan)Cl_2].H_2O$	6.5	5.9	8,023	6,821
$[Ru_2(hqcdmn)Cl_2].H_2O$	17.3	16.8	20,858	16,680
$[Ru_2(hqcdac)Cl_2].H_2O$	12.4	11.8	15,111	11,842
$[Ru_2(hqcap)Cl_2(H_2O)].H_2O$	16.2	15.7	15,782	12,596
$[Ru(hqcaap)Cl(H_2O)_2].H_2O$	8.8	7.4	8,219	5,800

[a] General reaction conditions: 0.34 mol benzene/ 0.28 mol toluene , 80 °C temperature, 30 bar dihydrogen pressure, 2 mg catalyst, 600 rpm stirring speed, 2 h reaction time.

Among these complexes, $[Ru_2(hqcdmn)Cl_2].H_2O$ was found to be the most active. Hence a detailed study was carried out on the activity of this complex towards the hydrogenation of benzene and toluene. The reactions were performed under solvent free conditions by variation of catalyst and substrate concentrations, dihydrogen pressure, reaction time and temperature of reaction mixtures. At 60 °C, and 30 bar hydrogen pressure, turnover frequencies 7362 h^{-1} and 5873 h^{-1} have been found for the hydrogenation of benzene and toluene respectively. This value is much higher than that reported for some of the mononuclear ruthenium-based catalysts in the homogeneous hydrogenation of arenes [41,42]. This higher turnover frequency may be due to the presence of electron rich nitrogen atoms in the heterocyclic Schiff base which tends to make the central Ru(II) cations more electron rich and thus promote the overlap of the filled metal d orbital and the empty sigma antibonding molecular orbital of the H_2. This effect in turn would favor the cleavage of the H−H bond, which is a crucial step in the hydrogenation reaction [43].

8.3.1.1 Effect of catalyst concentration

To study the influence of catalyst concentration on the reduction of benzene and toluene, quantity of the catalyst were varied in the range (1.41-7.05) × 10^{-6} mol, while the substrate concentration (0.34 mol benzene/0.28 mol toluene), dihydrogen pressure (30 bars) and the temperature (60 ºC) were kept constant (Tables 2 and 3). In both cases an increase in catalyst concentration was found to raise the percentage conversion. However, with increase in catalyst concentration, there occurs a change in the product distribution. At lower concentrations of the catalyst the fully hydrogenated product predominant while at increased catalyst concentrations partially hydrogenated product, which dominates. This would be due to the increase in catalytic active ruthenium sites with increase in catalyst concentration.

Table 2: Effect of the $[Ru_2(hqcdmn)Cl_2].H_2O$ in the hydrogenation of benzene [a]

[catalyst] (10^{-6} mol)	[benzene] (mol)	H_2 pressure (bar)	Temperature (°C)	Conversion (%)	Selectivity (%) [b]	
					CA	CE
1.41	0.34	30	60	10.2	85	15
2.82	0.34	30	60	12.3	84	16
4.23	0.34	30	60	13.0	83	17
5.64	0.34	30	60	13.2	83	17
7.05	0.34	30	60	13.5	82	18

[a] General reaction conditions: 0.34 mol benzene , 60 °C temperature, 30 bar dihydrogen pressure, 2.82×10^{-6} mol catalyst, 600 rpm stirring speed, 2 h reaction time. [b] CA = cyclohexane, CE = cyclohexene and the product selectivity is CA (or CE) / (CA + CE)

Table 3: Effect of the $[Ru_2(hqcdmn)Cl_2].H_2O$ in the hydrogenation of toluene [a].

[catalyst] (10^{-6} mol)	[toluene] (mol)	H_2 pressure (bar)	Temperature (°C)	Conversion (%)	Selectivity (%) [b]	
					MCA	MCE
1.41	0.28	30	60	11.7	86	14
2.82	0.28	30	60	11.8	85	15
4.23	0.28	30	60	12.6	84	16
5.64	0.28	30	60	12.9	84	16
7.05	0.28	30	60	13.2	83	17

[a] General reaction conditions: 0.28 mol toluene , 60 °C temperature, 30 bar dihydrogen pressure, 2.82×10^{-6} mol catalyst, 600 rpm stirring speed, 2 h reaction time. [b] MCA = methyl cyclohexane, MCE = methyl cyclohexene and the product selectivity is MCA (or MCE) / (MCA + MCE)

8.3.1.2 Effect of dihydrogen pressure

To analyse the dependence of dihydrogen pressure on the reduction of benzene, a series of experiments were carried out by varying the pressure over the range of 10 to 50 bar at 60 °C keeping both substrate concentration (0.34 mol benzene/0.28 mol toluene) and the catalyst loading (2.82×10^{-6} mol) constant. A favourable effect of conversion is observed with an increase of hydrogen pressure from 10 up to 50 bars. The complex is more selective for fully hydrogenated product and this selectivity also increases as the hydrogen pressure increases (Tables 4 and 5).

Table 4: Effect of dihydrogen pressure in the hydrogenation of benzene [a]

[catalyst] (10^{-6} mol)	[benzene] (mol)	H_2 pressure (bar)	Temperature (°C)	Conversion (%)	Selectivity (%) [b]	
					CA	CE
2.82	0.34	10	60	4.1	64	36
2.82	0.34	20	60	8.6	80	20
2.82	0.34	30	60	12.3	84	16
2.82	0.34	40	60	14.6	85	15
2.82	0.34	50	60	16.8	85	15

[a] General reaction conditions: 0.34 mol benzene , 60 °C temperature, 30 bar dihydrogen pressure, 2.82×10^{-6} mol catalyst, 600 rpm stirring speed, 2 h reaction time. [b] CA = cyclohexane, CE = cyclohexene and the product selectivity is CA (or CE) / (CA + CE)

Table 5: Effect of dihydrogen pressure in the hydrogenation of toluene [a].

[catalyst] (10^{-6} mol)	[toluene] (mol)	H_2 pressure (bar)	Temperature (°C)	Conversion (%)	Selectivity (%) [b]	
					MCA	MCE
2.82	0.28	10	60	4.0	63	37
2.82	0.28	20	60	8.4	80	20
2.82	0.28	30	60	11.8	85	15
2.82	0.28	40	60	14.0	86	14
2.82	0.28	50	60	15.1	86	14

[a] General reaction conditions: 0.28 mol toluene , 60 °C temperature, 30 bar dihydrogen pressure, 2.82×10^{-6} mol catalyst, 600 rpm stirring speed, 2 h reaction time. [b] MCA = methyl cyclohexane, MCE = methyl cyclohexene and the product selectivity is MCA (or MCE) / (MCA + MCE)

8.3.1.3 Effect of substrate concentration

The effect of substrate concentration on the hydrogenation was studied by varying its concentration in the range 0.34 mol-0.56 mol and 0.28 mol -0.47 mol for benzene and toluene respectively at a constant catalyst concentration of 2.82×10^{-6} mol at 60 °C and at 30 bar hydrogen pressure (Tables 6 and 7). The percentage conversion decreases where as selectivity towards the fully reduced product increases.

Table 6: Effect of substrate in the hydrogenation of benzene [a]

[catalyst] (10^{-6} mol)	[benzene] (mol)	H_2 pressure (bar)	Temperature (°C)	Conversion (%)	Selectivity (%) [b]	
					CA	CE
2.82	0.34	30	60	12.3	84	16
2.82	0.39	30	60	10.7	85	15
2.82	0.45	30	60	10.0	86	14
2.82	0.51	30	60	7.7	87	13
2.82	0.56	30	60	7.3	88	12

[a] General reaction conditions: 0.34 mol benzene , 60 °C temperature, 30 bar dihydrogen pressure, 2.82×10^{-6} mol catalyst, 600 rpm stirring speed, 2 h reaction time. [b] CA = cyclohexane, CE = cyclohexene and the product selectivity is CA (or CE) / (CA + CE)

Table 7: Effect of substrate in the hydrogenation of toluene [a].

[catalyst] (10^{-6} mol)	[toluene] (mol)	H_2 pressure (bar)	Temperature (°C)	Conversion (%)	Selectivity (%) [b]	
					MCA	MCE
2.82	0.28	30	60	11.8	85	15
2.82	0.33	30	60	10.9	87	13
2.82	0.38	30	60	9.5	88	12
2.82	0.42	30	60	8.4	88	12
2.82	0.47	30	60	7.3	88	12

[a] General reaction conditions: 0.28 mol toluene , 60 °C temperature, 30 bar dihydrogen pressure, 2.82×10^{-6} mol catalyst, 600 rpm stirring speed, 2 h reaction time. [b] MCA = methyl cyclohexane, MCE = methyl cyclohexene and the product selectivity is MCA (or MCE) / (MCA + MCE)

8.3.1.4 Effect of temperature

The effects of temperature on the hydrogenation of benzene and toluene were investigated in the range 40-120 °C, all other parameters being kept constant (Tables 8 and 9). Percentage conversion and selectivity towards fully reduced product is seen to increase with elevation of temperature.

Table 8: Effect of temperature in the hydrogenation of benzene [a]

[catalyst] (10^{-6} mol)	[benzene] (mol)	H_2 pressure (bar)	Temperature (°C)	Conversion (%)	Selectivity (%) [b]	
					CA	CE
2.82	0.34	30	60	12.3	84	16
2.82	0.34	30	40	4.7	74	26
2.82	0.34	30	80	17.3	85	15
2.82	0.34	30	100	20.9	85	15
2.82	0.34	30	120	23.2	86	14

[a] General reaction conditions: 0.34 mol benzene , 60 °C temperature, 30 bar dihydrogen pressure, 2.82×10^{-6} mol catalyst, 600 rpm stirring speed, 2 h reaction time. [b] CA = cyclohexane, CE = cyclohexene and the product selectivity is CA (or CE) / (CA + CE)

Table 9: Effect of temperature in the hydrogenation of toluene [a].

[catalyst] (10^{-6} mol)	[toluene] (mol)	H_2 pressure (bar)	Temperature (°C)	Conversion (%)	Selectivity (%) [b]	
					MCA	MCE
2.82	0.28	30	40	4.5	75	25
2.82	0.28	30	60	11.8	85	15
2.82	0.28	30	80	16.8	86	14
2.82	0.28	30	100	20.0	86	14
2.82	0.28	30	120	22.7	86	14

[a] General reaction conditions: 0.28 mol toluene , 60 °C temperature, 30 bar dihydrogen pressure, 2.82×10^{-6} mol catalyst, 600 rpm stirring speed, 2 h reaction time. [b] MCA = methyl cyclohexane, MCE = methyl cyclohexene and the product selectivity is MCA (or MCE) / (MCA + MCE)

8.3.1.4 Effects of reaction time

In order to study the effect of time, reactions were carried out for 4 h with 2.82×10^{-6} mol of catalyst, substrate concentration of 0.34 mol benzene/0.28 mol toluene, 30 bar pressure at 60 °C with a stirring speed of 600 rpm. The products were analysed at 15 minute intervals and the results are shown in Figure 1. Conversion of benzene and toluene increases linearly with increase in time. In both the cases, the selectivity does not change significantly as the time elapses.

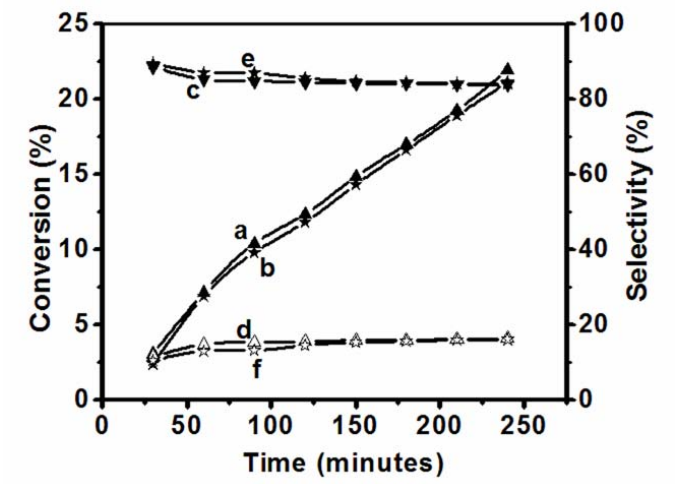

Figure 1: Effect of time; where a = conversion of benzene, b = conversion of toluene, c = CA selectivity for the hydrogenation of benzene, d = CE selectivity for the hydrogenation of benzene, e = MCA selectivity for the hydrogenation of toluene and f = MCE selectivity for the hydrogenation of toluene

8.3.2 Kinetics of hydrogenation of benzene using $[Ru_2(hqcdmn)Cl_2].H_2O$

The kinetics of hydrogenation of benzene was studied employing the initial rate method [44]. Initial rates were obtained by fitting the concentration–time data into the polynomial of the form $[C] = a_0 + a_1t + a_2t^2 + \cdots$ where C and t represent concentration and time, respectively. $a0$, $a1$, $a2$, etc. are constants. The coefficient of 't' gives the initial rate. This was done using Microsoft Excel. Catalytic runs were carried out at different catalyst and substrate concentrations and dihydrogen pressures. The data thus obtained is summarised in Table 10. Gas chromatographic estimation of the reaction mixture was done at intervals 15 min.

8.3.2.1 Order with respect to catalyst

The concentration of the catalyst was varied in the range of 1.41×10^{-6} to 7.05×10^{-6} mol l^{-1} range, (Table 10), while the benzene concentration (0.34 mol l^{-1}), dihydrogen pressure (30 bars or 1.02 mol l^{-1}) and the temperature (60 °C) were kept constant. A plot of initial rate versus concentration of the catalyst (Figure 2) yields a

straight line passing through the origin, suggesting first order with respect to the catalyst.

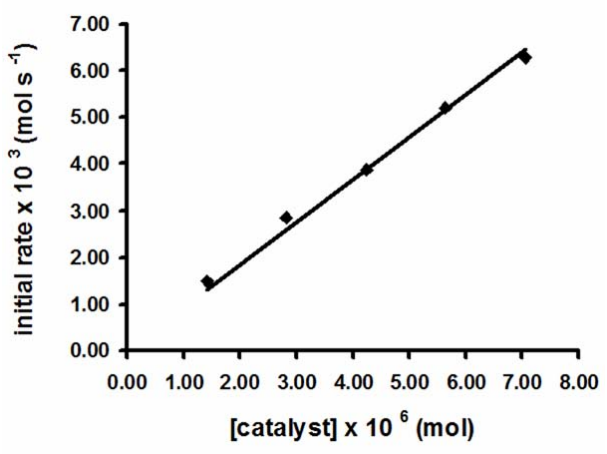

Figure 2: Plot of initial rate versus catalyst concentration

8.3.2.2 Order with respect to substrate

The effect of benzene concentration was studied in the range 0.34 to 0.56 mol l^{-1} (Table 10) keeping constant catalyst concentration (2.82×10^{-5} mol l^{-1}) and dihydrogen pressure (30 bars or 1.02 mol l^{-1}) at 60 ºC. A plot of initial rate versus [benzene] was a straight line (Figure 3) passing through origin indicating first order with respect to benzene.

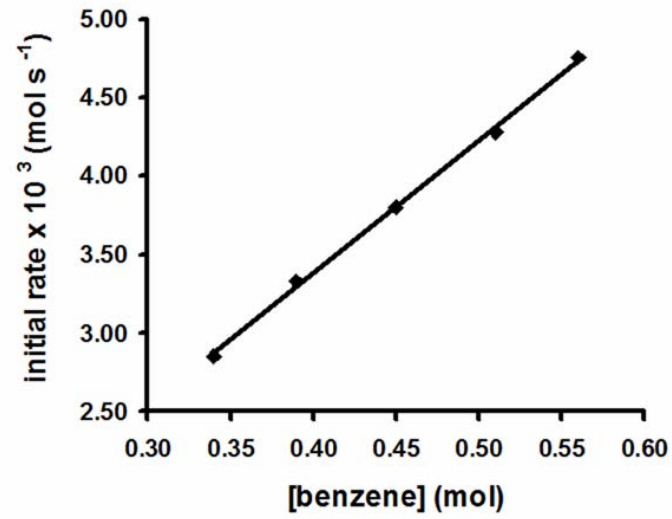

Figure 3: Plot of initial rate versus concentration of benzene

8.3.2.3 Order with respect to H_2

The effect of dihydrogen pressure at 60 ºC was studied in the range, 10 to 50 bar (0.34 to 1.70 mol l^{-1}) (Table 10), with 0.34 mol l^{-1} of benzene and 2.82×10^{-5} mol l^{-1} catalyst. A plot of reciprocal of the initial rate versus the reciprocal dihydrogen pressure gives a straight line (Figure 4) with intercept, indicating Michaelis-Menten type of kinetics with respect to dihydrogen.

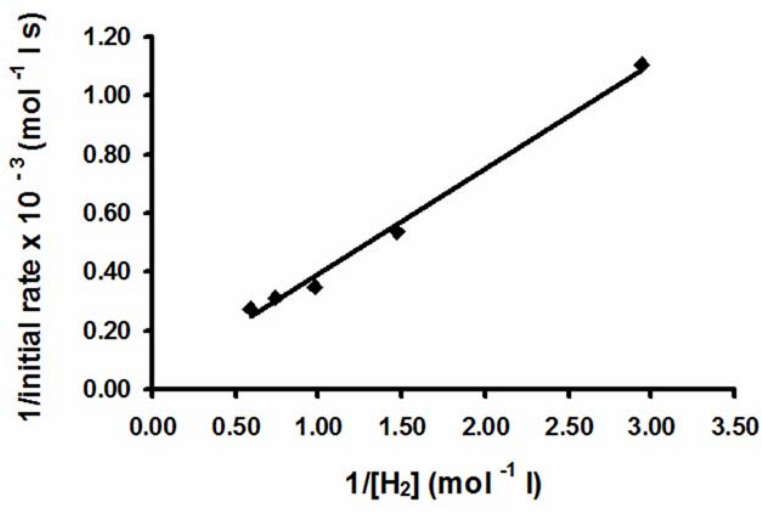

Figure 4: Plot of 1/initial rate versus 1/dihydrogen pressure

8.3.2.4 Derivation of experimental rate law

The results discussed above suggest that ruthenium(II) complex catalyses the hydrogenation of benzene according to the empirical rate equation,

From the kinetic data, the empirical rate equation can be expressed as,

$$\text{Rate} = \frac{-d[B]}{dt} = \frac{\{a\,[\text{benzene}][H_2][\text{catalyst}]\}}{\{b + c\,[H_2]\}} \qquad (1)$$

As mentioned above, the reaction follows Michaelis-Menten kinetics with respect to [H_2]. In order to verify whether H_2 is coordinated to the catalyst, the intermediate complex was separated from the reaction mixtures. The IR spectrum (Figure 5) of the intermediate complex exhibits bands at 938 and 1560 cm^{-1} due to the symmetric and asymmetric M−H_2 stretches, respectively [45]. Presence of the H−H stretch at 2963 cm^{-1} and δ M−H bands at 697 and 468 cm^{-1} in the spectrum confirm the formation of a η^2−dihydrogen complex [45,46]. Furthermore, the peak corresponding to coordinated water (at 3442 cm^{-1}) was not observed in the intermediate, suggesting that the coordination of the dihydrogen is through replacement of the coordinated water. Thus the kinetic analysis presented above allows proposing the following mechanism for the hydrogenation of benzene catalyzed by [Ru_2(hqcdmn)Cl_2].H_2O.

$$[\text{catalyst}] + H_2 \overset{K}{\Leftrightarrow} [\text{catalyst}(H_2)] \quad (2)$$

$$[\text{catalyst}(H_2)] + B \xrightarrow[slow]{k_1} [\text{catalyst}(H_2)B] \quad (3)$$

$$[\text{catalyst}\ (H_2)B] + H_2 \xrightarrow[fast]{} BH_2 + [\text{catalyst}(H_2)] \quad (4)$$

$$BH_2 + [\text{catalyst}(H_2)] + H_2 \xrightarrow[fast]{} BH_4 + [\text{catalyst}(H_2)] \quad (5)$$

$$BH_4 + [\text{catalyst}(H_2)] + H_2 \xrightarrow[fast]{} BH_6 + [\text{catalyst}(H_2)] \quad (6)$$

where 'B' represents benzene and 'catalyst' represents [[Ru_2(hqcdmn)Cl_2].H_2O]. This mechanism leads to the rate equation,

$$\text{Rate} = \frac{-d[B]}{dt} = k_1[\text{catalyst}(H_2)]_e[B] \quad (7)$$

where $[\text{catalyst}(H_2)]_e = K\,[\text{catalyst}]_e[H_2]_e$ (from equation 2) and $[\text{catalyst}]_e$ = $[\text{catalyst}]o - [\text{catalyst}(H_2)]_e = \frac{[catalyst]_o}{1+K[H_2]_e}$. Since $[H_2] >> [\text{catalyst}\ (H_2)]$, the

equilibrium concentration of dihydrogen, $[H_2]_e$ can be assumed to be equal to its initial concentration,$[H_2]_o$.

Thus rate equation (7) can be written as,

$$\text{Rate} = \frac{-d[B]}{dt} = \frac{k_1 K[catalyst]_o[H_2]_o[B]_o}{\{1+K[H_2]_o\}} \qquad (8)$$

where the subscript 'o' stands for initial concentration.

Equation (8) is similar to the experimentally observed rate equation. Hence, the proposed mechanism explains all the observed kinetic results. The kinetic data for benzene suggests that an intermediate hydride/dihydrogen complex is the catalytically active species that controls the overall hydrogenation rate. Ruthenium hydride and dihydrogen complexes of ruthenium are recognized as active precatalysts or intermediates in the catalytic cycles of many hydrogenation reactions [47-57]. Thus it is to be inferred that the present complex acts as a catalyst precursor for the hydrogenation of benzene and toluene.

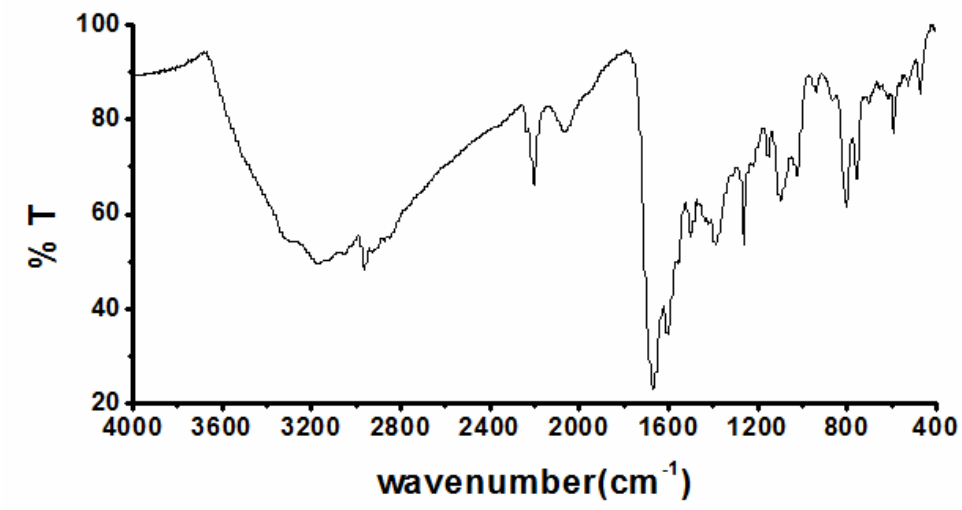

Figure 5: FT-IR spectrum of the intermediate ruthenium hydride complex

Table 10: The kinetic data for the $[Ru_2(hqcdmn)Cl_2].H_2O$ catalyzed hydrogenation of benzene [a].

[catalyst] (10^{-6} mol l^{-1})	[benzene] (mol l^{-1})	H_2		Initial rate
		Pressure (bar)	Concentration (mol l^{-1})	
1.41	0.34	30	1.02	1.48×10^{-3} mol s^{-1}
2.82	0.34	30	1.02	2.85×10^{-3} mol s^{-1}
4.23	0.34	30	1.02	3.88×10^{-3} mol s^{-1}
5.64	0.34	30	1.02	5.20×10^{-3} mol s^{-1}
7.05	0.34	30	1.02	6.28×10^{-3} mol s^{-1}
2.82	0.39	30	1.02	3.33×10^{-3} mol s^{-1}
2.82	0.45	30	1.02	3.80×10^{-3} mol s^{-1}
2.82	0.51	30	1.02	4.28×10^{-3} mol s^{-1}
2.82	0.56	30	1.02	4.75×10^{-3} mol s^{-1}
2.82	0.34	10	0.34	0.91×10^{-3} mol l^{-1} s^{-1}
2.82	0.34	20	0.68	1.86×10^{-3} mol l^{-1} s^{-1}
2.82	0.34	30	1.02	2.85×10^{-3} mol l^{-1} s^{-1}
2.82	0.34	40	1.36	3.21×10^{-3} mol l^{-1} s^{-1}
2.82	0.34	50	1.70	3.65×10^{-3} mol l^{-1} s^{-1}

[a] Other reaction conditions: 60 °C temperature, 600 rpm stirring speed and 2 h reaction time.

We carried out the same reaction under identical conditions with out the catalyst, with the organic ligand, with $RuCl_3.3H_2O$. In all these three cases no hydrogenation product was detected at the end of the reaction. These results proved that the hydrogenation was catalyzed by the added complex catalysts. Finke and co-workers [58-60] have reported that the hydrogenation of benzene under vigorous conditions (50-100 °C) using metal complexes proceeds through the formation of M(0) nanoclusters, which are not seen by naked eye. Here at the end of the reaction there were no black particles of ruthenium metal in the reaction mixture and the addition of mercury, as a selective poison for colloidal/nanoparticle catalysts, to the reaction system did not significantly affect the percentage conversion of benzene [61]. From these evidences we conclude that the hydrogenation in our system might have proceeded through a homogeneous mechanism and not through the formation of M(0) nanoparticles.

Conclusions

This chapter deals with the application of the ruthenium(II) complexes in the hydrogenation of benzene and toluene. All the complexes were screened for their catalytic activity and were found to be effective catalysts in the reduction of benzene and toluene. Catalytic experiments were carried out in a 100 mL bench top mini-reactor made of stainless steel 316 (Autoclave Engineers, Division of Snap-tite, Inc. PA). Partial as well as fully hydrogenated products were obtained during the reaction. A detailed kinetic study was carried out with $[Ru_2(hqcdmn)Cl_2].H_2O$ as the catalyst as it gave maximum conversion in the screening study. Influence of various parameters on the rate of reaction was investigated. Turn over frequencies 7362 h^{-1} and 5873 h^{-1} have been found for the reduction of benzene (0.34 mol) and toluene (0.28 mol) respectively at 60 ºC with 2.82 × 10^{-6} mol catalyst and at a hydrogen pressure of 30 bar. An intermediate hydride complex, believed to be the catalytically active species, has been isolated and identified by FT-IR spectroscopy. This active species is presumed to control the overall hydrogenation rate.

References

[1] L. Canali, D.C. Sherrington. Chemical Society Reviews, 28 (1999) 85−93.

[2] T. Katsuki. Chemical Reviews, 140 (1995) 189−214.

[3] K.C. Gupta, A.K. Sutar, Coordination Chemistry Reviews, 252 (2008) 1420−1450.

[4] R. Karvembu, R. Prabhakaran, K. Natarajan. Coordination Chemistry Reviews, 249 (2005) 911−918.

[5] K.O. Xavier, J. Chacko, K.K.M. Yusuff. Applied Catalysis A: General, 258 (2) (2004) 251−259.

[6] N.R. Suja, K.K.M. Yusuff. Journal of Applied Polymer Science, 91 (6) (2004) 3710−3719.

[7] S.C. Pearly, N. Sridevi, K.K.M. Yusuff. Journal of Applied Polymer Science, 105 (3) (2007) 997−1002.

[8] P.S. Chittilappilly, N. Sridevi, K.K.M. Yusuff. Journal of Molecular Catalysis A: Chemical, 286 (2008) 92−97.

[9] R. Drozdzak, B. Allaert, N. Ledoux, I. Dragutan, V. Dragutan, F. Verpoort. Coordination Chemistry Reviews, 249 (2005) 3055−3074.

[10] K. Abdur-Rashid, S.E. Clapham, A. Hadzovic, J.N. Harvey, A.J. Lough, R.H. Morrs. Journal of the American Chemical Society, 124 (2002) 15104−15118.

[11] P.J. Baricelli, L. Izaguirre, J. Lopez, E. Lujano, F. Lopez-Linares. Journal of Molecular Catalysis A: Chemical, 208 (2004) 67−72.

[12] B. Chen, U. Dingerdissen, J.G.E. Krauter, H.G.J. Lansink Rotgerink, K. Mobus, D.J. Ostgard, P. Panster, T.H. Riermeier, S. Seebald, T. Tacke, H. Trauthwein. Applied Catalysis A: General, 280 (2005) 17−46.

[13] E.G. Fidalgo, L. Plasseraud, G. Suss-Fink. Journal of Molecular Catalysis A: Chemical, 132 (1998) 5−12.

[14] R. Noyori, S. Hashiguchi. Accounts of Chemical Research, 30 (1997) 97−102.

[15] K. Nomura, H. Ogura, Y. Imanishi. Journal of Molecular Catalysis A: Chemical, 178 (2002) 105−114.

[16] D.U. Parmar, S.D. Bhatt, H.C. Bajaj, R.V. Jasra. Journal of Molecular Catalysis A: Chemical, 202 (2003) 9−15.

[17] C.A. Sandoval, T. Ohkuma, K. Muniz, R. Noyori. Journal of the American Chemical Society, 125 (2003) 13490−13503.

[18] G.C. Bond, F. Garin, G. Maire. Applied Catalysis, 41 (1988) 313−335.

[19] C. Morin, D. Simon, P. Sautet. Surface Science, 600 (2006) 1339−1350.

[20] P.A. Rautanen, J.R. Aittamaa, A.O.I. Krause. Industrial and Engineering Chemistry Research, 39 (11) (2000) 4032−4039.

[21] M.C. Rakowski, F.J. Hirsekorn, L.S. Stuhl, E.L. Muetterties. Inorganic Chemistry, 15 (1976) 2379−2382.

[22] A. Stanislaus, B.H. Cooper. Catalysis Reviews - Science and Engineering, 36 (1) (1994) 75−123.

[23] A. Andriollo, A. Bolivar, F.A. Ldpez, D.E. Pdez. Inorganica Chimica Acta, 238 (1995) 187−192.

[24] P.J. Baricelli, G. Rodriguez, M. Rodriguez, E. Lujano, F. Lopez-Linares. Applied Catalysis A: General, 239 (2003) 25−34.

[25] C. Daguenet, R. Scopelliti, P.J. Dyson. Organometallics, 23 (2004) 4849−4857.

[26] D.G. Holah, A.N. Hughes, B.C. Hui, C.T. Kan. Journal of Catalysis, 48 (1977) 340−344.

[27] I.M. Angulo, E. Bouwman. Journal of Molecular Catalysis A: Chemical, 175 (2001) 65−72.

[28] I.M. Angulo, S.M. Lok, V.F. Quiroga Norambuena, M. Lutz, A. L. Spek, E. Bouwman. Journal of Molecular Catalysis A: Chemical, 187 (2002) 55−67.

[29] C. Daguenet, P. J. Dyson. Catalysis Communications, 4 (2003) 153−157.

[30] J. Lin, C.U. Pittman Jr. Journal of Organometallic Chemistry, 512 (1996) 69−78.

[31] Z. Yang, M. Ebihara, T. Kawamura. Journal of Molecular Catalysis A: Chemical, 158 (2000) 509−514.

[32] A.F. Borowski, S. Sabo-Etienne, B. Chaudret. Journal of Molecular Catalysis A: Chemical, 174 (2001) 69−79.

[33] J.A. Widegren, M.A. Bennett, R.G. Fink. Journal of the American Chemical Society, 125 (34) (2003) 10301−10310.

[34] E. L. Muetterties, J. R. Bleeke. Accounts of Chemical Research, 12 (9) (1979) 324−331.

[35] N.S. Venkataramanan, G. Kuppuraj, S. Rajagopal. Coordination Chemistry Reviews, 249 (2005) 1249−1268.

[36] V. Dragutan, I. Dragutan, L. Delaude, A. Demonceau. Coordination Chemistry Reviews, 251 (2007) 765–794.

[37] E.A. Cagnola, M.E. Quiroga, D.A. Liprandi, P.C. L'Argentiere. Applied Catalysis A: General, 2004, 274, 205−212.

[38] A. Boettcher, H. Elias, E.G. Jaeger, H. Langfelderova, M. Mazur, L. Muller, H. Paulus, P. Pelikan, M. Rudolph, M. Valko. Inorganic Chemistry, 32 (1993) 4131−4138.

[39] P. Chen, B. Fan, M. Song, C. Jin, J. Ma, R. Li. Catalysis Communications, 7 (2006) 969−973.

[40] R.L. Augustine. Heterogeneous Catalysis for the Synthetic Chemist. Marcel Dekker, New York, 1996 (Chapter 17).

[41] L. Zhang, Y. Zhang, X-G Zhou, R-X Li, X-J Li, K.C. Tin, N-B Wong, Journal of Molecular Catalysis A: Chemical, 256 (2006) 171–177.

[42] A. F. Borowski, S. Sabo-Etienne, B. Chaudret. J. Journal of Molecular Catalysis A: Chemical, 174 (2001) 69–79.

[43] P. Chen, B. Fan, M. Song, C. Jin, J. Ma, R. Li. Catalysis Communications, 7 (2006) 969-973.

[44] S. Mayadevi, N. Sridevi, K.K.M. Yusuff. Indian Journal of Chemistry Section A: Inorganic, Bio-inorganic, Physical, Theoretical and Analytical Chemistry, 37 (1998) 413–417.

[45] G. Y. Kubas. Accounts of Chemical Research, 21 (1988) 120-128.

[46] P. J. Jessop, R. H. Morris. Coordination Chemistry Reviews, 121 (1992) 155-284.

[47] B.R. James. Catalysis Today, 37 (1997) 209-221.

[48] R. Noyori, T. Ohkuma. Angewandte Chemie International Edition, 40 (2001) 40-74.

[49] G. Zassinovich, G. Mestroni, S. Gladiali. Chemical Reviews, 92 (5) (1992) 1051-1069.

[50] T. Naota, H. Takaya, S.-I. Murahashi. Chemical Reviews, 98 (7) (1998) 2599-2660.

[51] R.A. Sanchez-Delgado, M. Rosales. Coordination Chemistry Reviews, 196 (2000) 249-280.

[52] J.E. Backvall. Journal of Organometallic Chemistry, 652 (2002) 105-111.

[53] F. Joo. Accounts of Chemical Research, 35 (2002) 738-745.

[54] G.J. Kubas, Metal Dihydrogen and Sigma-Bond Complexes, Kluwer Academic Publishers/Plenum Press, New York, 2001.

[55] M.A. Esteruelas, L.A. Oro. Chemical Reviews, 98 (1998) 577-588.

[56] S. Sabo-Etienne, B. Chaudret. Coordination Chemistry Reviews, 178-180 (1998) 381-407.

[57] S.E. Clapham, A. Hadzovic, R.H. Morris. Coordination Chemistry Reviews, 248 (2004) 2201–2237.

[58] J.A. Widegren, R.G. Finke. Journal of Molecular Catalysis A: Chemical, 191 (2003) 187–207.

[59] C.M. Hagen, J.A. Widegren, P.M. Maitlis, R.G. Finke. Journal of the American Chemical Society, 127 (2005) 4423−4432.

[60] Y. Lin, R.G. Finke. Inorganic Chemistry, 33 (1994) 4891−4910.

[61] T. Suarez, A. Guzman, B. Fontal, M. Reyes, F. Bellandi, R.R. Contreras, P. Cancines, G. Leon, L. Rojas. Transition Metal Chemistry, 31 (2006) 176–180.

Summary And Conclusion

Details of the studies on the synthesis, spectral characterization and catalytic applications of some new transition metal complexes of the Schiff bases derived from 3-hydroxyquinoxaline-2-carboxaldehyde are presented in this thesis. The thesis is divided into eight chapters. Contents of the various chapters are briefly described as follows:

Chapter 1

This chapter involves a general introduction to Schiff bases and a brief discussion of their applications in various catalytic processes. The synthetic methodologies and various applications of quinoxalines are also discussed in this chapter for the reason that we employed 3-hydroxyquinoxaline-2-carboxaldehyde, for the preparation of the Schiff base ligands. The scope of the present work and the possible application of these complexes in various fields are also discussed in this chapter.

Chapter 2

Chapter 2 deals with the details on various experimental and characterization techniques employed in the present study. Information about the synthesis and spectral characterization of the five new Schiff bases, N,N'-bis(3-hydroxyquinoxaline-2-carboxalidene)1,8-diaminonaphthalene (hqcdan-H_2), N,N'-bis(3-hydroxyquinoxaline-2-carboxalidene)2,3- diaminomaleonitrile (hqcdmn-H_2), N,N'-bis(3-hydroxyquinoxaline-2-carboxalidene)trans-(R,R')1,2-

diaminocyclohexane (hqcdac-H_2), 3-hydroxyquinoxaline-2-carboxalidene-2-aminophenol (hqcap-H_2) and 3-hydroxyquinoxaline-2-carboxalidene-4-aminoantipyrine (hqcaap-H), are also included in this chapter. These Schiff bases formed via the condensation of 3-hydroxyquinoxaline-2-carboxaldehyde with the amines 1,8-diaminonaphthalene, 2,3-diaminomaleonitrile, trans-(R,R')1,2-diaminocyclohexane, 2-aminophenol and 4-aminoantipyrine have been characterised with the aid of spectroscopic techniques such as FT-IR, UV-visible, NMR. These Schiff bases, like the other 2-hydroxyquinoxaline analogues, exhibit prototropic tautomerism.

Chapter 3

Oxovanadium(IV) complexes, $[(VO)_2(hqcdan)SO_4].H_2O$, $[(VO)_2(hqcdmn)SO_4].H_2O$, $[(VO)_2(hqcdac)SO_4].H_2O$, $[(VO)_2(hqcap)_2].H_2O$ and $[(VO)_2(hqcaap)_2SO_4].2H_2O$, were synthesised and characterised by elemental analysis, FT-IR, UV-visible, TG-DTA-DTG, EPR, AAS, cyclic voltammetry, conductance and magnetic susceptibility measurements. The cyclic voltammograms for all the complexes in DMSO consist of an irreversible reduction wave due to reduction of V^{IV} to V^{III} and an irreversible oxidation wave due to the oxidation of V^{IV} to V^{V}. The V=O stretching frequencies of these complexes are comparatively lower than that of other penta-coordinated oxovanadium(IV) complexes indicating that the V=O bond is weakened by strong σ and π electron donation by the electron rich Schiff base ligands to the antibonding orbital of the V=O group. Also these lower values for V=O stretching frequencies suggest the absence of −V=O—V=O− chain structure in these complexes. The presence of chelating bidentate coordination of the SO_4^{2-} group in each complex is evidenced by the presence of a triply degenerate ν_3 and single ν_1 bands in the IR spectra. The electronic spectra of all the complexes in methanol exhibit only a single d-d band and are dominated by ligand centered bands. However, the solid state diffuse reflectance spectra of these

complexes exhibit d-d bands corresponding to the electronic transitions of the square pyramidal oxovanadium complex ($^2B_2 \rightarrow {}^2A_1$, $^2B_2 \rightarrow {}^2B_1$, and the split $^2B_2 \rightarrow {}^2E$ transitions). The ESR spectra of all the complexes in DMF at LNT display well resolved axial anisotropy with typical eight-line pattern characteristic of square pyramidal oxovanadium(IV) complexes. The presence of lattice water molecules in these complexes is confirmed by the TG weight loss below 130 °C. Thus, all these complexes have a binuclear structure with square-pyramidal geometry around each vanadium centre.

Chapter 4

In this chapter, a discussion on the synthesis and characterization of copper(II) complexes, $[Cu_2(hqcdan)Cl_2].H_2O$, $[Cu_2(hqcdmn)Cl_2]$, $[Cu_2(hqcdac)Cl_2].H_2O$, $[Cu_2(hqcap)_2]$ and $[Cu(hqcaap)Cl(H_2O)_2]$, has been presented. The presence of coordinated and lattice water in these complexes are evidenced from the FT-IR and TG data. The complex, $[Cu(hqcaap)Cl(H_2O)_2]$, exhibits a magnetic moment value of 1.76 BM as expected for a mononuclear copper(II) octahedral complex, where as in all other cases, subnormal magnetic moment values were observed suggesting binuclear nature of the complexes. A two-stepped cyclic voltammogram were observed for all the complexes. The first redox peak appearing in the positive potential range corresponds to $Cu_2^{II,II}/Cu_2^{II,I}$ redox couple, whereas the second peak appearing in the negative potential range is attributable to the $Cu_2^{II,I}/Cu_2^{I,I}$ redox processes. Cyclic voltammogram of the mononuclear copper(II) complex also exhibits two irreversible one-electron waves due to the Cu^{III}/Cu^{II} couple and Cu^{II}/Cu^{I} couple. FT-IR spectra reveal that the azomethine stretching frequency increases for all the complexes suggesting complex formation. The diffuse reflectance spectra of the binuclear complexes exhibit the three spin allowed transitions, viz., $^2B_{1g} \rightarrow {}^2A_{1g}$ ($d_{x2-y2} \rightarrow d_{z2}$), $^2B_{1g} \rightarrow {}^2B_{2g}$ ($d_{x2-y2} \rightarrow d_{xy}$) and $^2B_{1g} \rightarrow {}^2E_g$ ($d_{x2-y2} \rightarrow d_{xz}$, d_{yz}), expected for square-planar complexes.

However in solution spectra (in methanol) only one broad band was observed. The electronic spectral data for the complex, $[Cu(hqcaap)Cl(H_2O)_2]$, suggest an octahedral geometry. EPR spectra of all the complexes were recorded in polycrystalline state and in DMF solution at 77 K. The presence of half-field signals in the spectra of $[Cu_2(hqcdmn)Cl_2]$ and $[Cu_2(hqcdac)Cl_2].H_2O$ supports the binuclear structure for these complexes.

Chapter 5

Chapter 5 deals with the synthesis and characterization of the ruthenium(II) complexes, $[Ru_2(hqcdan)Cl_2].H_2O$, $[Ru_2(hqcdmn)Cl_2].H_2O$, $[Ru_2(hqcdac)Cl_2].H_2O$, $[Ru_2(hqcap)Cl_2(H_2O)].H_2O$ and $[Ru(hqcaap)Cl(H_2O)_2].H_2O$. The presence of coordinated and lattice water molecules in the complexes could be confirmed form the TG and IR studies. All the complexes are diamagnetic and EPR silent suggesting that the ruthenium is in the +2 oxidation state. A two-stepped cyclic voltammogram was observed for all the ruthenium(II) complexes. The first redox peak appearing in the positive potential range for the binuclear complexes corresponds to $Ru_2^{III,III}/Ru_2^{III,II}$ redox couple, where as the second redox couple appearing in the negative potential range is attributable to the $Ru_2^{III,II}/Ru_2^{II,II}$ redox processes. Cyclic voltammogram of the mononuclear ruthenium(II) complex also exhibits two irreversible one-electron waves due to the Ru^{IV}/Ru^{III} couple and Ru^{III}/Ru^{II} couple. An increase in azomethine stretching frequency was observed in the IR spectra of all the complexes. Presence of the three bands corresponding to the electronic transitions, $^1A_{1g} \rightarrow {}^1E_g$, $^1A_{1g} \rightarrow {}^1B_{1g}$ and $^1A_{1g} \rightarrow {}^1A_{2g}$ in the diffuse reflectance spectra of the binuclear complexes suggests a square planar geometry. The electronic spectrum of $[Ru(hqcaap)Cl(H_2O)_2].H_2O$ suggests an octahedral structure.

Chapter 6

Details on the catalytic activity studies of the oxovanadium(IV) complexes, $[(VO)_2(hqcdan)SO_4].H_2O$, $[(VO)_2(hqcdmn)SO_4].H_2O$, $[(VO)_2(hqcdac)SO_4].H_2O$, $[(VO)_2(hqcap)_2].H_2O$ and $[(VO)_2(hqcaap)_2SO_4].2H_2O$, in the liquid phase oxidation of cyclohexene are presented in this chapter. All the complexes are found to catalyze liquid phase oxidation of cyclohexene using H_2O_2 as oxidant. More selectivity was observed for allylic oxidation products rather than that for epoxidation product. The oxovanadium(IV) complex of the Schiff base, N,N'-bis(3-hydroxyquinoxaline-2-carboxalidene)2,3-diaminomaleonitrile, exhibits comparatively better catalytic activity and a detailed investigation was carried out with this complex. A low H_2O_2 efficiency seen for this reaction might be due to the high activity of the complex towards the decomposition of hydrogen peroxide.

Chapter 7

Studies on the catalytic activity of the copper(II) complexes (synthesis of which are presented in chapter 4) in the liquid-phase hydroxylation of phenol using H_2O_2 as an oxidant are presented in this chapter. Catechol and hydroquinone are the sole products of the reaction. All the complexes were screened for their activity towards the hydroxylation of phenol. The complex, $[Cu_2(hqcdmn)Cl_2]$, gave maximum conversion in the screening studies and detailed investigations were carried out with this complex. The effect of amount of catalyst, reaction time, reaction temperature, amount of oxidant, and that of the amount of solvent on the reaction were studied. It was found that there exists an optimum value for the catalyst amount, temperature and time. Increase in the amount of H_2O_2 has a positive effect on the reaction, while the quantity and nature of solvent have no significant effect.

Chapter 8

This chapter deals with the application of the ruthenium(II) complexes (synthesis of which are presented in chapter 5) in the hydrogenation of benzene and toluene. All the complexes were screened for their catalytic activity and were found to be effective catalysts in the reduction of benzene and toluene. Catalytic experiments were carried out in a 100 mL bench top mini-reactor. Both partial and complete reduction products were obtained during the hydrogenation. A detailed kinetic study was carried out with $[Ru_2(hqcdmn)Cl_2].H_2O$, as it exhibited maximum catalytic activity in the screening study. Influence of various parameters on the rate of reaction was investigated. Turnover frequencies of 7362 h^{-1} and 5873 h^{-1} have been found for the reduction of benzene (0.34 mol) and toluene (0.28 mol) respectively at 60 ºC with 2.82×10^{-6} mol catalyst and at a hydrogen pressure of 30 bar. These values are much higher than that of some of the reported ruthenium catalysts for the homogeneous aromatic hydrogenation reactions. An intermediate hydride complex, believed to be the catalytically active species, has been isolated and identified by FT-IR spectroscopy. This active species is presumed to control the overall hydrogenation rate.

List of Publications

1. **V. Arun**, P.P. Robinson, S. Manju, P. Leeju, G. Varsha, V. Digna, K.K.M. Yusuff, "A novel fluorescent bisazomethine dye derived from 3- hydroxyquinoxaline-2-carboxaldehyde and 2,3-diaminomaleonitrile" Dyes and Pigments 82(3) (2009) 268-275.

2. **V. Arun**, N. Sridevi, P.P. Robinson, S. Manju, K.K.M. Yusuff, "Ni(II) and Ru(II) Schiff base complexes as catalysts for the reduction of benzene" J. Mol. Catal. A: Chem. 304(1-2) (2009) 191-198.

3*. D. Varghese, **V. Arun**, M. Sebastian, P. Leeju, G. Varsha, K.K.M. Yusuff, "N,N'-Bis[(E)-quinoxalin-2-ylmethylidene]ethane-1,2-diamine" Acta Cryst. E65 (2009) o435.

4*. G. Varsha, **V. Arun**, M. Sebastian, P. Leeju, D. Varghese, K.K.M. Yusuff, "(Z)-2-Amino-3-[(E)-benzylideneamino]-but-2-enedinitrile" Acta Cryst. E65 (2009) o919.

5*. P.P. Robinson, **V. Arun**, S. Manju, C.U. Aniz, K.K.M. Yusuff, "Oxidation kinetics of nickel nano crystallites obtained by controlled thermolysis of diaqua-bis(ethylenediamine)nickel(II) nitrate" Journal of Thermal Analysis and Calorimetry, doi: 10.1007/s10973-009-0209-y

* Not related to the work presented in this thesis